

**CONSEQUENCES AND PREVENTION OF ELEVATED CIRCULATING
TYROSINE DURING NITISINONE THERAPY IN ALKAPTONURIA**

RÓISÍN LEWIS

A thesis submitted in partial fulfilment of the requirements of Liverpool John
Moore's University for the degree of Doctor of Philosophy

March 2018

Acknowledgements

Foremost, I would like to express my sincerest thanks and gratitude to my director of studies, Professor Jonathan Jarvis, for the opportunity to undertake this PhD project and for his support, scholarly guidance and the provision of resources to complete my research. I also profusely thank Dr Hazel Sutherland, for her expertise as a mouse whisperer and for being a friend as well as a very able mentor - her kindness (and coffee!) has helped fuel much of the laboratory work contained within this thesis.

I would like to offer a special note of thanks to my additional supervisors, Professor Jim Gallagher and Professor Lakshminarayan Ranganath, for their support and valued input throughout this research. Many thanks are also extended to Dr Craig Keenan for his assistance with the laborious task of chondrocyte quantification and for his general comedic value (that laugh!). Thank you to all members of the AKU research group at the University of Liverpool and Royal Liverpool University Hospital. Special mention must go to Professor Edward Lock, for constantly offering his knowledgeable opinion on perplexing findings long into his retirement. My sincerest thanks are also extended to the staff of the Liverpool John Moores University Life Sciences Support Unit, the unsung heroes of animal work - Steve, Roy, Joe and Ste.

I am extremely thankful to my parents, Jude and Mick, and Sister, Hannah, for their continuous words of encouragement to finish my research. I am eternally grateful also to my grandparents, John and Doreen, for their belief and confidence in everything I do. Special thanks are also extended to my partner, Andrew Mason, for his love, kindness and endless support during my perpetual student status. I would like to dedicate this thesis to the memory of his father, Christopher Ian Mason (1955-2018), who passed away shortly before its completion.

Alkaptonuria (AKU) is an ultra-rare, autosomal recessive disorder of tyrosine catabolism due to mutations within the homogentisate 1,2-dioxygenase (HGD) gene. The resulting enzyme deficiency leads to accumulation of homogentisic acid (HGA) and deposition of melanin-like pigment polymers in the connective tissues of the body in a process called ochronosis. This leads to debilitating early onset osteoarthropathy, renal damage and aortic valve disease. As a multisystem disorder, AKU results in progressive and chronic pain and severe morbidity. Most management approaches for AKU are palliative and rely largely on analgesia and arthroplasty. Several therapeutic approaches have been tested with low degrees of clinical effectiveness. Nitisinone is a promising drug that blocks the enzyme catalysing the formation of HGA and thus lowers its plasma concentration. HGA lowering therapy has been widely used in another rare inborn error of metabolism, Hereditary Tyrosinemia type 1 (HT-1) for over 20 years. Nitisinone is highly efficacious in terms of its metabolic effect as it decreases HGA to very low levels, but there is limited toxicology data available for its use in AKU. There are also concerns relating to the adverse side effects of elevated tyrosine and potential neurotoxicity if treatment was implemented in children.

The work presented within this thesis presents novel findings to inform the future licensing process for the use of nitisinone in AKU and investigates the safety of implementing treatment in younger patients. Nitisinone treatment had no detrimental effect on learning, memory or motor function in young AKU or wild type mice. The thesis also includes new data from mouse dosing studies concerning the correlation between plasma HGA and ochronotic pigmentation and reveals that plasma HGA must be lowered to a critical level before pigmentation is beneficially reduced. Finally, this thesis reports on the lability of the arteriovenous metabolome relating to AKU and initiates a discussion relating to the HPPA to HPLA excretory conversion pathway along with important considerations for collection, analysis and comparison of blood samples in future studies.

Abbreviations

ACC - Articular calcified cartilage

AKU - Alkaptonuria

BQA - Benzoquinone acetic acid

CSF - Cerebrospinal fluid

ECM - Extracellular matrix

ENU - N-ethyl N-nitrosourea

FAH - Fumarylacetoacetase

HAC – Hyaline articular cartilage

HGA - Homogentisic acid

HGD - Homogentisate 1,2-dioxygenase

HPPD - 4-hydroxyphenylpyruvate dioxygenase

HT-1 - Hereditary tyrosinemia type 1

HT-2 - Hereditary tyrosinemia type 2

HT-3 - Hereditary tyrosinemia type 3

IGST - Inverted grid suspension test

LTDRS - Long-term dose response study

MAA - Maleylacetoacetic acid

MTPT - 1-methyl-4-phenyl-1,2,3,6-tetrahydropyridine

MWM - Morris water maze

NFR – Nuclear fast red

NMR – Nuclear magnetic resonance

NTBC - 2-(2-nitro-4-trifluoromethylbenzoyl)-1,3-cyclohexanedione

OA - Osteoarthritis

PKU – Phenylketonuria

RT-PCR – Reverse transcription-polymerase chain reaction

TAT - Tyrosine aminotransferase

WT - Wild type

Table of Contents

Acknowledgements	i
Abstract	ii
Abbreviations	iii-iv
Table of Contents	v-xi
Table of Figures	xii-xvi
Tables	xvii
1. Introduction	1
1.1 ALKAPTONURIA	2
1.1.1 History	3
1.1.2 Epidemiology	4
1.1.3 Pathophysiology and diagnosis	4
1.1.4 HGD Gene	5
1.1.5 Ochronosis	6
1.1.6 Current therapeutic options	8
1.1.6.1 Ascorbic acid	8
1.1.6.2 Low protein diet	8
1.1.6.3 Nitisinone	9
1.1.6.3.1 Nitisinone induced tyrosinemia	9
1.2 HGD-/- AKU MOUSE MODEL	12
1.3 BEHAVIOURAL STUDIES	13
1.3.1 Morris Water Maze	14
1.4 MOTOR FUNCTION ASSESSMENT	16
1.4.1 Rota-rod	17
1.4.2 Inverted grid suspension test	18
1.4.3 Catwalk XT gait analysis	19
2. Materials and Methods	20
2.1 ETHICAL APPROVAL	21

2.6.6 Sectioning of tissue	32
2.6.7 Subbing of slides	32
2.6.7.1 Preparation of subbing solution	32
2.6.7.2 Subbing procedure	33
2.6.8 Tissue staining	33
2.6.8.1 Schmorl's stain	33
2.6.8.1.1 Preparation of Schmorl's incubating solution	33
2.6.8.1.2 Schmorl's staining procedure	34
2.7 HISTOLOGICAL ANALYSIS	34
2.7.1 Tibio-femoral joints from long-term dose response study	34
2.7.2 Light microscopy	34
2.7.3 Quantification of ochronotic pigmentation	34
2.8 REDUCTION OF MOUSE ANXIETY	36
2.9 MOUSE IDENTIFICATION	37
2.10 MORRIS WATER MAZE	37
2.10.1 Introduction	37
2.10.2 MWM equipment	38
2.10.3 Health and safety	38
2.10.4 Preparation of MWM pool	39
2.10.5 MWM testing procedure	39
2.10.5.1 General information	39
2.10.5.2 Visible platform task (day 1)	40
2.10.5.3 Hidden platform task (day 2-5)	40
2.10.5.4 Probe test (day 6)	40
2.11 MOTOR FUNCTION ASSESSMENT	43
2.11.1 Rota-rod	43
2.11.1.1 Introduction	43
2.11.1.2 Rota-rod equipment	43
2.11.1.3 General information	43
2.11.1.4 Positioning mice on the Rota-rod	43
2.11.1.5 Testing procedure	44

2.11.2 Inverted grid suspension test	45
2.11.2.1 Inverted grid suspension test equipment	45
2.11.2.2 Testing procedure	46
2.12 CATWALK XT GAIT ANALYSIS	46
2.12.1 Introduction	46
2.12.2 Mice	47
2.12.3 Bodyweight	47
2.12.4 Equipment	48
2.12.5 General information	48
2.12.6 Training procedure	48
2.12.7 Test procedure	49
2.12.8 Run classification	49
2.12.9 Catwalk gait analysis parameters	50
2.12.9.1 Static parameters	50
2.12.9.2 Dynamic parameters	51
2.13 ARTERIOVENOUS METABOLOME STUDY (CHAPTER 5)	51
2.13.1 Mice	51
2.14 STATISTICAL ANALYSIS	52
2.14.1 Normality and homogeneity of variance	52
2.14.2 Morris water maze data	52
2.14.3 Motor function test data	52
2.14.4 Long-term dose response study data	52
2.14.5 Arteriovenous metabolome data	53
3. Analysis of learning, memory and motor function in nitisinone treated and control cohorts of AKU (Hgd^{-/-}) and wild type BALB/c mice	54
3.1 INTRODUCTION	55
3.2 HYPOTHESIS AND AIM OF STUDY	56
3.3 RESULTS	57
3.3.1 Plasma metabolites	57

3.3.2 Morris water maze	59
3.3.2.1 Visible platform (Day 1)	59
3.3.2.2 Hidden Platform (Day 2-5)	63
3.3.2.3 Probe Trial (Day 6)	67
3.3.3 Motor function analysis	69
3.3.3.1 Rota-rod	69
3.3.3.2 Inverted grid suspension test	70
3.3.4 Catwalk XT gait analysis	71
3.3.4.1 Bodyweight	72
3.3.4.2 Stance Phase	73
3.3.4.3 Swing Phase	74
3.3.4.4 Duty Cycle	75
3.3.4.5 Regularity index and stride length	77
3.3.4.6 Maximum contact intensity (paw weight bearing)	78
3.3.4.7 Print area	79
3.4 DISCUSSION	80
3.4.1 Morris water maze	80
3.4.2 Motor Function Analysis	81
3.4.3 Catwalk XT gait analysis	82
3.4.4 Limitations	84
4. Balancing the reduction of plasma HGA and elevation of tyrosine in the treatment of AKU with nitisinone - a long-term dose response study in BALB/c Hgd^{-/-} mice	85
4.1 INTRODUCTION	86
4.2 HYPOTHESIS AND AIM OF STUDY	87
4.3 RESULTS	88
4.3.1 Plasma metabolites	88
4.3.1.1 Tyrosine	88
4.3.1.2 HGA	92
4.3.1.3 Phenylalanine	96
4.3.1.4 HPPA	99

4.3.1.5 HPLA	102
4.3.2 Pigmentation quantification	107
4.3.2.1 Inter-observer variability	109
4.3.3 Pigmentation in the BALB/c Hgd ^{-/-} tibio-femoral joint	111
4.3.3.1 Control mice	111
4.3.3.2 Nitisinone 0.125mg/L	115
4.3.3.3. Nitisinone 0.5mg/L	118
4.3.3.4 Nitisinone 2mg/L	121
4.3.4 Relationship between HGA and ochronotic pigmentation	127
4.4 DISCUSSION	129
4.4.1 HGA and ochronotic pigmentation	129
4.4.2 Dosing to reduce elevation of tyrosine	130
4.4.3 HPPA and HPLA	131
4.4.4 HGA variability	132
4.4.5 Mid-term and terminal bleed metabolite discrepancies	133
4.4.6 Limitations	135
5. Investigating the arteriovenous blood metabolome relating to Alkaptonuria in the	136
BALB/c Hgd^{-/-} mouse	
5.1 INTRODUCTION	137
5.1.1 Study 1	138
5.1.2 Study 2	139
5.1.3 Study 3	139
5.1.4 Study 4	140
5.2 HYPOTHESIS AND AIM OF STUDY	142
5.3 RESULTS	143
5.3.1 Effect of sample collection tube	143
5.3.2 Differences in metabolites between tail bleeds	145
5.3.3 Differences in metabolites between sample site	146
5.3.4 Five consecutive tail bleeds	148
5.3.5 Cull method	151

5.3.6 Combined data from terminal arterial bleeds to assess cull method	154
5.3.7 Combined data from venous tail and terminal bleeds	157
5.4 DISCUSSION	161
6. General Discussion	166
7. Future work	173
7.1 Investigate differences between arteriovenous metabolome in AKU humans	174
7.2 Heterozygous mice for further MWM trials	174
7.3 Measuring catecholamines in the mouse brain	174
7.4 Gait analysis with weight matched Hgd ^{-/-} and WT mice	175
7.5 Quantification of OA in Hgd ^{-/-} nitisinone treated mice	175
7.6 Cull method effect on HPPA/HPLA	175
8. References	176
Appendix: Long-term dose response study metabolite data and pigmented chondrocyte counts	192

Table of Figures

Chapter 1

- Figure 1.1 - Diagram detailing the enzyme defect in AKU and formation of ochronotic pigment 2

Chapter 2

- Figure 2.1 - Area of ochronotic pigmentation quantification in the mouse tibio-femoral joint 35
- Figure 2.2 - Classification of pigmentation for quantification of pigmented chondrons in the BALB/c Hgd^{-/-} tibio-femoral joint 36
- Figure 2.3 - Morris water maze pool quadrants, platform location and cardinal/ordinal compass point starting positions 42
- Figure 2.4 - Morris water maze equipment set up 42
- Figure 2.5 - Rota-rod apparatus 44
- Figure 2.6 - Inverted grid suspension test apparatus set up 45
- Figure 2.7 - The catwalk XT platform and illumination of footprints in a mouse traversing the glass walkway 47
- Figure 2.8 - Footprint classification after data acquisition in the Catwalk XT platform 50

Chapter 3

- Figure 3.1 - Plasma tyrosine and HGA levels (mean \pm sem) in BALB/c Hgd^{-/-} and WT control and nitisinone treated mice 58
- Figure 3.2 - Mean escape latency (\pm SEM) of BALB/c Hgd^{-/-} and WT mice during visible platform trials in the MWM 60
- Figure 3.3 - Mean swimming speed (\pm SEM) of BALB/c Hgd^{-/-} and WT mice during visible platform trials in the MWM 61
- Figure 3.4 - Mean swimming distance (\pm SEM) of BALB/c Hgd^{-/-} and WT mice during visible platform trials in the MWM 62
- Figure 3.5 - A: Mean escape latency (\pm SEM) B: Mean swimming speed (\pm SEM) C: Mean swimming distance (\pm SEM) of BALB/c Hgd^{-/-} and WT mice during hidden platform trials in the MWM 64
- Figure 3.6 - Mean escape latency (\pm SEM) of BALB/c Hgd^{-/-} and WT mice in the MWM: comparison of first and last run of hidden platform trials 66

Figure 3.7 – Mean percentage of time spent in target quadrant (\pm SEM) during probe trial of the MWM in BALB/c Hgd ^{-/-} and WT nitisinone treated and control mice	68
Figure 3.8 - Mean (\pm SEM) performance of BALB/c Hgd ^{-/-} and WT control and treated mice on the Rota-rod	69
Figure 3.9 - Mean (\pm SEM) latency to fall on the inverted grid suspension test in BALB/c Hgd ^{-/-} and WT control and treated mice	70
Figure 3.10 - Bodyweight of male and female BALB/c Hgd ^{-/-} and WT mice tested with the Catwalk gait analysis platform	72
Figure 3.11 - Mean (\pm SEM) stance phase for male and female BALB/c Hgd ^{-/-} and WT mice	73
Figure 3.12 - Mean (\pm SEM) swing phase for male and female BALB/c Hgd ^{-/-} and WT mice	74
Figure 3.13 - Mean (\pm SEM) duty cycle for male and female BALB/c Hgd ^{-/-} and WT mice	76
Figure 3.14 - Mean (\pm SEM) regularity index (A) and stride length (B) for male and female BALB/c Hgd ^{-/-} and WT mice	77
Figure 3.15 - Mean (\pm SEM) maximum contact intensity for male and female BALB/c Hgd ^{-/-} and WT mice.	78
Figure 3.16 - Mean (\pm SEM) print area for male and female BALB/c Hgd ^{-/-} and WT mice	79

Chapter 4

Figure 4.1 - Effects of nitisinone on plasma tyrosine levels after 20 weeks treatment in BALB/c Hgd ^{-/-} mice	89
Figure 4.2 - Effects of nitisinone on plasma tyrosine levels after 40 weeks treatment in BALB/c Hgd ^{-/-} mice	90
Figure 4.3 - Comparison of the effect of nitisinone dose on plasma tyrosine levels after 20 (mid) and 40 weeks (term) treatment in BALB/c Hgd ^{-/-} mice	91
Figure 4.4 - Effect of nitisinone on plasma HGA after 20 weeks treatment in BALB/c Hgd ^{-/-} mice	92
Figure 4.5 - Effect of nitisinone on plasma HGA levels after 40 weeks treatment in BALB/c Hgd ^{-/-} mice	93
Figure 4.6 - Comparison of effects of nitisinone dose on plasma HGA levels after 20 (mid) and 40 (term) weeks treatment in BALB/c Hgd ^{-/-} mice	94

Figure 4.7 - Effect of nitisinone on plasma phenylalanine after 20 weeks treatment in BALB/c Hgd-/- mice	96
Figure 4.8 - Effects of nitisinone on plasma phenylalanine after 40 weeks treatment in BALB/c Hgd-/- mice	97
Figure 4.9 - Comparison of the effects of nitisinone dose on plasma phenylalanine levels after 20 (mid) and 40 (term) weeks treatment in BALB/c Hgd-/- mice	98
Figure 4.10 - Effect of nitisinone dose on plasma HPPA levels after 20 weeks treatment in BALB/c Hgd-/- mice	99
Figure 4.11 - Effect of nitisinone dose on plasma HPPA levels after 40 weeks treatment in BALB/c Hgd-/- mice	100
Figure 4.12 - Comparison of the effects of nitisinone dose on plasma HPPA levels after 20 (mid) and 40 (term) weeks treatment in BALB/c Hgd-/- mice	101
Figure 4.13 - Effect of nitisinone dose on plasma HPLA levels after 20 weeks treatment in BALB/c Hgd-/- mice	102
Figure 4.14 - Effect of nitisinone dose on plasma HPLA levels after 40 weeks treatment in BALB/c Hgd-/- mice	103
Figure 4.15 - Comparison of the effects of nitisinone dose on plasma HPLA levels after 20 (mid) and 40 (term) weeks treatment in BALB/c Hgd-/- mice	104
Figure 4.16 - Overall effect of nitisinone dose on plasma metabolites measured after 20 weeks treatment (mid bleed) in BALB/c Hgd-/- mice	105
Figure 4.17 - Overall effect of nitisinone dose on plasma metabolites measured after 40 weeks treatment (terminal bleed) in BALB/c Hgd-/- mice	106
Figure 4.18 - Quantification of pigmented chondrocytes counts showing both classification methods - cellular staining only and peri-cellular and cellular staining combined. Stained with Schmorls reagent	108
Figure 4.19 - Inter-observer variability and correlation of cellular pigmentation quantification method	110
Figure 4.20 - Pigmentation in 43 week old, BALB/c Hgd-/- control mouse (30.4)	112
Figure 4.21 - Ochronotic pigmentation throughout the articular calcified cartilage of the lateral and medial aspects of the tibio-femoral joint of a 43 week old, BALB/c Hgd-/- control mouse (30.4)	113
Figure 4.22 - Overview of pigmentation of the articular calcified cartilage in the tibio-femoral joint of two 43 week old, BALB/c Hgd -/- control mice	114

Figure 4.23 - Ochronotic pigmentation in the articular calcified cartilage of the tibio-femoral joint of 43 week old, BALB/c Hgd ^{-/-} mice receiving 0.125mg nitisinone.	116-117
Figure 4.24 - Overview of entire tibio-femoral joint of a 43 week old, BALB/c Hgd ^{-/-} mouse receiving 0.125mg nitisinone for 40 weeks	118
Figure 4.25 - Ochronotic pigmentation in 43 week old BALB/c Hgd ^{-/-} mice receiving 0.5mg nitisinone for 40 weeks	119
Figure 4.26 - Overview of entire tibio-femoral joint in 43 week old BALB/c Hgd ^{-/-} mouse receiving 0.5mg nitisinone for 40 weeks.	120
Figure 4.27 - Very low levels of ochronotic pigmentation in the ACC of the medial femoral condyle and medial tibial plateau in 43 week old mice receiving 2mg nitisinone for 40 weeks	122
Figure 4.28 - Overview of entire tibio-femoral joint of 43 week old, BALB/c Hgd ^{-/-} mouse (13.6) receiving 2mg nitisinone for 40 weeks	123
Figure 4.29 - Comparison of ochronotic pigmentation within the ACC of the medial femoral condyle and medial tibial plateau in 43 week old Hgd ^{-/-} BALB/c mice receiving 0mg (A), 0.125mg (B), 0.5mg (C) and 2mg (D) nitisinone for 40 weeks	124-125
Figure 4.30 - Hyaline articular cartilage damage and signs of osteoarthritis in the tibio-femoral joint of 43 week old, control and nitisinone treated BALB/c Hgd ^{-/-} mice	126
Figure 4.31 - The relationship between plasma HGA concentration and ochronotic pigmentation is not linear	127
Figure 4.32 - The correlation of plasma HGA and ochronotic pigmentation after 40 weeks nitisinone treatment in BALB/c Hgd ^{-/-} mice	128

Chapter 5

Figure 5.1 - Differences in metabolites between mid-term and terminal bleeds in BALB/c Hgd ^{-/-} mice from the long-term dose response study	141
Figure 5.2 - Collection tube had no significant effect on metabolite values between brachial arterial blood samples in control or nitisinone treated BALB/c Hgd ^{-/-} mice	144
Figure 5.3 - Plasma HGA values decrease between two consecutive tail bleeds sampled seconds apart	145

Figure 5.4 - HGA values were significantly lower in brachial bleeds in control mice, HGA and HPPA were significantly lower in brachial bleeds and HPLA was significantly higher in brachial bleeds in nitisinone treated mice	147
Figure 5.5 - Control mice showed variation in HGA between tail bleeds	148
Figure 5.6 - Variation in HGA is masked by the therapeutic effect of nitisinone in treated Hgd^{-/-} mice	150
Figure 5.7 - Tail bleed HGA values in control mice once again showed high intra and inter-mouse variability	152
Figure 5.8 - HPPA values in treated mice followed the same trend as observed in previous studies – lower levels in terminal arterial bleeds compared to tail bleeds. HPLA was much less variable with similar concentrations across bleeds	153
Figure 5.9 - Culling with Pentoject had a significant effect on HPPA and HPLA terminal arterial plasma values compared to manual culling in nitisinone treated Hgd^{-/-} mice (B, C). Cull method had no significant effect on HGA values in terminal arterial bleeds of control Hgd^{-/-} mice (A).	155
Figure 5.10 - Administration of Pentoject has a significant effect on terminal bleed HPPA and HPLA plasma values of Hgd^{-/-} BALB/c nitisinone treated mice	156
Figure 5.11 - Plasma HGA was lower in blood sampled from brachial vessels (terminal) compared to peripheral venous blood (tail) in BALB/c Hgd^{-/-} mice	158
Figure 5.12 - Plasma HPPA was lower (A) and HPLA higher (B) in blood sampled from brachial vessels (terminal) compared to peripheral venous blood (tail) in BALB/c Hgd^{-/-} mice.	159
Figure 5.13 - Phenylalanine was slightly elevated in blood sampled from brachial vessels (terminal) compared to peripheral venous blood (tail) in nitisinone treated BALB/c Hgd^{-/-} mice	160
Figure 5.14 - Tyrosine showed no significant fluctuations between plasma sample Site in control or nitisinone treated BALB/c Hgd^{-/-} mice.	160

Tables

Chapter 2

Table 2.1 - Details of individual BALB/c mice used within this thesis	24-27
Table 2.2 - Platform location and starting directions for the Morris water maze behavioural experiment	41

Chapter 3

Table 3.1 - Mean Gallagher proximity measures during probe trial of the MWM in BALB/c Hgd ^{-/-} and WT nitisinone treated and control mice	68
---	----

Chapter 4

Table 4.1 - Coefficient of variation for HGA from mid and term bleeds.	95
Table 4.2 - Quantification of mean pigmentation in the tibio-femoral joint of 43 week old control and nitisinone treated BALB/c Hgd ^{-/-} mice	110

Chapter 5

Table 5.1 - Tukey multiple comparisons results from ANOVA post hoc tests of combined venous tail and brachial arterial bleed data (n=21 mice)	157
---	-----

1. Introduction

1.1 ALKAPTONURIA

Alkaptonuria (AKU) is an ultra-rare, autosomal recessive condition commonly referred to as “black bone disease”. The condition is a disorder of phenylalanine and tyrosine catabolism due to mutations within the homogentisate 1,2-dioxygenase (HGD) gene. The resulting enzyme deficiency leads to accumulation of homogentisic acid (HGA) and deposition of melanin-like pigment polymers in the connective tissues of the body in a process called ochronosis. This leads to debilitating early onset osteoarthropathy, osteopenia, tendon and ligament ruptures, renal damage and aortic valve disease. As a multisystem disorder, AKU results in progressive and chronic pain and severe morbidity.

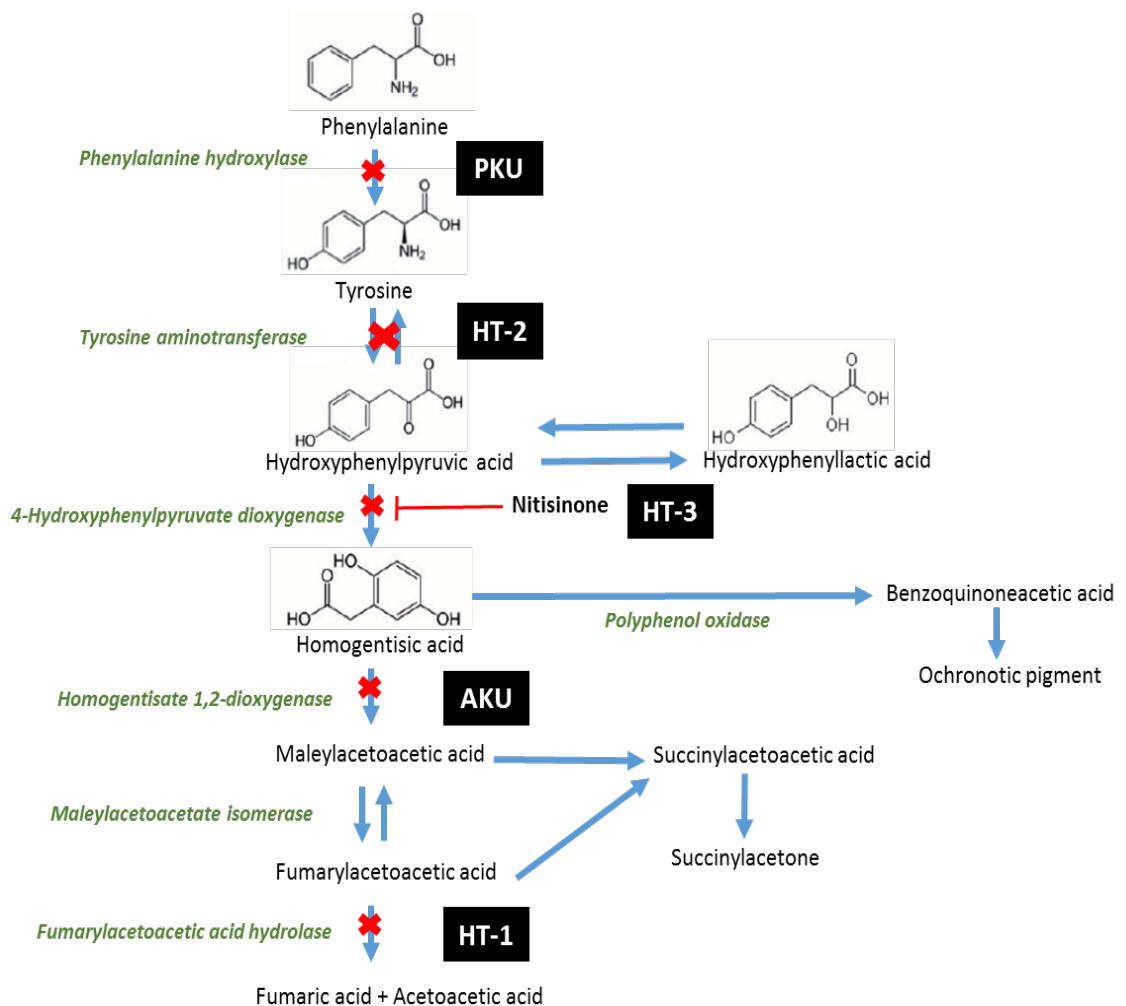


Figure 1.1 - Diagram detailing the enzyme defect in AKU and formation of ochronotic pigment. Other conditions of the tyrosine pathway are also included: phenylketonuria (PKU) and hereditary tyrosinemia type 1, 2 and 3 (HT-1, HT-2, HT-3).

1.1.1 History

Sir A E Garrod notably described the “chemical individuality”, congenital nature and familial prevalence of AKU in a series of papers published between 1899-1907 [1-5]. He later presented the condition as one of the first inborn errors of metabolism during his Croonian lecture series in 1908 [6]. Here, he described how the condition followed the laws of Mendelian inheritance, by observing how children of unaffected parents could suffer from the condition and that incidences of AKU were higher in the offspring of consanguineous marriages. He also reported evidence in relation to a defective gene in AKU and made links to how dietary intake of tyrosine affected the amount of HGA excreted in individuals with AKU [4]. Neubauer and colleagues aided with this understanding by mapping the tyrosine-degradation pathway a year later. They discovered that oral administration of phenylalanine or tyrosine to AKU patients resulted in urinary excretion of large quantities of HGA, concluding it must be an intermediary metabolite of the two [7]. Preceding Garrod’s lectures, several other cases of Alkaptonuria are described in the literature with the earliest known case found in the Egyptian mummy, Harwa, dating back to 1500 BC [8, 9]. The term “alcapton” was devised in 1859 by Boedeker meaning “to greedily swallow alkali” when he referred to a reducing compound present in a patient’s urine with an affinity for alkali [10]. The term ochronosis was devised by Rudolph Virchow in 1866, when he observed that upon microscopic inspection, the macroscopic blue-black pigmentation in the connective tissues of an elderly male post-mortem were actually yellow ochre coloured [11]. Alcapton was later isolated and named homogentisic acid (HGA) in 1891 by Wolkow and Baumann. [12]. Between 1947-1956, Siřaj and colleagues significantly contributed to the knowledge of AKU by collecting a set of 102 patients and detailing the clinical manifestations and development of the condition culminating in the first international publication [13-15]. In 1958, La Du and colleagues demonstrated the absence of HGD enzyme activity in liver homogenates from a liver biopsy extracted during abdominal surgery of a 57 year old, male AKU patient. This represented biochemical proof that the mutation in AKU is associated with a single enzyme arising from a defective gene [16, 17]. This gene was localised and mapped to chromosome 3q2 by Pollak and colleagues in 1993 [18].

1.1.2 Epidemiology

The incidence of AKU is estimated at 1 in 250,000 to 1 in 1,000,000 in most populations [19]. As of 2013, there were 950 reported cases of AKU across 40 countries worldwide [20]. There are incidences of countries with a higher prevalence of the condition such as Slovakia, India and Jordan where the incidence is as high as 1 in 19000 [21, 22]. This is predominantly due to the founder effect, where there is establishment of a new population by a small number of original founders resulting from migration. Higher numbers of consanguineous marriage taking place within these regions has led to a loss of genetic variation and higher incidences of the condition [23].

1.1.3 Pathophysiology and diagnosis

Phenylalanine and tyrosine are obtained through diet and endogenous protein turnover for the production of hormones, melanin and synthesis of new proteins within the body. AKU is a disorder of phenylalanine and tyrosine catabolism due to mutations within the homogentisate 1,2-dioxygenase (HGD) gene (HGNC:4892). The encoded HGD enzyme (EC 1.13.11.5) is responsible for converting HGA into the pathway intermediate, Maleylacetoacetic acid (MAA) with around 95% of dietary tyrosine metabolised in this way [24]. The genetic mutation within AKU results in a deficiency of the HGD enzyme, blocking the tyrosine catabolic pathway at the level of HGA. HGA is the hallmark metabolite of AKU and accounts for the clinical features synonymous with the condition - homogentisic aciduria, ochronosis and ochronotic osteoarthritis [24]. These clinical features present at different stages of life with homogentisic aciduria – urinary excretion of HGA, being present from birth. HGA readily oxidises into benzoquinone acetic acid (BQA) which forms discolouring melanin-like, pigment polymers. Daily urinary excretion of HGA occurs in gram quantities; this darkens upon standing and is usually the first sign towards diagnosis in children. Over a period of years, HGA accumulates and pigment polymers are deposited into cartilage and connective tissues in a process called ochronosis. This results in macroscopic blue/black discolouration of the affected tissues - the origin of the term “black bone disease”. Accumulation of ochronosis over time alters the mechanical properties of the connective tissues and cartilage causing them to become brittle. This leads to degradation of the articular surface, relative unloading and therefore absorption of the

subchondral bone, osteoarthritis and eventual collapse of the load-bearing joints in many patients. Accumulation and polymerisation of HGA cause the multisystem manifestations of AKU including severe early onset osteoarthropathy, osteopenia, renal, gall, prostatic and salivary gland calculi and renal damage [24-27]. Post-mortem analysis of the cardiovascular involvement in AKU has shown pigmentation of the heart valves that is associated with calcification and clinically significant aortic stenosis. Intense pigmentation has also been observed within the fibrolipid components of atherosclerotic plaques [103]. Obvious clinical features include darkening of the sclera and cartilage of the ears, black earwax and discolouration of the sweat and sweat glands. Joint involvement in AKU is associated with severe morbidity including chronic pain and decreased quality of life with orthopaedic surgical intervention often required by patients in their early thirties. Weight-bearing joints are primarily affected (vertebral column, hips and knees) although smaller synovial joints often become symptomatic between 30-40 years [44, 52]. Despite homogentisic aciduria from birth, symptoms including joint involvement are often absent in youth followed by progressive disease development from the third decade of life, explaining why AKU was often missed in the past and diagnosis occurred in adulthood for the majority of cases. Thankfully, this is not the case for the present day due to the internet and the work of the AKU society providing information to aid with early diagnosis. A rapid semi-quantitative reliable method of diagnosis of AKU is via pigment development of urine spots applied to alkalisated paper. Diagnosis is usually confirmed with analysis of urine and plasma HGA using high performance liquid chromatography and mass spectrometry [28-30].

1.1.4 HGD Gene

The HGD gene has a genomic location of 3q13.33 spanning 14 exons and containing 54,404 base pairs. The functional HGD gene encodes a 445 amino acid protein structure consisting of a hexamer formed by a dimer of trimers that metabolises HGA to MAA [31]. HGD gene expression in humans is apparent in multiple tissues of the body including the kidney, liver, prostate, small intestine and colon [33]. Laschi and colleagues reported expression in osteoarticular cells by testing human normal and AKU cells for HGD gene expression by reverse transcription-polymerase chain reaction (RT-PCR) and Western blotting. They revealed expression in chondrocytes, synoviocytes and osteoblasts [32]. The HGD enzyme is predominantly produced by hepatocytes in the liver and within the kidney [33]. The

defect of AKU is caused by recessive mutations of the HGD gene that directly or indirectly affect active site residues, subunit interactions and overall protein folding structure resulting in the total loss of function or reduced HGD enzyme production associated with AKU. There are currently 129 mutations in the HGD mutation database with over 60% of these being missense. These mutations are distributed throughout the HGD gene but a higher prevalence is found in exons 6, 8, 10, and 13 [34, 35]. No correlations between type of HGD mutation and the severity of the disorder have been observed.

1.1.5 Ochronosis

Ochronosis of tissues in AKU is thought to follow localised changes in composition and organisation of the extracellular matrix (ECM) prior to spreading to chondrocytes. Taylor and colleagues examined cartilage matrix components in samples obtained from hip and knee surgeries of AKU, OA and non-OA patients. They reported disorganisation and a reduction in extractable glycosaminoglycans as well as a very low cell turnover state in the ECM of cartilage from the AKU patients compared with OA and non-OA [36, 37]. Whether this disorganisation is a cause or consequence of pigmentation is currently unknown. By comparing samples obtained at various stages of the disease, ochronotic pigmentation is thought to initiate in the calcified zone of articular cartilage in both mice and humans with progression of pigmentation following a similar age related pattern. Further work by Taylor and colleagues described these progressive stages in the Hgd^{-/-} mouse [71]. Early stage pigmentation is present within the pericellular matrix of chondrocytes as early as 15 weeks. By 40 weeks, pigmentation has progressed to the cellular compartment in many of the chondrons of the articular calcified cartilage. At 65 weeks, advanced stage, extensive pigmentation is apparent throughout the femoral and tibial articular cartilage although some chondrocytes appear to be at an earlier stage of the pigmentation process even though they are very near to others with intense pigmentation, suggesting that the process is not uniform throughout. No end stage “blanket pigmentation” is observable in the mouse but is found in AKU patients. This disparity between species, despite a very similar biochemical status, is thought to be due to a number of factors including the shorter lifespan of the mouse, quadrupedal locomotion reducing load bearing and faster metabolic and cellular turnover of HGA adducted proteins prior to polymerisation. These factors may all contribute to the reduction in severity of the condition in the Hgd^{-/-} mouse [70, 71].

Investigation of pigmented cartilage specimens from AKU patients by Taylor and colleagues revealed a distinct pattern of binding of ochronotic pigment [38]. They reported a periodic banding pattern of ochronotic shards on individual collagen fibres, which suggested a possible preferential binding site for HGA and concluded other local factors must be involved in promoting or inhibiting the ochronotic pigmentation process along with HGA. In support of this, nuclear magnetic resonance (NMR) investigation into ochronotic cartilage by Chow also found a marked decrease in collagen molecular order and demonstrated that the ochronotic deposits altered the fibre structure by “invasion and crosslinking” [39]. Additional work by Taylor and colleagues [40] characterised the progression of pigmentation reporting that intact cartilage is resistant to pigmentation and focal changes to the calcified cartilage occur prior to initiation of pigment deposition. Pigmentation then spreads throughout the cartilage, altering its mechanical properties, with advanced stage ochronosis leading to aggressive resorption of calcified cartilage and loss of the subchondral plate. This group has suggested that the stiffening of the cartilage shields the underlying bone from normal mechanical stresses leading to bone resorption and final catastrophic collapse of the joint structure. The intermediate steps resulting in the production of ochronotic pigment polymers remains to be fully elucidated but several mechanisms or contributing factors have been suggested. In a separate paper, Taylor and colleagues suggested that tyrosinase might be implicated in the ochronosis that occurs in AKU [41]. They proposed that changes in the substrate specificity of tyrosinase, a polyphenol oxidase involved in the production of melanin from tyrosine, might be the missing link involved in the pigmentation process whereby HGA is polymerised under certain conditions instead of or in addition to tyrosine. Other evidence suggests damage is more likely attributable to the enzyme HGA polyphenol oxidase, and its product BQA binding and altering the structural integrity of the connective tissues. This leads to free radical production as a result of the oxidative process, which may incite further damage by promoting inflammation [42]. Decreased activity of lysyl hydroxylase, an enzyme important for pyridinoline cross-linking and stabilisation of cartilage has also been observed in patients with ochronosis [42, 43].

1.1.6 Current therapeutic options

Most management approaches for AKU are palliative and rely largely on analgesia and arthroplasty. Several therapeutic approaches have been tested with low degrees of clinical effectiveness. Future treatment options such as gene or enzyme replacement therapy would effectively cure AKU by replacing the defective HGD enzyme, ensuring HGA is broken down as in the healthy individual but unfortunately, these treatment options are not yet available.

1.1.6.1 Ascorbic acid

Ascorbic acid has antioxidant properties that were proposed could prevent the oxidative formation of BQA from HGA by inhibiting HGA polyphenol oxidase, in turn reducing ochronosis [44, 48]. This was shown to be achievable *in vitro* with the use of 10 mM ascorbic acid [45] but such concentrations are impossible to achieve *in vivo*. Administration of ascorbic acid to AKU patients was shown to reduce urinary BQA but no effect was observed for HGA excretion [46]. Furthermore, a study by Wolff *et al* demonstrated two fold increases in urinary excretion of HGA in ascorbic acid treated infants with AKU, presumably through its effect as a cofactor on the immature HPPD enzyme [47]. Alongside concerns about the effect of increased HGA on formation of renal oxalate stones, therapy with ascorbic acid for AKU is generally regarded as ineffective. Other antioxidants including phytic acid, taurine, ferulic acid and lipoic acid have been shown to have some efficacy in counteracting the production of BQA [49] but it is believed efforts are better spent in researching a therapy that blocks the formation of HGA itself.

1.1.6.2 Low protein diet

As HGA is a product of tyrosine catabolism, limiting dietary intake of phenylalanine and tyrosine is a seemingly logical therapy for AKU. A study by de Haas and colleagues [50] showed low protein diet to be effective for the reduction of HGA in patients under 12 but past this age, any effect was negligible. Behavioural influences were noted within the study presumed due to the severe dietary restriction. Although rational, restriction of dietary protein requires strict supervision and personal discipline, and poor compliance is often

encountered. Furthermore, reports of efficacy in treatment with a low protein diet remain to be proven in long-term studies [19, 24].

1.1.6.3 Nitisinone

Nitisinone or 2-(2-nitro-4-trifluoromethylbenzoyl)-1,3-cyclohexanedione (NTBC) was originally developed as one of the first synthetic triketone herbicides by Zeneca Agrochemicals [51]. Some plants and lichens produce natural triketones, such as production of leptospermone by the bottlebrush plant (*Callistemon citrinus*) [53]. Triketones suppress the growth of surrounding plants by selective inhibition of hydroxyphenylpyruvate dioxygenase (HPPD; EC 1.13.11.27) to prevent the production of HGA and synthesis of plastoquinone and ubiquinone. These function as transporters in the electron transport chain of photosynthesis and play crucial roles in plant growth. Electron exchange is impeded in the affected plant leading to reduced chlorophyll production, bleaching and suppression of growth [54]. Nitisinone is a related chemical entity, and has been developed, tested and licenced as an orally administered, HPPD blocking therapy that has already been widely used in another rare inborn error of metabolism, Hereditary Tyrosinaemia type 1 (HT-1) for over 20 years. Nitisinone is highly efficacious in terms of its metabolic effect for AKU as it decreases HGA to very low levels in the AKU mouse [71, 72] and humans [55, 56]. A recent human study investigating the effect of once daily nitisinone on 24-hour urinary HGA excretion in AKU patients observed a clear dose response relationship with 8mg per day reducing urinary HGA levels by 98.8% [55]. A second phase of the study is ongoing, involving 140 patients across Europe, and is due to finish in 2019. Half of the patients will receive nitisinone with the study aiming to compare the treated and untreated patients after four years to assess the effects of nitisinone via blood biochemical measurements and the AKUSSI, a combinatorial clinical assessment tool for clinical severity [165].

1.1.6.3.1 Nitisinone induced tyrosinemia

As part of its mechanism of action of inhibiting HPPD, the enzyme catalysing the formation of HGA, nitisinone also causes undesirable 'upstream' increases in circulating tyrosine.

Upon commencement of nitisinone treatment, a protein-restricted diet is advised to control the amount of circulating tyrosine provided from food although patient compliance varies. Previous studies of nitisinone use in AKU have shown serum tyrosine to increase from ~50mM baseline up to 1500mM in extreme cases (average 800mM), though these values are usually well tolerated [56]. In some treated patients, however, oculocutaneous adverse reactions relating to elevated circulating tyrosine may occur including conjunctivitis, corneal opacity, keratitis, photophobia and eye pain. Tyrosine has low solubility compared to most amino acids and readily crystallizes in tissues at high concentrations, deposition of crystals can occur in the cornea resulting in an inflammatory response. Two published reports of tyrosine keratopathy in AKU detail occurrence at low nitisinone doses – 1mg and 2mg daily with serum tyrosine measured at 941mM and ~550mM respectively. Both cases recovered fully upon cessation of treatment with one able to restart nitisinone with reduced dietary protein intake [57]. The other case was twice restarted on nitisinone but due to reoccurring ocular symptoms, treatment was permanently stopped. The study concluded that this patient showed predisposition to toxicity independent of peak plasma tyrosine levels (his was approximately 200mM below the average for the treated cohort) and that this contra-indication to treatment may occur in about 5% of AKU patients on nitisinone [58]. Although tyrosine is elevated in nitisinone treated AKU patients, Taylor and colleagues have shown this does not contribute to, or exacerbate, the process of ochronosis [59].

The tyrosinemia post-nitisinone resembles the metabolic status in genetic deficiency of HPPD; a condition termed hereditary tyrosinemia type 3 (HT-3) (Figure 1.1). Increased plasma tyrosine levels from birth have been proposed as a contributing factor to the impaired cognitive function and intermittent ataxia observed in some patients with HT-3. Nitisinone was originally developed as a herbicide, for this reason there is limited toxicology data available for its use as a HGA lowering therapy in AKU. Continuous and long-term monitoring of the efficacy, toxicity and safety post-nitisinone is currently ongoing as suggested in a best practice review by Ranganath and colleagues [24]. The issues relating to tyrosine toxicity as a result of HPPD inhibition must be considered when implementing treatment. Clearance of excess tyrosine is dependent on tyrosine aminotransferase (TAT) (EC 2.6.1.5). This is the first and rate-limiting enzyme within the catabolic pathway (Figure

1.1), the activity of which differs between species - rat: 1.7 ± 0.2 , mouse 7.8 ± 1.5 , human 7.17 ± 1.17 [60, 61]. The significantly lower hepatic TAT activity in the rat results in greater accumulation of tyrosine and is responsible for the higher incidence of toxicities observed within the species. Toxicity testing for mesotrione, another triketone herbicide with a shorter half-life than nitisinone, has shown a clear plasma tyrosine concentration threshold for ocular toxicity in rats (approximately 1000 μ mol/L) above which the incidence of corneal lesions, but also elevated liver and kidney weights and reduced bodyweight, increases significantly. [60, 62-64]. Ocular toxicity in the mouse occurred with mesotrione but at much higher doses, attributable to the higher TAT activity in this species enabling efficient tyrosine clearance. This also indicated that humans are likely less prone to ocular toxicity due to having similar TAT activity as mice.

Within AKU, symptoms accumulate over time due to high HGA levels. Commencement of nitisinone therapy from birth has the potential to reduce and maintain low HGA levels throughout life and thus prevent or substantially delay the pathological complications associated with the condition. A primary concern of such a course of treatment is that the elevated circulating tyrosine may cause intellectual impairment particularly if administered in childhood during brain development [110]. Similar concerns have been raised in HT1 patients treated with nitisinone in whom the treatment is lifesaving. Within this condition, mutations within the fumarylacetoacetate hydrolase gene (FAH; HGNC:3579) result in FAH enzyme deficiency (EC 3.7.1.2) and accumulation of the substrate fumarylacetoacetate and succinylacetone, large quantities of which are hepato- and nephrotoxic. Several studies examining the use of nitisinone in early treated children with HT1 have shown patients scoring lower than average in assessments of intelligence, cognitive development, motor function and speech, which the authors of the study have linked to the elevation of plasma tyrosine [112]. Significant elevation of tyrosine in the cerebrospinal fluid (CSF) and impaired serotonin synthesis has also been observed in HT1 patients receiving nitisinone treatment [65]. Serotonin is involved in regulation of mood, motivation and arousal; it could therefore influence learning and memory [66]. Toxicity studies evaluating inhibition of HPPD in neonatal animals have indicated no increased sensitivity to elevated tyrosine compared with adults [60]. The effect of nitisinone in utero has been evaluated using rabbits, rats and mice and shown reproductive toxicity but at doses 2.5-125 times higher than used in HT1

patients. The doses used in AKU patients are lower still. There is little information relating to nitisinone toxicity *in utero* for humans. Three cases of women with HT1 who received nitisinone throughout pregnancy are described in the literature with the children reported as suffering no adverse effects and displaying normal psychomotor development within the first years of life [67-69].

1.2 HGD-/- AKU MOUSE MODEL

The effects of early nitisinone therapy and high circulating tyrosine levels can be assessed using the AKU mouse model (Hgd^{-/-}). This model was developed at the Institut Pasteur in 1994 having been recognised during a chemical mutagenesis study using N-ethyl N-nitrosourea (ENU) intraperitoneal injection (250mg/kg). Confirmation of AKU in the mice was by observed darkening of the urine when pipetted onto filter paper soaked in 0.5M sodium hydroxide [73]. The aku gene mutation, later mapped to murine chromosome 16, is a missense mutation at intron 12 (GTAAGT to GAAAGT) causing the complete deletion of exon 12. This leads to a frame-shift and premature stop codon in the fourth codon of exon 13 [74]. The resulting phenotype is analogous to one of the known mutations responsible for AKU in humans (D16Mit4 locus in the mouse, homologous to human 3q), producing a HGD deficient mouse with similar blood chemistry to human AKU and urine containing HGA that blackens upon oxidation. The AKU mouse model is a vital tool for testing potential therapies including nitisinone and any possible developmental neurotoxicity that could result from therapy prior to use in children.

Taylor and colleagues first observed ochronosis within the AKU Hgd^{+/-} FAH^{-/-} mouse (a mouse that can model either HT-1 or AKU depending on selection conditions) [71]. They described macroscopic ochronotic renal nodules and microscopic pigmentation throughout the kidneys. Various stages of ochronotic pigmentation were also observed at the subchondral junction of the distal femur at 13 months of age. Further work by Preston and colleagues [70] described pigmentation of the articular cartilage apparent as early as 15 weeks that steadily increased with age. Commencement of nitisinone therapy resulted in a reduction of plasma HGA throughout the mouse' lifetime and completely prevented further accumulation of pigment at a dose of 4mg/L. Previous studies in Hgd^{-/-} mice within our lab

have used 4mg/L nitisinone as this was the dose originally determined by the Grompe lab that allowed the FAH^{-/-} HT-1 mouse model to survive [75]. This FAH^{-/-} model was the precursor strain from which the Hgd^{-/-} mouse used within this thesis was derived. Previous Hgd^{-/-} mouse work assessing the nitisinone dose response has included a mid-life study carried out by Keenan and colleagues [72] in which 54-week-old mice were treated with an ad libitum supply of water containing doses between 0.125-4mg/L of nitisinone for 13 days. Plasma HGA concentrations were highly variable in AKU mice but HGA responded in a dose-dependent manner to nitisinone treatment. Higher concentrations of nitisinone resulted in greater suppression of plasma HGA and removal of nitisinone after 13 days resulted in plasma HGA levels returning to pre-treatment levels. Studies have shown progressive pigmentation of chondrocytes in the mouse model but no severe osteoarthropathy along with few overt effects on welfare [70-72].

1.3 BEHAVIOURAL STUDIES

Animals are an invaluable tool in biomedical research for the understanding of disease and development of novel treatments. Animal models of cognitive impairment have long been used to determine the neural basis of cognitive functioning, helping to enhance our understanding of the networks involved in learning and memory. These have led to a greater understanding of neurodegenerative diseases such as Parkinson's and Alzheimer's as well as psychiatric disorders such as schizophrenia, depression and bipolar disorder [88, 173]. Behavioural pharmacology allows the efficacy and toxicity of a pharmaceutical intervention to be evaluated by observing the neurocognitive effect in the form of behavioural responses [76]. Mice are widely used in behavioural studies to approximate human responses as they share many of the same important brain functions— learning, memory, anxiety and circadian rhythm. Many factors can alter behaviour in mice including general health, background strain (differences in anxiety/aggression), age, sex and environment (diet, housing, noise). These factors must be considered and standardised when testing to ensure influence on behaviour is minimal [77]. Mice are nocturnal animals; several recent studies have shown light exerts widespread effects on physiology and behaviour and that testing during the light phase can induce pronounced behavioural inhibition and cognitive disruption. Testing during the inactive period may also be detrimental to the animal's welfare due to increased stress [78-81]. For this reason, a

reverse light cycle was implemented for all experiments within this thesis to ensure testing took place during the active phase and behaviour was less likely to be affected by perturbations of circadian rhythm. This ensured neurocognitive testing was more sensitive in detecting any treatment related effects. Diet, strain, housing and time of testing were standardised. As there have been concerns that the tyrosinemia in nitisinone treated HT-1 patients and high tyrosine from birth in HT-3 may contribute to the cognitive impairment and lower intelligence observed in some patients, a behavioural test of learning and memory - indicators of cognition, could examine these in nitisinone treated Hgd^{-/-} mice. It is important to evaluate the effects of nitisinone related tyrosinemia in an AKU murine phenotype prior to use in children to ensure the elevated tyrosine is not neurotoxic to the developing brain.

1.3.1 Morris Water Maze

The Morris water maze (MWM) is a widely accepted behavioural task for assessing hippocampal dependent learning and retrieval of spatial memory in rodents. Mice or rats swim within a pool, first to measure their ability to learn the position of a submerged platform, and then to measure their ability to recall the platforms position after a period of time. Richard Morris originally developed the MWM in 1981 at the University of St Andrews to test spatial localisation in the rat and to investigate the controversies surrounding the neural basis of spatial learning and working memory (82, 83). The MWM protocol can be adapted for many neurobehavioural applications including validation of rodent disease models and evaluation of drug treatments and the related effects on cognition, learning and memory [84]. Advantages of the MWM include insensitivity to variances in bodyweight, absence of non-performers (close to 100% rodents will perform swimming tasks) and minimal training compared to other behavioural tasks [86]. The motivation to escape in the MWM is also uniform between animals, which is not the case for other behavioural tasks. Submersion in water tends to be constant at motivating escape for all test subjects. In behavioural tasks containing food as a stimulus on the other hand, motivation can differ depending on differences in appetite between animals. During the MWM task, the use of external visual cues aids the rodent in determining the location of a submerged platform from varying starting positions within a circular pool. The rodent cannot see the platform as the water is opaque via the addition of non-toxic tempera paint.

Alternatively, a black pool is used with a clear plastic platform, as within this thesis. An additional advantage of a water-based task is that rodents cannot rely on odour trails from previous test subjects as an escape cue. Within the MWM, the use of external navigatory cues allows for the allocentric processing of the hippocampus and entorhinal cortex to be tested. Allocentric navigation is object centred, in that the use of external cues and their location relative to one another enables the location of another object or place to be determined [85]. For example, perception of a landmark such as a tall monument in the distance, provides relational information about one's own location compared to other landmarks and can be used as an aid for navigation.

The place cells of the hippocampus are considered to play a primary role in acquisition and retrieval of spatial information as well as the consolidation of spatial memory. These place cells form an internal spatial map that continuously updates as an organism moves to allow awareness of its location within an environment [86]. Communication between hippocampal place cells and other place cells in the entorhinal cortex forms a hippocampal–entorhinal circuit with the entorhinal cortex also containing grid cells used to map larger spaces [86, 92]. Lesions or damage within these regions has been shown to have a detrimental effect on performance within the MWM. Riedel and colleagues reported serious impairment of MWM performance in rats who had inactivated hippocampal networks using AMPA receptor antagonists. These transmembrane glutamate receptors mediate fast synaptic transmission within the hippocampus [90]. Furthermore, animals with damage to other areas of the brain including the basal forebrain, striatum and cerebellum all exhibit deficits within the MWM, suggesting navigation is dependent on the coordinated action of numerous brain regions, which together contribute to a functional neuronal network [84]. Activation of dopaminergic receptors, specifically D1R and D5R of the prefrontal cortex, striatum and hippocampus has also been shown to be necessary for normal spatial information processing. Sariñanaa *et al* used *in situ* hybridisation probes to show that forebrain D5R activation plays a unique role in spatial learning and memory in conjunction with D1R activation. Interestingly, their data also suggested that prefrontal cortical and striatal, but not hippocampal D1R activation was essential for this process [93].

Performance and analysis of the MWM test is automated by tracking and analysis software which measures the position of the mouse continuously and calculates parameters such as path latency, path length and swim speed. A progressive reduction of these parameters during testing indicates spatial learning of the platform location [86]. The task involves a number of consecutive days of training followed by a probe test on the final day to assess the consolidation and retrieval of memory. The probe is not only an important assessment of the learning and acquisition of memory that has taken place over the previous days of testing, but also a test of long term memory consolidation. The MWM is an aversively motivated behavioural task and therefore stress is a continuous factor to consider when analysing results. Stress is known to influence cognitive function and has been shown to affect acquisition and retention of memory within the MWM. De Quervain and colleagues reported impaired probe trail performance in rats after they had received a foot shock and concluded that this was due to increased plasma corticosterone levels [89]. For this reason, supplementary stress must be actively minimised during testing. Within this thesis, this was achieved by following proven stress reducing handling techniques and by allowing adequate prior acclimatisation to the testing environment. This is detailed further within the methods section in chapter 2. For the Hgd^{-/-} mouse and in the context of this thesis, the MWM has proved to be a valuable tool to assess whether elevation of tyrosine by nitisinone therapy has an effect on spatio-temporal awareness, place learning and memory. These studies therefore address concerns regarding the potential for neurotoxicity of tyrosine in the hereditary tyrosinemias, including nitisinone treated HT-1 patients.

1.4 MOTOR FUNCTION ASSESSMENT

Motor function assessment is the one of the most accessible domains of mouse behavioural science and forms an important part of the evaluation of animal behaviour. Assays for grip strength, motor coordination, balance, swimming speed and gait analysis are all widely used to assess motor function in various mouse models [94-95]. The type of assessment differs depending on whether the purpose is to monitor a treatment or to analyse a phenotype associated with a particular genetic mutation. As different tests assess different aspects of motor performance, it is often not sufficient to run a single test, therefore a range of tests are simultaneously required to ensure comprehensive evaluation and identification of subtle changes. Behavioural experiments, such as the MWM, measure

motor responses to sensory information e.g. processing visual information (3D visual cues) to induce a motor response (swimming to a submerged platform), it is thus important to consider the effects of motor functioning to ensure the behavioural data is properly interpreted [95]. Along with spatial learning, coordinated limb use during voluntary locomotion can also be assessed when mice are swimming in the MWM. Swimming has been shown to be a sensitive test of motor coordination in wild type and rodent models of disease [174-176]. Alongside motor assessment, a functional observational battery can be carried out to further detect any obvious behavioural effects of treatment. This is a neurobehavioral tool consisting of a series of observations that can be made while mice are in their home cage, with sufficient frequency to ensure detection of any behavioural or neurological abnormalities [177]. Behaviour and appearance of the animal are observed to look for any indications of neurotoxicity (in this case, as a result of nitisinone therapy or elevated tyrosine levels). Signs of neurotoxicity include convulsions, tremors, increased levels of lacrimation or salivation, piloerection, diarrhoea and increased vocalisation.

1.4.1 Rota-rod

The Rota-rod is a commonly used test of motor coordination and balance in the mouse, originally developed by a Dunham and Miya in 1957 and specifically designed to measure neurological deficits in rodents [97]. It has since been fully automated and is now one of the most popular tests of motor function owing to its ease of use and sensitivity. During the Rota-rod test, mice are placed on a horizontal, rotating rod arranged at a small distance from floor level, low enough for a fall to be innocuous to test subjects but high enough to induce the mouse's natural avoidance to fall. The mice must walk forwards to remain upright and maintain their balance to stay on the rotating rod, which continuously accelerates at a speed of 4-40rpm over 300 seconds. When the mouse is unable to continue, it falls onto a magnet trip plate, which records the latency to fall and speed of rotation at the time of fall. Mice with abnormalities affecting coordination or balance will tend to exhibit lower latencies to fall. Wang and colleagues showed mice with surgical destabilisation of the medial meniscus, for example, a commonly used model of OA, had statistically significantly lower latency times to fall compared to age matched naïve mice at 8 and 16 weeks after surgery [98]. Mouse models of Parkinson's disease also affect performance on the Rota-rod. Within the MTPT model, a Parkinson's phenotype is induced

via damage to the nigrostriatal dopaminergic system by MTPT injection. This has been shown to lead to reduced Rota-rod latencies both short and long term [178]. Interestingly, a recent paper by Giraldo *et al* that employed a genetic (α -synuclein) Parkinson's mouse model, reported abnormal locomotor behaviour but significantly increased latencies on the Rota-rod compared to control mice [179]. The authors suggested that the longer latencies to fall could be due to the mice exhibiting reduced anxiety levels due to elevated extracellular dopamine in the striatum produced by dysfunctional striatum-basal ganglia circuits. Increased levels of dopamine occurs in the early stages of Parkinson's disease, which can lead to increased general activity and repetitive behaviours [179]. The Rota-rod will enable assessment of coordination and balance within nitisinone treated and control Hgd^{-/-} and WT mice. The elevation of tyrosine post-nitisinone resembles the metabolic status in HT-3 where HPPD is also inhibited and occasional loss of balance and ataxia have been reported. It is therefore important to examine the effect of elevated tyrosine in nitisinone treated mice to investigate if this is the cause of the motor dysfunction observed in HT-3.

1.4.2 Inverted grid suspension test

The inverted grid suspension test (IGST) is a widely used, non-invasive general measure of grip strength originally devised by Kondziela in 1964 [180]. The test measures the ability of the mouse to remain clinging to an inverted wire mesh grid, suspended a small distance above a soft surface during which the latency to fall is measured. The test assesses the combined grip strength of both fore and hind limbs. Grip strength tests are highly specific in that they attempt to measure a single, well-defined aspect of behaviour, they are therefore combined with other motor function tests, in this case the Rota-rod, swimming within the MWM and gait analysis. Most healthy mice will easily reach the maximum grip latency time. The IGST has been used in mice to measure tolerance to drugs such as ethanol (which induces myorelaxation). The test has also been used to assess gross strength and disease progression in mouse models of muscular dystrophy and in mice with cerebellar dysfunction [95, 181].

1.4.3 Catwalk XT gait analysis

The CatWalk XT platform is a computer-assisted automated quantitative gait analysis system that allows simultaneous quantification of a large number of both static and dynamic gait parameters during voluntary walking. Briefly, the apparatus consists of an enclosed walkway on a glass plate that is traversed by a mouse from one side to the other. Green light enters at the long edge of the glass plate and is completely internally reflected. Light is able to escape only at those areas where the animal's paws make contact with the glass plate; as a result, the light is scattered which results in illumination of the exact area of contact. The image is captured by the camera and stored on a computer for analysis. The Catwalk platform has been used to measure numerous disease models leading to gait abnormality in rodents. These have included spinal cord injury, Parkinson's disease, cerebellar ataxia and osteoarthritis [122, 131]. The platform has been shown to be capable of detecting very subtle alterations in gait as well as minor changes in neurological function [183]. In the context of AKU, ochronosis has been shown to pathologically alter gait in humans [96] but the effect of ochronosis on gait within the Hgd^{-/-} mouse model is currently unknown. The Catwalk XT gait analysis platform will therefore be used to investigate whether any significant differences in gait are present between Hgd^{-/-} and WT mice prior to treatment with nitisinone.

2. Materials and Methods

2.1 ETHICAL APPROVAL

2.1.1 Procedures

All procedures within this thesis were performed in accordance with the Animals Scientific Procedures Act (1986) and licensed by the United Kingdom Home Office under a project license granted to Professor Jonathan Jarvis (PPL 40/3743) and a personal license granted to Róisín Lewis (PIL I8B47F4AC).

2.2 MICE

2.2.1 Breeding

Four Hgd^{-/-} breeding pairs on a BALB/c.129/sv background were obtained from the University of Liverpool colony. This colony was originally established from breeders obtained from Dr. X Montagutelli (Pasteur Institute, France). Control wild type (WT) mice on a BALB/cAnNCrl background were purchased from Charles River laboratories (UK).

2.2.2 Mouse husbandry

Mice were bred, housed and maintained within the Liverpool John Moores University Life Sciences Support Unit in accordance with Home Office UK guidelines. Mice were maintained on an ad libitum supply of vegetal diet A30RMB (SAFE, Augy, France) and drinking water. A reverse light cycle (16-hour light/8-hour dark) was introduced to ensure behavioural testing took place during the active phase.

2.2.3 Genotyping

Genotyping was carried out at the University of Liverpool prior to obtaining the Hgd^{-/-} breeding pairs. Genomic DNA was extracted from tail tips using DNeasy Blood and Tissue kits (Qiagen, UK), and the Hgd gene typed as previously described [119] with slight modifications. Primer sequences were:

- forward primer 5'-CATTTTCACCGTGCTGACTG-3'
- reverse primer 5'-TTTAGTCGCTGCATCACCTG-3'

A 25µl PCR reaction mix contained 12.5µl of HotStarTaq Mastermix (Qiagen, UK), 1µl of each 100mM primer stock, 2µl of DNA sample and 8.5µl of water. PCR conditions were: 15min at 95°C + 30 cycles (30s at 94°C, 30s at 52°C, 1min at 72°C) + 7min at 72°C. A 1.5µl aliquot of product was digested at 37°C with 0.3µl of HpyCH4III, 1.5µl of New England BioLabs Buffer 4 and 11.7µl of water, for at least 2hrs. Samples were electrophoresed for 30min at 200V on a 3% agarose gel containing SybrSafe (Invitrogen, UK). Wild type samples produced 170bp and 120bp digest bands, and mutant samples a nondigested 290bp band. Stability of the mutation and the effectiveness of nitisinone were continuously monitored by stability of urinary and plasma HGA in treated and untreated AKU mice. No signs of reversion of the mutation have been observed in five years of breeding of the homozygous colony within University of Liverpool/Liverpool John Moores University.

2.2.4 Treatment

2.2.4.1 Nitisinone

Nitisinone powder was obtained as a personal gift from Dr Edward Lock from original development batches supplied for research. Purity was confirmed by mass spectrometry analysis performed by the Department of Clinical Biochemistry and Metabolic Medicine at the Royal Liverpool University Hospital (RLUH).

2.2.4.1.1 Preparation of nitisinone stock solution

3.04M Nitisinone

75mM NaHCO₃

To prepare 200ml:

- 3g NaHCO₃ to 30ml RNAase free water (Sigma, UK)
- Swirled and placed in oven at 55°C
- Once dissolved 200mg NTBC added, returned to oven
- Once dissolved 170ml water added to make a 1mg/ml stock solution
- 1ml aliquots into eppendorfs and frozen at -20°C

These 1ml stock solutions were then ready to add to 250ml water bottles to produce 4mg/L concentrations when required and facilitated simple further dilution to produce additional doses.

2.2.4.1.2 Nitisinone - Morris water maze & motor function testing

Two cohorts (1 WT, 1 Hgd^{-/-}) of 12 female BALB/c mice were provided with an ad libitum supply of drinking water containing 4mg/L nitisinone. A further two cohorts (1 WT, 1 Hgd^{-/-}) of 12 female BALB/c mice acted as controls with no nitisinone treatment. All mice were aged between 12-24 weeks upon commencing treatment. A different set of mice were used to assess gait on the Catwalk XT platform. These consisted of two cohorts (WT n=8, Hgd^{-/-} n=12) of male BALB/c mice and two cohorts (WT n=10, Hgd^{-/-} n=7) of female BALB/c mice.

2.2.4.1.3 Nitisinone - Long-term dose response study

Four cohorts of seven male BALB/c Hgd^{-/-} mice were administered nitisinone straight from weaning (aged 3 weeks) for a period of forty weeks. Cohorts were group housed and provided with an ad libitum supply of drinking water containing either 2mg/L, 0.5mg/L, 0.125mg/L or 0mg (control) of nitisinone.

2.2.4.1.4 Nitisinone - Arteriovenous metabolome study

Twelve male BALB/c Hgd^{-/-} mice were provided with an ad libitum supply of drinking water containing 4mg/L nitisinone for one week. Nine male BALB/c Hgd^{-/-} mice acted as control and received no nitisinone treatment. All mice were aged between 18-36 weeks upon commencing treatment.

Mouse ID	Genotype	Sex	Age (weeks)	Experiment	Treatment cohort
CHgd 100.1	Hgd -/-	F	23.8	MWM/Motor function	0mg Control
CHgd 100.2	Hgd -/-	F	23.8	MWM/Motor function	0mg Control
CHgd 105.1	Hgd -/-	F	21.3	MWM/Motor function	0mg Control
CHgd 105.2	Hgd -/-	F	21.3	MWM/Motor function	0mg Control
CHgd 105.3	Hgd -/-	F	21.3	MWM/Motor function	0mg Control
CHgdJ 2.1	Hgd -/-	F	22.0	MWM/Motor function	0mg Control
CHgdJ 5.1	Hgd -/-	F	20.7	MWM/Motor function	0mg Control
CHgdJ 5.3	Hgd -/-	F	20.7	MWM/Motor function	0mg Control
CHgdJ 11.1	Hgd -/-	F	14.9	MWM/Motor function	0mg Control
CHgdJ 11.2	Hgd -/-	F	14.9	MWM/Motor function	0mg Control
CHgdJ 12.1	Hgd -/-	F	13.3	MWM/Motor function	0mg Control
CHgdJ 15.1	Hgd -/-	F	12.3	MWM/Motor function	0mg Control
CHgd 100.3	Hgd -/-	F	24.6	MWM/Motor function	NTBC 4mg/L
CHgd 100.4	Hgd -/-	F	24.6	MWM/Motor function	NTBC 4mg/L
CHgd 106.1	Hgd -/-	F	21.3	MWM/Motor function	NTBC 4mg/L
CHgd 106.2	Hgd -/-	F	21.3	MWM/Motor function	NTBC 4mg/L
CHgd 106.3	Hgd -/-	F	21.3	MWM/Motor function	NTBC 4mg/L
CHgdJ 2.2	Hgd -/-	F	22.0	MWM/Motor function	NTBC 4mg/L
CHgdJ 5.2	Hgd -/-	F	20.7	MWM/Motor function	NTBC 4mg/L
CHgdJ 5.4	Hgd -/-	F	20.7	MWM/Motor function	NTBC 4mg/L
CHgdJ 9.5	Hgd -/-	F	15.7	MWM/Motor function	NTBC 4mg/L
CHgdJ 11.3	Hgd -/-	F	14.9	MWM/Motor function	NTBC 4mg/L
CHgdJ 11.4	Hgd -/-	F	15.9	MWM/Motor function	NTBC 4mg/L
CHgdJ 12.2	Hgd -/-	F	13.3	MWM/Motor function	NTBC 4mg/L
CHgdJ 13.1	Hgd -/-	M	3.0	LTDRS	NTBC 2mg/L
CHgdJ 13.2	Hgd -/-	M	3.0	LTDRS	NTBC 2mg/L
CHgdJ 13.3	Hgd -/-	M	3.0	LTDRS	NTBC 2mg/L
CHgdJ 13.4	Hgd -/-	M	3.0	LTDRS	NTBC 2mg/L
CHgdJ 13.5	Hgd -/-	M	3.0	LTDRS	NTBC 2mg/L
CHgdJ 13.6	Hgd -/-	M	3.0	LTDRS	NTBC 2mg/L
CHgdJ 13.7	Hgd -/-	M	3.0	LTDRS	NTBC 2mg/L
CHgdJ 22.1	Hgd -/-	M	3.0	LTDRS	NTBC 0.5mg/L
CHgdJ 24.1	Hgd -/-	M	3.0	LTDRS	NTBC 0.5mg/L
CHgdJ 24.2	Hgd -/-	M	3.0	LTDRS	NTBC 0.5mg/L
CHgdJ 26.1	Hgd -/-	M	3.0	LTDRS	NTBC 0.5mg/L
CHgdJ 26.2	Hgd -/-	M	3.0	LTDRS	NTBC 0.5mg/L
CHgdJ 26.3	Hgd -/-	M	3.0	LTDRS	NTBC 0.5mg/L
CHgdJ 26.4	Hgd -/-	M	3.0	LTDRS	NTBC 0.5mg/L
CHgdJ 29.1	Hgd -/-	M	3.0	LTDRS	NTBC 0.125mg/L
CHgdJ 29.2	Hgd -/-	M	3.0	LTDRS	NTBC 0.125mg/L
CHgdJ 29.3	Hgd -/-	M	3.0	LTDRS	NTBC 0.125mg/L
CHgdJ 29.3	Hgd -/-	M	3.0	LTDRS	NTBC 0.125mg/L
CHgdJ 29.5	Hgd -/-	M	3.0	LTDRS	NTBC 0.125mg/L

CHgdJ 29.6	Hgd -/-	M	3.0	LTDRS	NTBC 0.125mg/L
CHgdJ 29.7	Hgd -/-	M	3.0	LTDRS	NTBC 0.125mg/L
CHgdJ 30.1	Hgd -/-	M	3.0	LTDRS	0mg Control
CHgdJ 30.2	Hgd -/-	M	3.0	LTDRS	0mg Control
CHgdJ 30.3	Hgd -/-	M	3.0	LTDRS	0mg Control
CHgdJ 30.4	Hgd -/-	M	3.0	LTDRS	0mg Control
CHgdJ 30.5	Hgd -/-	M	3.0	LTDRS	0mg Control
CHgdJ 30.6	Hgd -/-	M	3.0	LTDRS	0mg Control
CHgdJ 30.7	Hgd -/-	M	3.0	LTDRS	0mg Control
CHgdJ 42.2	Hgd -/-	M	38.4	Catwalk XT	0mg Control
CHgdJ 42.3	Hgd -/-	M	38.4	Catwalk XT	0mg Control
CHgdJ 42.4	Hgd -/-	M	38.4	Catwalk XT	0mg Control
CHgdJ 47.1	Hgd -/-	M	31.9	Catwalk XT	0mg Control
CHgdJ 47.2	Hgd -/-	M	31.9	Catwalk XT	0mg Control
CHgdJ 47.3	Hgd -/-	M	32.2	Catwalk XT	0mg Control
CHgdJ 47.4	Hgd -/-	M	32.2	Catwalk XT	0mg Control
CHgdJ 47.5	Hgd -/-	M	32.2	Catwalk XT	0mg Control
CHgdJ 49.1	Hgd -/-	M	28.5	Catwalk XT	0mg Control
CHgdJ 49.2	Hgd -/-	M	28.5	Catwalk XT	0mg Control
CHgdJ 51.1	Hgd -/-	M	17.5	Catwalk XT	0mg Control
CHgdJ 51.2	Hgd -/-	M	17.5	Catwalk XT	0mg Control
CHgdJ 46.2	Hgd -/-	F	33.7	Catwalk XT	0mg Control
CHgdJ 46.3	Hgd -/-	F	33.7	Catwalk XT	0mg Control
CHgdJ 48.1	Hgd -/-	F	32.5	Catwalk XT	0mg Control
CHgdJ 48.2	Hgd -/-	F	32.5	Catwalk XT	0mg Control
CHgdJ 48.3	Hgd -/-	F	32.5	Catwalk XT	0mg Control
CHgdJ 50.1	Hgd -/-	F	25.9	Catwalk XT	0mg Control
CHgdJ 50.2	Hgd -/-	F	25.9	Catwalk XT	0mg Control
CHgdJ 38.1	Hgd -/-	M	36.0	AV metab study 1	NTBC 4mg/L
CHgdJ 38.2	Hgd -/-	M	36.0	AV metab study 1	NTBC 4mg/L
CHgdJ 38.3	Hgd -/-	M	36.0	AV metab study 1	NTBC 4mg/L
CHgdJ 38.4	Hgd -/-	M	36.0	AV metab study 1	NTBC 4mg/L
CHgdJ 38.5	Hgd -/-	M	36.0	AV metab study 1	NTBC 4mg/L
CHgdJ 41.1	Hgd -/-	M	23.1	AV metab study 1	0mg Control
CHgdJ 41.2	Hgd -/-	M	23.1	AV metab study 1	0mg Control
CHgdJ 41.3	Hgd -/-	M	23.1	AV metab study 1	0mg Control
CHgdJ 42.1	Hgd -/-	M	18.1	AV metab study 1	0mg Control
CHgdJ 43.3	Hgd -/-	M	24.6	AV metab study 2	0mg Control
CHgdJ 44.1	Hgd -/-	M	23.0	AV metab study 2	0mg Control
CHgdJ 44.2	Hgd -/-	M	28.9	AV metab study 3	NTBC 4mg/L
CHgdJ 44.3	Hgd -/-	M	28.9	AV metab study 3	NTBC 4mg/L
CHgdJ 46.1	Hgd -/-	M	25.4	AV metab study 3	NTBC 4mg/L
CHgdJ 59.1	Hgd -/-	M	18.6	AV metab study 4	0mg Control
CHgdJ 59.2	Hgd -/-	M	18.6	AV metab study 4	NTBC 4mg/L

CHgdJ 59.3	Hgd -/-	M	18.6	AV metab study 4	NTBC 4mg/L
CHgdJ 59.4	Hgd -/-	M	18.6	AV metab study 4	NTBC 4mg/L
CHgdJ 52.1	Hgd -/-	M	29.6	AV metab study 4	NTBC 4mg/L
CHgdJ 55.1	Hgd -/-	M	20.7	AV metab study 4	0mg Control
CHgdJ 55.2	Hgd -/-	M	20.7	AV metab study 4	0mg Control
WT BC/J 5.1	WT	F	13.1	MWM/Motor function	0mg Control
WT BC/J 5.2	WT	F	13.1	MWM/Motor function	0mg Control
WT BC/J 5.3	WT	F	13.1	MWM/Motor function	0mg Control
WT BC/J 5.4	WT	F	13.1	MWM/Motor function	0mg Control
WT BC/J 5.5	WT	F	13.1	MWM/Motor function	0mg Control
WT BC/J 8.1	WT	F	24.0	MWM/Motor function	0mg Control
WT BC/J 8.2	WT	F	24.0	MWM/Motor function	0mg Control
WT BC/J 10.1	WT	F	21.6	MWM/Motor function	0mg Control
WT BC/J 10.2	WT	F	21.6	MWM/Motor function	0mg Control
WT BC/J 10.3	WT	F	21.6	MWM/Motor function	0mg Control
WT BC/J 10.4	WT	F	21.6	MWM/Motor function	0mg Control
WT BC/J 10.5	WT	F	21.6	MWM/Motor function	0mg Control
WT BC/J 6.1	WT	F	13.1	MWM/Motor function	NTBC 4mg/L
WT BC/J 6.2	WT	F	13.1	MWM/Motor function	NTBC 4mg/L
WT BC/J 6.3	WT	F	13.1	MWM/Motor function	NTBC 4mg/L
WT BC/J 6.4	WT	F	13.1	MWM/Motor function	NTBC 4mg/L
WT BC/J 6.5	WT	F	13.1	MWM/Motor function	NTBC 4mg/L
WT BC/J 8.3	WT	F	24.0	MWM/Motor function	NTBC 4mg/L
WT BC/J 8.4	WT	F	24.0	MWM/Motor function	NTBC 4mg/L
WT BC/J 8.5	WT	F	24.0	MWM/Motor function	NTBC 4mg/L
WT BC/J 8.6	WT	F	24.0	MWM/Motor function	NTBC 4mg/L
WT BC/J 12.1	WT	F	18.6	MWM/Motor function	NTBC 4mg/L
WT BC/J 13.1	WT	F	18.4	MWM/Motor function	NTBC 4mg/L
WT BC/J 13.2	WT	F	18.4	MWM/Motor function	NTBC 4mg/L
WT BC/J 36.1	WT	F	44.0	Catwalk XT	0mg Control
WT BC/J 36.2	WT	F	44.0	Catwalk XT	0mg Control
WT BC/J 36.3	WT	F	44.0	Catwalk XT	0mg Control
WT BC/J 36.4	WT	F	44.0	Catwalk XT	0mg Control
WT BC/J 39.1	WT	F	41.1	Catwalk XT	0mg Control
WT BC/J 39.2	WT	F	41.1	Catwalk XT	0mg Control
WT BC/J 39.3	WT	F	41.1	Catwalk XT	0mg Control
WT BC/J 39.4	WT	F	41.1	Catwalk XT	0mg Control
WT BC/J 39.5	WT	F	41.1	Catwalk XT	0mg Control
WT BC/J 39.6	WT	F	41.1	Catwalk XT	0mg Control
WT BC/J 44.1	WT	M	17.3	Catwalk XT	0mg Control
WT BC/J 44.2	WT	M	17.3	Catwalk XT	0mg Control
WT BC/J 44.3	WT	M	17.3	Catwalk XT	0mg Control
WT BC/J 44.4	WT	M	17.6	Catwalk XT	0mg Control
WT BC/J 46.1	WT	M	12.6	Catwalk XT	0mg Control
WT BC/J 46.2	WT	M	12.6	Catwalk XT	0mg Control
WT BC/J 46.3	WT	M	12.6	Catwalk XT	0mg Control

WT BC/J 46.4	WT	M	12.6	Catwalk XT	0mg Control
--------------	----	---	------	------------	-------------

Table 2.1 – Details of individual BALB/c mice used within this thesis. Age in weeks indicates age at commencement of treatment. MWM/Motor function and Catwalk XT – chapter 3. Long-term dose response study (LTDRS) – Chapter 4. Arteriovenous metabolome studies (AV Metab Study 1-4) – Chapter 5.

2.3 PLASMA SAMPLING

2.3.1 Venous tail bleeds

To measure plasma metabolites mid-study, plasma samples were obtained from tail bleeds. Mice were warmed in an incubator (mediHEAT, Peco Services, UK) at 37°C for approximately 5 minutes to aid with vasodilation prior to sample collection. Mice were then eased into a Broome style rodent restrainer (Plas Labs™) to minimise distress and risk of injury. A shallow incision was made to one of the lateral caudal tail veins with a sterile scalpel blade and a blood sample collected. These were collected into microvette collection tubes (Sarstedt, CB 300) and stored at 4 °C prior to processing within 2 h, using an adaptation of the Bory method [29, 104]. Briefly, whole blood was centrifuged at 1500g for 10 min at 4°C and the plasma deproteinised by adding 5.8 M perchloric acid (Sigma, UK) equivalent to 10% of the plasma volume. Acidified supernatant was stored at -20°C. Volumes of blood taken were kept within Home Office limits. This is a maximum of 15% total blood volume within one month and a maximum of 10% total blood volume within any one bleed. We calculated our samples using a lower blood volume of 65ml/kg body weight and the minimum body weight within each study to ensure the blood removal was below the limits. Tail bleeds were approximately 50- 70 µl, giving 15µl acidified plasma.

2.3.2 Terminal bleeds

Immediately after culling, an incision was made within the left axilla and blood collected from the underlying brachial vessels into monovette collection tubes (Sarstedt, S-monovette® K3E). These were stored at 4°C prior to processing within 2 h, using the same method as detailed above.

2.3.3 Morris water maze and motor function assessment (chapter 3)

Tail bleed samples were collected after 2 weeks to measure metabolites and confirm efficacy of nitisinone treatment prior to commencing behavioural and motor function studies. Efficacy of nitisinone in treated Hgd^{-/-} and wild type mice was indicated by elevated tyrosine. Hgd^{-/-} treated mice would also show a reduction in plasma HGA.

2.3.4 Long-term dose response study (chapter 4)

Mid-term tail bleeds were collected at 20 weeks and terminal bleeds collected at 40 weeks.

2.3.5 Arteriovenous metabolome study (chapter 5)

Consecutive tail bleed samples were collected immediately followed by culling (pentoject/cervical dislocation) and terminal bleed sample collection.

2.3.6 Analysis of plasma metabolites

The concentrations of plasma tyrosine, HGA, phenylalanine, HPPA and HPLA were measured by liquid chromatography tandem mass spectrometry. All analyses were performed on an Agilent 6490 Triple Quadrupole mass spectrometer with Jet-Stream[®] electrospray ionisation (ESI-MS/MS) coupled with an Agilent 1290 infinity UHPLC pump and HTC autosampler. This method incorporates reverse-phase chromatographic separation on an Atlantis C18 column (100mmx3.0mm, 3 μ m). Initial conditions of 80:20 water:methanol with 0.1% formic acid (v/v) increased linearly to 10:90 over five minutes. Matrix-matched calibration standards and quality controls were utilised with appropriate isotopically labelled internal standards. Quantitation was achieved in multiple reaction mode (MRM) with two product ion transitions for both tyrosine (positive ionisation) and HGA (negative ionisation). Samples were prepared by dilution in a combined internal standard solution (final concentrations of 0.4 μ mol/L 13C6-HGA and 2 μ mol/L d2-tyrosine in 0.1% formic acid (v/v) in deionised water). All quantitation analyses were performed by the Department of Clinical Biochemistry and Metabolic Medicine at the Royal Liverpool University Hospital (RLUH). A detailed protocol of analysis is described by Hughes et al [28].

2.4 SCHEDULE 1 HUMANE CULLING METHODS

All mice were humanely killed using methods detailed under Schedule 1 of the Animals (Scientific Procedures) Act 1986 [181] with all persons carrying out the procedure having received prior training and deemed confident and competent in using the specified techniques.

2.4.1 Pentोजect (pentobarbitone) overdose

Mice were euthanised by lethal dose of Pentोजect (sodium pentobarbitone 20% w/v) administered intraperitoneally to minimise any distress. This led to rapid loss of consciousness and death by respiratory arrest within 3-5 minutes. Death was confirmed via cervical dislocation.

2.4.2 Cervical dislocation

Mice were manually euthanised by pressing a rod at the base of the skull and pulling the animal backwards to sever the spinal cord at the base of the brain resulting in rapid loss of consciousness and death. The use of this method was necessary within the arteriovenous metabolome study to ensure no pharmacological method of culling would affect blood metabolites.

2.5 HARVESTING OF THE TIBIO-FEMORAL JOINT

Once mice were confirmed dead, the skin was removed from the hind limbs exposing the full anatomy of the joint. The surround leg musculature was dissected away and the joint dissected out by cutting close to the femoral head. The tibia was then cut above the ankle to leave a complete tibio-femoral joint. The joint was rinsed in phosphate buffered saline (PBS) and fixed with 10% phosphate buffered formalin solution (PBFS) prior to decalcification and embedding.

2.6 HISTOLOGY

2.6.1 Reagents

Potassium ferricyanide, ferric chloride, and nuclear fast red (NFR) were purchased from VWR, UK. Ethylenediaminetetraacetic acid (EDTA), chromic potassium sulphate, bovine gelatine and DPX mounting medium were purchased from Sigma, UK. Premium frosted glass slides and 50mm cover slips were purchased from VWR, UK. Histological methods were followed as published in a paper by Keenan *et al* [72].

2.6.2 Tissue fixation

Carcasses of mice used in the behavioural and motor function studies (chapter 3) and long-term dose response study (chapter 4) were fixed to enable future analysis of tissues if necessary. Tissues harvested were immediately fixed in 10% phosphate buffered formalin solution (PBFS) at room temperature to prevent autolysis. PBFS was changed regularly when pH indicator showed acidosis to maintain fixation. The amount of fixative used was generally 15-20 times greater than the tissue volume.

2.6.2.1 Preparation of PBFS

10mM Sodium phosphate dibasic (Na_2HPO_4)

32mM Potassium phosphate (KH_2PO_4)

123mM Sodium chloride (NaCl)

3.7% (v/v) Formaldehyde

To prepare 2.5L:

- 250ml of Formaldehyde (37% w/v)
- 250ml of phosphate buffered solution (PBS) (10x)
- 2000ml distilled water
- pH adjusted to 7.2-7.4
- Few drops of phenol red (pH indicator, 0.01% in water) added and solution mixed. Phenol red is orange/pink at neutral pH, purple if alkaline and yellow when acidic.

2.6.3 Decalcification of mineralised tissue

Decalcification is the process of removing calcium from mineralised tissue. This was necessary to section and analyse the tibio-femoral joints from mice within the long-term dose response study (chapter 4). Decalcification was performed using 12% EDTA, a chelating agent that binds calcium.

2.6.3.1 Preparation of decalcifying solution

12% (w/v) EDTA

To prepare 2.5L:

- 300g of EDTA
- 2000ml d.H₂O
- Few drops of phenol red indicator added and solution mixed
- pH adjusted to 8 to dissolve EDTA (NaOH pellets)
- Once dissolved pH was adjusted to 7.2–7.4
- Solution was then made up to a final volume of 2500ml

Following fixation, mineralized tissues were placed into EDTA for an initial period of 24hrs. The EDTA solution was then changed and tissues left to decalcify for a further 6 days. Decalcification was complete when tissues were flexible and soft enough to bend.

2.6.4 Processing of tissue

Following decalcification, the tibio-femoral joints were removed from EDTA and washed several times with PBS. They were then processed, first through increasing grades of ethanol (70% (15mins), 90% (30mins), and 100% (x4) (1hr)) to dehydrate the tissue. Once dehydrated, tissues were cleared using two changes of xylene (45 minutes in each) before being passed through two changes of paraffin wax (1hr in each) to complete the processing. Processing was performed using a Leica TP1020 tissue processor (Leica, Germany).

2.6.5 Embedding of tissue

Following processing, the tibio-femoral joints were placed into heated metallic moulds, submerged in molten paraffin wax and embedded in the coronal plane to enable simultaneous evaluation of the medial and lateral surfaces as recommended by the Osteoarthritis Research Society International (OARSI) histopathology initiative [105]. A plastic chuck was placed on top of the mould to allow sectioning of the block. Blocks were cooled to solidify and then removed from their metallic mould.

2.6.6 Sectioning of tissue

Tissue blocks were cut to remove excess wax, and shaped to have a trapezoid cutting surface. Blocks were initially trimmed at 10µm until the tissue could be viewed through the block. Sections were then taken every 5µm before being mounted on subbed slides and placed in an incubator at 50°C overnight. Sections from the knee joints of all mice were taken every 5µm from posterior to anterior until the whole joint had been sectioned. Blocks were sectioned using a Leica RM2245 semi-automated microtome (Leica, Germany).

2.6.7 Subbing of slides

Microscope slides were subbed with a gelatine solution to help sections adhere to the slide.

2.6.7.1 Preparation of subbing solution

0.1% (w/v) Bovine gelatine

0.35mM Chromic potassium sulphate

To prepare 400ml:

- 400ml distilled water
- 0.8g type B bovine gelatine
- Gelatine dissolved in distilled water with heat – not exceeding 50°C
- 0.08g chromic potassium sulphate added when gelatine dissolved

2.6.7.2 Subbing procedure

- Slides rinsed in 100% ethanol for 30 seconds
- Left to dry for 5 minutes
- Slides then immersed in subbing solution for 30 seconds
- Dried overnight at room temperature – cover slides to prevent dust building up

2.6.8 Tissue staining

2.6.8.1 Schmorl's stain

Schmorl's stain demonstrates reducing substances in paraffin sections such as melanin, which reduce ferricyanide to ferrocyanide, producing varying shades of blue with a positive result. Melanin and ochronotic pigment are proposed to have similar structures and are both derived from the tyrosine catabolic pathway. By modifying the procedure to include a longer incubation time, Schmorl's stain has been shown to identify the presence of ochronotic pigmentation in murine and human tissues [106].

2.6.8.1.1 Preparation of Schmorl's incubating solution

46mM Ferric chloride

3mM Potassium ferricyanide

To prepare 50ml:

- 0.5g Ferric chloride in 50ml d.H₂O (1%)
- 0.1g Potassium ferricyanide in 10ml d.H₂O (1%)
- Add 37.5ml ferric chloride solution to 5ml potassium ferricyanide solution.
- Make up to 50ml with d.H₂O (7.5ml)

This solution was used fresh and prepared immediately before use.

2.6.8.1.2 Schmorl's staining procedure

- Slides were deparaffinised in two changes of xylene - 5 minutes in each
- Hydrated through ethanol (100%, 100%, 70%, 70% - 2 minutes in each) to water
- Immersed in Schmorl's stain for up to 15 minutes
- Washed well in running cold water to remove any residual ferricyanide
- Treated with 1% acetic acid for 5 minutes to prevent over-staining
- Counterstained in nuclear fast red (NFR) for 3-5 minutes
- Washed in running cold water to remove any residual NFR
- Dehydrated through ethanol (70%, 70%, 100%, 100% - 2 minutes in each)
- Cleared in two changes of xylene - 3 minutes in each
- Mounted with DPX and left to dry

2.7 HISTOLOGICAL ANALYSIS

2.7.1 Tibio-femoral joints from long-term dose response study (chapter 4)

The first ten sections that encompassed both the medial and lateral tibial plateaus and femoral condyles were selected as representative for each mouse, stained and analysed via light microscopy.

2.7.2 Light microscopy

Tibio-femoral joint pigmentation quantification was carried out using a Nikon Eclipse Ci microscope fitted with a Ds-Fi2 camera. A Zeiss Axio Imager 2 was used for acquiring panoramic images. NIS Br elements was used for image analysis.

2.7.3 Quantification of ochronotic pigmentation

From the stained sections, the most complete section that included the entire tibio-femoral joint was selected for quantification. The total number of pigmented chondrons present in the articular calcified cartilage and entheses of the femoral condyles, tibial plateaus and intercondylar regions was quantified (Fig. 2.1). Two sections from each cohort were quantified by a second blinded observer to assess inter-observer reliability. As previously

demonstrated by Preston et al [70], pigmentation can be classified via staging - early stage, peri-pigmentation of the peri-cellular matrix forming a halo around chondrocytes and later stage, cellular pigmentation with advancement into the cellular compartment and dark staining of the nuclei of the chondrocytes (Fig. 2.2). In consideration of this, two counts for each section was carried out. The first included just later stage cellular pigmentation and the second included peri-pigmented and cellular pigmented chondrocytes combined.

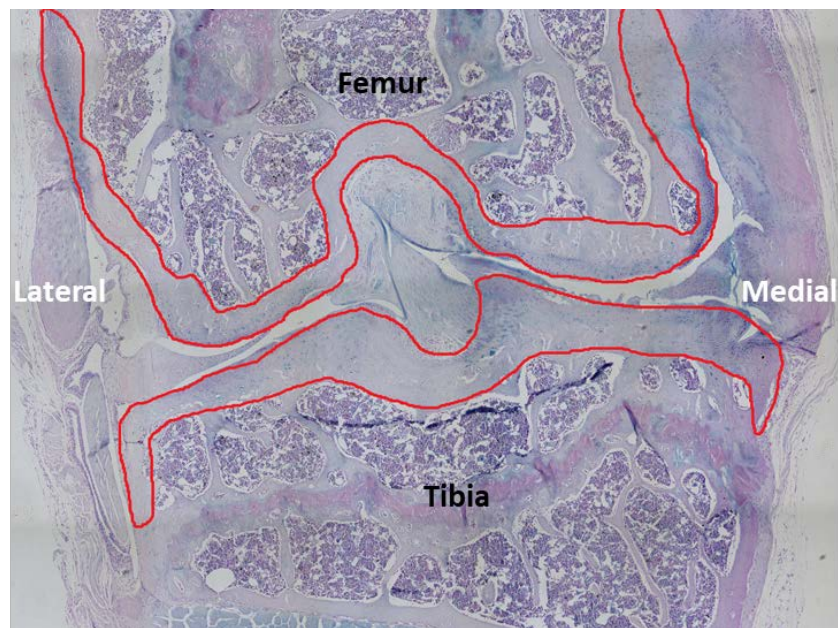


Figure 2.1 - Area of ochronotic pigmentation quantification in the mouse tibio-femoral joint. The area inside the red line was quantified encompassing the articular calcified cartilage of the medial and lateral tibial plateaus, femoral condyles and entheses.

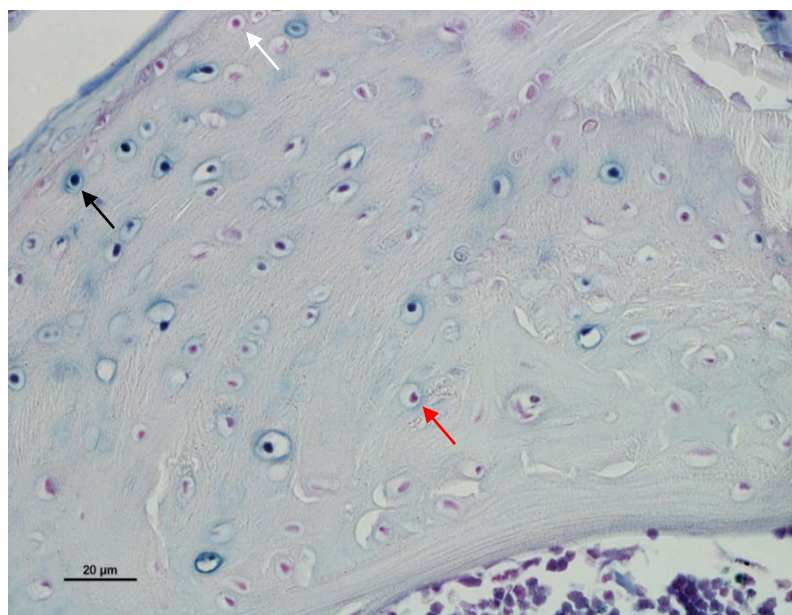


Figure 2.2 - Classification of pigmentation for quantification of pigmented chondrons in the BALB/c Hgd^{-/-} tibio-femoral joint. White arrow: unpigmented chondrocyte. Red arrow: Peri-pigmentation in the peri-cellular matrix forming a halo around chondrocytes of the articular calcified cartilage. Black arrow: Cellular pigmentation showing advancement into the cellular compartment and dark staining of the nuclei. Bar:20um. Stained with Schmorls.

2.8 REDUCTION OF MOUSE ANXIETY

A visit to the University of Liverpool's Leahurst animal campus was arranged to speak with Professor Jane Hurst, Head of Mammalian Behaviour & Evolution at the Institute of Integrative Biology. Professor Hurst is widely regarded in the field of animal behaviour and has published several methods to aid in reduction of handling related anxiety in mice [106-108]. Her methods include the use of handling tubes and cupping methods instead of the usual laboratory method of tail handling which can be aversive and impair reliability of behavioural test results. The use of handling tubes and cupping was implemented for all mice within this thesis. Prior to testing, mice were handled daily for 2 weeks to reduce anxiety during testing. This was carried out within the testing room to ensure they also became used to being transported from their home room. For each day of behavioural, motor function and gait analysis testing, mice were transported to the testing room and

allowed to acclimatise to their surroundings for 30 minutes prior to beginning trials. Lights were dimmed or switched off as testing took place during the mice's dark cycle (most active period). Noise was kept to a minimum and no other person was permitted to enter the room during testing to minimise aversive stimulus.

2.9 MOUSE IDENTIFICATION

Mice were both tail and ear marked to ensure easy recognition during testing. Tails were marked with non-toxic marker. Mice were submerged in water during Morris water maze trials so tail marking was repeated daily before beginning trials. Ears were also marked using an ear punch (Interfocus, UK) to ensure mice were distinguishable if tail marks had faded.

2.10 MORRIS WATER MAZE

2.10.1 Introduction

The Morris water maze (MWM) is a widely accepted behavioural task for assessing spatial learning and memory in rodents, originally developed by Richard Morris in 1981 at the University of St Andrews (82, 83). During the MWM task, the use of external visual cues aids the rodent in determining the location of a submerged platform from varying starting positions within a circular pool of water (Fig. 2.3, Fig 2.4). The use of external navigatory cues allows for the allocentric processing of the hippocampus and entorhinal cortex to be tested. The task involves a number of consecutive days of training followed by a probe test on the final day to assess the consolidation and retrieval of memory. Performance and analysis of the test is automated by tracking and analysis software which measures parameters such as path latency, path length and swim speed.

2.10.2 MWM equipment

MWM equipment was obtained from HVS image (Buckinghamshire, UK) unless otherwise stated and included:

- Tracking and analysis software (HVS image 2014 for Windows)
- Laptop with Microsoft Windows operating system (Toshiba, Japan)
- Large area high resolution camera with varifocal lens and ceiling mount
- Long-range wireless mouse
- Black polypropylene seamless pool, 150cm diameter, height 60cm
- Clear platform, diameter 10cm, height 29.5cm with stable 30x30cm base
- Curtains to mount around pool area to minimise additional spatial cues
- Water pump to empty pool (Karcher GP40, Amazon, UK)
- 200 watt thermostat water heater (Eheim, Germany)
- 3D high contrast visual cues to mount around pool during hidden trials – small plastic chair, large inflatable ball, large 3 gallon plastic bucket, 1m long cylindrical tube (Amazon, UK)
- Digital thermometer (Andrew James, Amazon, UK)
- Flexible PVC tubing to fill pool (Amazon, UK)
- Milton sterilising liquid (P&G, UK)
- Pool tester kit for the measurement of pH and Chlorine (OPC, UK)
- Red warming lamp (Ecoglow 20, Brinsea, UK)
- 4 x 50 watt floor lamps (GU10, ML Accessories Ltd, UK) to provide diffuse lighting and minimised reflections in pool.

2.10.3 Health and safety

Before beginning MWM trials, time was taken to ensure the equipment set up met health and safety standards. As several electrical devices (water heater, pump and floor lamps) were being used in an area with a large pool of water, steps had to be taken to minimise risk of injury to mice and users of the animal facility including fitting residual circuit breakers to all plugs and taping down all trip hazards with high contrast tape. The head of health and safety and estate management inspected the test area to ensure all precautionary measures had been taken and these departments were liaised with regularly. As the probe test of the Morris water maze experiment had to be performed on a

Saturday, out of hours access had to be authorised by the Dean and head of security services and further health and safety assessment completed.

2.10.4 Preparation of MWM pool

At the beginning of a test week, the pool was filled with tap water and a water temperature of 24-26°C reached. Mice are prone to stress from hypothermia therefore it was crucial this temperature was maintained throughout testing. Water temperature was maintained overnight via the use of a water heater with thermostat. Filling the pool took approximately one hour due to the large quantity of water required to reach a depth of 28 cm. A body of water at this temperature poses a risk of Legionella therefore Milton sterilising liquid was added and the pH and chlorination of the pool assessed daily to ensure a safe environment for mice and other users of the animal facility. The pool water was also cleaned of visible debris multiple times a day during testing and thoroughly cleaned with ethanol solution once emptied with a water pump on a weekly basis.

2.10.5 MWM testing procedure

2.10.5.1 General information

To enter the pool, each mouse was gently lifted and placed onto the arm of the experimenter to carry them to the pool. To begin a trial, the mouse was gently placed into the water immediately facing the perimeter (away from centre of pool) in the required starting position. The experimenter immediately started the tracking software by clicking the wireless mouse whilst quickly leaving the pool area to avoid becoming a spatial cue. Each mouse performed five trials per day during visible and hidden platform tasks and was allowed a maximal time of 90 seconds to locate the platform. Finding the platform was defined as staying on it for at least two seconds; mice that crossed the platform without stopping were left to swim. Mice that located the platform were left on the platform for 15 seconds before being retrieved. When mice did not locate the platform in the maximal time allowed, they were gently guided to it using a hand and allowed to independently climb onto it and spend 15 seconds on the platform before being retrieved - these mice were assigned a latency of 90 seconds. The starting time of the experiment was kept constant each day for all cohorts. Between individual trials, mice were given an inter-trial interval of

15 minutes and placed under a red warming lamp to minimise fatigue and risk of hypothermia.

2.10.5.2 Visible platform task (day 1)

During visible platform trials, a high contrast black and yellow striped flag was mounted onto the platform within the pool with the platform itself being 1.5cm higher than the water level. The visible platform task enabled the mouse to learn the task of finding and mounting the platform, associating it as the goal (escape route), whilst ensuring the mice had no visual or motor impairments that could affect the subsequent days of the experiment. During the visible platform task, the entry point remained the same whilst the platform position within the pool was varied for each of the five trials (Table 2.1).

2.10.5.3 Hidden platform task (day 2-5)

Before beginning hidden platform trials, 3D visual cues were mounted around each side of the pool to aid with spatial navigation. The striped flag was removed from the platform and the pool was filled with additional water to submerge the platform by 5-8 millimetres to ensure it was hidden. Hidden platform trials took place over four days with each mouse performing five trials per day. The platform location was fixed but the mouse's entry point was varied (Table 2.1). In total, each mouse performed twenty hidden platform trials over the four hidden platform testing days. Performance during training was measured by escape latency, swimming speed and path distance.

2.10.5.4 Probe test (day 6)

The probe test was completed around 20 hours after the final hidden platform trial on the following day. The platform was removed from the pool and each mouse completed a single, 30 second trial entering the pool diagonally opposite from where the platform was previously located. The probe trial is an important assessment of any spatial learning that has taken place over the previous four days testing and also tests long term memory consolidation and retrieval. Preference and increased time spent in the target quadrant is indicative that the mouse was able to memorise and recall the location of the platform.

Spatial retention in the probe trial was measured by the percentage of total time spent in each quadrant and a proximity measure of average distance to platform site (Gallagher's measure).

	Day 1 (Visible)		Day 2 (Hidden)	Day 3 (Hidden)	Day 4 (Hidden)	Day 5 (Hidden)	Day 6 (Probe)
	Platform location	Starting direction	Platform location: SW Starting direction as follows:				No platform
Trial 1	Centre	S	E	SE	E	N	NE
Trial 2	NE	S	NE	N	NW	E	
Trial 3	SE	S	NW	NW	NE	S	
Trial 4	SW	S	SE	NE	N	W	
Trial 5	NW	S	N	E	SE	N	

Table 2.2 - Platform location and starting directions for the Morris water maze behavioural experiment. Starting directions were changed quasi-randomly. During hidden platform trials when the platform is fixed in the SW quadrant, starting directions in close proximity to this quadrant (S, W, SW) are initially unused as this increases the chance of mice finding the platform by merely bumping into it.

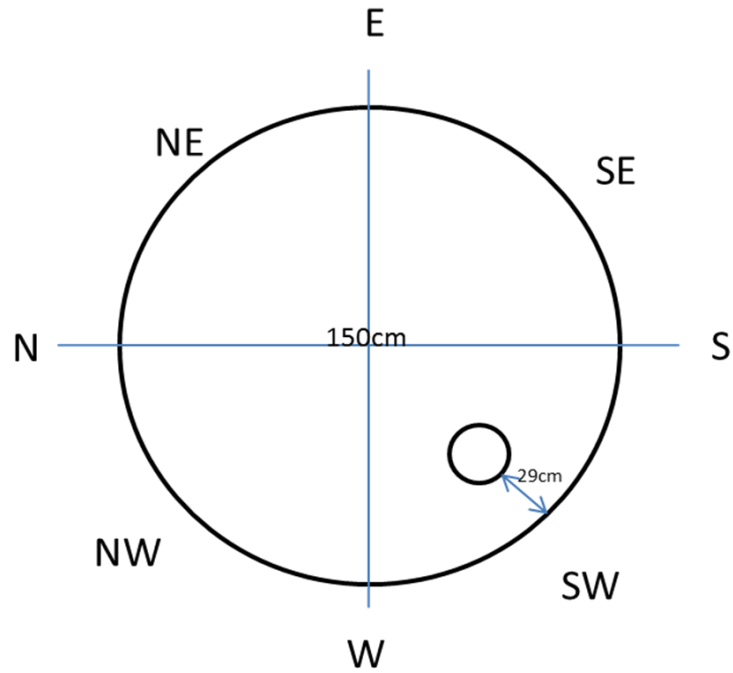


Figure 2.3 – Morris water maze pool quadrants, platform location and cardinal/ordinal compass point starting positions. Automated tracking software analyses the mouse’s position with the four pool quadrants.

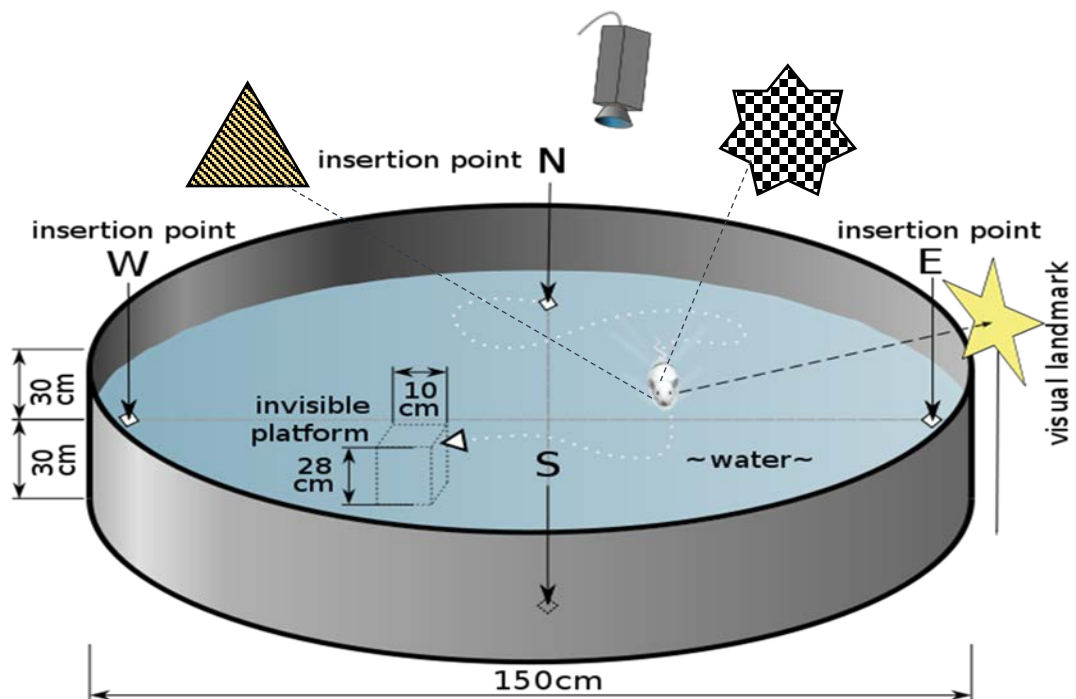


Figure 2.4 – Morris water maze equipment set up. High contrast 3D spatial cues are mounted around the pool during hidden platform trials to aid with spatial navigation to the submerged platform. Image edited and reused from Wikimedia commons [87]

2.11 MOTOR FUNCTION ASSESSMENT

2.11.1 Rota-rod

2.11.1.1 Introduction

The rota-rod test is used to assess motor coordination and balance in rodents. Mice must maintain their balance to stay on a rotating rod that continuously accelerates at a speed of 4 rotations per minute (rpm) to 40rpm over 300 seconds. The rota-rod consists of five 3cm diameter cylinders with six 25cm diameter dividers to form five lanes, each 5.7cm wide, enabling five mice to be tested simultaneously. The height to fall is 16cm and the rod is textured to ensure the mice can maintain an adequate grip. When a mouse falls off its cylindrical section of the rod onto the plate below, the plate trips and the corresponding magnetic switch is activated, thereby recording the latency to fall in seconds (Fig. 2.5).

2.11.1.2 Rota-rod equipment

- Rota-rod (4700, Ugo Basile, VA, Italy)
- 50% EtOH to clean apparatus after each use
- Blue tissue roll

2.11.1.3 General information

Motor function testing was carried out one week after mice completed MWM trials to minimise effects of fatigue. Mice were acclimatised to the rota-rod apparatus prior to testing by completing 3 trials whilst the rod rotated at 4rpm for 1-2 minutes at hourly intervals the day prior to testing. This allowed mice to become accustomed to the task and minimised anxiety related effects on performance. Mice completed three days of rota-rod testing with three trials per day, each separated by a 15 minute inter-trial interval. It was possible to run the next batch of mice consecutively in one trial before moving to the next.

2.11.1.4 Positioning mice on the Rota-rod

The mice could not be lowered directly onto the rota-rod from above as they would spread

their legs and block entry between the discs. It was therefore necessary to use a method whereby the mice were flipped up onto the rod by the tail, landing right side up but dorsal side in first between the rotating discs. This technique was innocuous for test subjects and was perfected using wild type mice prior to testing.

2.11.1.5 Testing procedure

The rota-rod was set to accelerating mode with the rod initially rotating at a constant speed of 4rpm to allow positioning of all the mice in their respective lanes. Once mice were positioned walking forwards, the start button was pressed and the rod began accelerating from 4 rpm to 40 rpm over 300 seconds. When mice fell, the latency to fall was automatically recorded then transferred onto the data sheet. During testing, if a mouse gripped the rod and completed a full passive rotation, the fall plate was tripped by the experimenter to stop the timer for that mouse as passive rotation was considered a failure in performance akin to falling. After each set of five mice had completed a trial, the apparatus was cleaned with water then 50% ethanol solution and wiped dry prior to testing the next set.



Figure 2.5 - Rota-rod apparatus (4700, Ugo Basile, Italy).

2.11.2 Inverted grid suspension test

The inverted grid suspension test (IGST) is a widely used, non-invasive general measure of grip strength. The test measures the ability of the mouse to remain clinging to an inverted wire mesh grid suspended a small distance above a soft surface (Fig. 2.6).

2.11.2.1 Inverted grid suspension test equipment

- Clear hollow acrylic cylinder, 30cm long x 20cm diameter
- Wire mesh with 1 cm² grids
- Stopwatch
- Soft rodent bedding to cushion fall
- 50% EtOH to clean apparatus after each use
- Blue tissue roll

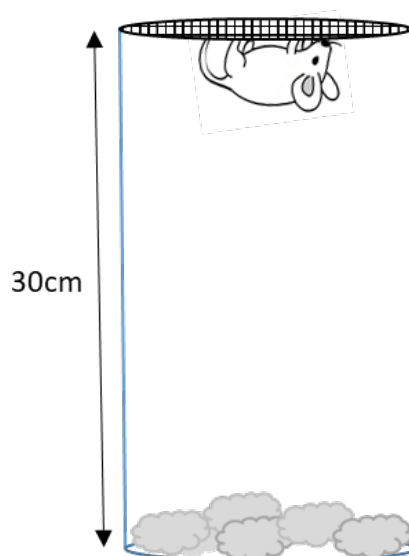


Figure 2.6 – Inverted grid suspension test apparatus set up.

2.11.2.2 Testing procedure

Mice were placed in the cylinder topped with the wire mesh. Once mice had a sustained grip, the cylinder was slowly inverted onto the table top so that mice were suspended from the grid. Rodent bedding was positioned under the cylinder to cushion the fall. The stopwatch was started as soon as the cylinder was inverted and the latency to fall recorded. Mice completed three trials with a 1 minute inter-trial interval. A maximal hanging time of 180 seconds was allowed and the mean of the three trials analysed. Apparatus was thoroughly cleaned after each mouse had completed three trials.

2.12 CATWALK XT GAIT ANALYSIS

2.12.1 Introduction

The CatWalk XT platform is a computer-assisted automated quantitative gait analysis system that allows simultaneous quantification of a large number of both static and dynamic gait parameters during voluntary walking. It consists of an enclosed walkway on a glass plate that is traversed by a mouse from one side of the walkway to the other. Green light enters at the long edge of the glass plate and is completely internally reflected. Light is able to escape only at those areas where the animal's paws make contact with the glass plate; as a result, the light is scattered which results in illumination of the exact area of contact (Fig 2.7). The image is captured by the camera and stored on a computer for analysis.

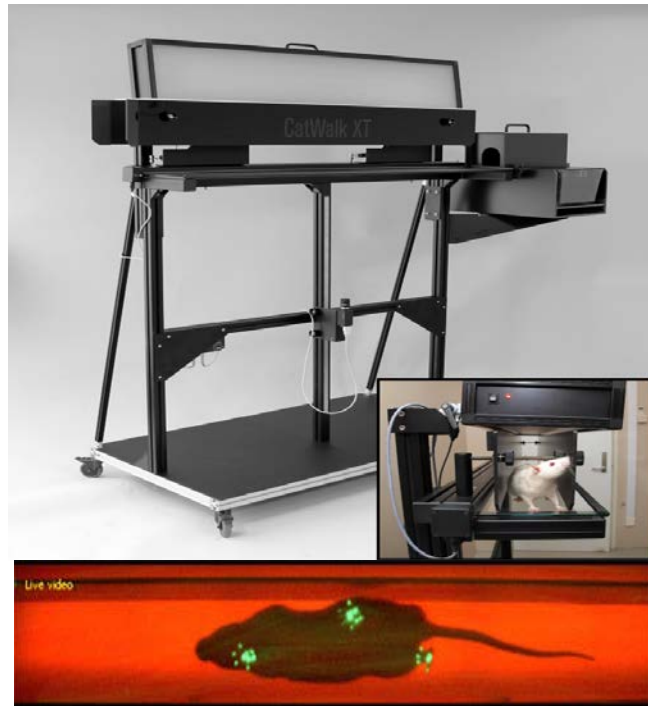


Figure 2.7 – The catwalk XT platform and illumination of footprints in a mouse traversing the glass walkway.

2.12.2 Mice

The Catwalk XT gait analysis platform assessed a cohort of 19 BALB/c Hgd^{-/-} mice (12 male, 7 female) and a separate control cohort of 18 BALB/c wild type mice (8 male, 10 female) to investigate whether any significant differences in gait were present between genotypes prior to treatment with nitisinone. Mice within this study received no treatment with nitisinone as we wished to assess whether joint ochronosis affected gait in the Hgd^{-/-} mice, as observed in human AKU patients. Hgd^{-/-} cohorts age ranged between 17 to 39 weeks, as by this age the ochronotic phase of the disease is observed within the joints of these mice [70].

2.12.3 Bodyweight

Bodyweight was measured daily during testing using weighing scales and the average weight used for analysis.

2.12.4 Equipment

- Catwalk XT system (10.6, Noldus, Netherlands) including high speed camera
- Computer running Microsoft Windows and Catwalk 10.6 analysis software
- 1% EtOH to clean apparatus after each use
- Blue tissue roll
- Microfibre glass cleaning cloth

2.12.5 General information

The walkway area was defined and software calibrated for mouse footprint analysis prior to beginning gait analysis. This was only necessary to complete once as the layout of the walkway and the calibration was stored within the application. Each mouse's identification number (eg Hgd^{-/-} 40.4, WT 35.6) and group (eg Hgd^{-/-} female, WT male) was inputted prior to beginning acquisition so each mouse could be easily selected and run data acquired. It was essential to ensure the glass walkway was clean and free of streaks for every recorded run as even small smears or dirt particles would affect the scattering of light resulting in erroneous recording of paw prints. Each mouse was required to perform three compliant trials (see below) with the most consistent run selected for grouped analysis. Catwalk XT software automatically performed all data analysis.

2.12.6 Training procedure

Before acquiring runs, mice needed to learn to cross the walkway without interruptions (such as stopping or rearing on to its hindlimbs) so all animals started from a similar baseline, this was considered a "compliant run". This was important in order to be able to compare different runs and pick up gait abnormalities that were the result of effects of treatment or in this case, genotype, rather than differences in quality of runs. Mice were habituated to the CatWalk system by individually placing them in the corridor for 1 minute over a number of consecutive days until they freely explored the walkway. One week prior to starting gait analysis, mice were trained to run across the glass plate with a minimum of three runs per day. This was achieved by placing a goal box at the end of the walkway with

bedding and littermates from the mouse's home cage to act as an olfactory stimulatory cue. In total, training took place over a two-week period prior to beginning gait analysis.

2.12.7 Test procedure

In the *Experiment Explorer*, under *Acquisition*, the corresponding trial for the mouse being tested was highlighted and *Acquire Runs* selected. The *Snap Background* button was selected to acquire a background image of the empty, clean walkway – this step had to be completed before every trial so data acquisition could take place. *Start Acquisition* was selected and the apparatus was then ready to begin data acquisition indicated by the *Status* changing to “waiting for run to start”. The mouse was placed into the corridor from the side with acquisition starting automatically as soon as the animal's contour was detected. The *Status* changed to ‘recording Run#’. More than one compliant run could be acquired by either taking the animal out of the corridor and placing it back in on the other side or by letting it turn around independently and run the opposite way along the walkway. When the set number of compliant runs has been acquired, the *Acquisition Finished Tasks* dialogue window opened and the next trial for the corresponding next mouse could be selected.

2.12.8 Run classification

Acquired runs had to be reviewed and footprints classified prior to analysis. Footprint classification could be automated or manual. All prints were automatically classified and then reviewed, with any wrong prints reclassified manually (Fig. 2.8).

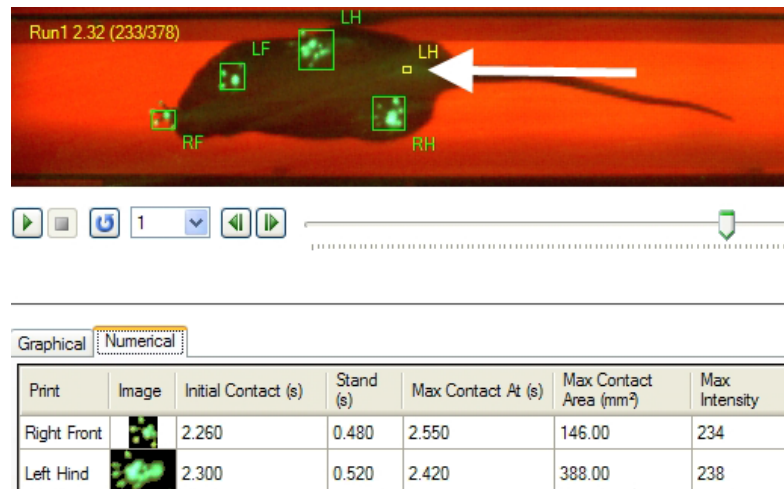


Figure 2.8 – Footprint classification after data acquisition in the Catwalk XT platform. Prints were automatically classified and then reviewed to detect erroneous prints, which could then be manually corrected. White arrow indicates an erroneous left hindlimb (LH) print that was deleted and reclassified.

2.12.9 Catwalk gait analysis parameters

The following parameters were selected for analysis to enable comprehensive assessment of gait in the Hgd^{-/-} and wild type mice:

2.12.9.1 Static parameters

- Regularity index: measurement of interlimb coordination. Expresses the number of normal step sequence patterns relative to the number of paw placements. This parameter can be used for the assessment of ataxia.
- Stride length: distance between successive placements of the same paw. Stride length must be the same for all limbs if the animal is using a consistent gait pattern. Rodent models of rheumatic arthritis have decreased stride length, shorter stride to reduce weight bearing.
- Maximum contact intensity: light intensity ranging from 0–255 arbitrary units. Intensity of the print depends on the degree of contact between a paw and the

glass plate and increases with increasing weight. This parameter is used to assess neuropathic pain where intensity would be reduced in a painful paw.

- Paw print area: complete surface area contacted by the paw during a stance phase. Decreased print area is found in systematic models of arthritis. Main parameter associated with osteoarthritis.

2.12.9.2 Dynamic parameters

- Stance phase: duration in seconds of contact of a paw with the glass plate in a step cycle (stance phase + swing phase). Stance phase is decreased in rodent models of arthritis. This is the weight-bearing phase – pain would present as reduction in stance phase.
- Swing phase: duration in seconds of no contact of a paw with the glass plate in a step cycle. Swing phase is increased if the stance phase is decreased as the animal tries to reduce weight on limbs by spending less time in the weight-bearing phase.
- Duty cycle: stance duration as a percentage of the step cycle duration = stance phase/(stance + swing phases) × 100.

2.13 ARTERIOVENOUS METABOLOME STUDY (CHAPTER 5)

2.13.1 Mice

A cohort of 12 nitisinone treated BALB/c Hgd^{-/-} mice and a control cohort of 9 BALB/c Hgd^{-/-} receiving no treatment were divided between four separate smaller studies detailed below. Metabolite data was analysed from each separate study and then combined for further analysis. All mice were male and aged between 20-35 weeks upon commencing treatment.

2.14 STATISTICAL ANALYSIS

2.14.1 Normality and homogeneity of variance

Data was assessed for normality and homogeneity of variance prior to analysis using the Shapiro-Wilk and Brown-Forsythe test respectively. This confirmed the majority of data had a Gaussian distribution. Some metabolite and Morris water maze latency data failed the normality test due to outliers or mixed distributions but as ANOVA and T tests are considered robust to the assumption of normality due to making statistical inferences about means it was not necessary to transform the data. All statistics were calculated using GraphPad Prism 7 for Windows (GraphPad, CA, USA).

2.14.2 Morris water maze data

Means of the five trials for each day and each mouse were calculated to give a single escape latency, path length and path distance for each test subject. Subject means for the four days of hidden platform trials were analysed by three way ANOVA with genotype and treatment as a between-subjects factor and day as a within-subject factor. Data from Morris water maze visible platform and probe trial were subjected to a two-way ANOVA between genotype and treatment. When the ANOVA detected significant effects, pairwise differences between means for a given variable were evaluated using post hoc Tukey or Sidak multiple comparison test with significance set at $P < 0.05$.

2.14.3 Motor function testing data

Latency to fall on the Rota-rod was analysed by three way ANOVA with genotype and treatment as a between-subjects factors and day as a within subject factor with post hoc Tukey multiple comparison test. Latency to fall on the inverted grid suspension test was analysed by two way ANOVA with between subject factors of genotype and treatment.

2.14.4 Long-term dose response study data

Comparisons of metabolites and pigmentation between control and nitisinone treated groups were performed using a one-way ANOVA with Dunnetts post hoc test. Comparisons

of metabolites between mid and term bleeds were performed using paired two-way students t tests. Results were considered statistically significant at $p < 0.05$. An intraclass and Pearson's correlation coefficient test with absolute agreement was carried out for pigmentation counts to assess inter-observer variability.

2.14.5 Arteriovenous metabolome data

Comparisons of metabolites between bleed site and cull method were performed using two way repeated measured ANOVA with bleed as a repeated measures factor and treatment as a between subject factor. Pairwise differences between means for a given metabolite were evaluated using Tukey or two-way student's t tests.

3. Analysis of learning, memory and motor function in nitisinone treated and control cohorts of AKU (Hgd^{-/-}) and wild type (WT) BALB/c mice.

3.1 INTRODUCTION

Nitisinone is currently being trialled as a HGA lowering therapy for AKU patients over the age of 18. It has been widely used in children with hereditary tyrosinemia type 1 (HT1) for over 20 years where therapy is life saving and must be initiated as early as possible to prevent the fatal hepatic and renal manifestations associated with the disease. Nitisinone has dramatically increased survival rates in HT1 but some researchers have suggested an associated cognitive impairment in some children when reaching school age [111-114]. As part of its mechanism of action of inhibiting 4-hydroxyphenylpyruvate dioxygenase (HPPD), nitisinone causes increases in circulating tyrosine. There is concern that this tyrosinemia may be a contributing factor to the intellectual impairment observed in some children, particularly as treatment is started early in life during essential stages of brain development [110]. There are other possible causes for educational delay in HT1 patients such as liver dysfunction in early life, but for the purpose of this thesis, we wished to search for evidence of adverse effects of tyrosinemia on cognitive function in nitisinone treated mice.

Several studies assessing the neurocognitive outcome of nitisinone use in early treated, HT1 patients have shown conflicting results ranging from normal IQ with no impairment to a high number of patients performing below normal in the assessment of psychomotor development and intellectual functioning [111-113]. None of these studies were able to identify a clear correlation between metabolic control and cognitive function although the most recent study from García and colleagues (2017) found a significant correlation between tyrosine/phenylalanine ratio and IQ concluding that some patients with HT1 treated with nitisinone are at risk of presenting developmental delay and impaired cognitive functioning [114]. The tyrosinemia post nitisinone also resembles the metabolic status in hereditary tyrosinemia Type 3 (HT-3) where there is increased plasma tyrosine from birth due to genetic deficiency of HPPD. The neurological manifestations associated with the condition such as delayed cognitive and intellectual development, intermittent ataxia and seizures have been linked to the elevated blood levels of tyrosine [115].

Nitisinone is a promising HGA lowering treatment but there is limited toxicology data available for its use in AKU. Some may argue that as sufferers of AKU have no clinical symptoms until adulthood there is no need to treat early, however, murine studies have indicated the process of ochronosis starts from as early as 15 weeks and cumulatively leads

to joint damage [70, 71]. Commencing treatment early in children with AKU could potentially reduce accumulation of damage over time due to high HGA levels and improve prognosis later in life. However, the side effect of elevated tyrosine poses potential safety issues to the developing brain that must be investigated prior to use in children.

3.2 HYPOTHESIS AND AIM OF STUDY

Hypothesis: Nitisinone treatment causes significant changes in learning, memory and motor control in Hgd^{-/-} and WT mice.

This study aimed to assess the effects of nitisinone-induced elevation of tyrosine on learning and memory, indicators of cognition, using the Morris water maze (MWM) in the AKU (Hgd^{-/-}) BALB/c mouse. As ataxia has been reported in some HT-3 patients, where elevated tyrosine levels are present from birth, motor function was also assessed using the Rota-rod and Inverted Grid Suspension Test. The Catwalk XT gait analysis platform was used on a separate cohort of male and female, Hgd^{-/-} and wild type (WT) mice to investigate whether any significant differences in gait were present prior to treatment with nitisinone. This type of analysis has not previously been reported for AKU mice. The Catwalk XT automated system enabled a comprehensive assessment of static and dynamic gait parameters.

3.3 RESULTS

3.3.1 Plasma metabolites

After 1 week of treatment with nitisinone (4mg/L), plasma tyrosine was elevated in Hgd^{-/-} treated and WT treated mice (1390±68.0 and 1242±59.8 umol/L respectively) (Fig. 3.1A). HPPD inhibition reduced plasma HGA to very low levels in Hgd^{-/-} treated mice compared to control (10.3±1.2 and 142.5±10.8 umol/L respectively) (Fig. 3.1B). Measuring these metabolites confirmed nitisinone treatment was effective prior to performing further cognitive and motor function assessment and treatment was continued at the same dose throughout the testing period.

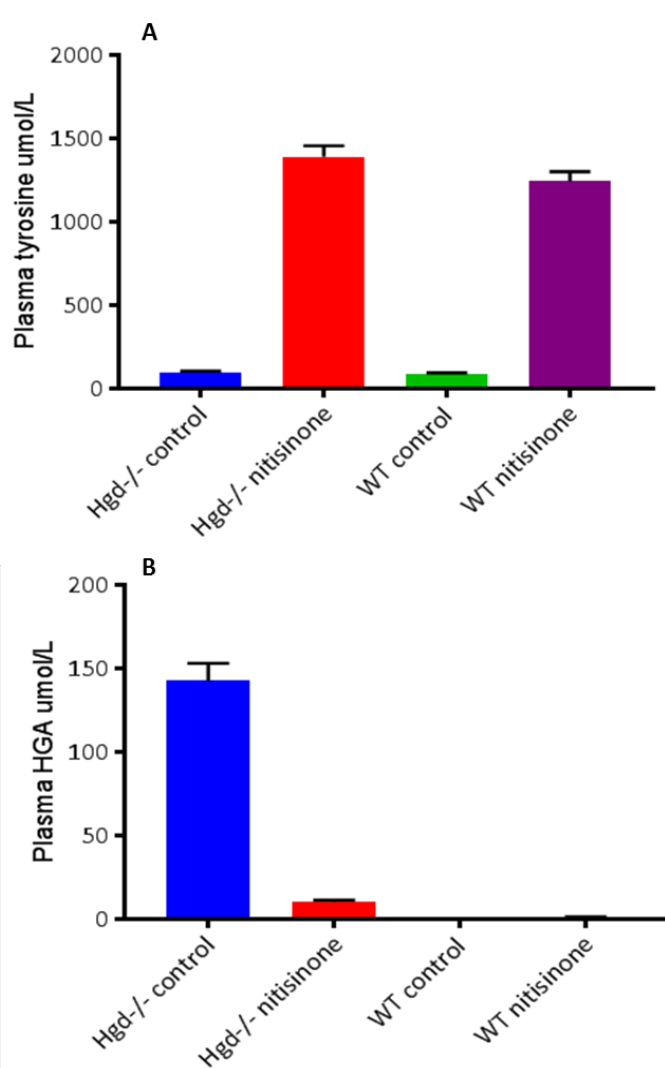


Figure 3.1 – Plasma tyrosine and HGA levels in BALB/c Hgd^{-/-} and WT control and nitisinone treated mice. Results confirmed nitisinone (4mg/L) elevated plasma tyrosine in Hgd^{-/-} treated and WT treated mice (A). This was to ensure MWM and motor function testing assessed the effects of tyrosinemia (elevation of tyrosine) in both genotypes. Plasma HGA was reduced to low levels in Hgd^{-/-} treated mice, which further confirmed effectiveness of nitisinone treatment prior to starting cognitive and motor function assessment (B). Mean \pm SEM values shown, n=12 per cohort.

3.3.2 Morris water maze

3.3.2.1 Visible platform (day 1)

Escape latency decreased over the five trials of the visible platform test on day 1. All cohorts showed they were able to see the platform and learn the task of mounting the platform to escape the pool suggesting no apparent visual or swimming deficits were present that would affect subsequent hidden platform trials (days 2 to 5 of testing). There was a significant effect of trial number on latency ($F(4, 220) = 12.27$ $P < 0.0001$) as the mice became more accustomed to the task and escaped the pool quicker. Hgd^{-/-} control and treated mice were significantly slower at escaping during trial 4 than WT treated mice ($P = 0.0146$ and 0.0324 respectively) (Fig. 3.2A). The significant effects of trial and genotype ($F(1, 220) = 7.961$ $P = 0.0052$) on escape latency are clearer when the first and last trial of the visual platform task are plotted (Fig. 3.2B). Swimming speed did not vary significantly between cohorts indicating no gross motor deficits were present that would affect further trials (Fig. 3.3). Swimming distance decreased significantly in all cohorts over the five trials as the mice learnt the location of the platform and swam a more direct path ($F(4, 220) = 10.47$ $P < 0.0001$). However, Hgd^{-/-} control mice swam a significantly further distance than WT treated mice during trial 2 ($P = 0.0380$) (Figure 3.4A). Overall, Hgd^{-/-} mice swam a significantly further distance than WT mice during visible trials shown by a main effect of genotype on swimming distance ($F(1, 220) = 7.68$ $P = 0.0061$) (Figure 3.4B).

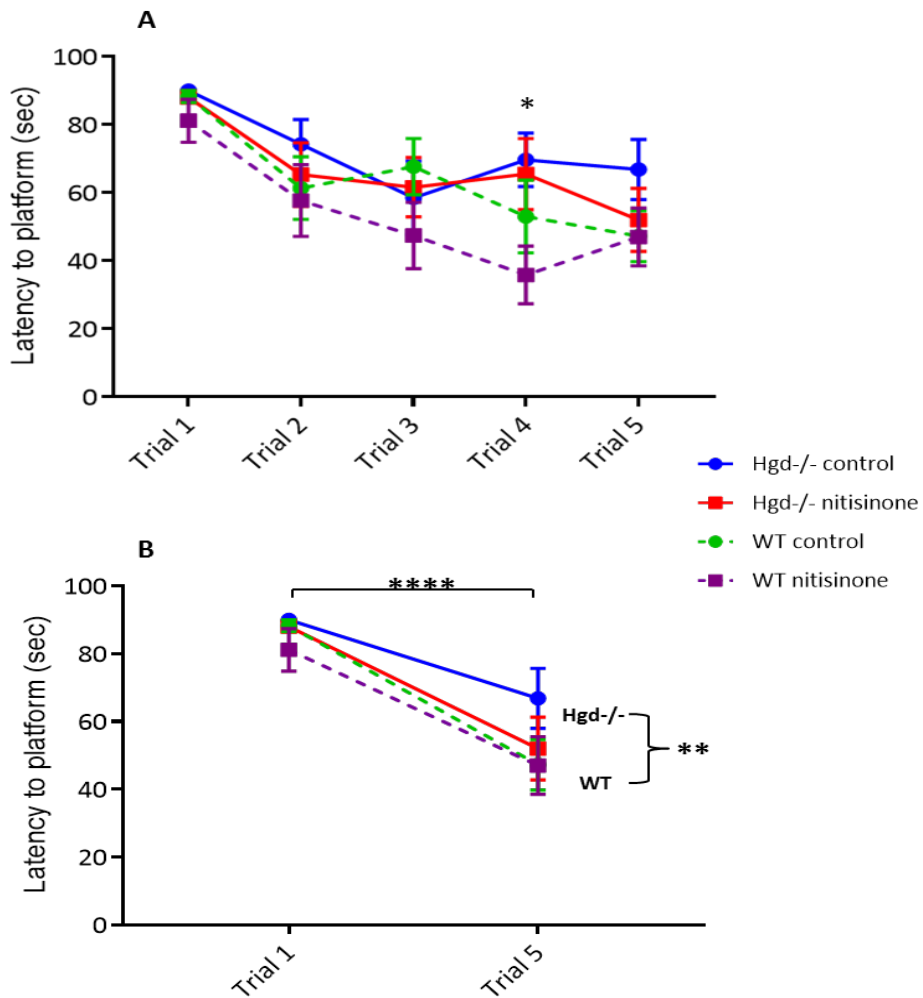


Figure 3.2 - Mean escape latency (\pm SEM) of BALB/c Hgd-/- and WT mice during visible platform trials in the MWM, n=12 per cohort. **A: All groups showed a progressive decrease in latency over the five training trials. This indicates all treatment groups were able to recognise and learn the task of finding and mounting the platform, suggesting no visual or motor defects prior to beginning hidden platform trials. **B.** The significant effect of trial on latency and the learning process is apparent when comparing the first and last trial of the day ($F(4, 220) = 12.27 P < 0.0001$). At this early stage, analysis of data also showed genotype to be a significant factor in performance ($F(1, 220) = 7.961 P = 0.0052$).**

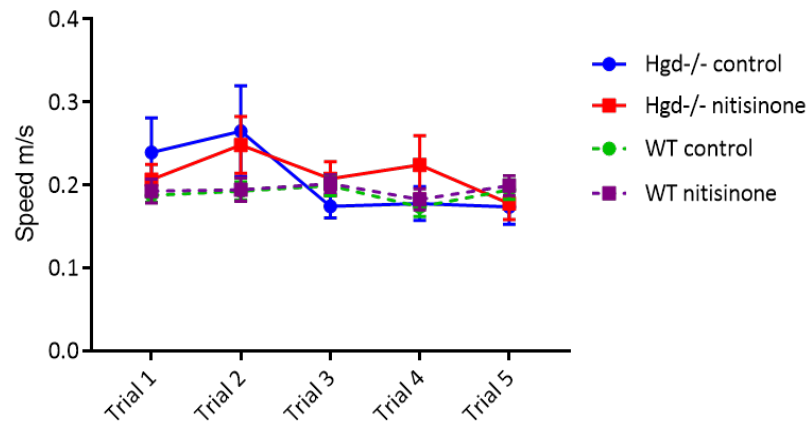


Figure 3.3 - Mean swimming speed (\pm SEM) of BALB/c Hgd-/- and WT mice during visible platform trials in the MWM, n=12 per cohort. Swim speed did not vary significantly between cohorts suggesting no obvious deficits in swimming ability or motivation to swim.

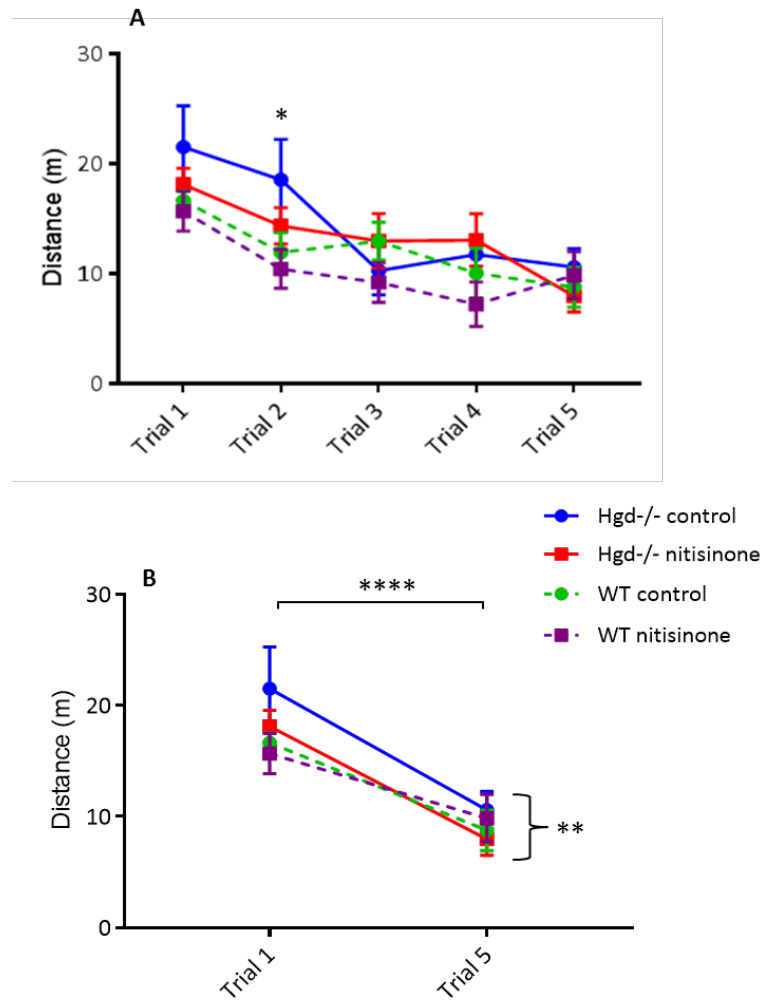


Figure 3.4 - Mean swimming distance (\pm SEM) of BALB/c Hgd-/- and WT mice during visible platform trials in the MWM, n=12 per cohort. **A: All groups showed a progressive decrease in distance over the 5 training trials indicating mice learnt to take a more direct path to the target platform with each trial. Hgd-/- control mice swam a significantly longer distance ($P=0.0380$) than WT treated mice during trial 2. **B:** The significant effect of trial on distance is apparent when the first and last trial of the day are compared ($F(4,220) = 10.47$ $P<0.0001$). Genotype was also found to have a significant effect on swimming distance ($F(1,220) = 7.68$ $P=0.0061$).**

3.3.2.2 Hidden platform (day 2-5)

During hidden platform trials a main effect of genotype on escape latency was observed ($F(1,176) = 12.39$ $P=0.0006$). Both WT cohorts found the hidden platform significantly quicker over consecutive days compared with Hgd^{-/-} mice (Fig. 3.5A). Test day had a nearly significant effect on escape latency ($F(3,176) = 2.631$ $P=0.0516$) as mice showed an overall decrease in latency over the hidden platform trials but this decrease was not steady over subsequent days. Importantly, treatment with nitisinone had no significant effect on latency for any cohort ($F(3,176) = 0.1713$ $P=0.6794$). All cohorts showed a progressive decrease in swimming speed over the hidden trials confirmed by a significant main effect of test day on swimming speed ($F(3,176) = 6.501$ $P=0.0003$). This could indicate the mice were becoming more accustomed to the task and less anxious about being in the pool (Fig. 3.5B). There was no main effect of genotype or treatment on swimming speed but a significant genotype x treatment interaction was present ($F(1,176) = 5.77$ $P=0.0173$) as WT control mice swam faster than WT treated mice, whereas Hgd^{-/-} treated mice were faster than Hgd^{-/-} control mice. All cohorts showed a progressive decrease in swimming distance over the hidden platform trials as they swam a more direct path to the platform, confirmed by a significant effect of day on swimming distance ($F(3,176) = 16.76$ $P<0.0001$). WT mice treated with nitisinone swam a significantly shorter distance than Hgd^{-/-} control, Hgd^{-/-} treated and WT control mice on day 3 ($P=0.0262$, $P=0.0193$ and $P=0.0195$ respectively). WT treated mice also swam a significantly shorter distance than Hgd^{-/-} treated mice on day 5 ($P=0.0341$) (Fig. 3.5C). A significant genotype x treatment interaction was also observed for swimming distance ($F(1,176) = 4.853$ $P=0.0289$).

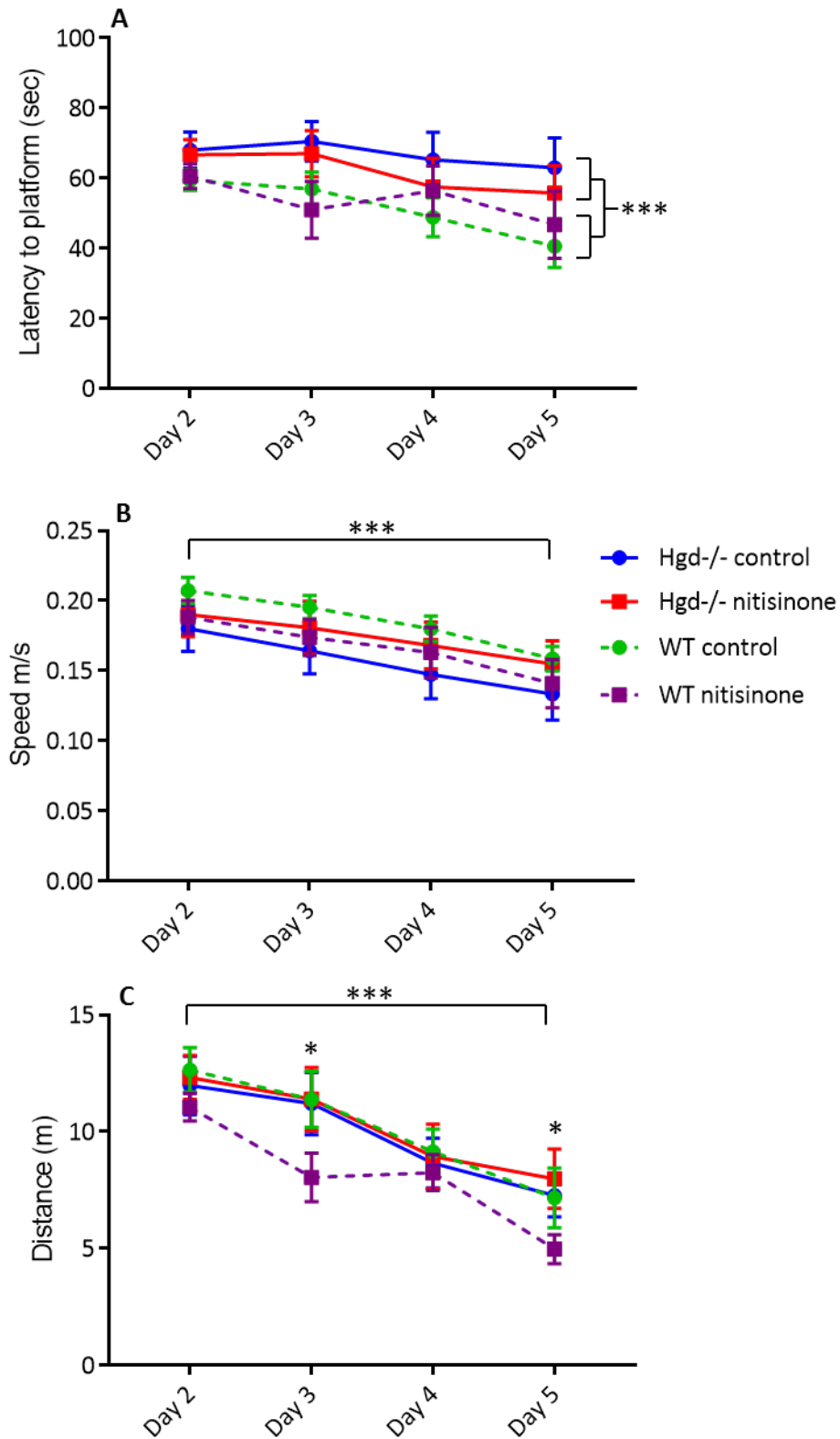


Figure 3.5 - A: Mean escape latency (\pm SEM) B: Mean swimming speed (\pm SEM) C: Mean swimming distance (\pm SEM) of BALB/c Hgd^{-/-} and WT mice during hidden platform trials in the MWM, n=12 per cohort. A: During hidden trials, a main effect of genotype on latency was observed ($F(1,176) = 12.39$ $P=0.0006$). Both WT cohorts found the platform quicker

over consecutive days compared with Hgd^{-/-} cohorts. Treatment with nitisinone and test day had no significant effect on escape latency. **B:** All cohorts showed a decrease in swim speed over the hidden trials confirmed by a significant effect of test day on swim speed ($F(3,176) = 6.501$ $P=0.0003$). **C:** All cohorts showed a decrease in swimming distance over the hidden platform trials confirmed by a significant effect of day on distance ($F(3,176) = 16.76$ $P<0.0001$). WT treated mice swam a significantly shorter distance than other cohorts on day 3 and day 5. **B & C:** A significant genotype x treatment interaction was also observed for swimming speed and distance ($F(1,176) = 5.77$ $P=0.0173$ and $F(1,176) = 4.853$ $P=0.0289$ respectively).

When the latency of the first and last trial of the hidden platform days are plotted, the significant effect of genotype is more apparent. Hgd^{-/-} cohorts took longer to find the platform and showed no significant improvement over the four days of hidden platform testing. Hgd^{-/-} treated mice performed marginally better than Hgd^{-/-} control mice but this was not statistically significant. WT cohorts showed substantial improvement and located the platform quicker with each testing day. WT control mice showed the greatest improvement out of all cohorts with the largest decrease in latency from first to last trial. Again, there was no significant effect of nitisinone treatment on either genotype (Fig. 3.6).

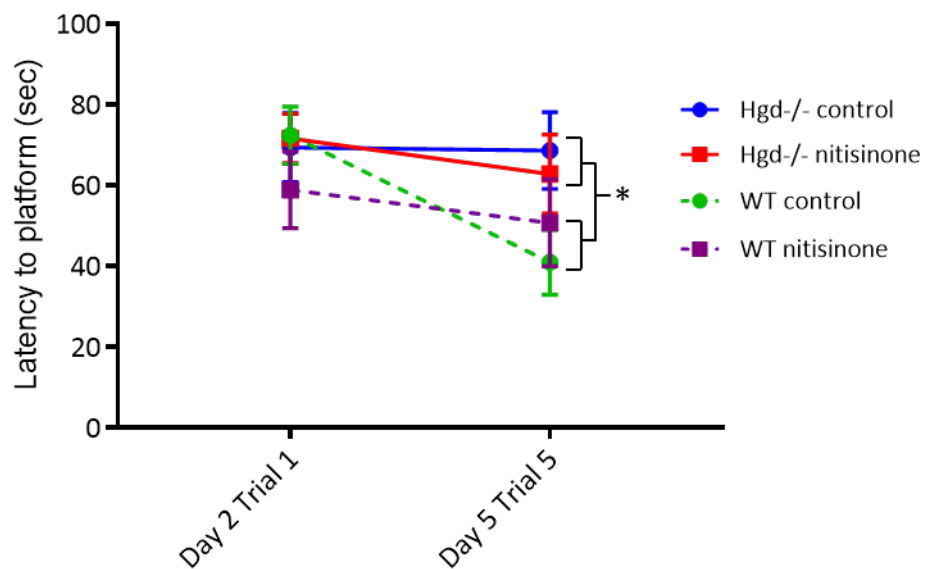


Figure 3.6 - Mean escape latency (\pm SEM) of BALB/c Hgd^{-/-} and WT mice in the MWM: comparison of first and last run of hidden platform trials, n=12 per cohort. A significant effect of genotype on escape latency is apparent ($F(1,88) = 3.961$ $P=0.0497$). WT cohorts were quicker at finding the hidden platform. WT control mice were quickest to find the platform followed by WT treated with nitisinone. Hgd^{-/-} cohorts did not improve significantly over the hidden platform trials with Hgd^{-/-} control mice appearing to show no improvement in escape latency of the four hidden days testing.

3.3.2.3 Probe trial (day 6)

During the probe trial, the platform was removed from the pool and each mouse performed a single trial. The target quadrant refers to the previous location of the platform during hidden platform trials. Preference to the target quadrant, indicated by >25% time spent within that quadrant, is indicative of the mouse's ability to learn and consolidate spatial memory during hidden platform trials and the ability to recall this location the following day. The probe trial was carried out the day after the final hidden platform trial to ensure it was not assessing short-term memory. Both WT cohorts showed preference to the target quadrant whilst Hgd $-/-$ cohorts showed no preference. This significant genotypic effect was confirmed by ANOVA ($F(1, 44) = 0.5.992$ $P=0.0184$). Nitisinone treatment had no effect on target quadrant preference ($F(1, 44) = 0.01134$ $P=0.9157$) (Fig. 3.7). Gallagher's proximity measure confirmed WT cohorts were in closer proximity to the target quadrant throughout the probe trial (Table 3.1).

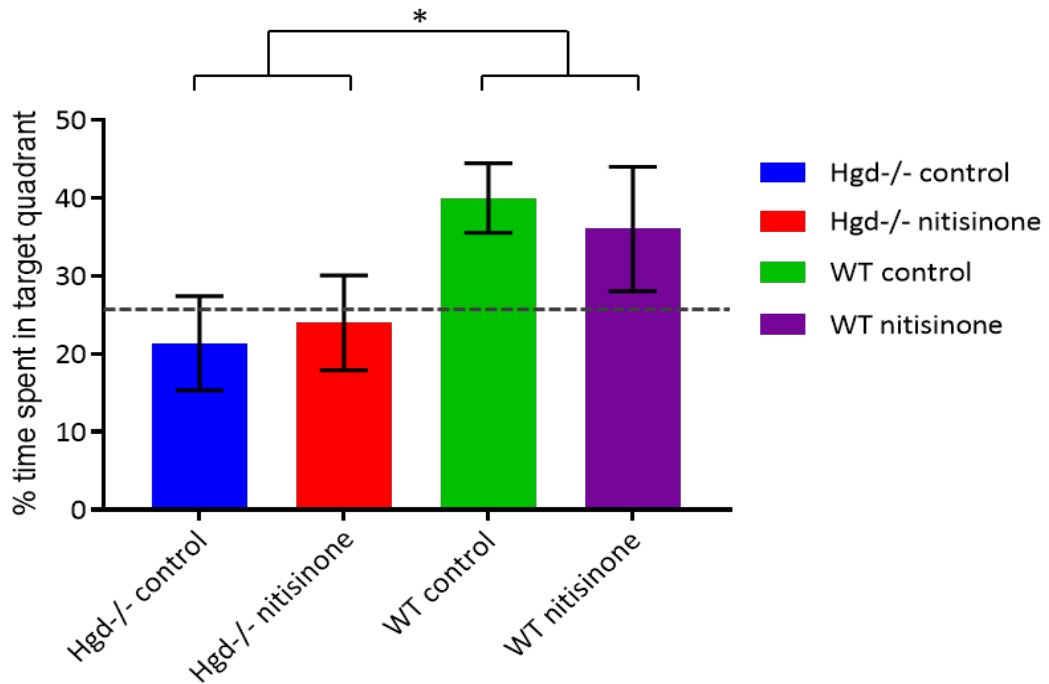


Figure 3.7 – Mean percentage of time spent in target quadrant (\pm SEM) during probe trial of the MWM in BALB/c Hgd-/- and WT nitisinone treated and control mice. Preference is indicated by >25% time spent within a quadrant. WT cohorts showed preference to the target quadrant indicating spatial learning and memory retrieval. Both Hgd-/- cohorts showed no preference to the target quadrant. This significant genotypic effect was confirmed by ANOVA ($F(1, 44) = 0.5992$, $P = 0.0184$). Treatment did not significantly affect quadrant preference suggesting nitisinone does not reduce learning performance. Differences in spatial learning between Hgd -/- and WT mice appears to be due to genotype and not nitisinone treatment.

Hgd-/- control	Hgd-/- nitisinone	WT control	WT nitisinone
0.7592	0.7117	0.5517	0.6425

Table 3.1 - Mean Gallagher proximity measures during probe trial of the MWM in BALB/c Hgd-/- and WT nitisinone treated and control mice, n=12 per cohort. The average distance in metres from the platform over the whole trial, corrected for start point and using every sample point for distance from the platform. Higher values indicate less spatial knowledge. This measure confirmed WT cohorts showed more preference to the target quadrant by being in closer proximity to the previous location of the platform throughout the probe trial.

3.3.3 Motor function analysis

3.3.3.1 Rota-rod

Within the Rota-rod test mice walk on an accelerating motorised rod; the latency to fall for each mouse is automatically recorded with a higher latency to fall indicative of a better performance. Hgd^{-/-} cohorts performed significantly better (spent longer on the motorised rod) than WT cohorts across all Rota-rod trials ($F(1, 16) = 68.68$ $P < 0.0001$) (Fig. 3.8). Hgd^{-/-} cohorts also performed significantly better during each of the three days compared to WT cohorts ($F(1, 16) = 4.874$ $P = 0.0422$) (day 1: $P = 0.0016$, day 2: $P = 0.0011$, day 3: $P < 0.0001$). In agreement with MWM trials, treatment with nitisinone had no significant effect on performance. All cohorts showed improvement in performance over the three days testing but this was greatest in Hgd^{-/-} cohorts indicated by a significant genotype x day interaction ($F(1, 16) P = 0.0192$).

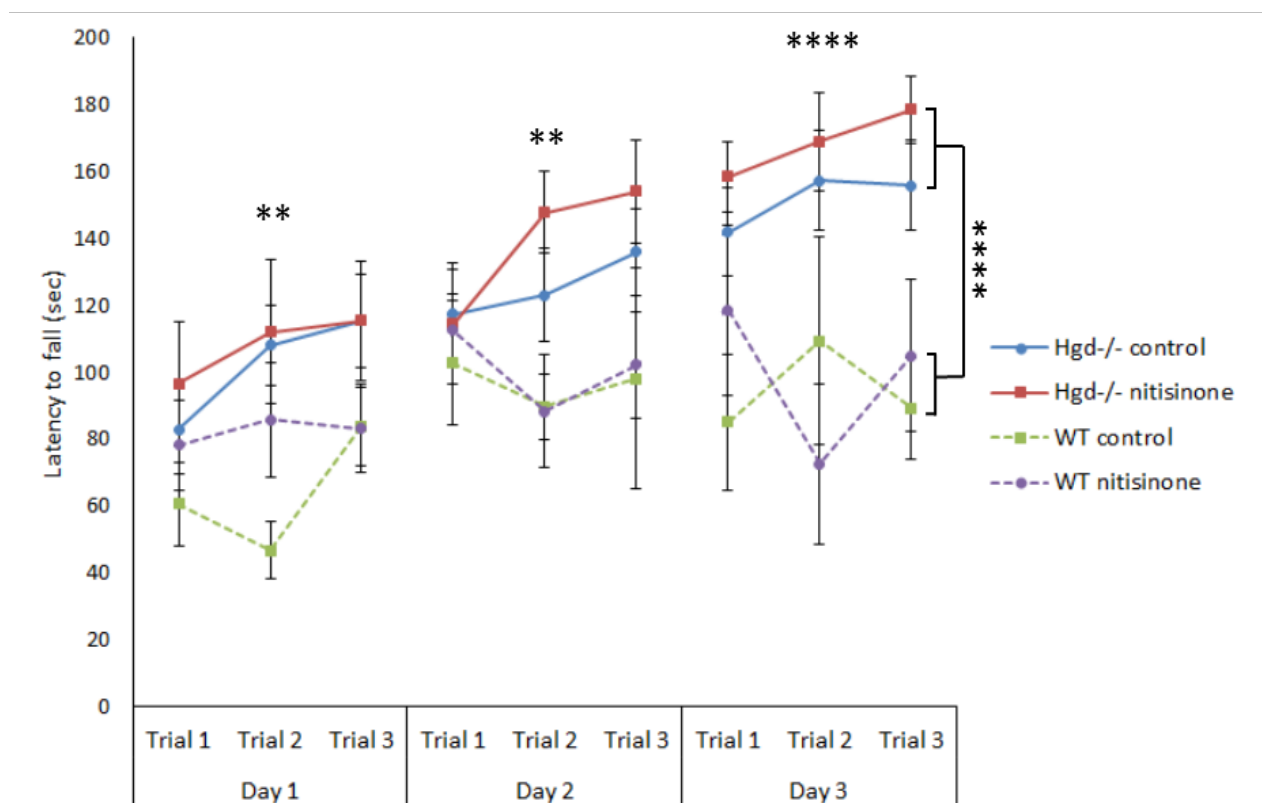


Figure 3.8 - Mean (\pm SEM) performance of BALB/c Hgd^{-/-} and WT control and treated mice on the Rota-rod. Both WT cohorts fell earlier than Hgd^{-/-} cohorts across the 3 days of testing. Hgd^{-/-} cohorts showed greatest improvement in performance. Genotype and day were significant factors of performance. ** = $P < 0.01$ **** = $P < 0.0001$

3.3.3.2 Inverted grid suspension test

Performance varied on the inverted grid test between cohorts with WTs performing marginally better than Hgd^{-/-} cohorts (Figure 3.9). Two way ANOVA showed no significant effects of genotype or treatment with nitisinone on latency to fall ($F(1, 137) = 3.262$ $P=0.0731$ and $F(1, 137) = 1.028$ $P=0.3125$ respectively).

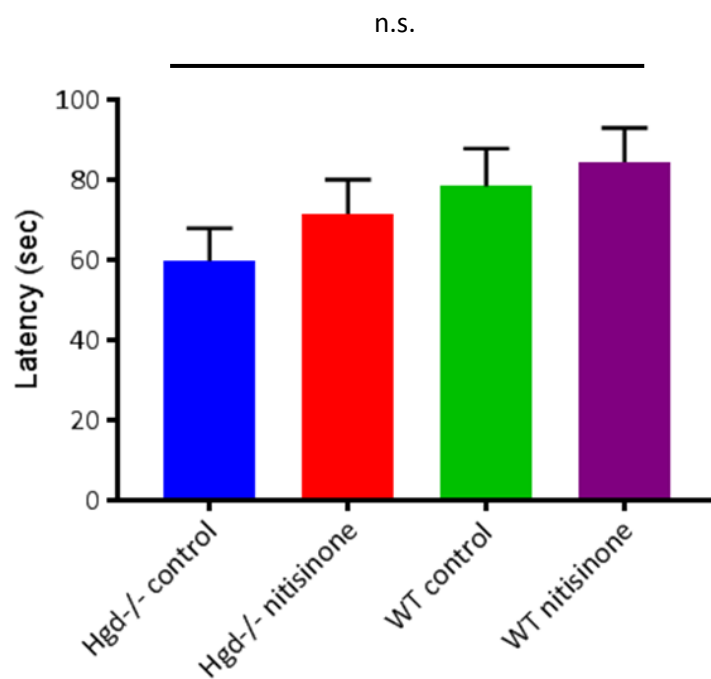


Figure 3.9 - Mean (\pm SEM) latency to fall on the inverted grid suspension test in BALB/c Hgd^{-/-} and WT control and treated mice. Hgd^{-/-} and WT cohorts showed a similar performance with no significant effects of genotype or treatment with nitisinone on latency.

3.3.4 Catwalk XT gait analysis

The Catwalk XT gait analysis platform was used on a separate cohort of male and female, Hgd^{-/-} control and WT control mice to investigate whether any significant differences in gait were present between genotypes prior to treatment with nitisinone. Mice within the subsequent study therefore received no treatment with nitisinone as we wished to assess whether gait was affected by joint ochronosis as previously demonstrated in human AKU patients [96]. This type of analysis has not previously been reported for Hgd^{-/-} mice. The Catwalk XT automated system enabled a comprehensive assessment of static and dynamic gait parameters.

3.3.4.1 Bodyweight

Bodyweight varied significantly between male cohorts due to the age of mice when available for testing since we had a limited timeframe of access to the gait analysis platform. Hgd^{-/-} males were older (17-38 weeks) and significantly heavier than WT males (12-17 weeks). This was taken into consideration when comparing gait analysis parameters affected by weight and body size such as print area and stride length. Bodyweight did not differ significantly between female cohorts (Fig. 3.10). Hgd^{-/-} cohorts age ranged between 17 to 39 weeks, as we wished to analyse gait when the ochronotic phase of the disease had initiated within the joints. A natural history study by Preston and colleagues showed pigmented chondrocytes to be present in the BALB/c Hgd^{-/-} mouse knee from 15 weeks of age and then progressively increasing across the mouse's lifespan [70].

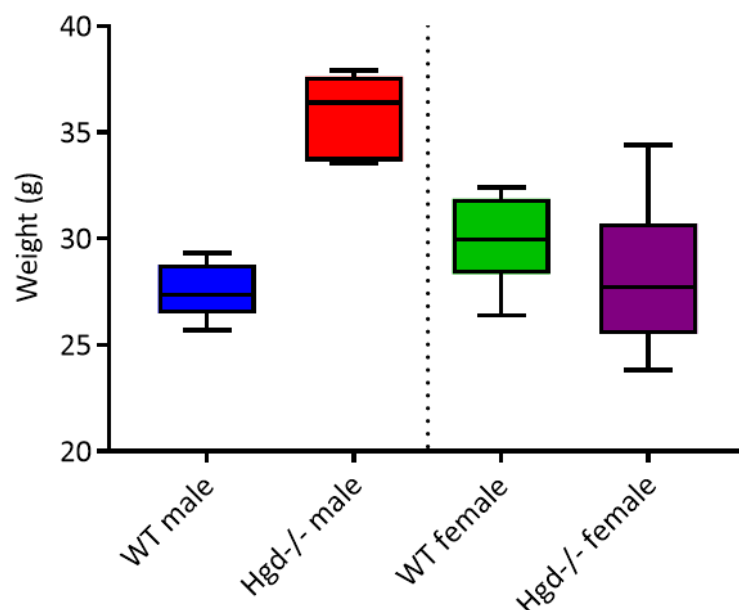


Figure 3.10 - Bodyweight of male and female BALB/c Hgd^{-/-} and WT mice tested with the Catwalk gait analysis platform. Hgd^{-/-} male mice were significantly heavier than WT male mice due to age differences.

3.3.4.2 Stance phase

Male Hgd^{-/-} mice had significantly longer stance phases of the left and right hind limbs compared to WT males ($t(18) = 2.41$, $P = 0.0269$ and $t(18) = 2.965$, $P = 0.0083$ respectively). Both hindlimbs showed an increase of approximately 0.04 seconds or 28% compared to WT males. Female cohorts had similar stance phases for all limbs analysed with no significant differences between genotype (Fig. 3.11).

Stance Phase

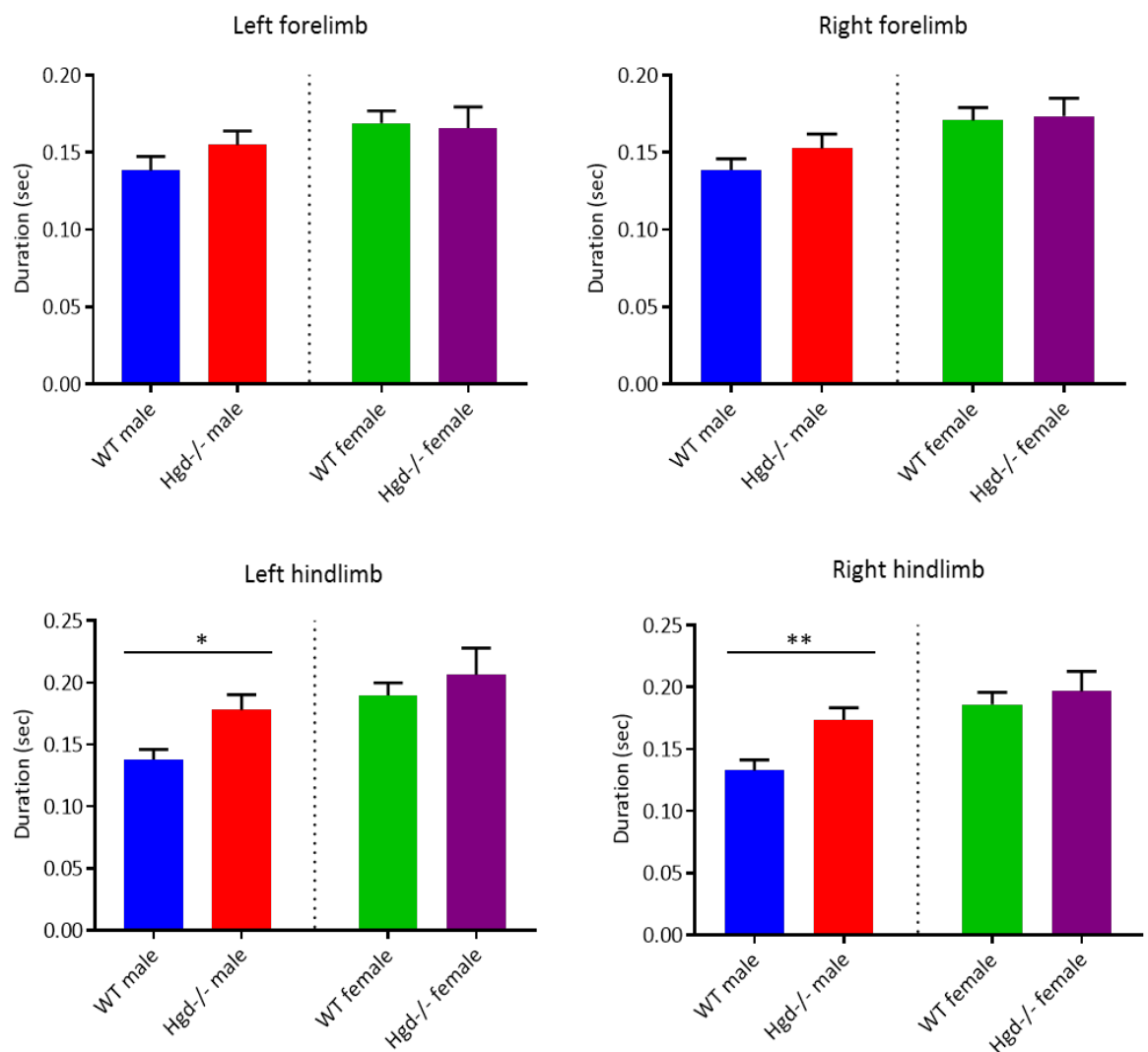


Figure 3.11 - Mean (\pm SEM) stance phase for male and female BALB/c Hgd^{-/-} and WT mice.

Male Hgd^{-/-} mice had significantly longer hindlimb stance phases compared to male WT.

Female cohorts showed no significant differences for any limb. * = $P < 0.05$, ** = $P < 0.01$

3.3.4.3 Swing phase

Male Hgd^{-/-} mice had significantly shorter left and right hindlimb swing phases compared with WT males ($t(18) = 4.184$, $P = 0.0006$ and $t(18) = 4.321$, $P = 0.0004$ respectively). These were decreased by approximately 0.02 seconds or 18% compared with WT males. This decrease in swing phase coincides with the increase in stance phase of the step cycle within these limbs. Female cohorts had similar swing phases for all limbs analysed with no significant differences between genotypes (Fig. 3.12).

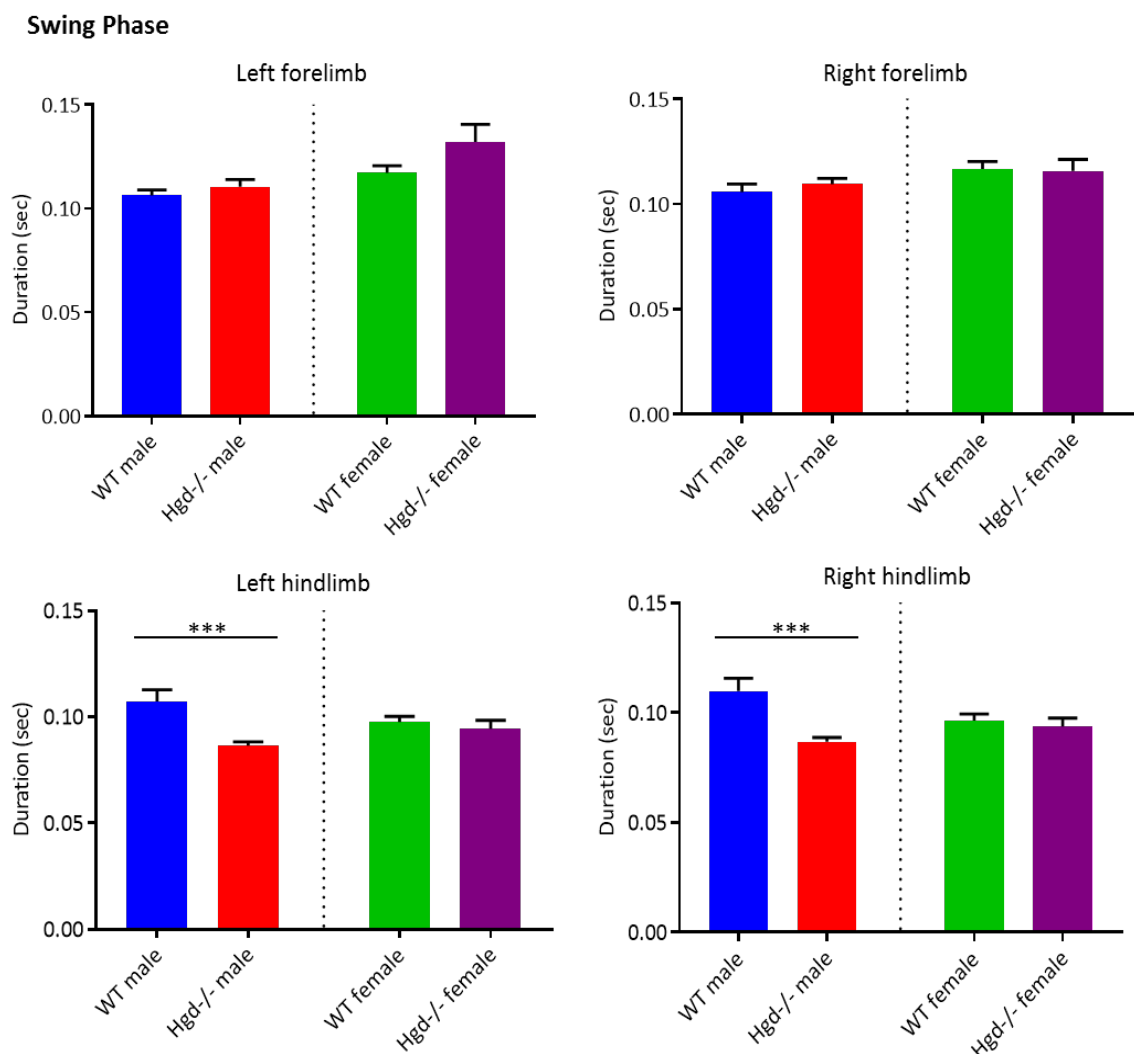


Figure 3.12 - Mean (\pm SEM) swing phase for male and female BALB/c Hgd^{-/-} and WT mice. Male Hgd^{-/-} mice had significantly shorter hindlimb swing phases compared to male WT. Female cohorts showed no significant differences for any limb. *** = $P < 0.001$.

3.3.4.4 Duty cycle

Duty cycle expresses the weight bearing stance duration as a percentage of the step cycle duration. Male Hgd^{-/-} mice had significantly higher duty cycles of the left and right hindlimb compared with WT males ($t(18) = 3.843$, $P = 0.0012$ and $t(18) = 4.463$, $P = 0.0003$ respectively). These were both increased by approximately 10% compared with WT males. This coincides with the differences observed in the swing and stance phases of the step cycle within these limbs previously discussed. Hgd^{-/-} females had a reduced duty cycle in the left forelimb (-3.9%) compared with the same limb in WT females ($t(15) = 2.515$, $P = 0.0238$). The duty cycle of other limbs in female cohorts showed no significant differences (Fig. 3.13).

Duty cycle

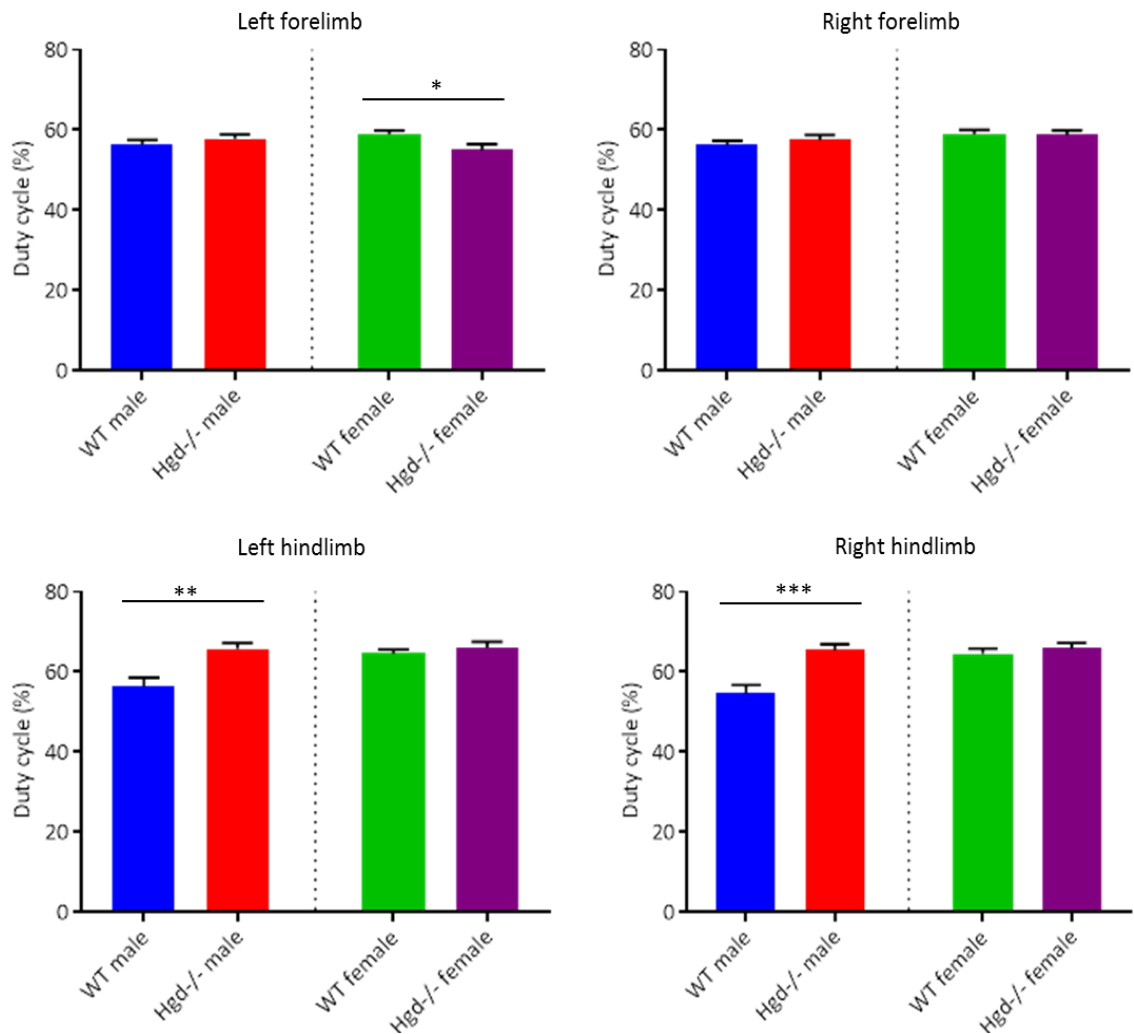


Figure 3.13 - Mean (\pm SEM) duty cycle for male and female BALB/c Hgd^{-/-} and WT mice. This represents the weight bearing stance phase as percentage of the entire step cycle duration (stance phases + swing phases). Male Hgd^{-/-} mice had significantly higher duty cycles of the hind limbs compared to male WTs. Hgd^{-/-} females had a reduced duty cycle in the left forelimb compared with the same limb in WT females * = P<0.05, ** = P<0.01, *** = P<0.001.

3.3.4.5 Regularity index and stride length

All cohorts had a regularity index near 100% indicating no abnormalities of interlimb coordination (Fig. 3.14A). Stride length was the same for all limbs indicating the mice were using a consistent gait pattern. One-way ANOVA of stride length within cohorts did not reveal any significant differences between limbs therefore the combined data for all four limbs was used for analysis between cohorts. Hgd^{-/-} males mice had a significantly larger stride length compared with WT males ($t(6) = 14.39, P < 0.0001$). Female cohorts had similar stride lengths (Fig. 3.14B).

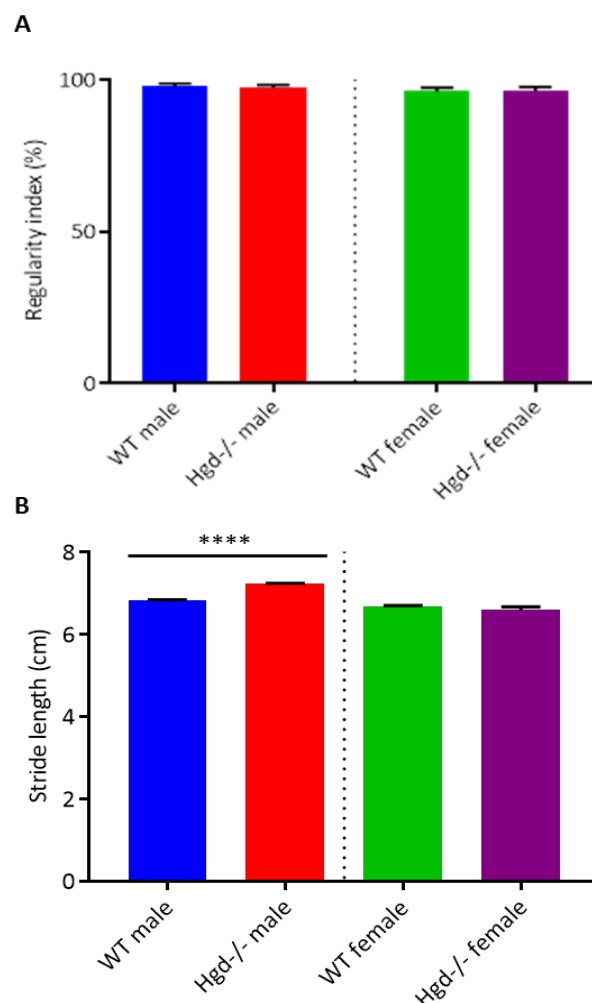


Figure 3.14 - Mean (\pm SEM) regularity index (A) and stride length (B) for male and female BALB/c Hgd^{-/-} and WT mice. All cohorts had a regularity index near 100% indicating no abnormalities in interlimb coordination (A). Hgd^{-/-} males had a significantly larger stride length than WT males. Female cohorts had similar stride lengths (B). **** = $P < 0.0001$

3.3.4.6 Maximum contact intensity (paw weight bearing)

Intensity of the print depends on the degree of contact between a paw and the glass plate and intensifies with increased weight bearing. Hgd^{-/-} female mice had significantly reduced contact intensity for all four paws compared with WT females (left forelimb: $t(15) = 5.515$, $P < 0.0001$, right forelimb: $t(15) = 4.071$, $P < 0.0010$, left hindlimb: $t(15) = 3.126$, $P < 0.0069$, right hindlimb: $t(15) = 2.391$, $P < 0.0304$). Male Hgd^{-/-} mice exhibited an increase in contact intensity of the left hindlimb compared with the same limb in WT males ($t(18) = 2.381$, $P < 0.0285$). No other significant limb differences were apparent between male cohorts (Fig. 3.15).

Maximum contact intensity

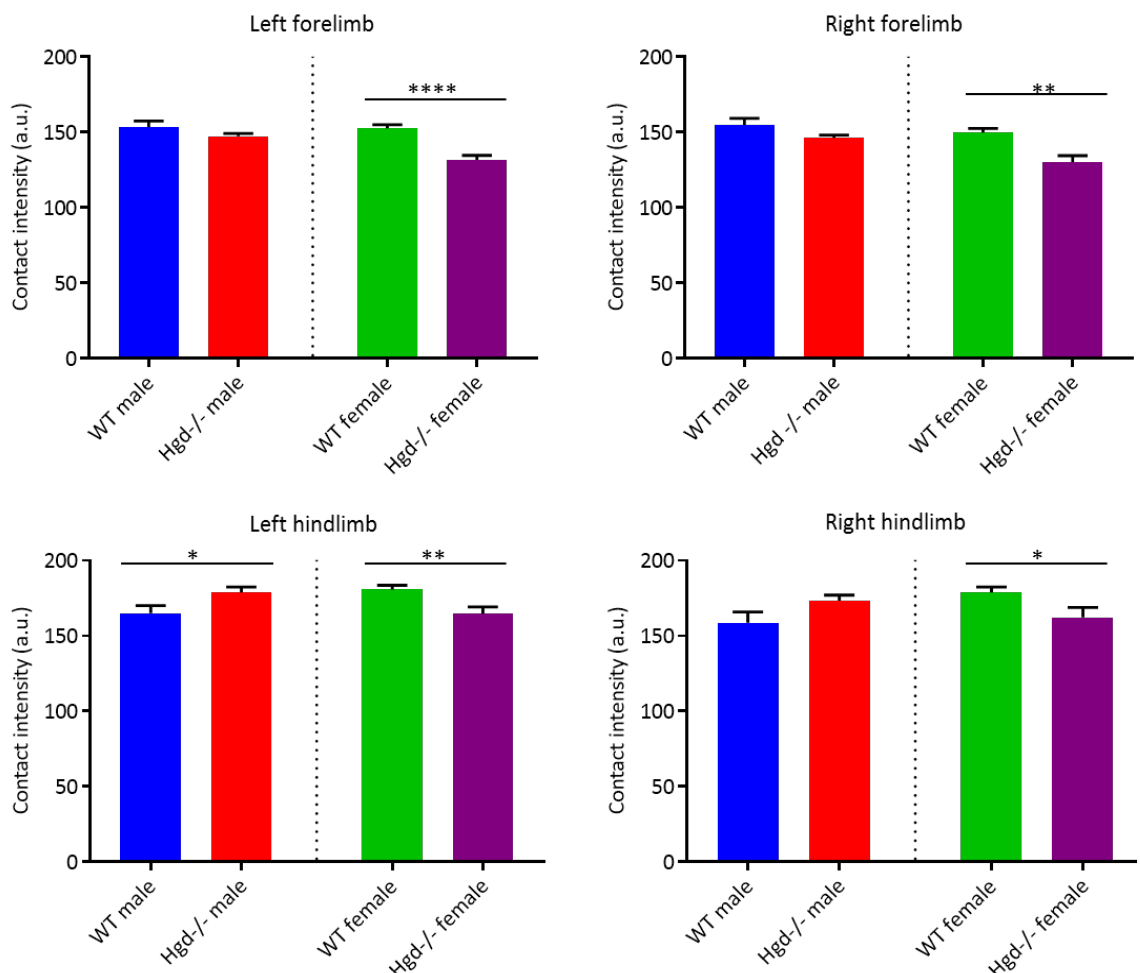


Figure 3.15 - Mean (\pm SEM) maximum contact intensity (arbitrary units ranging between 0 – 255) for male and female BALB/c Hgd^{-/-} and WT mice. Female Hgd^{-/-} mice had significantly reduced contact intensity in all four limbs compared to WT females. Male Hgd^{-/-}

/- mice showed an increase in contact intensity of the left hindlimb. * = $P < 0.05$, ** = $P < 0.01$, **** = $P < 0.0001$.

3.3.4.7 Print area

Hgd^{-/-} males had significantly larger print areas in all four limbs compared with WT males (left forelimb: $t(18) = 7.4$, $P < 0.0001$, right forelimb: $t(18) = 7.784$, $P < 0.0001$, left hindlimb: $t(18) = 7.11$, $P < 0.0001$, right hindlimb: $t(18) = 6.962$, $P < 0.0001$). Hgd^{-/-} female and WT females had similar print areas with no significant differences between limbs (Fig. 3.16).

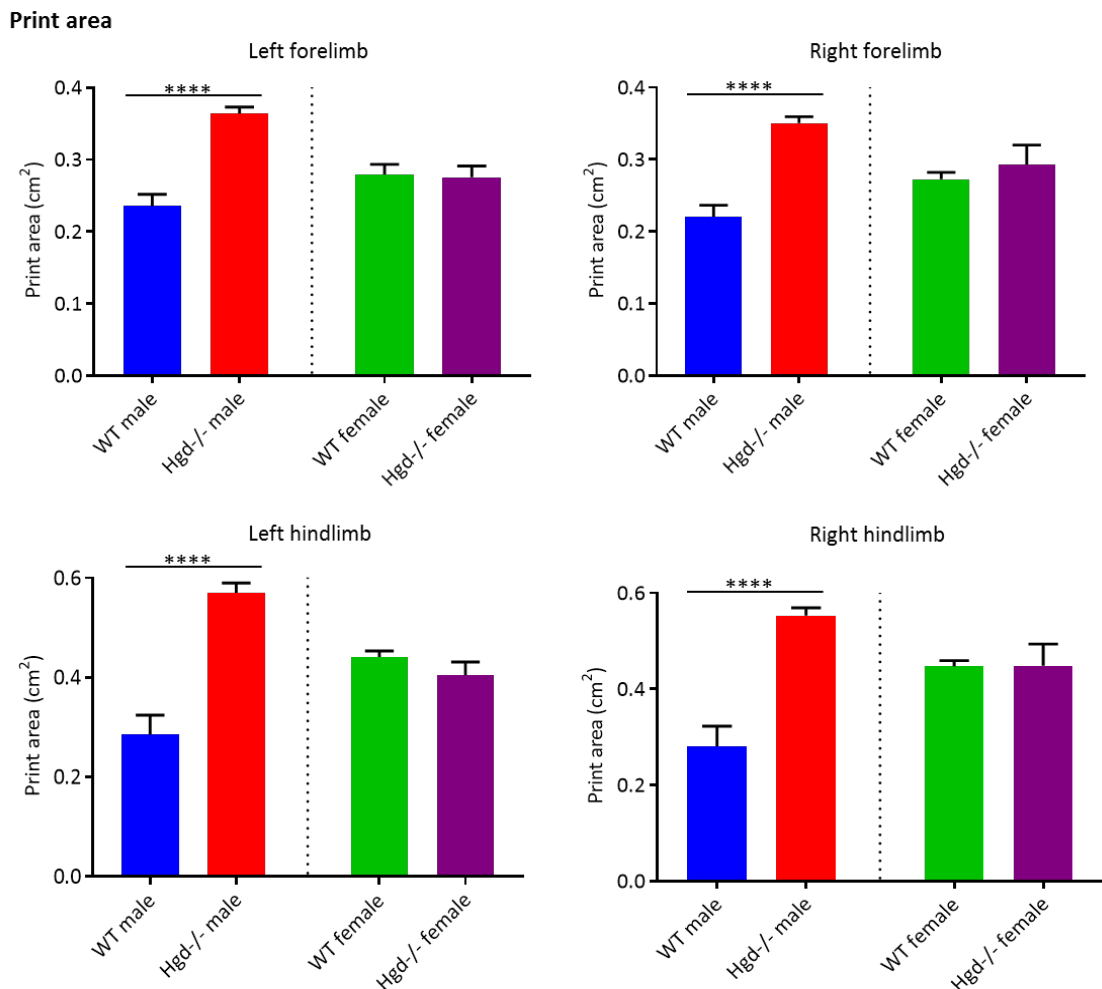


Figure 3.16 - Mean (\pm SEM) print area for male and female BALB/c Hgd^{-/-} and WT mice. Male Hgd^{-/-} mice had significantly larger print areas in all four limbs compared to WT males. Female cohorts had similar print areas with no significant differences between limbs. **** = $P < 0.0001$.

3.4 DISCUSSION

This study aimed to determine whether tyrosinemia as a potentially adverse side effect of nitisinone therapy has consequences relating to spatial learning, memory or motor function in Hgd^{-/-} or WT BALB/c mice. High levels of tyrosine have been linked to the delayed cognitive development and learning difficulties found in some patients with hereditary tyrosinemia type 1 (HT-1) who receive lifesaving nitisinone treatment from early life. The neurological and motor dysfunction associated with hereditary tyrosinemia type 3 (HT-3) has also been linked to the high levels of tyrosine present from birth within the condition [115]. The hypothesis at the beginning of this chapter was not supported by the results therefore the principle of using nitisinone in younger patients is valid.

3.4.1 Morris water maze

The MWM results indicated significant differences in spatial learning and memory between genotype but no significant effects of nitisinone treatment. This supports the earlier use of nitisinone in AKU patients. A recent AKU patient study investigating subclinical ochronotic features in alkaptonuria (SOFIA) observed pigmentation in the ear cartilage biopsy of a 16-year old male demonstrating that ochronosis can occur in AKU patients before this age [165]. This suggests that starting nitisinone therapy in childhood would likely be beneficial for patient prognosis. The genotypic differences were apparent from the first day of testing and remained a continuous finding across various measured parameters. WT control and treated mice showed significant improvements in performance throughout the hidden trials with the probe trial confirming they were able to form and recall spatial memory and utilise this for navigation (Fig. 3.7). Hgd^{-/-} control and treated mice showed minimal improvement throughout hidden trials and showed no preference to the target quadrant during the probe trial. This is an important finding as it may be an indication that Hgd^{-/-} mice are less able to use hippocampal dependent learning for navigation or could illustrate deficits in the mesolimbic dopaminergic pathway involved in motivation, in this case to escape the pool of water. Importantly, treatment with nitisinone or the related elevation in tyrosine did not have a significant effect on performance for any cohort in the MWM and there were no indications that treatment was detrimental to the learning process. This is in agreement with findings from a recent study by Hillgartner and colleagues who investigated learning in tyrosinemia type 1 (HT-1) and WT mice treated with nitisinone. HT-

1 mice showed slower learning and altered behaviour, which the authors concluded was a result of the HT-1 genotype and not due to treatment with nitisinone [116].

The results highlight that it would be useful to perform future trials with a control colony that were as matched to the Hgd^{-/-} mice as possible. It would be helpful to repeat some of the measurements in heterozygous mice generated by crossing some of the homozygous colony back with WT mice and selecting the heterozygotes that have the mutation in only one allele (Hgd^{+/-}). Time and resources were not sufficient to allow implementation of this proposed study within the present thesis but this should influence future work.

3.4.2 Motor function analysis

No obvious motor deficits were revealed in the Rota-rod or inverted grid suspension test in Hgd^{-/-} mice. Hgd^{-/-} cohorts performed better than WT in the accelerating Rota-rod test and improved with each trial indicating no deficits in coordination or motor function. Hgd^{-/-} and WT mice treated with nitisinone actually performed better than controls within the Rota-rod test although treatment was not a statistically significant factor (Fig. 3.8). The inverted grid suspension test showed no significant effect of genotype or nitisinone treatment (Fig. 3.9). Large intra-cohort variation was apparent but as this is an assessment of grip strength and the ability for the mouse to support its bodyweight this can be subject to normal variation between mice, as would be the case with human subjects. Similar to the Rota-rod, Hgd^{-/-} and WT cohorts receiving nitisinone performed marginally better than controls suggesting acute increases in circulating tyrosine due to nitisinone treatment may have aided with performance. Tyrosine is a precursor to the catecholamine neurotransmitters including dopamine which is involved in motivation, arousal and learning [117]. Previous studies have shown even single doses of tyrosine to have a significant effect on working memory especially in times of neurotransmitter depletion such as during a stressful or cognitively demanding task [118, 119]. Motor function could also be visually assessed by swimming ability in MWM – all cohorts swam at roughly the same speed showing no specific deficit in swimming ability. Swimming is non-weight bearing so this was a useful measure to remove variations due to bodyweight.

Throughout testing there were no obvious indicators of discomfort or pain (vocalisation, grimace, weight loss, piloerection) apparent in the Hgd^{-/-} mice, which may have been expected if mice were experiencing the same ochronotic arthropathy found in human AKU patients. Hgd^{-/-} mice were past the age that ochronotic pigmentation has been shown to initiate although none were past 25 weeks suggesting the painful osteoarthritis that might be associated with later stage ochronosis was not present. Hgd^{-/-} mice were noticeably more docile, less motivated to avoid human contact and easier to handle than WT mice after the same amount of prior handling. Anxiety related urination was also notably less although this was not quantitatively measured. AKU patients often report having depressed mood and fatigue [24, 27, 100] – this may also be the case for Hgd^{-/-} mice. Reduced motivation, anxiety and fear responses could indicate involvement of the mesolimbic dopaminergic pathway associated with these states. Dopamine is one of the neuromodulators most potently acting on the mechanisms underlying these. Disruptions within this pathway, perhaps due to synthesis of ochronotic pigment (also found to be similar to neuromelanin, itself produced from L-DOPA), may be taking place within AKU along with enhanced pigment production by the melanin-synthetic enzyme tyrosinase as suggested by Taylor and colleagues [41]. A murine study by Eisenhofer found changes in the function and expression of tyrosinase with advancing age whereby melanin synthesis became more pronounced and dopamine synthesis decreased [120]. Usually, tyrosinase converts tyrosine to a quinone intermediary to form melanin but in the AKU individual, and as Taylor [41] suggests, perhaps tyrosinase polymerises HGA instead leading to ochronotic pigment production. Eisenhofers findings also suggest this may contribute to why pigmentation increases with age in AKU as tyrosinase-dependent melanin synthesis, or in the case of AKU, ochronotic pigment synthesis, becomes more pronounced. The reduced tyrosinase-dependent dopamine production could also explain why patients experience low mood and fatigue.

3.4.3 Catwalk XT gait analysis

The Catwalk gait analysis system was able to detect small but significant differences in voluntary gait during movement at self-selected speed across a small distance. The analysis of the data showed differences within dynamic gait parameters (stance phase (Fig. 3.11), duty cycle (Fig. 3.13)) of Hgd^{-/-} males compared with WT males, indicated that these mice were spending a longer time during the weight bearing phases of the step cycle on their

hind limbs. A reason for this could simply be due to the Hgd^{-/-} males having a larger bodyweight and size (Fig. 3.10). Hgd^{-/-} males also had slight increases in both forelimb stance phases compared to WT males although these differences were not statistically significant. Gait characteristics are influenced by animal size with larger animal having been shown to have increased stance time and stride lengths [121]. Conversely, forelimb duty cycles showed no increase in the Hgd^{-/-} males, which would be expected if the differences were solely due to increased body size.

Previous studies investing gait in rodent models of arthritis have found these mice show a reduction in the weight bearing phases of an affected limb in an attempt to reduce load bearing that would cause pain [122, 123]. This is the case for unilateral models of arthritis where the condition is induced in a limb via injection of an irritant substance or mechanical damage caused by compression of the joint [109]. Transgenic models of osteoarthritis (OA) present with bilateral compensations due to systematic joint pathology [124-126]. By increasing the percentage of time spent on both hind limbs, the percentage of time a single hind limb must bear weight without contralateral support is reduced [127, 128]. This would represent a closer model to the Hgd^{-/-} mouse due to joint ochronosis also being systematic within load bearing joints. The increases observed in Hgd^{-/-} stance phase and duty cycle of the hindlimbs could be a sign that Hgd^{-/-} males are experiencing some change in hindlimb sensitivity and compensate with an altered gait pattern to minimise weight bearing on a single limb. Higher hind-limb stance times have been observed in type IX collagen deficient mice that prematurely develop osteoarthritis but this was combined with a slower velocity and shorter stride length in order to reduce force on the affected joint [129-131]. This was not the case for Hgd^{-/-} males who had a similar velocity and significantly larger stride length than WT males (Fig. 3.14B). Considering this, the differences in the dynamic gait parameters observed in Hgd^{-/-} male could be due to a slight pathologically altered gait, but is most likely due to larger bodyweight and size, as any effects were very small and nowhere near those observed in mice with induced OA. The only effect observed in female cohorts was a reduced maximum contact intensity in Hgd^{-/-} mice compared to WTs (Fig. 3.15). This parameter is often used to assess neuropathic pain whereby intensity would be reduced in a painful paw [132-134]. In this case, Hgd^{-/-} females showed a reduction across all four paws therefore this effect is mostly likely due to small differences in bodyweight between the female cohorts as WT females were slightly heavier. Regularity index and

stride lengths were similar for both genotypes and sexes and showed a consistent gait pattern and good interlimb coordination indicating no signs of ataxia. Overall gait analysis showed only minor effects that were dissimilar to those observed in mouse models of OA suggesting no obvious signs of pathologically altered gait.

3.4.4 Limitations

Mice ages varied within and between Hgd^{-/-} and WT cohorts due to constraints with colony size although the mean age (weeks) for cohorts used within the MWM, rotarod and IGST were similar (Hgd^{-/-} treated: 19.7, Hgd^{-/-} control: 19.2, WT treated: 18.1, WT control: 18.5). These mice were neither young nor aged and consequently the difference in age did not likely have a significant effect on the learning process. Age differences between Hgd^{-/-} and WT cohorts within the catwalk XT platform caused an effect due to the related increase in bodyweight that occurs as mice age, this was taken into account when examining parameter affected by bodyweight. Closer age matching should be considered for future experiments to remove this variable.

The findings of this chapter are promising for the use of nitisinone as a HGA reducing therapy in children with AKU. Behavioural and motor function assessment indicated no detrimental effects of nitisinone treatment or the associated tyrosinemia on cognition or motor function. Any effects in mice appeared to be due to the Hgd^{-/-} genotype and not nitisinone treatment. These findings aid in addressing the concerns regarding the neurotoxicity of elevated tyrosine in nitisinone treated children.

4. Balancing the reduction of plasma HGA and elevation of tyrosine in the treatment of AKU with nitisinone - a long-term dose response study in BALB/c Hgd^{-/-} mice.

4.1 INTRODUCTION

Nitisinone is highly efficacious as a reversible inhibitor of 4-hydroxyphenylpyruvate dioxygenase (HPPD), the enzyme responsible for homogentisic acid (HGA) synthesis [63]. Previous murine and human studies investigating nitisinone use in AKU have shown reduction of HGA to very low levels [71, 72, 55, 56]. A dose of 8mg per day (0.114mg/kg for 70kg human) reduced urinary HGA levels by 98.8% in the recent SONIA1 human study with the reasonable assumption that this is low enough to prevent ochronosis [55]. Preston et al have shown that administration of nitisinone at 4mg/L (0.5-0.8mg/kg for 30g mouse) in the Hgd^{-/-} mouse reduced plasma HGA throughout the mouse' lifetime and completely prevented further deposition of ochronotic pigment from start of treatment [70]. This study by Preston and colleagues along with previous work within our own lab used 4mg/L nitisinone; the dose originally determined by the Grompe lab that enabled the HT-1 FAH^{-/-} mouse model to survive. This FAH^{-/-} model was the strain from which our AKU Hgd^{-/-} mouse was derived [75].

HT-1 mice and patients require nitisinone at much higher doses (1-2mg/kg per day) to prevent fatal complications [141]. It is important to determine a dose in the Hgd^{-/-} mouse that provides therapeutic reduction of HGA whilst also minimising the elevation of tyrosine so that this can guide the calculation of dosage for AKU patients. There have been incidences of AKU patients treated with nitisinone who have shown predisposition to tyrosine toxicity independent of peak plasma levels. This manifests as reversible corneal keratopathy that requires suspension of treatment or reduction of dose to resolve [56, 57]. Tailoring the dose of nitisinone to provide a balanced compromise of HGA reduction whilst minimising the degree of tyrosinemia could therefore also benefit these patients to ensure uninterrupted treatment. The only previous nitisinone dose response study in Hgd^{-/-} mice within the literature by Keenan and colleagues found plasma HGA concentrations responded in a dose dependent manner with higher concentrations of nitisinone resulting in greater suppression of plasma HGA [72]. This dose response study by Keenan *et al* was short term (13 days) and started Hgd^{-/-} mice on nitisinone treatment at 54 weeks of age to investigate the effect on plasma HGA. The study contained within this chapter was long-term (40 weeks) and treated weanling (3 weeks old) Hgd^{-/-} mice with nitisinone, when the ochronotic pigmentation phase of the disease had yet to initiate. We aimed to investigate

the lowest dose that would reduce HGA sufficiently to prevent deposition of ochronotic pigment in the tibio-femoral joint.

4.2 HYPOTHESIS AND AIM OF STUDY

Hypothesis: Ochronotic pigmentation of the tibio-femoral joint in the Hgd^{-/-} mouse shows a dose relationship with nitisinone via plasma HGA concentration.

The primary aim of this long-term dose response study was to determine the lowest dose of nitisinone required to sufficiently reduce plasma HGA levels and prevent ochronotic pigmentation of chondrocytes within the Hgd^{-/-} mouse tibio-femoral joint. A second objective was to determine whether plasma HGA levels and the amount of ochronotic pigmentation within the tibio-femoral joint were correlated. Although there are many intermediates in the tyrosine pathway, HGA is the metabolite understood to be primarily responsible for the disease pathology of AKU. Along with HGA and tyrosine, this study also measured the metabolites upstream from the mechanism of action of nitisinone (HPPA, HPLA and Phenylalanine) in case these gave an indication of potential rate-limiting steps in the production of HGA or elucidated the status of alternative catabolic or excretory pathways. Establishing the minimum effective dose required to reduce plasma HGA levels and prevent ochronosis whilst simultaneously attempting to minimise the adverse effects of tyrosinemia as a result of nitisinone treatment is important for a human therapeutic strategy. As stated by Introne and colleagues, this is fundamental in reducing the cost of lifetime treatment and minimising potential side effects [56].

4.3 RESULTS

4.3.1 Plasma metabolites

4.3.1.1 Tyrosine

There was a marked dose-related increase in tyrosine at 20 weeks that was statistically significant between groups ($F(3,23) = 245.18, P < 0.0001$) (Fig. 4.1). Tyrosine levels were lowest in control mice (mean (\pm SE) 60.6 ± 4.8 $\mu\text{mol/L}$) and increased with nitisinone dose – $257.0 \pm 41.9 \mu\text{mol/L}$, $796.7 \pm 56.0 \mu\text{mol/L}$ and $1455.3 \pm 45.5 \mu\text{mol/L}$ for 0.125mg, 0.5mg and 2mg nitisinone respectively. The dose response of tyrosine to nitisinone appears to plateau at plasma levels of around $1400 \mu\text{mol/L}$ in BALB/c Hgd^{-/-} and WT mice. Treatment with a higher 4mg/L nitisinone dose from previous experiments have also shown tyrosine elevated to similar levels (Chapter 3, Fig. 3.1A). Post hoc Dunnetts test showed all doses were elevated significantly compared with control levels. Tyrosine levels measured at 40 weeks remained elevated in a dose responsive manner and were significantly different between groups ($F(3,21) = 73.702, P < 0.0001$) (Fig. 4.2). Post hoc tests showed 0.5mg and 2mg were significantly elevated compared with control.

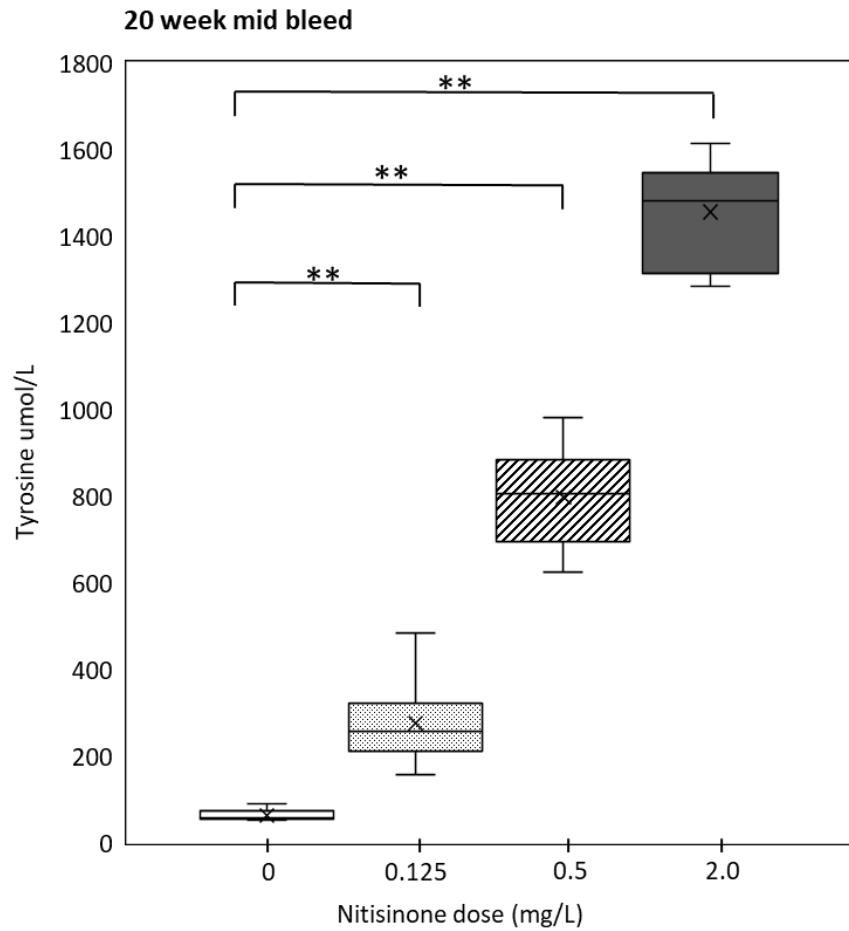


Figure 4.1 - Effects of nitisinone on plasma tyrosine levels after 20 weeks treatment in BALB/c Hgd^{-/-} mice. Tyrosine exhibited an elevated dose response with statistically significant differences between groups ($P < 0.0001$). Post hoc Dunnetts test showed all nitisinone doses resulted in significant elevation of tyrosine above control levels, 2mg cohort $n=7$, other cohorts $n=6$. ** = $P < 0.01$

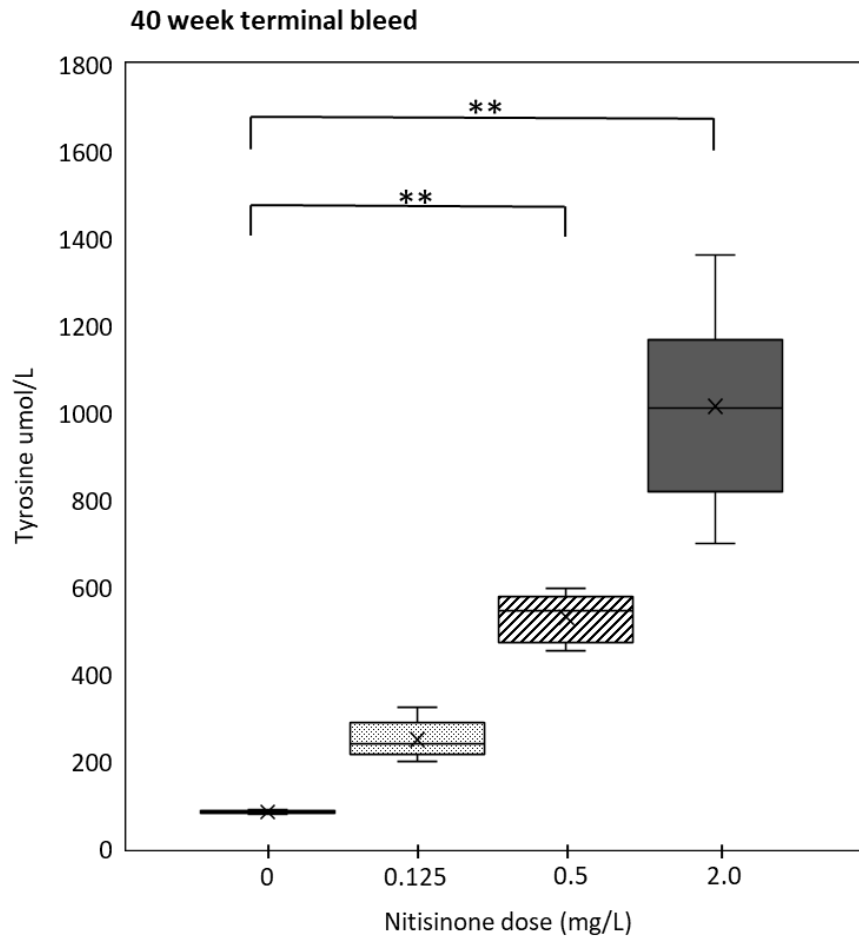


Figure 4.2 - Effects of nitisinone on plasma tyrosine levels after 40 weeks treatment in BALB/c Hgd^{-/-} mice. Tyrosine remained elevated in a dose responsive manner with significant differences between groups ($P < 0.0001$). Post hoc Dunnetts test showed significant elevation of tyrosine above control levels in 0.5mg and 2mg doses. 2mg cohort $n=7$, other cohorts $n=6$. ** = $P < 0.01$

Tyrosine levels showed variation between mid and term bleeds for the 0.5mg and 2mg nitisinone groups (Fig. 4.3). These were significantly lower in terminal bleeds compared with those measured in the mid bleed 20 weeks earlier. Paired t tests showed significant differences between mid and terminal bleeds for 0.5mg ($P=0.0013$) and 2mg nitisinone doses ($P=0.0004$). Although still elevated compared to control in both bleeds, mean tyrosine levels showed a reduction of 265.4 $\mu\text{mol/L}$ in the 0.5mg nitisinone group between bleeds and 440.3 $\mu\text{mol/L}$ in the 2mg nitisinone group between bleeds.

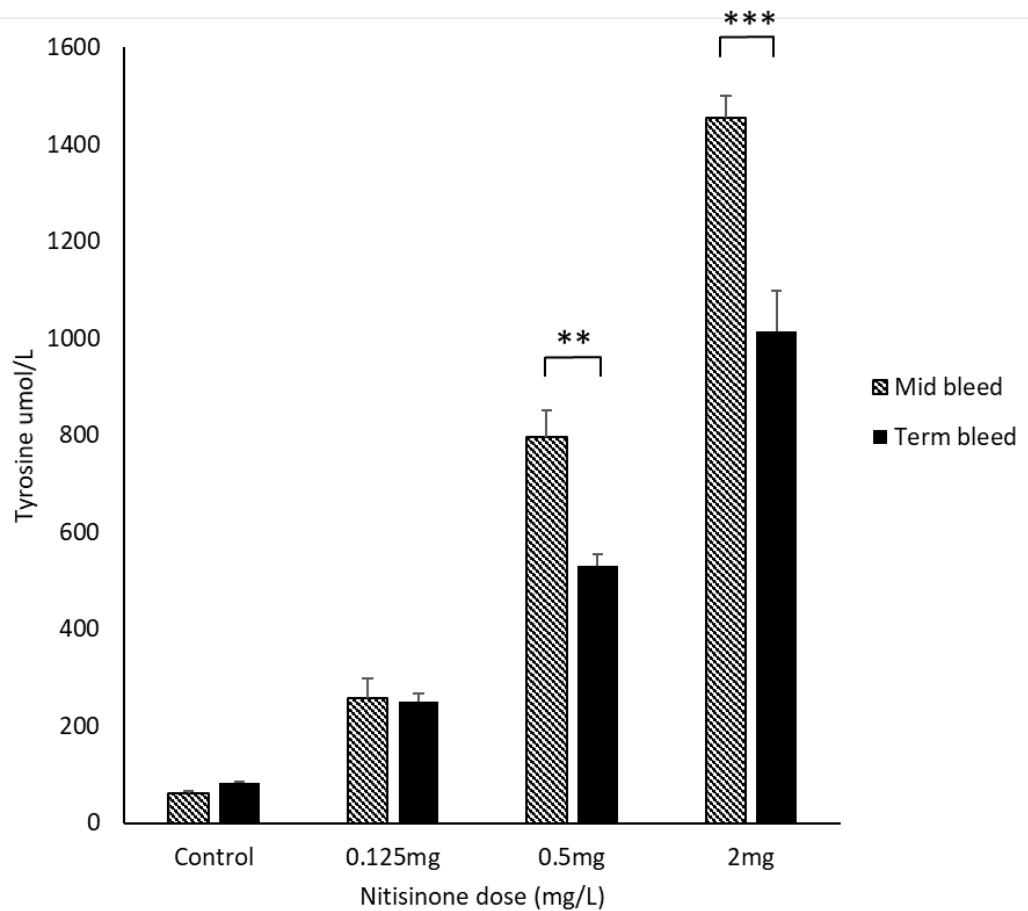


Figure 4.3 - Comparison of the effect of nitisinone dose on plasma tyrosine levels after 20 (mid) and 40 weeks (term) treatment in BALB/c Hgd^{-/-} mice. Elevation of tyrosine was lower after 40 weeks treatment in 0.5mg and 2mg nitisinone. 2mg cohort n=7, other cohorts n=6.. Significance from t test ** = $P<0.01$, *** = $P<0.001$. Mean \pm sem.

4.3.1.2 HGA

HGA levels measured at 20 weeks (mid-bleed) were significantly different between cohorts ($P=0.0009$) (Fig.4.4). There was high intra-cohort variability in HGA levels within control mice (range 147.6–356.7 $\mu\text{mol/L}$) and mice receiving 0.125mg (range 56.7-399.8 $\mu\text{mol/L}$) and 0.5mg nitisinone (range 133.4-357.6 $\mu\text{mol/L}$). Mice receiving 2mg nitisinone had the lowest HGA values and showed less variability between values (range 33.0-59.0 $\mu\text{mol/L}$). Mean HGA values showed a decreasing dose response as nitisinone dose increased. Dunnetts post hoc tests confirmed mice receiving 2mg nitisinone had significantly lower HGA levels compared with control ($P<0.01$). The 0.125mg and 0.5mg nitisinone dose lowered mean plasma HGA but this was not statistically significant compared with control.

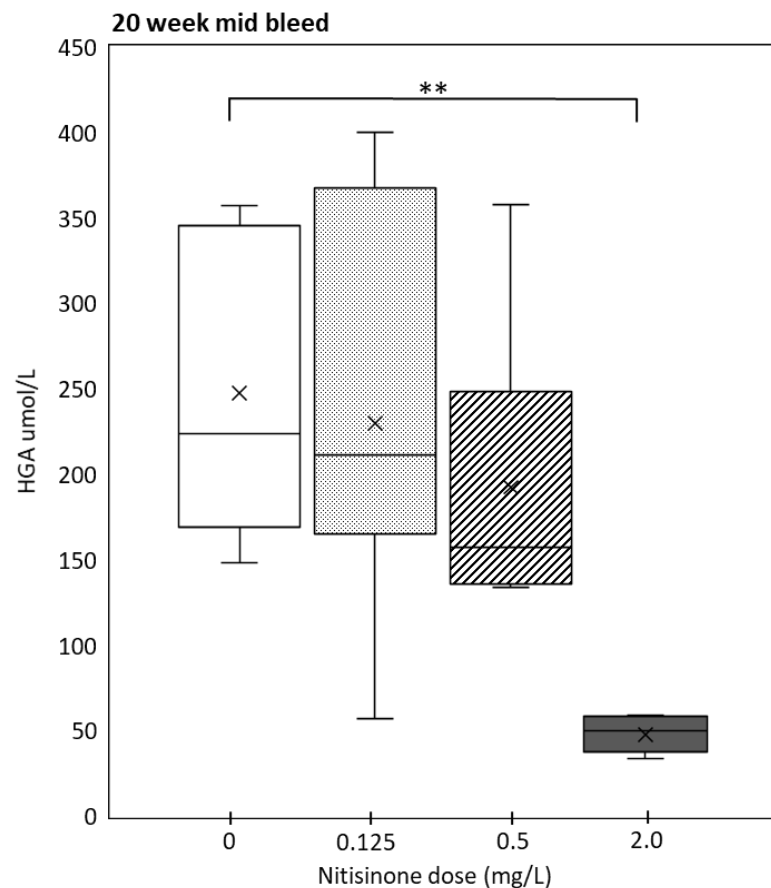


Figure 4.4 - Effect of nitisinone on plasma HGA after 20 weeks treatment in BALB/c Hgd^{-/-} mice. Large intra-cohort variation was apparent between control, 0.125mg and 0.5mg nitisinone. Post hoc Dunnetts test showed 2mg nitisinone significantly reduced HGA levels compared with control. 2mg cohort n=7, other cohorts n=6. ** = $P<0.01$

Terminal bleed plasma HGA levels showed a stronger, decreasing dose response relationship with significant differences between groups ($P < 0.0001$) (Fig. 4.5). Less intra-cohort variation was also apparent. Mice receiving 0.5mg and 2mg nitisinone showed significantly lower HGA values compared with control mice ($P < 0.01$). Mice receiving 0.125mg showed a reduction in HGA compared with control but also contained an outlier with a HGA value higher than that of control mice. One-way ANOVA with post hoc test was performed including and omitting this result, in each case 0.125mg nitisinone also resulted in a significant reduction in HGA compared with control ($P < 0.05$).

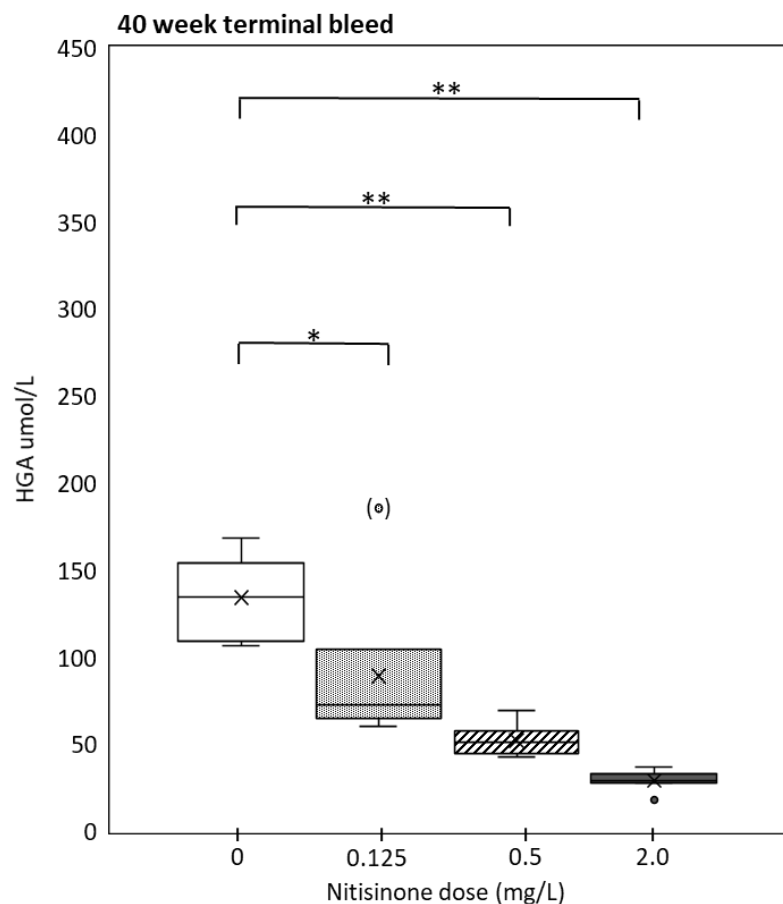


Figure 4.5 - Effect of nitisinone on plasma HGA levels after 40 weeks treatment in BALB/c Hgd^{-/-} mice. HGA reduced significantly in all mice receiving nitisinone compared with control. 2mg cohort n=7, other cohorts n=6. Significance from post hoc Dunnetts test * = $P < 0.05$, ** = $P < 0.01$

Plasma HGA levels were reduced within all dose cohorts including control between mid and term bleeds (Fig. 4.6). Terminal bleed HGA values were significantly lower in all treatment groups compared with mid bleed values collected 20 weeks previously within the same cohort. Unexpectedly, in view of previous work that showed a relatively constant HGA level across the mouse lifetime [70], mean HGA values were significantly reduced by 46% between mid and term bleeds in control mice ($P=0.0322$). A similar reduction was seen in mice receiving 2mg nitisinone ($\downarrow 40\%$, $P=0.0142$). Mice receiving 0.125mg and 0.5mg nitisinone followed the same trend with 61% ($P=0.0168$) and 73% ($P=0.0117$) reduction respectively in mean HGA levels in terminal bleeds compared with mid bleeds. This apparent discrepancy in plasma HGA is investigated further in chapter 5 of this thesis.

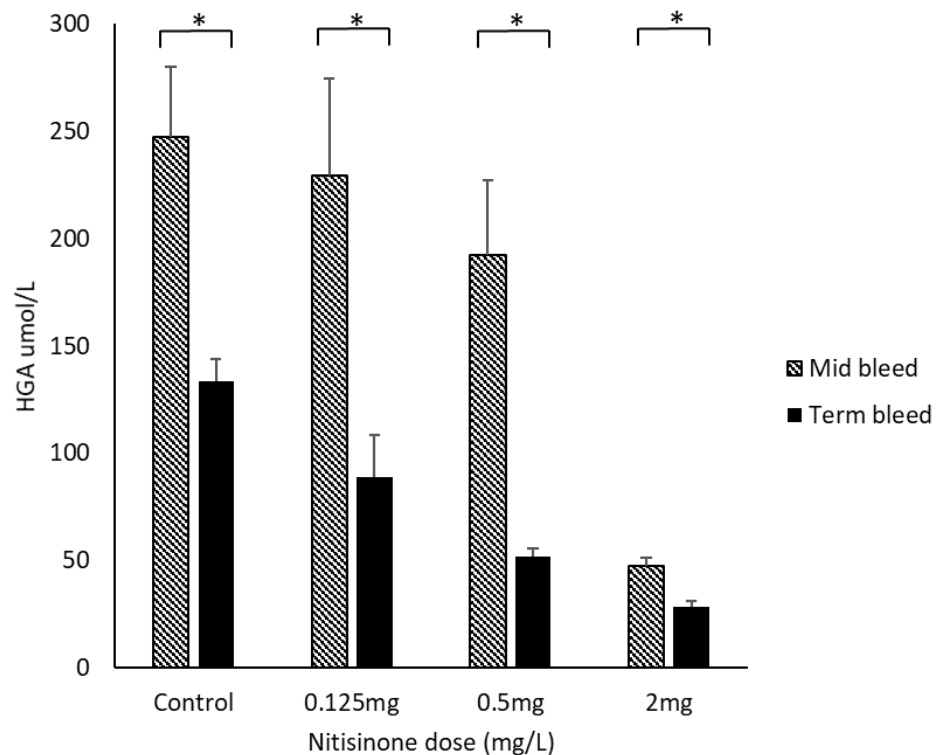


Figure 4.6 - Comparison of effects of nitisinone dose on plasma HGA levels after 20 (mid) and 40 (term) weeks treatment in BALB/c Hgd^{-/-} mice. Plasma HGA values were significantly lower in samples taken at 40 weeks in control and nitisinone treated mice compared to those sampled at 20 weeks. 2mg cohort n=7, other cohorts n=6. Significance from t test * = $P < 0.05$. Mean \pm sem.

There was high variability in plasma HGA concentrations consistent with that observed in AKU patients [55, 56, 58] and previous murine studies (70, 72). This variability was apparent within mice of the same cohort (often littermates of the same inbred strain) and within the same mouse at different time points. Variation in HGA was higher in 20 week mid bleed samples compared to 40 week term samples for all but the 0.125mg cohort due to a high value outlier at the terminal bleed (table 4.1).

Nitisinone Dose mg/L	HGA mid bleed coefficient of variation (%)	HGA term bleed coefficient of variation (%)
0	35.4	18.2
0.125	52.0	53.4
0.5	45.1	18.3
2.0	22.6	20.6

Table 4.1 – Coefficient of variation for HGA from mid and term bleeds. Variability was lowest in 2mg nitisinone at the mid-term bleed. Variability was lower in terminal compared to mid bleeds in all but the 0.125mg cohort due to a high outlier. 2mg cohort n=7, other cohorts n=6.

4.3.1.3 Phenylalanine

Phenylalanine plasma values sampled at the 20 week mid bleed showed significant variation between groups ($P < 0.0001$). Mice receiving 2mg nitisinone had significantly elevated levels compared with control mice ($P < 0.01$) (Fig 4.7). Phenylalanine did not fluctuate significantly compared with control in mice receiving 0.125mg or 0.5mg nitisinone. However, terminal bleed phenylalanine values showed no significant fluctuation compared to control mice for any nitisinone doses (Fig 4.8).

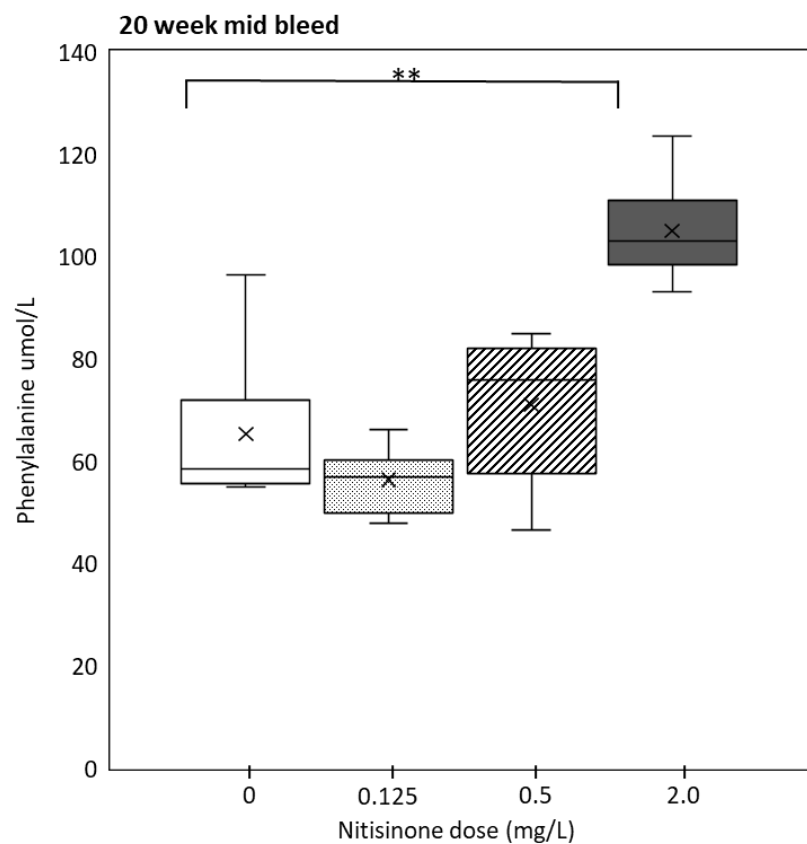


Figure 4.7 - Effect of nitisinone on plasma phenylalanine after 20 weeks treatment in BALB/c Hgd^{-/-} mice. Mice receiving the highest 2mg dose of nitisinone showed significantly elevated phenylalanine levels compared to control. 2mg cohort n=7, other cohorts n=6. Significance from post hoc Dunnetts test ** = $P < 0.01$.

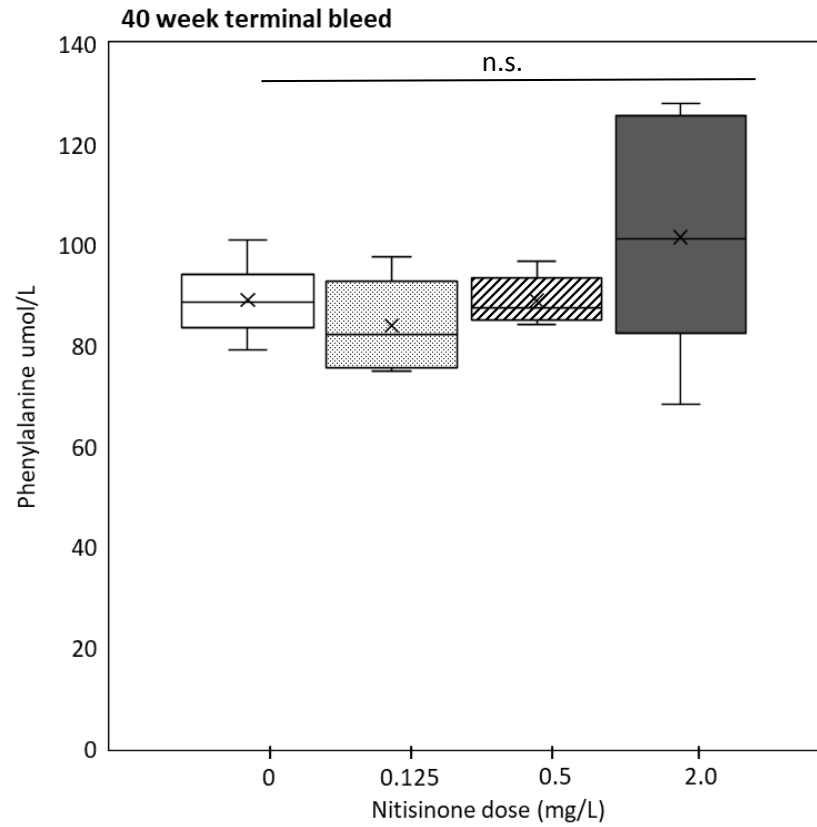


Figure 4.8 - Effects of nitisinone on plasma phenylalanine after 40 weeks treatment in BALB/c Hgd^{-/-} mice. No significant differences were apparent between cohorts. 2mg cohort n=7, other cohorts n=6.

A significant difference between mid and terminal bleeds was observed in control mice ($P=0.0035$) and in mice receiving 0.125mg nitisinone ($P=0.0001$) (Fig. 4.9) Mice receiving 0.5mg nitisinone also showed variation between mid and terminal bleed values but this was not statistically significant.

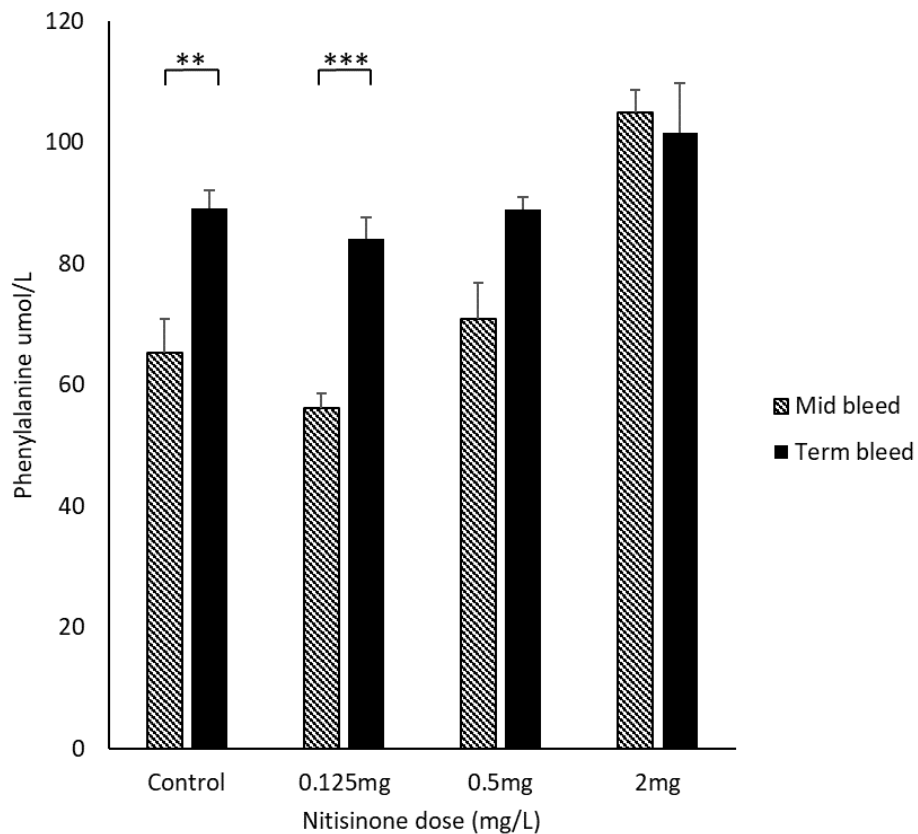


Figure 4.9 - Comparison of the effects of nitisinone dose on plasma phenylalanine levels after 20 (mid) and 40 (term) weeks treatment in BALB/c Hgd^{-/-} mice. Control and 0.125mg cohorts showed significantly elevated plasma phenylalanine in samples collected at 40 weeks compared to 20 weeks. Significance from t test ** = $P<0.01$, *** = $P<0.001$. Mean \pm sem, 2mg cohort $n=7$, other cohorts $n=6$.

4.3.1.4 HPPA

Plasma HPPA values measured at 20 weeks were significantly different between cohorts ($P < .0001$). HPPA was elevated in line with nitisinone dose (Fig. 4.10). All mice within the control cohort had HPPA values below the detection range ($< 10 \mu\text{mol/L}$), the value of $10 \mu\text{mol/L}$ was therefore assigned to the control group for analysis. Mice receiving 0.5 mg and 2 mg nitisinone showed significantly elevated HPPA levels compared with control ($P < 0.01$). Intra-cohort variation within the 0.5 mg and 2 mg dose mice was also higher compared with control and 0.125 mg cohorts.

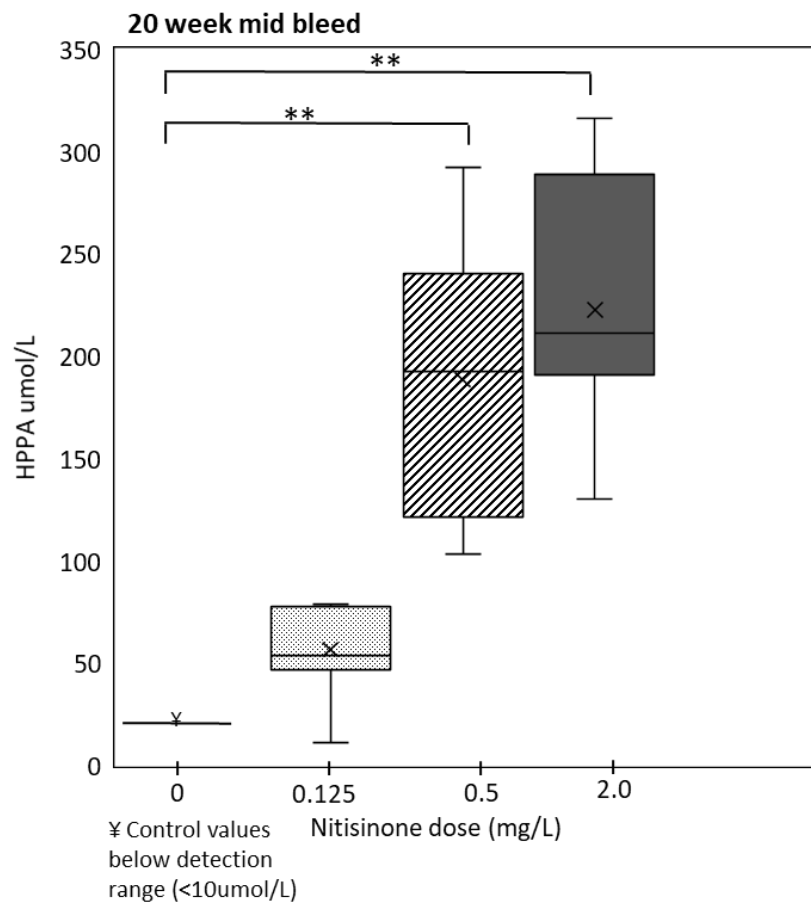


Figure 4.10 - Effect of nitisinone dose on plasma HPPA levels after 20 weeks treatment in BALB/c Hgd^{-/-} mice. HPPA shows a significant and elevated dose response to nitisinone. 2 mg cohort $n=7$, other cohorts $n=6$. Significance from post hoc Dunnetts test $** = P < 0.01$.

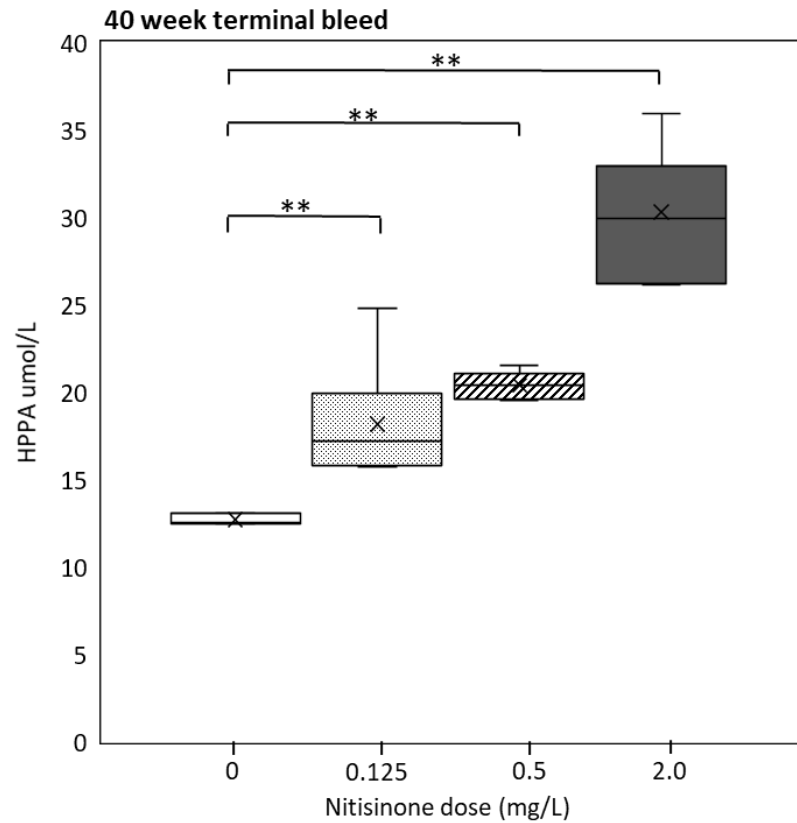


Figure 4.11 - Effect of nitisinone dose on plasma HPPA levels after 40 weeks treatment in BALB/c Hgd^{-/-} mice. An elevated dose response was still evident at 40 weeks although this was less marked than the response at 20 weeks and HPPA values were lower in all nitisinone treated cohorts. 2mg cohort n=7, other cohorts n=6. Significance from post hoc Dunnetts test ** = P<0.01.

Plasma HPPA values sampled at 40 weeks were significantly reduced compared to the 20 week mid bleed in nitisinone treated cohorts. Although a dose response was still evident with HPPA values highest in the 2mg cohort and these reducing in line with nitisinone dose (Fig. 4.11), all cohorts receiving nitisinone had HPPA values markedly lower, similar to the effect seen in HGA at 40 weeks (Fig. 4.6). T test results showed HPPA levels within cohorts were significantly reduced between mid and terminal bleeds for 0.125mg (P=0.0255), 0.5mg (P=0.0020) and 2mg (P=0.0002) nitisinone doses (Fig. 4.12). These and other metabolite discrepancies are addressed in chapter 5 of this thesis.

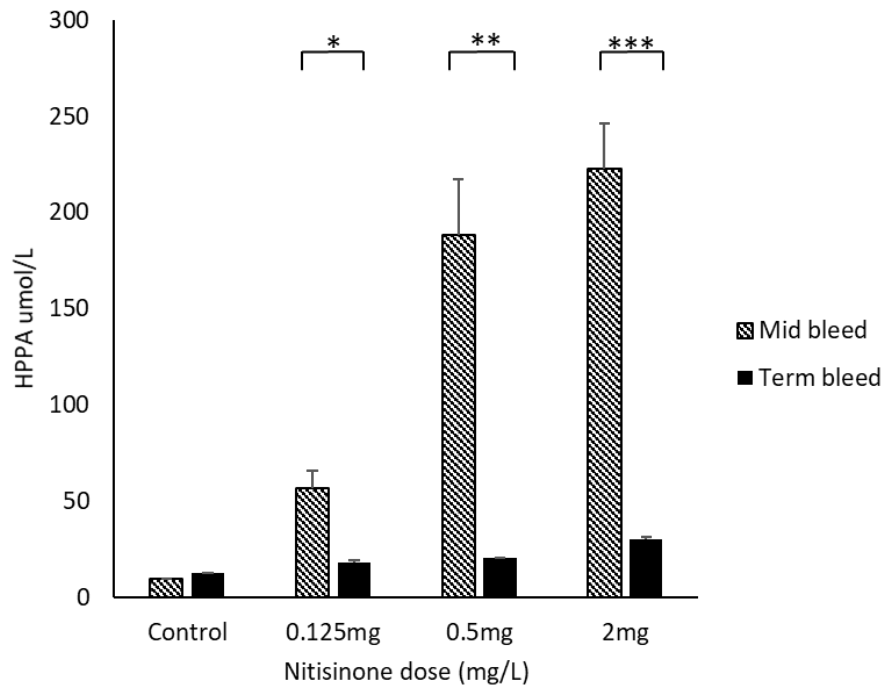


Figure 4.12 - Comparison of the effects of nitisinone dose on plasma HPPA levels after 20 (mid) and 40 (term) weeks treatment in BALB/c Hgd^{-/-} mice. Plasma HPPA was significantly reduced in nitisinone treated cohorts at 40 weeks. Significance from t tests * = $P < 0.05$, ** = $P < 0.01$, *** = $P < 0.001$. Mean \pm sem, 2mg cohort n=7, other cohorts n=6.

4.3.1.5 HPLA

Plasma HPLA levels at 20 weeks showed an elevated dose response in nitisinone treated cohorts compared to control with significant differences between cohorts ($P < 0.0001$) (Fig. 4.13). Control HPLA values were below detection rate ($< 5 \mu\text{mol/L}$) so these were set at $5 \mu\text{mol/L}$ for analysis. 0.125mg nitisinone dose caused elevation of HPLA compared to control but Dunnetts post hoc test showed this was not significant. 0.5mg and 2mg nitisinone caused significant elevation of HPLA compared with control ($P < 0.01$). A similar effect was observed for plasma HPLA at 40 weeks, which remained elevated in a dose responsive manner in mice receiving nitisinone compared with control (Fig. 4.14).

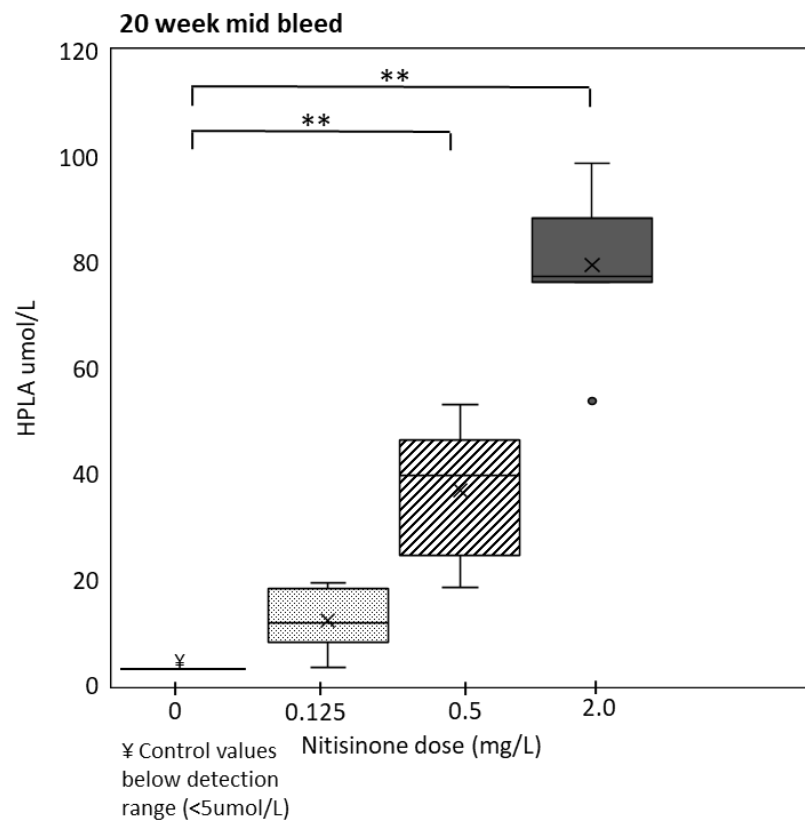


Figure 4.13 - Effect of nitisinone dose on plasma HPLA levels after 20 weeks treatment in BALB/c Hgd^{-/-} mice. 0.5mg and 2mg resulted in significantly elevated HPLA compared to control. 0.125mg had no significant effect on HPLA. 2mg cohort $n=7$, other cohorts $n=6$. Significance from post hoc Dunnetts test ** = $P < 0.01$.

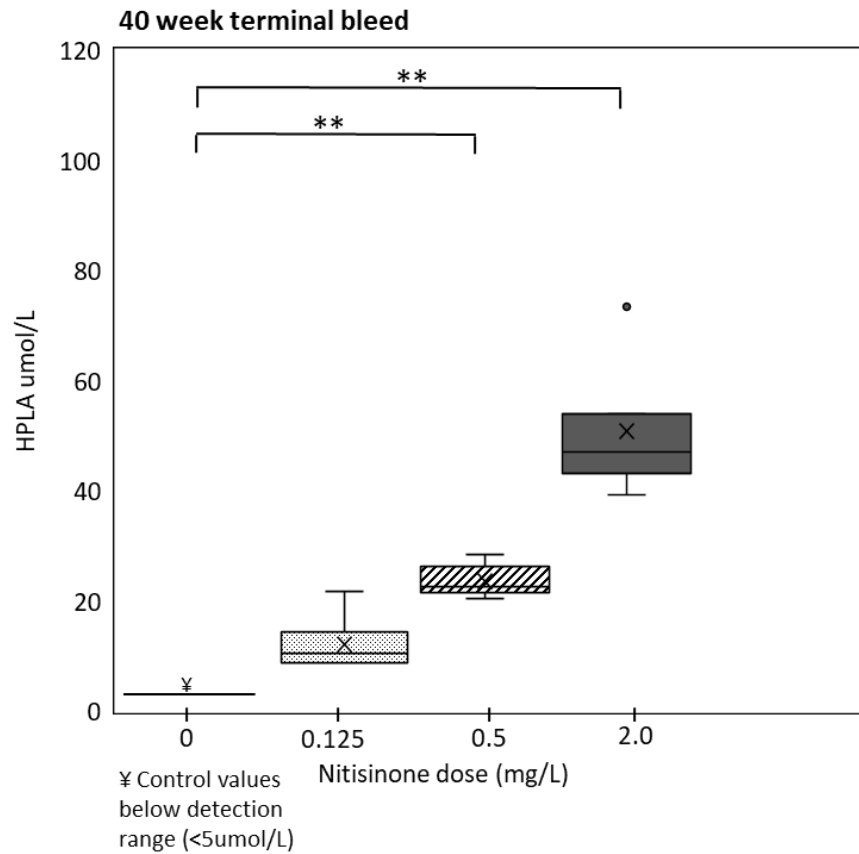


Figure 4.14 - Effect of nitisinone dose on plasma HPLA levels after 40 weeks treatment in BALB/c Hgd^{-/-} mice. 0.5mg and 2mg resulted in significantly elevated HPLA compared to control. 0.125mg had no significant effect on HPLA. 2mg cohort n=7, other cohorts n=6. Significance from post hoc Dunnetts test ** = P<0.01.

Mice receiving 0.5mg and 2mg nitisinone showed a significant reduction in mean plasma HPLA levels between 20 and 40 weeks bleeds (t test $P=0.0406$ and $P=0.0015$ respectively) (Fig. 4.15). Similar discrepancies were found HGA and HPPA (Fig. 4.6 and Fig. 4.12 respectively) in which plasma values were also significantly lower at 40 weeks compared to 20 weeks despite no change in treatment. These findings are investigated further in chapter 5 of this thesis.

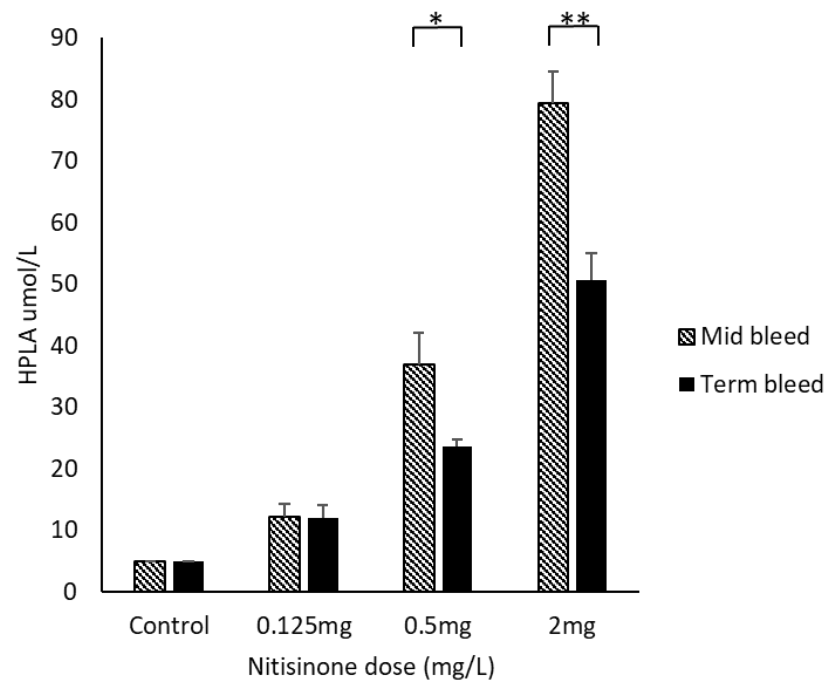


Figure 4.15 - Comparison of the effects of nitisinone dose on plasma HPLA levels after 20 (mid) and 40 (term) weeks treatment in BALB/c Hgd^{-/-} mice. Plasma HPLA was significantly lower at 40 weeks compared to 20 weeks in 0.5mg and 2mg nitisinone treated mice. Significance from t test * = $P<0.05$, ** = $P<0.01$. Mean \pm sem, 2mg cohort $n=7$, other cohorts $n=6$.

Overall, a systematic dose response to nitisinone was observed for all metabolites measured (Fig. 4.16, Fig 4.17). Phenylalanine appeared to be the most stable metabolite over the series of doses investigated displaying only minor fluctuations compared to control values. HGA, HPPA and HPLA values differed significantly within the same cohorts between mid and terminal plasma samples in nitisinone treated mice. Unexpectedly, HGA was also significantly different between mid and terminal samples in control mice who received no nitisinone treatment. These results prompted a further study to investigate whether this was a methodological or genuine finding, the results of which are presented and discussed in chapter 5 of this thesis.

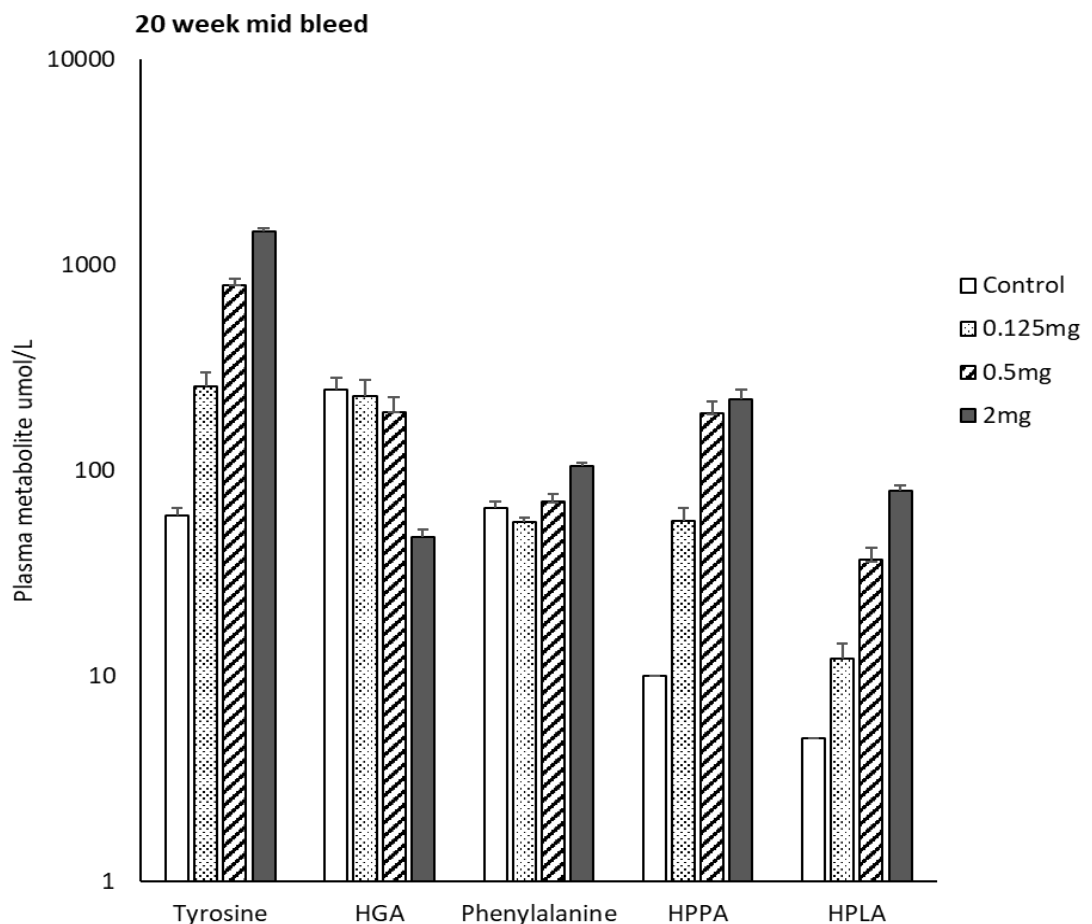


Figure 4.16 - Overall effect of nitisinone dose on plasma metabolites measured after 20 weeks treatment (mid bleed) in BALB/c Hgd^{-/-} mice. All metabolites showed a systematic dose response to nitisinone. Logarithmic scale to enable inclusion of tyrosine values and clarity of response in other metabolites. Mean \pm sem, 2mg cohort n=7, other cohorts n=6.

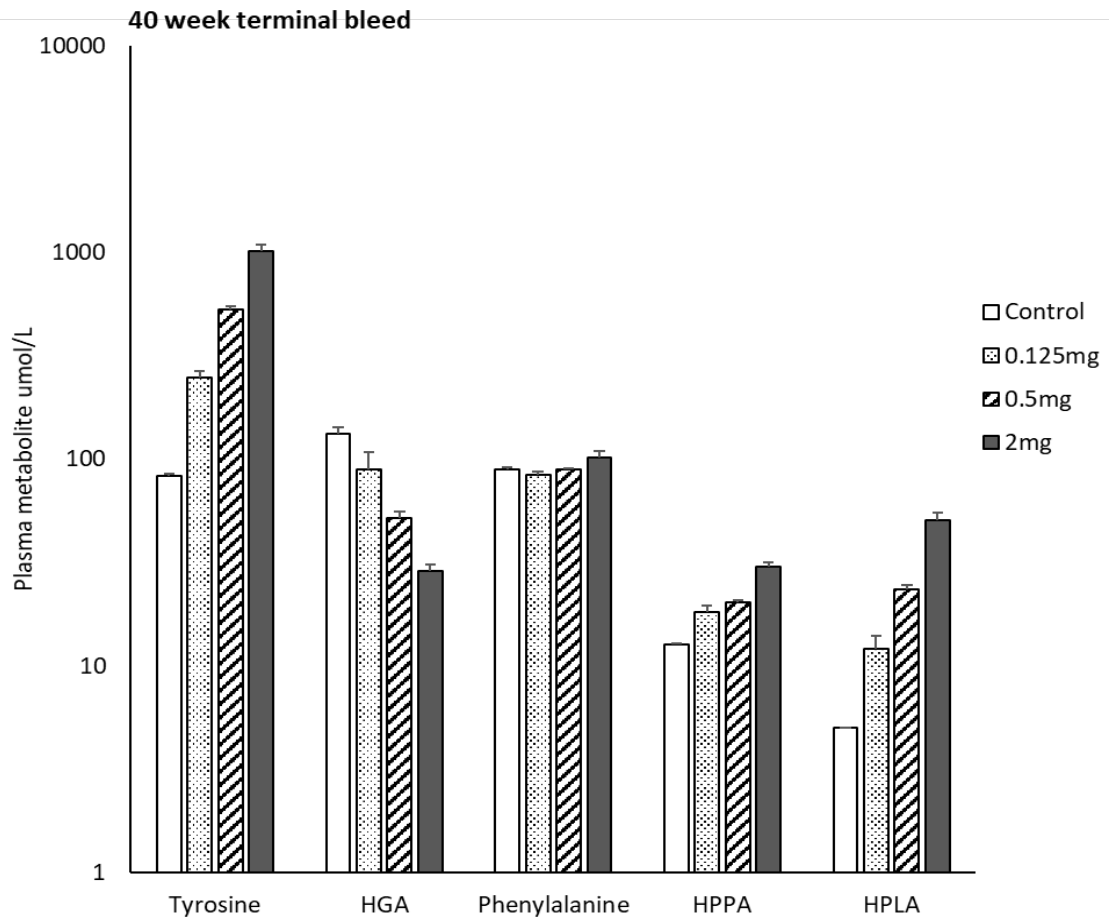


Figure 4.17 - Overall effect of nitisinone dose on plasma metabolites measured after 40 weeks treatment (terminal bleed) in BALB/c Hgd^{-/-} mice. All metabolites showed a similar systematic dose response to nitisinone as observed in the 20 week mid bleed although values for HGA, HPPA and HPLA had decreased. Logarithmic scale to enable inclusion of tyrosine values and clarity of response in other metabolites. Mean \pm sem, 2mg cohort n=7, other cohorts n=6.

4.3.2 Pigmentation quantification

Two classification methods were used for quantification of pigmentation in the Hgd/- mouse tibio-femoral joint – cellular staining only and peri-cellular and cellular staining combined. Both classification methods showed the same dose response for pigmentation measured in post mortem histological sections of the tibio-femoral joint – a decrease in pigmented chondrocytes for mice receiving 0.5mg and 2mg nitisinone compared with control (Fig. 4.18). Pigmentation was highest in control mice and those receiving 0.125mg nitisinone. Mice within these groups showed high intra-cohort variation in pigmentation levels. The lowest 0.125mg nitisinone dose did not significantly reduce pigmentation compared with control for either pigmentation classification method. A slight increase in mean(\pm sem) pigmentation was observed in the 0.125mg dose compared with control (184.8 \pm 25.3 pigmented chondrons per histological section increasing to 197.8 \pm 27.1 respectively). Mean pigmentation in the 0.5mg dose cohort was significantly lower compared with control in both classifications of pigmentation ($P < 0.01$). The 2mg/L dose further significantly lowered pigmentation compared with control ($p < 0.0001$). Overall, mean(\pm sem) cellular pigmentation levels reduced from 184.8 \pm 25.3 in the control group to 43.0 \pm 8.2 and 5.1 \pm 1.5 in the 0.5mg/L and 2mg/L group respectively.

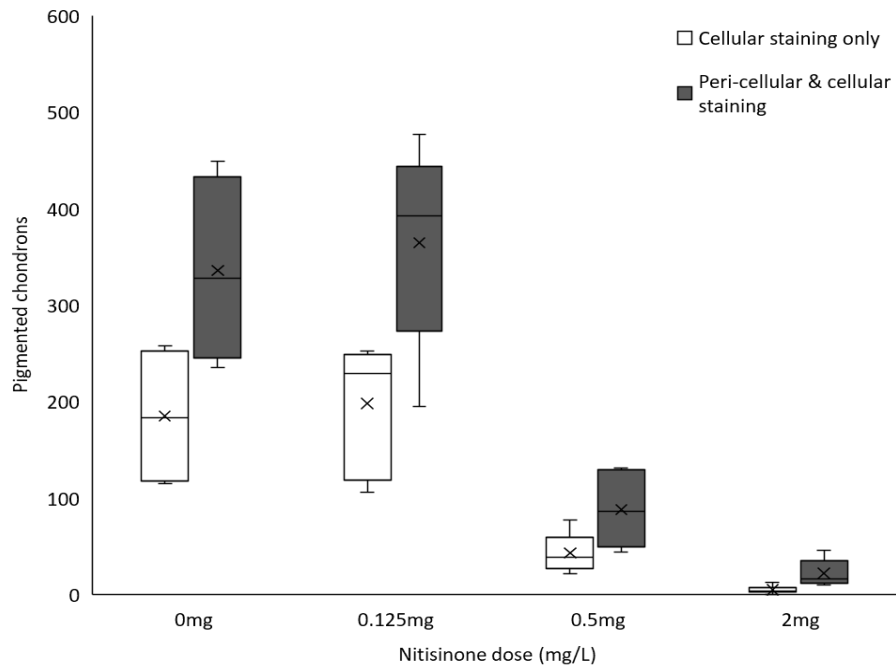


Figure 4.18 - Quantification of pigmented chondrocytes counts showing both classification methods - cellular staining only and peri-cellular and cellular staining combined, 2mg cohort n=7, other cohorts n=6. Stained with Schmorls reagent. Both classification systems show a significant dose response for pigmentation. The number of pigmented chondrocytes appeared to be unaffected by the lowest 0.125mg dose with pigmentation levels being similar to the control group. Pigmentation decreased by over 75% for the 0.5mg group when compared to the control and 0.125mg groups. A similar dose response trend was observed in mice receiving 2mg nitisinone with pigmentation showing a drop of around 75% compared with the 0.5mg dose.

4.3.2.1 Inter-observer variability

Both classification systems of pigmentation of chondrocytes produced consistent quantification with matching pigmentation trends for doses independent of the classification system used. To assess reliability of quantification, a second observer repeated cellular pigmentation counts for two sections from each cohort (Fig 4.19). An intraclass correlation coefficient (ICC) test with absolute agreement was run for pigmentation counts to assess inter-observer variability. The ICC was 0.96 and was significantly difference from 0 ($P = 0.001$) indicating excellent correlation and low inter-observer variability. Pearson's correlation coefficient was 0.9223 and indicated a positive linear correlation. This confirmed the reliability of the cellular pigmentation classification method. For this reason, the cellular classification quantified data was selected for use in subsequent analysis (Table 4.2).

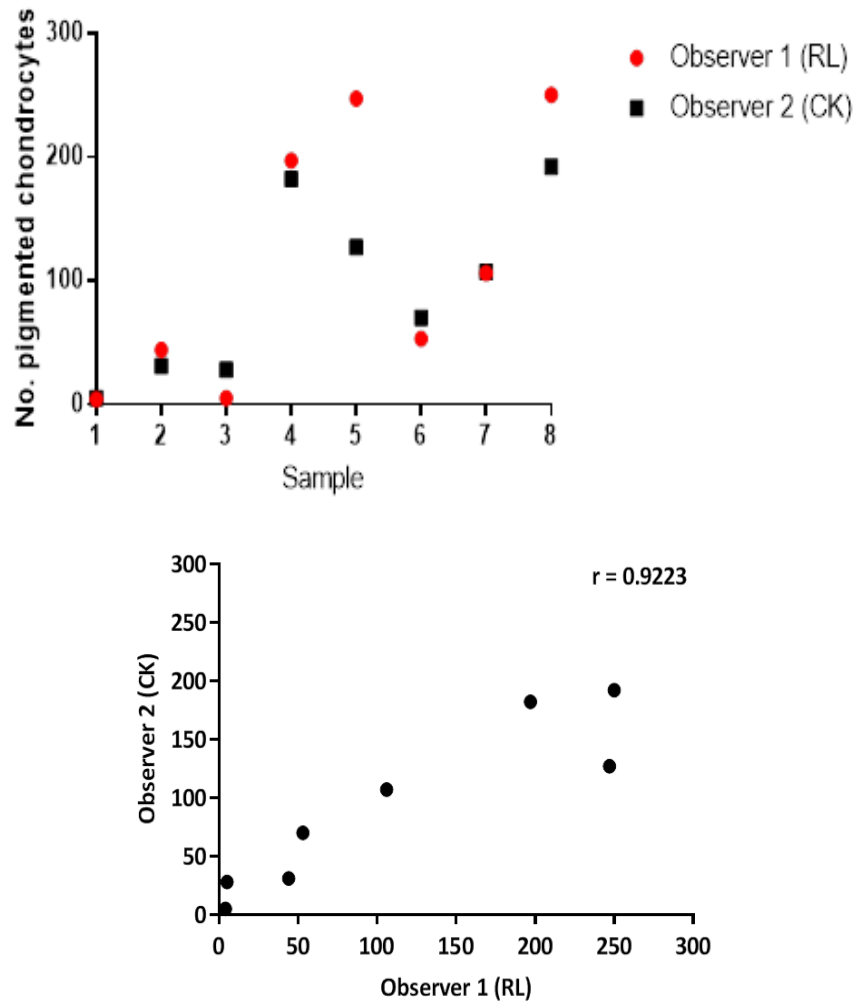


Figure 4.19 - Inter-observer variability and correlation of cellular pigmentation quantification method. Scatter charts demonstrating low variability in the number of pigmented chondrocytes between two independent observers (RL and CK).

Nitisinone Dose (mg/L)	n	Pigmentation classification	Mean	SD	SEM
0 control	7	Cellular	184.8	61.9	25.3
		Cellular + peri-cellular	335.8	92.2	37.6
0.125	6	Cellular	197.8	66.4	27.1
		Cellular + peri-celluar	364.7	104.0	42.5
0.5	6	Cellular	43.0	20.0	8.2
		Cellular + peri-cellular	88.0	37.7	15.4
2	6	Cellular	5.1	4.1	1.5
		Cellular + peri-cellular	21.9	13.7	5.2

Table 4.2 - Quantification of mean pigmentation in the tibio-femoral joint of 43 week old control and nitisinone treated BALB/c Hgd^{-/-} mice.

4.3.3 Pigmentation in BALB/c Hgd^{-/-} tibio-femoral joint

4.3.3.1 Control mice

Extensive cellular and peri-cellular ochronotic pigmentation was apparent throughout the articular calcified cartilage (ACC) of the tibio-femoral joint in control mice (Fig 4.21, Fig. 4.22). Pigmentation was also present in the intercondylar regions and fibrocartilaginous entheses where attachment of ligaments result in areas of high stress. (Fig. 4.20). Control mice showed high variation in pigmentation levels (cellular range: 119-258, peri-cellular range: 235-449) and had high levels of peri-pigmented chondrocytes in the early stages of ochronotic pigment deposition.

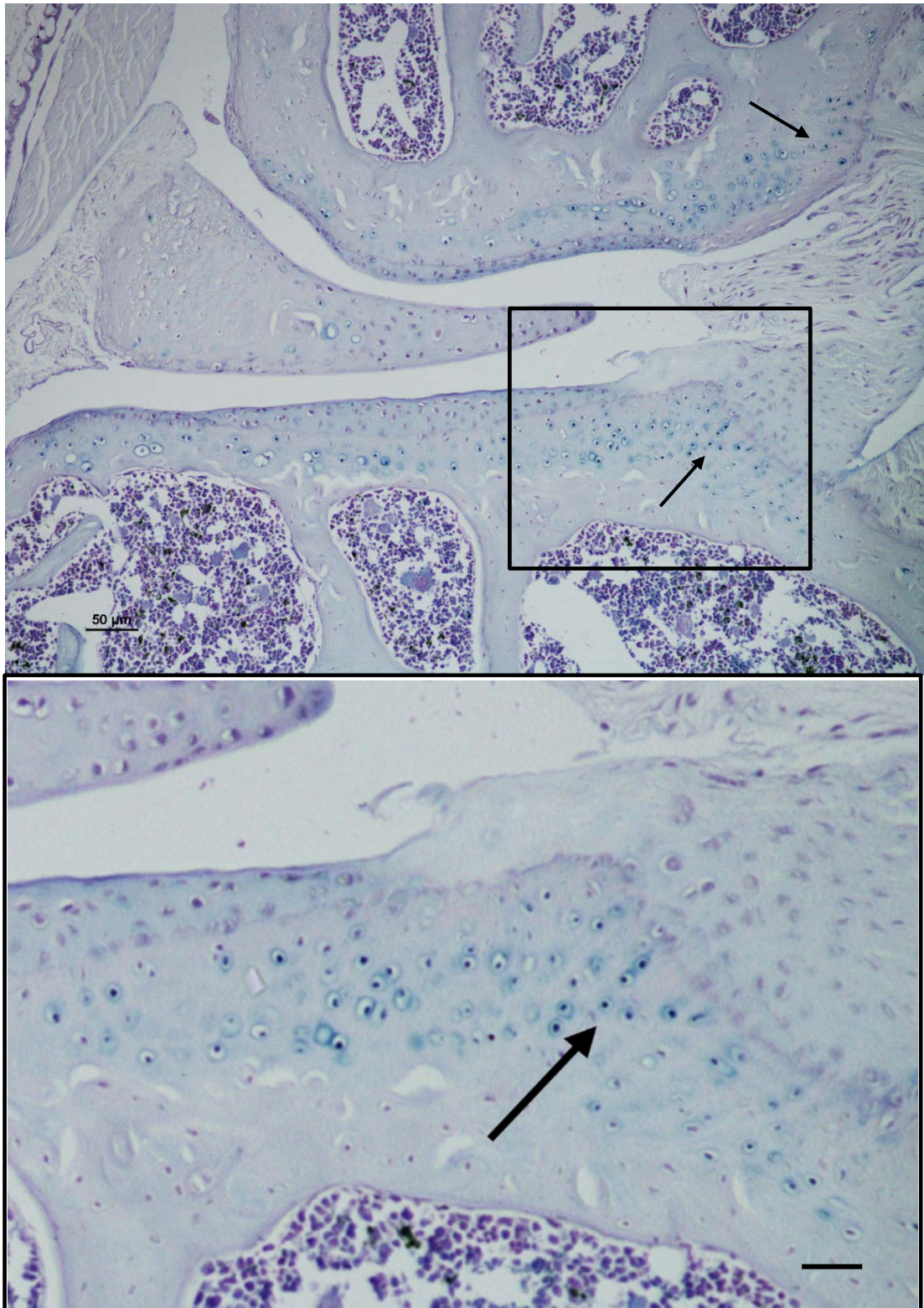


Figure 4.20 - Pigmentation in 43 week old, BALB/c Hgd^{-/-} control mouse (30.4). Extensive pigmentation of the ACC including heavily pigmented chondrocytes on the lateral tibial plateau and lateral femoral condyle (black arrows), close to the intercondylar region and attachment of cruciate ligament, areas of high stress. Stained with Schmorls reagent. Bar = 50um. Zoomed image bar = 20um.

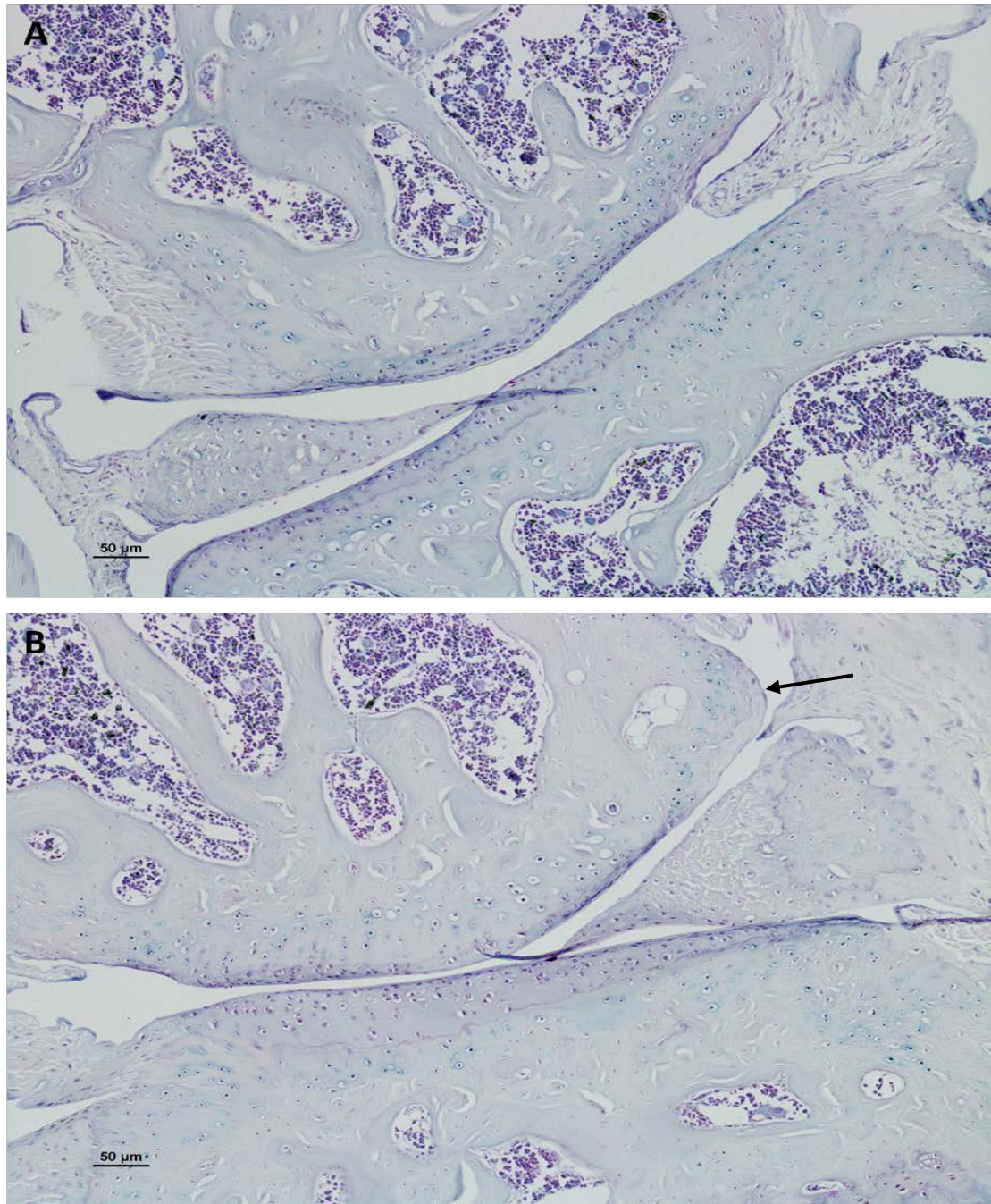


Figure 4.21 - Ochronotic pigmentation throughout the ACC of the lateral and medial aspects of the tibio-femoral joint of a 43 week old, BALB/c Hgd^{-/-} control mouse (30.4).
A: High levels of cellular pigmentation within the lateral femoral condyle and lateral tibial plateau. B: A heavily pigmented osteophyte was located on the medial femoral condyle (black arrow) - a hallmark of cartilage degradation and osteoarthritis. Stained with Schmorl's reagent. Bar = 50µm.

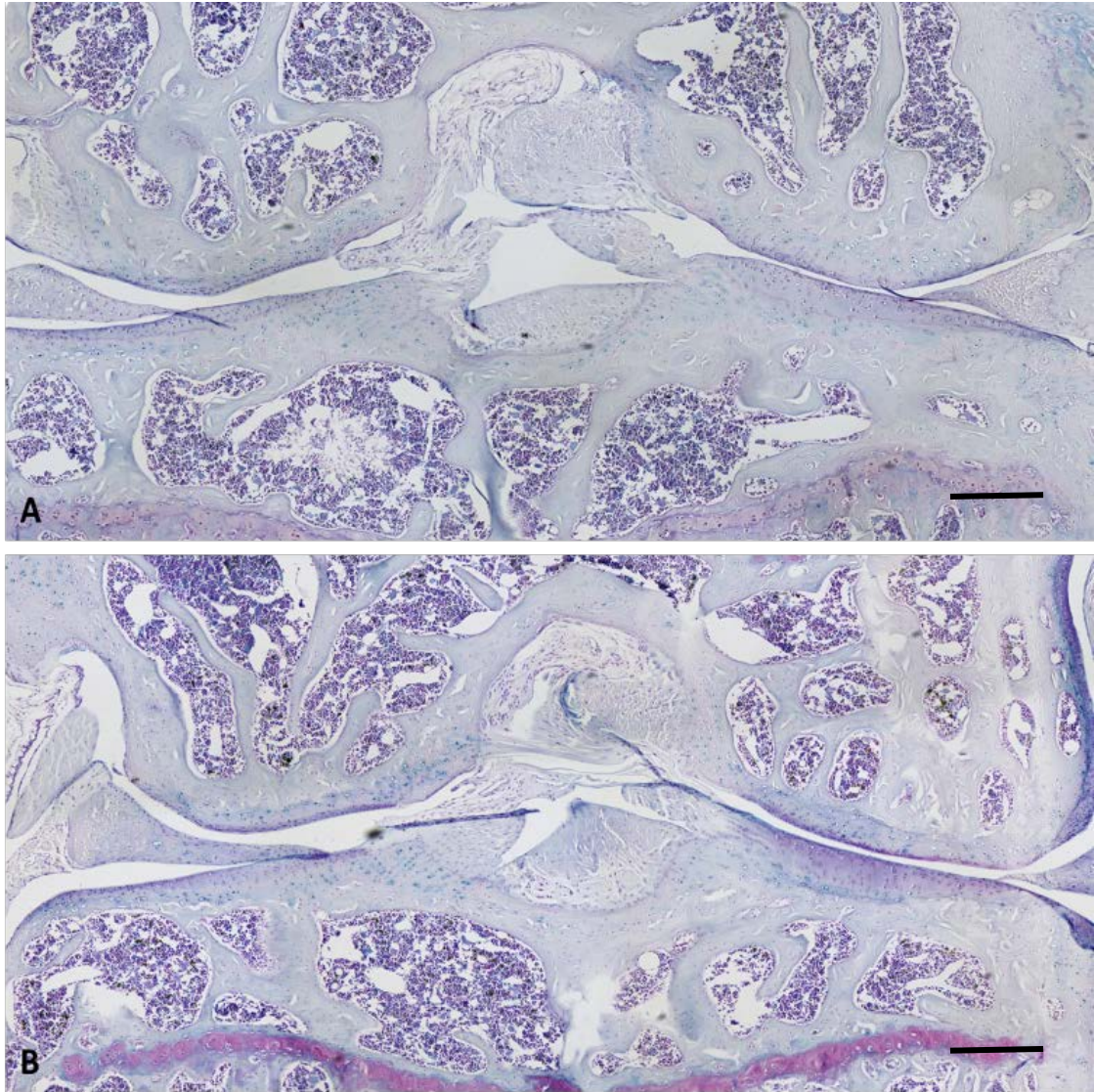
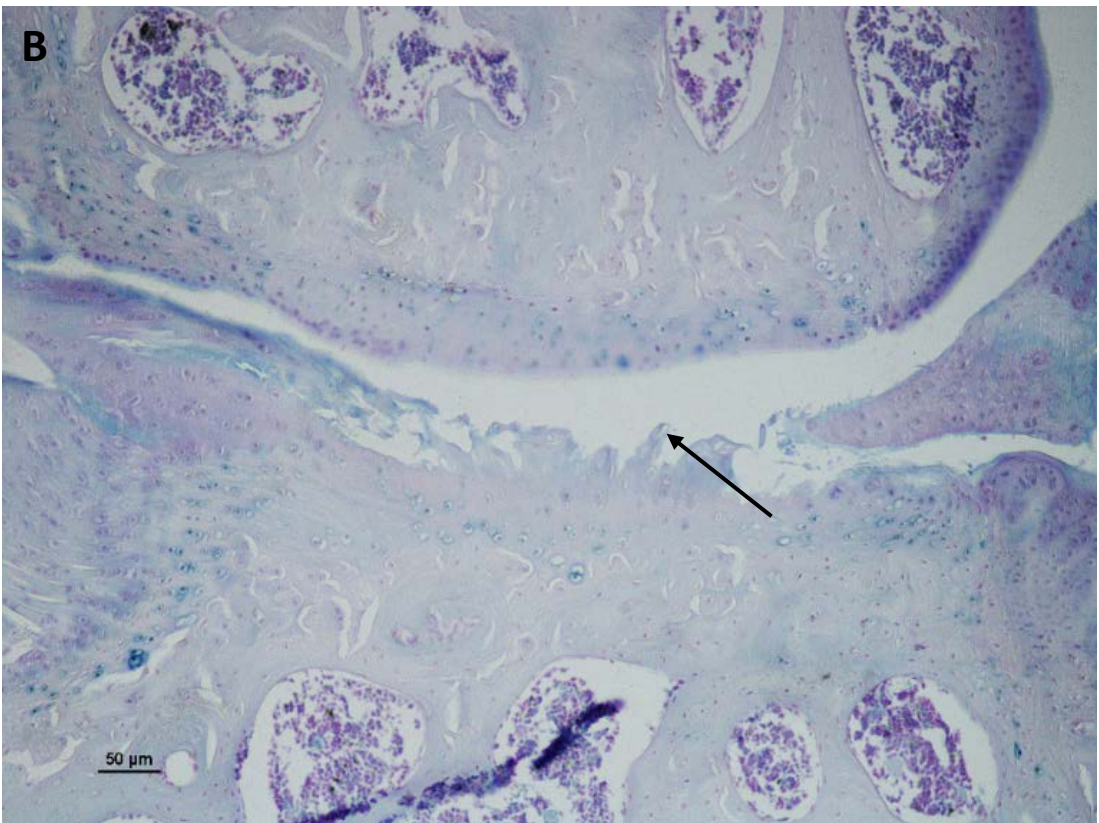
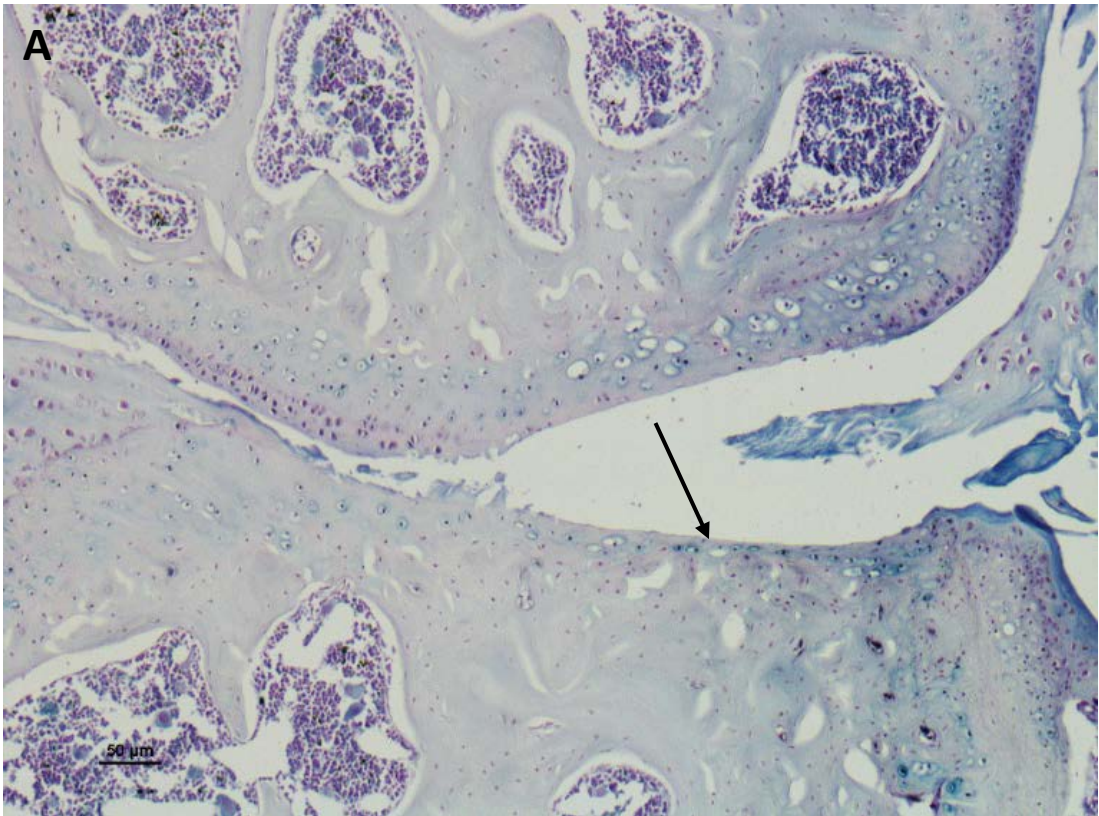


Figure 4.22 - Overview of pigmentation of the ACC in the tibio-femoral joint of two 43 week old, BALB/c Hgd $-/-$ control mice. A: mouse 30.1, B: mouse 30.6. These mice showed the highest pigmentation levels within the control cohort. Stained with Schmorls reagent. Bar=100um.

4.3.3.2 Nitisinone 0.125mg/L

Pigmentation levels did not differ significantly compared to control cohorts in mice receiving 0.125mg nitisinone. There was extensive cellular and peri-cellular pigmented chondrocytes throughout the ACC of the femur and tibia. (Fig. 4.23, Fig. 4.24). As with control mice, pigmentation spanned into the fibrocartilaginous entheses and intercondylar regions. Mice within this group showed high variation in pigmentation levels (cellular range 106 – 252, peri-cellular range 195-477) similar to the control group. Mean(\pm sem) pigmentation levels in this group were in fact slightly higher than control, 197.8 ± 27.1 and 184.8 ± 25.3 respectively.



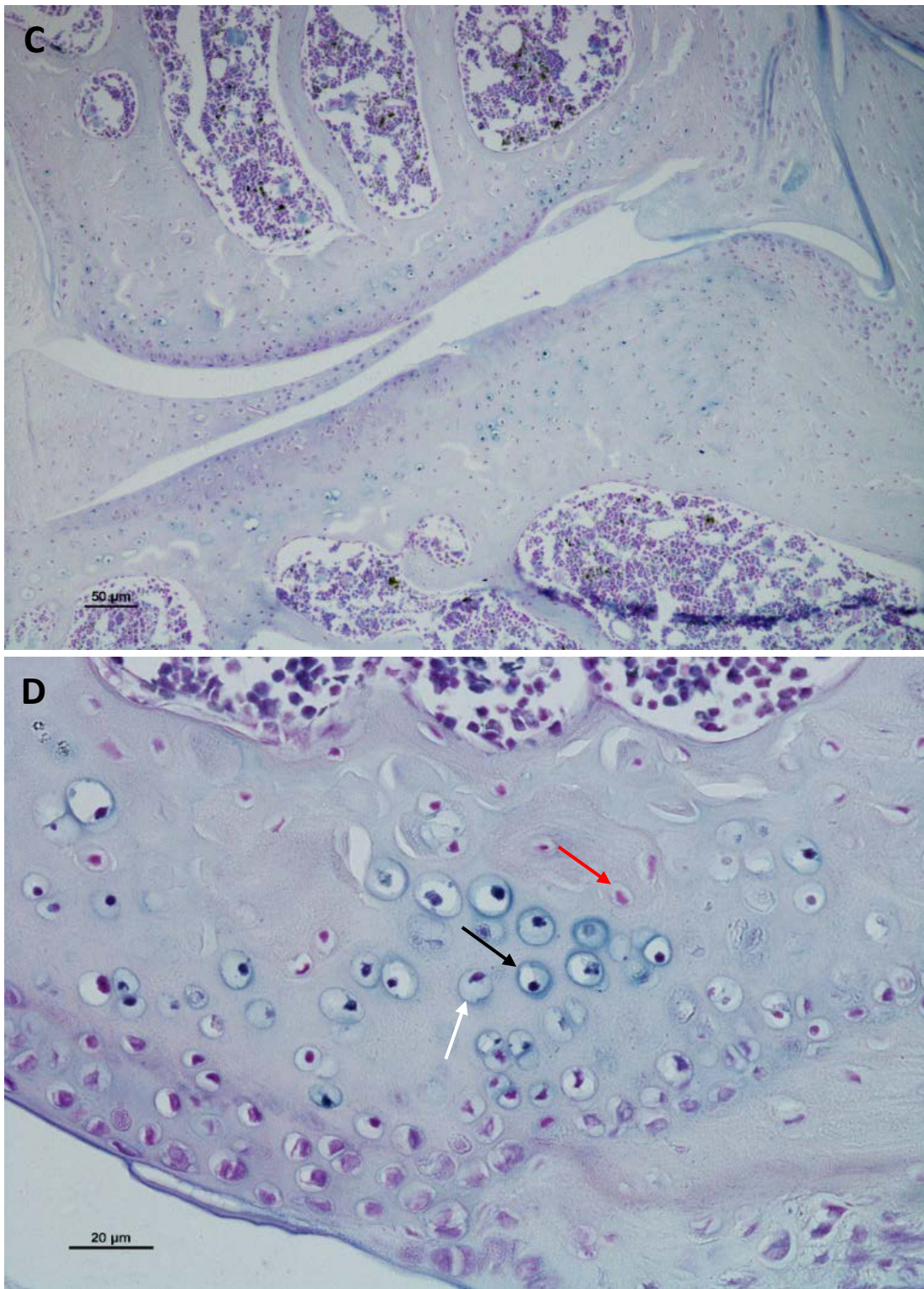


Figure 4.23 - Ochronotic pigmentation in the ACC of the tibio-femoral joint of 43 week old, BALB/c Hgd^{-/-} mice receiving 0.125mg nitisinone. Pigmentation levels were similar to that of control mice with cellular and peri-cellular pigmented chondrocytes widespread throughout the joint. **A & B:** Along with pigmentation in the medial femoral condyle and medial tibial plateau, there were also signs of osteoarthritis such as fibrillations and damage to the hyaline articular cartilage (arrowed). **C:** Pigmented chondrocytes throughout

the lateral tibial plateau and lateral femoral condyle. **D**: Chondrocytes showing different stages of ochronotic pigmentation – unpigmented (red arrow), peri-pigmented (white arrow) and cellular pigmented (black arrow) were present in close proximity throughout the ACC. Stained with Schmorls. A,B,C: bar=50um, D: bar=20um.

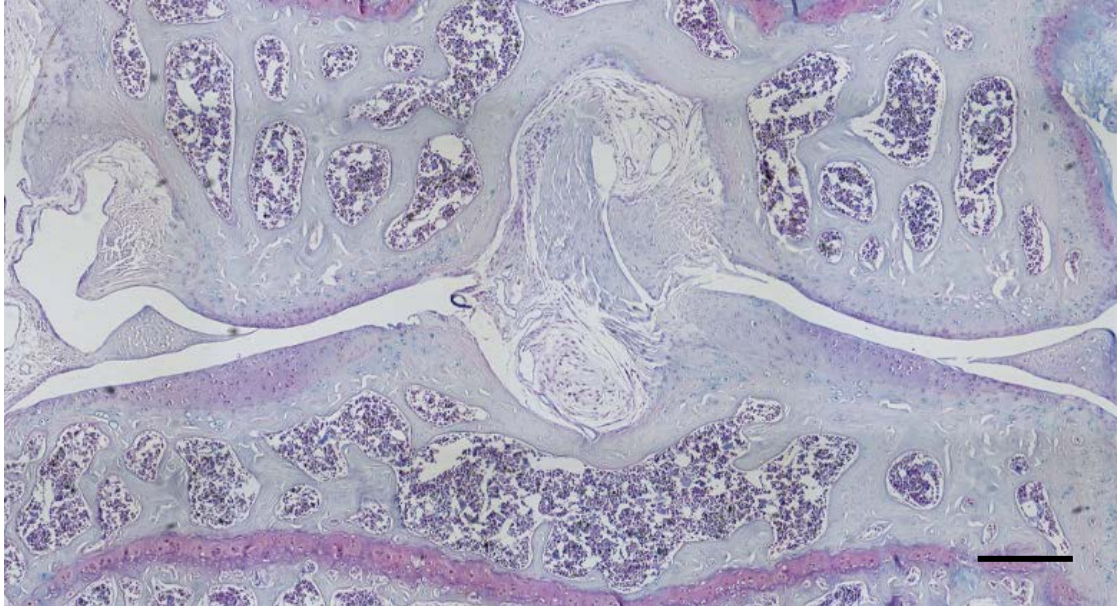


Figure 4.24 - Overview of entire tibio-femoral joint of a 43 week old, BALB/c Hgd-/- mouse receiving 0.125mg nitisinone for 40 weeks. Ochronotic pigmentation was widespread throughout the ACC. Levels of pigmentation were similar to control mice. Stained with Schmorls reagent. Bar = 100um.

4.3.3.3. Nitisinone 0.5mg/L

Ochronotic pigmentation levels in the 0.5mg nitisinone cohort were significantly lower compared with the control cohort ($P < 0.01$). Intra-cohort variation in pigmentation levels were also lower (cellular range 22-77, peri-cellular range 44-131). Cellular pigmentation appeared to be localised to areas of high stress such as the intercondylar area around the attachment of ligaments (Fig. 4.25A). Mice within this cohort had large areas of ACC with either early stage, peri-cellular pigmentation or unpigmented chondrocytes (Fig. 4.25B).

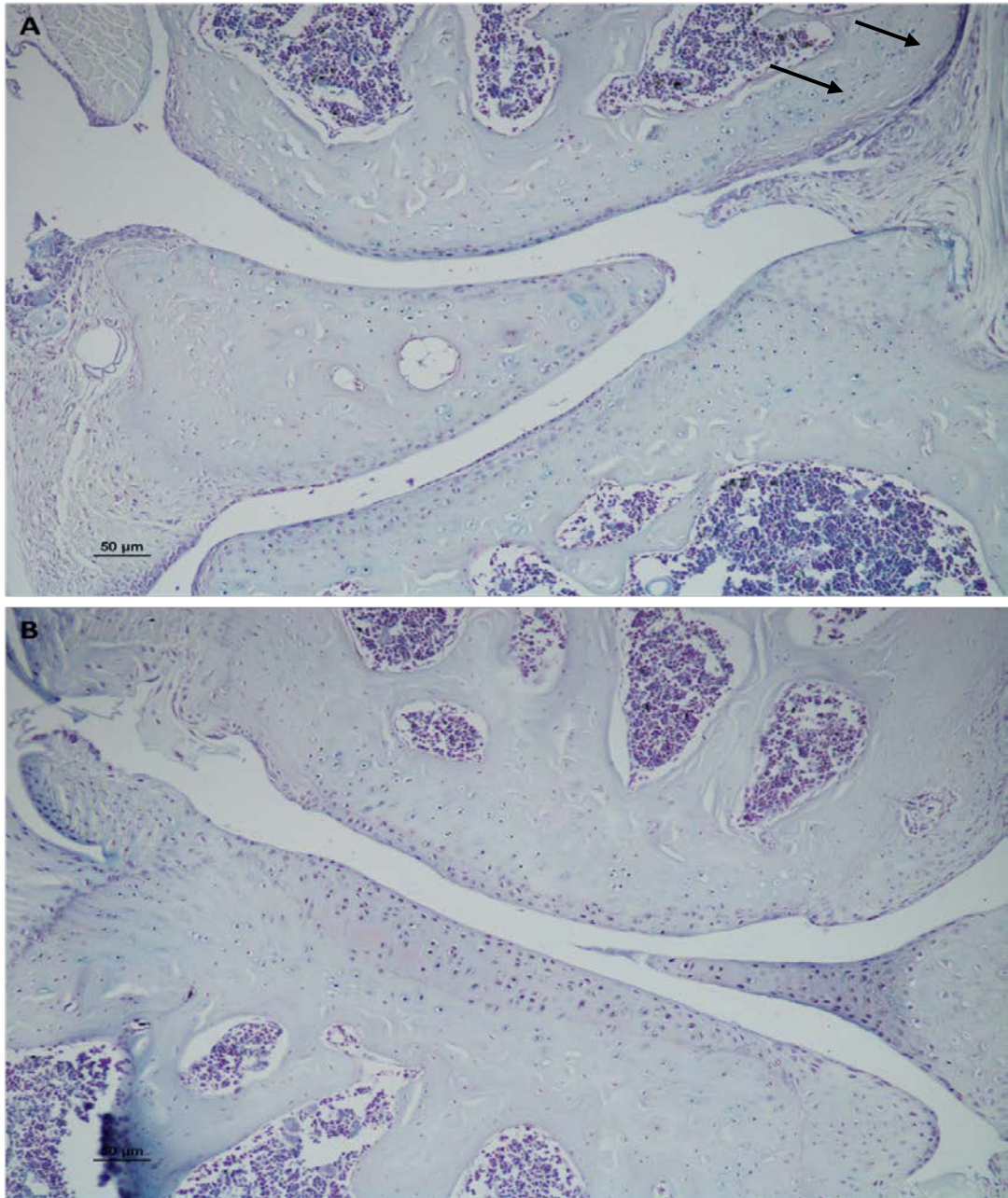


Figure 4.25 - Ochronotic pigmentation in 43 week old BALB/c Hgd^{-/-} mice receiving 0.5mg nitisinone for 40 weeks. A: Areas of cellular pigmentation were clustered around the insertion of ligaments in the lateral femoral condyle (arrowed). **B:** Large areas of the ACC in the medial femoral condyle and medial tibial plateau in mouse 26.2 showed very low levels of pigmentation and this was mostly early stage, peri-pigmentation. Stained with Schmorls. Bar=50um.

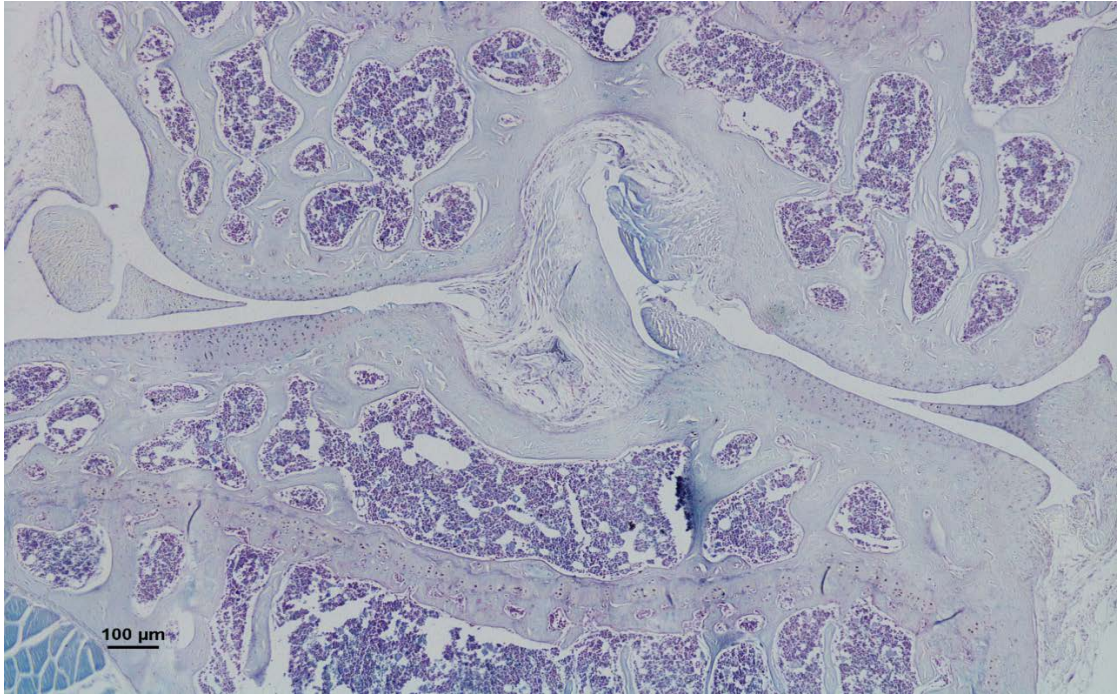


Figure 4.26 - Overview of entire tibio-femoral joint in 43 week old BALB/c Hgd^{-/-} mouse receiving 0.5mg nitisinone for 40 weeks. Pigmentation was significantly reduced compared with control mice. Stained with Schmorl's reagent. Bar=100um.

4.3.3.4 Nitisinone 2mg/L

Ochronotic pigmentation was reduced to very low levels in the 2mg nitisinone cohort with these being significantly lower than control levels ($P < 0.01$) (Fig. 4.27, Fig. 4.28). Intra-cohort variation in pigmentation levels were also lowest (cellular range 0-13, peri-cellular range 10-46).

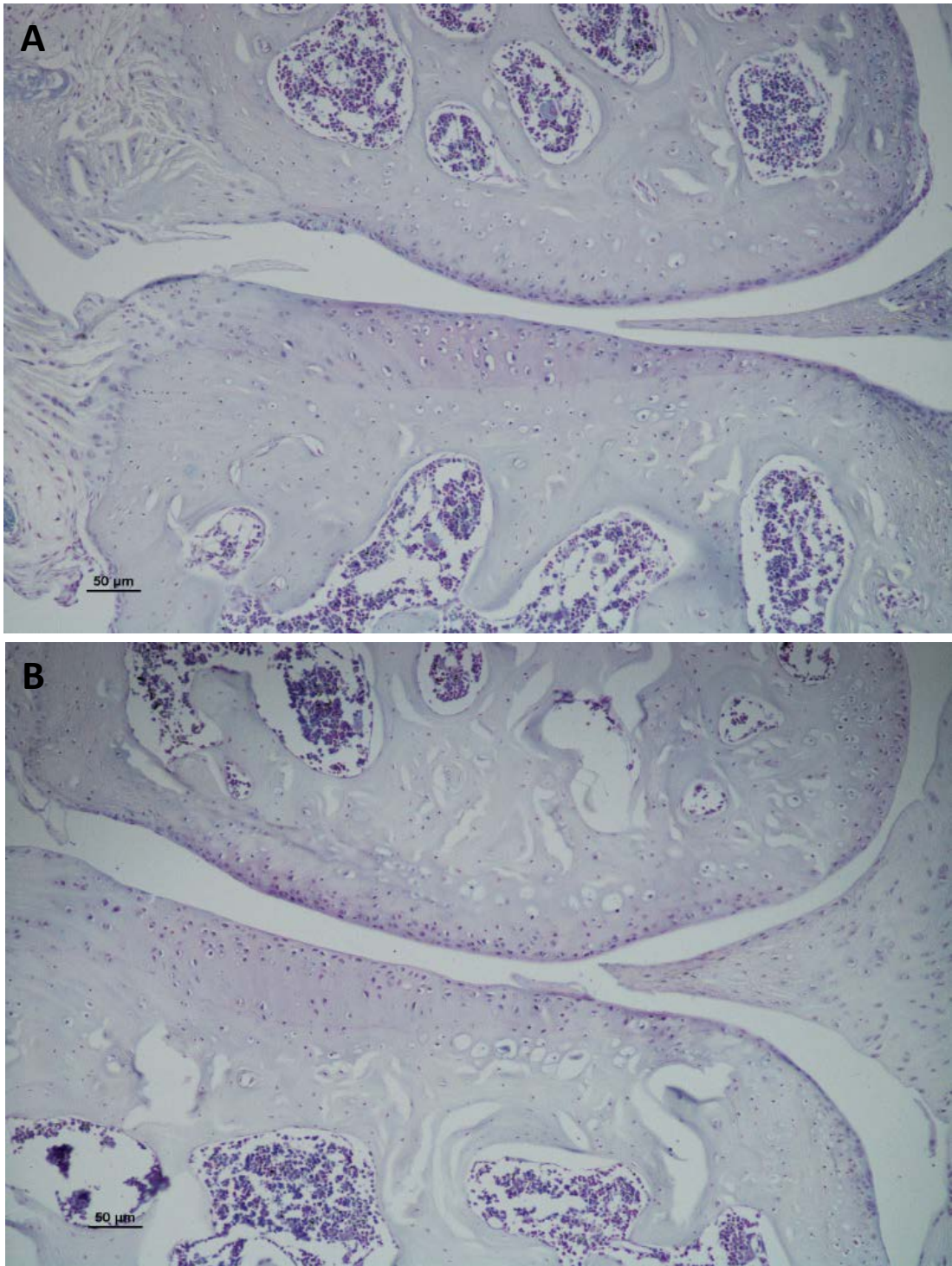


Figure 4.27 – A&B: Very low levels of ochronotic pigmentation in the ACC of the medial femoral condyle and medial tibial plateau in 43 week old mice receiving 2mg nitisinone for 40 weeks. Stained with Schmorls reagent. Bar=50um.

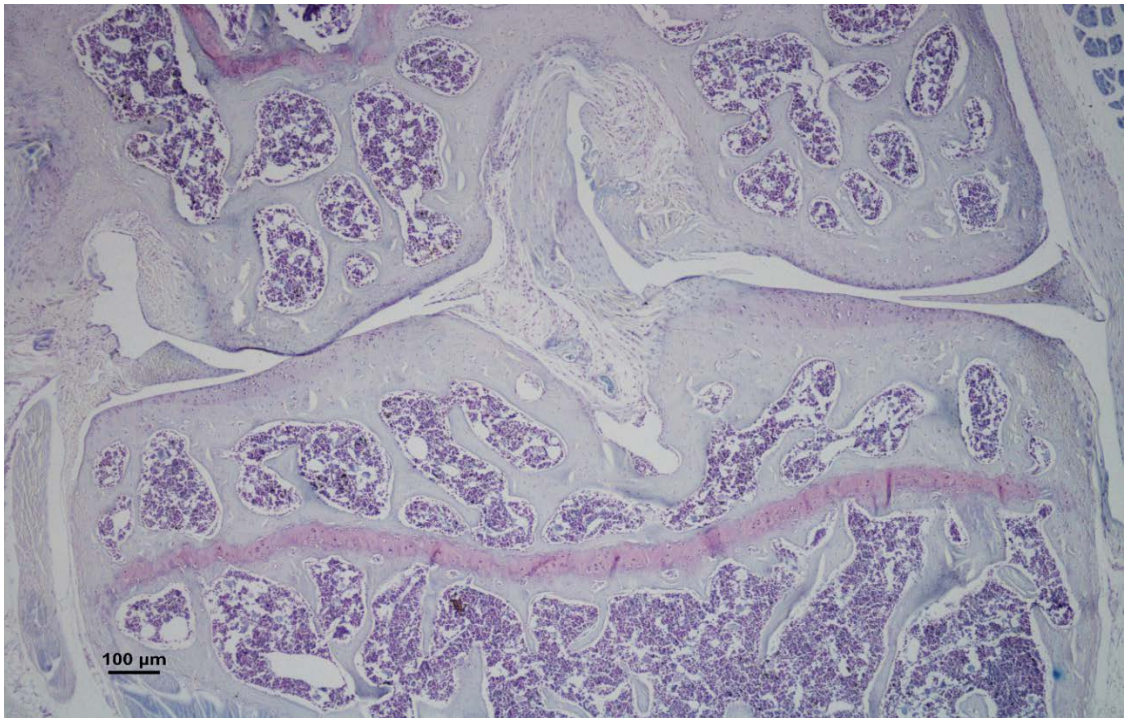
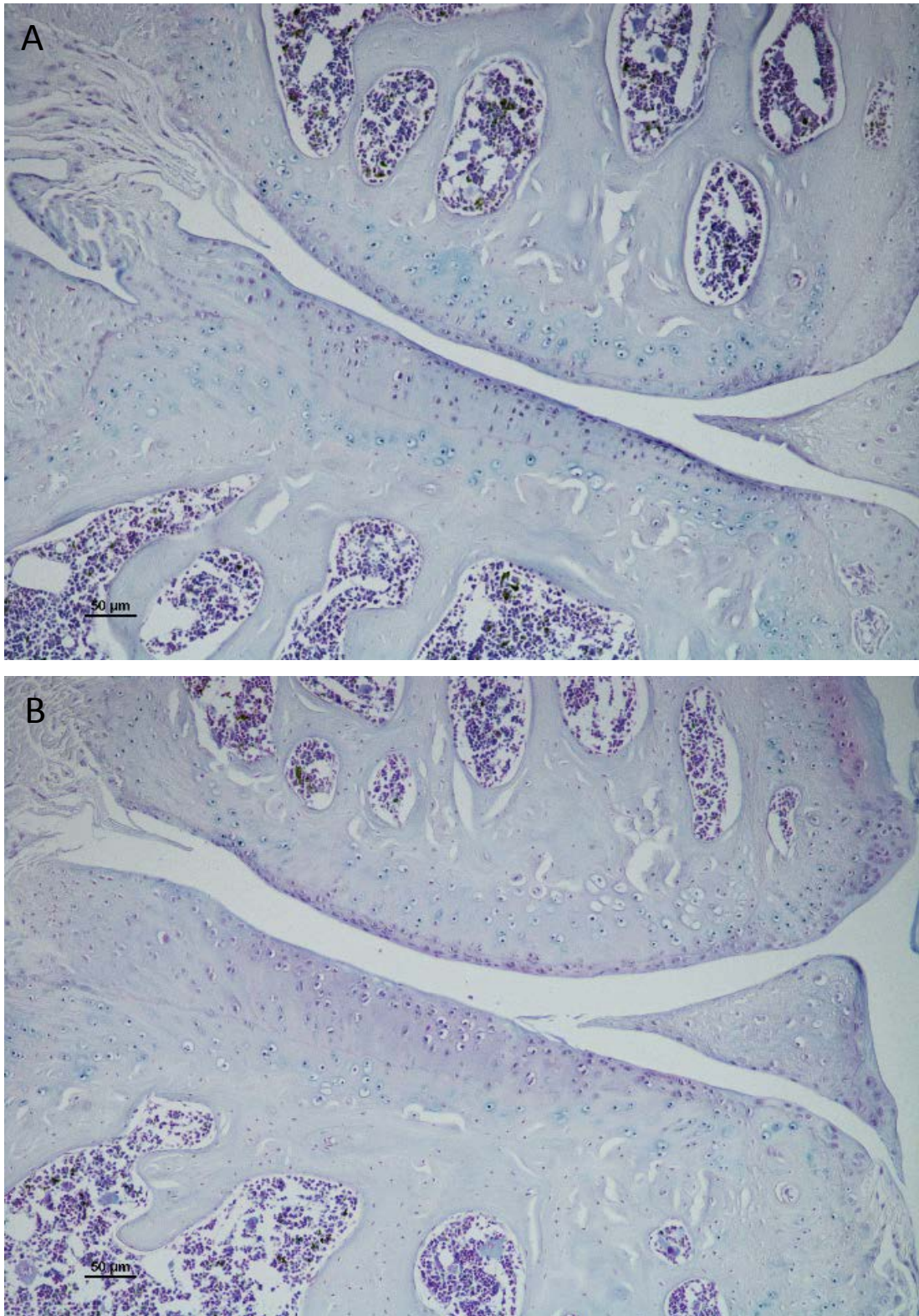


Figure 4.28 - Overview of entire tibio-femoral joint of 43 week old, BALB/c Hgd^{-/-} mouse (13.6) receiving 2mg nitisinone for 40 weeks. Very low levels of pigmentation throughout the ACC. Stained with Schmorls. Bar=100um.

Comparison of ochronotic pigmentation levels between cohorts showed a visible and clear dose response to nitisinone with pigmentation decreasing as nitisinone dose increased (Fig. 4.29).



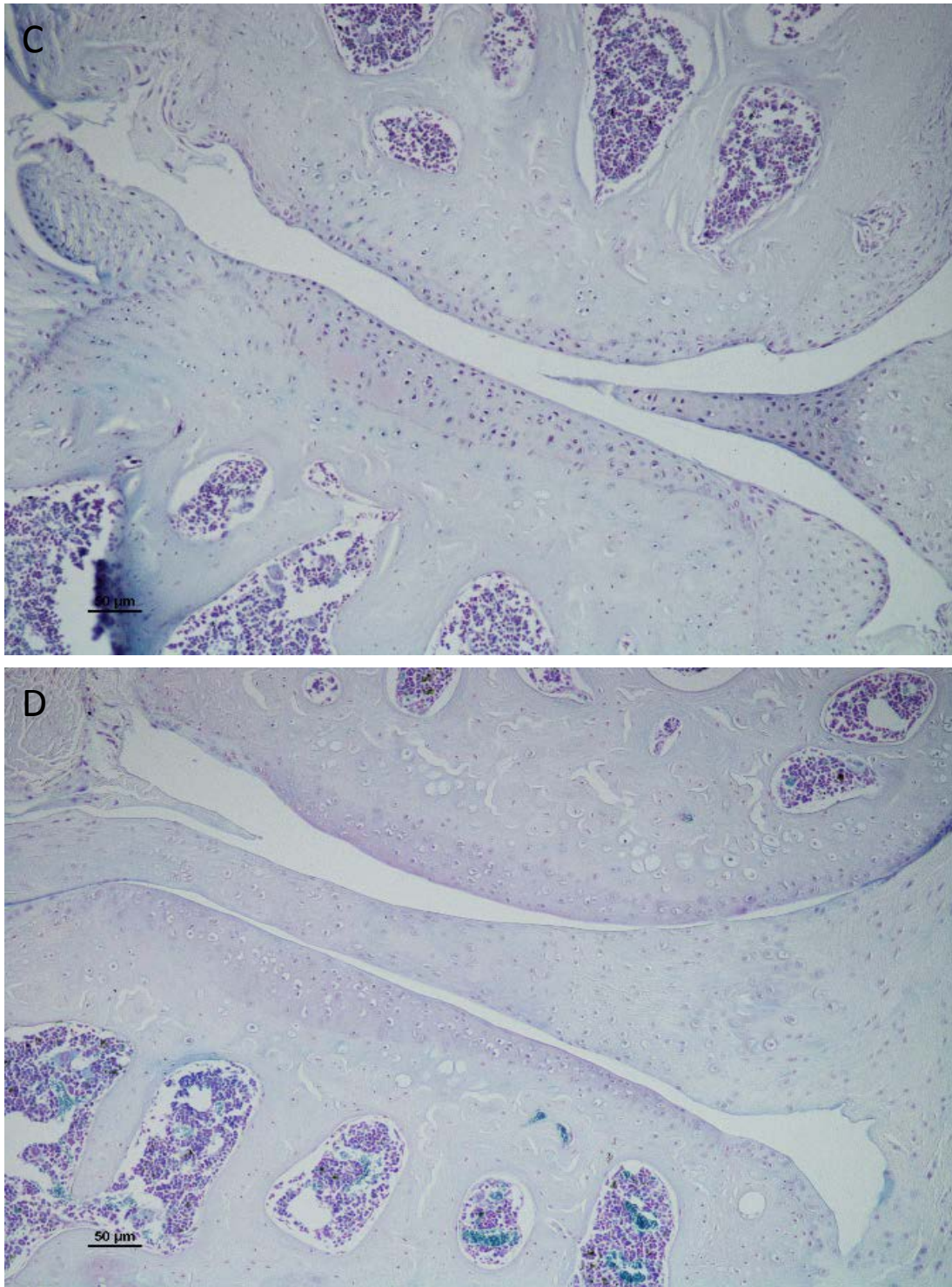


Figure 4.29 - Comparison of ochronotic pigmentation within the ACC of the medial femoral condyle and medial tibial plateau in 43 week old Hgd^{-/-} BALB/c mice receiving 0mg (A), 0.125mg (B), 0.5mg (C) and 2mg (D) nitisinone for 40 weeks. Control and 0.125mg cohorts showed similar high levels of pigmentation throughout the articular calcified cartilage. 0.5mg nitisinone resulted in a visible reduction in pigmentation. 2mg nitisinone reduced ochronotic pigmentation further to reach very low levels. Stained with Schmorls. Bar=50um.

Degradation of the hyaline articular cartilage and signs of osteoarthritis (OA) including fibrillations and osteophytes were apparent in several mice from control and nitisinone treated cohorts although these were not quantified (Fig. 4.30). These signs of OA were apparent even in mice who were receiving the higher doses of nitisinone who had therapeutically reduced plasma HGA from 3 weeks of age and displayed low levels of ochronotic pigmentation (Fig. 4.30 C & D). This suggests HGA/ochronotic pigmentation is not the only factor leading to joint arthropathy in AKU.

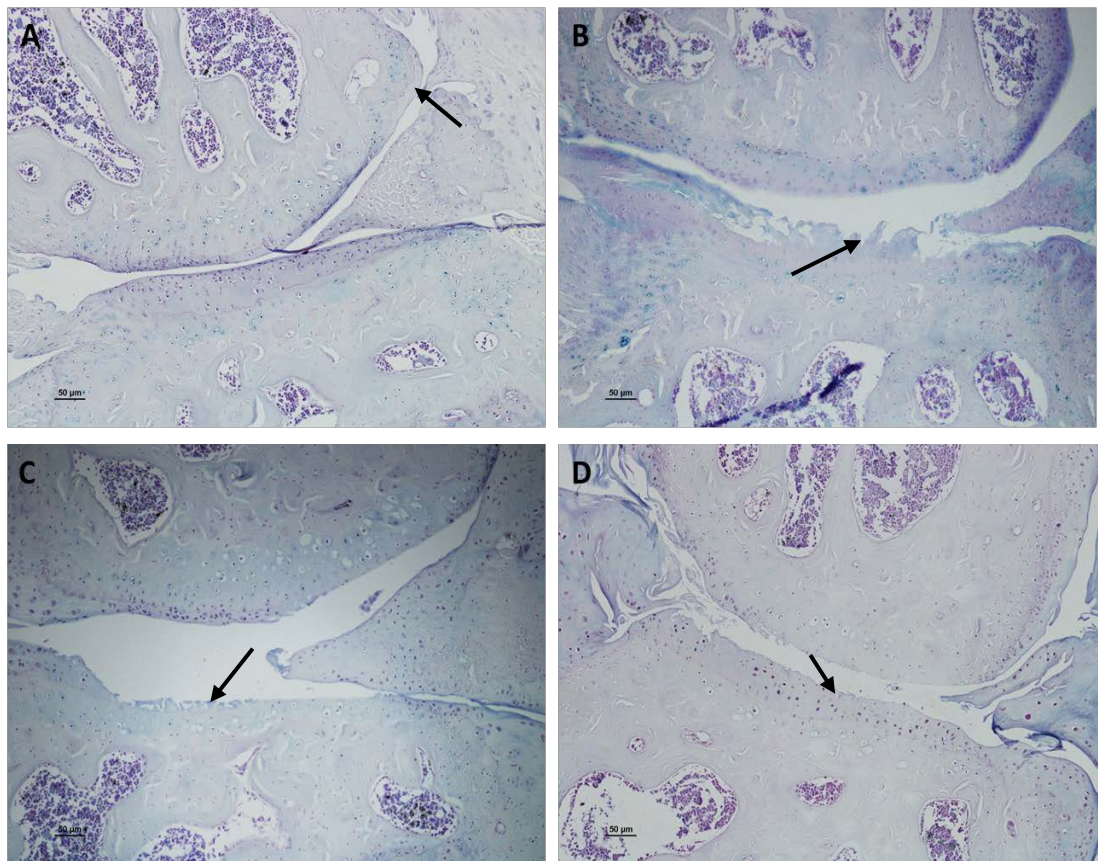


Figure 4.30 - Hyaline articular cartilage damage and signs of osteoarthritis in the tibio-femoral joint of 43 week old, control and nitisinone treated BALB/c Hgd $-/-$ mice. Several mice from control and nitisinone treated groups showed signs of osteoarthritis (arrowed) A: An osteophyte present on the medial femoral condyle of a control mouse. B: Fibrillations and hyaline articular cartilage damage of the medial tibial plateau in a mouse receiving 0.125mg nitisinone C: Severe damage to the hyaline articular cartilage of the medial tibial plateau, exposing the underlying articular calcified cartilage in a mouse receiving 0.5mg nitisinone. D: Fibrillations in the hyaline articular cartilage of the medial tibial plateau in a mouse receiving 2mg nitisinone. Stained with Schmorl's reagent. Bar=50µm.

4.3.4 Relationship between HGA and ochronotic pigmentation

Nitisinone lowered plasma HGA for all treated cohorts compared with control (Fig. 4.31). The lowest 0.125mg nitisinone dose reduced mean plasma HGA to 89 μ mol/L (133 μ mol/L in control) but this had no significant effect on pigmentation levels. Mean pigmentation levels were in fact slightly higher in the 0.125mg cohort compared with control levels. The 0.5mg nitisinone cohort had mean plasma HGA of 51.9 μ mol/L and with this, a beneficial effect of lowered HGA on pigmentation was observed resulting in a 77% reduction in pigmentation compared with control. The 2mg nitisinone cohort displayed a larger decrease in mean plasma HGA levels of 28.7 μ mol/L and a 97% reduction in pigmentation compared to control.

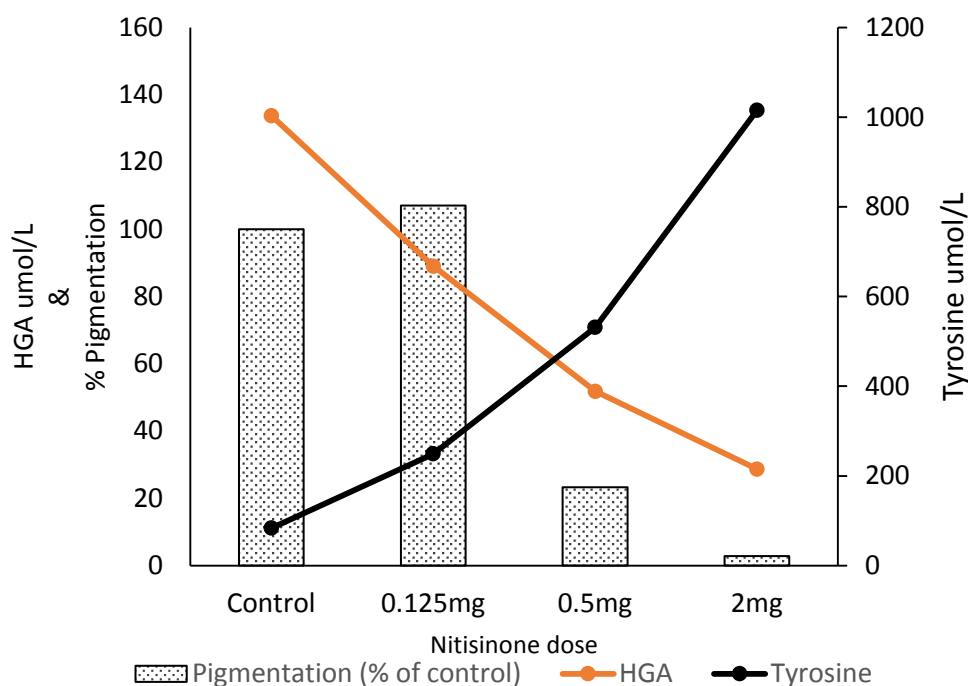


Figure 4.31 - The relationship between plasma HGA concentration and ochronotic pigmentation is not linear. The effect of 0.125mg nitisinone was not sufficient to see a reduction in ochronotic pigmentation of chondrocytes within the mouse tibio-femoral joint. The beneficial effect of HGA reduction on pigmentation is apparent in the 0.5mg cohort when plasma HGA reached ~50 μ mol/L resulting in a 75% reduction in pigmentation. The highest 2mg dose reduced HGA and pigmentation further. Terminal bleed HGA and tyrosine values plotted.

Over the series of doses, the relationship between plasma HGA concentration and number of pigmented chondrocytes was correlated. The lowest 0.125mg dose appeared to be effective in two individuals resulting in a reduction in pigmentation but this effect was not seen in the other four mice within the same cohort suggesting a dose around here is a critical point (Fig. 4.32). One mouse within this cohort also had a high plasma HGA value (185.4umol/L), higher than any values from the control cohort and seemingly an outlier, but interestingly this mouse had the third lowest pigmentation within the cohort. 0.5mg and 2mg nitisinone lowered plasma HGA sufficiently to reduce pigmentation in all individuals. 2mg also reduced intra-cohort variation in HGA and pigmentation levels with values from this cohort forming a distinct cluster.

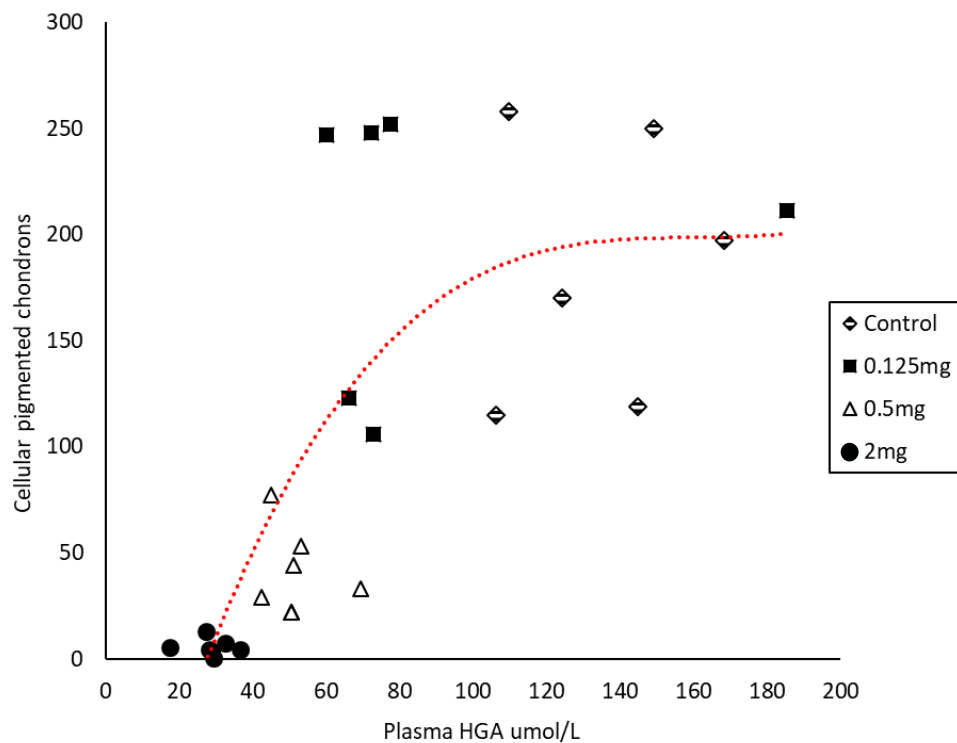


Figure 4.32 - The correlation of plasma HGA and ochronotic pigmentation after 40 weeks nitisinone treatment in BALB/c Hgd^{-/-} mice. Plasma HGA concentration and number of pigmented chondrocytes was correlated over the series of doses. This correlation became stronger as nitisinone dose increased. The lowest non-control dose (0.125mg) lowered plasma HGA in all mice within the cohort but pigmentation was only reduced in two individuals. 0.5mg and 2mg nitisinone lowered HGA sufficiently to reduce pigmentation in all mice suggesting a critical value of 60umol/L must be reached before pigmentation levels are affected.

4.4 DISCUSSION

This study set out to assess the long-term dose response of nitisinone administration in the Hgd^{-/-} mouse. Previous studies have observed the short-term response of plasma HGA concentration and investigated the long-term effect of midlife and lifetime administration of one dose (4mg/L) on ochronotic pigmentation [70, 72]. Predominantly, this study aimed to determine the minimum effective dose of nitisinone required to lower plasma HGA and reduce ochronotic pigmentation whilst minimising the elevation of tyrosine. The results support the hypothesis set out at the beginning of this chapter with additional context related to tyrosine concentration.

4.4.1 HGA and ochronotic pigmentation

Plasma HGA exhibited a dose related decrease and high sensitivity to nitisinone in all treated cohorts but the correlation between HGA concentration and ochronotic pigmentation was not linear. Pigmentation levels in control mice were consistent with those found in mice of a similar age (40 weeks) in a natural history of ochronosis study by Preston and colleagues [70]. Although mice receiving 0.125mg/L nitisinone showed a mean reduction in plasma HGA of 33% compared with control, pigmentation levels were only significantly reduced in two individuals within the cohort. A mouse within this cohort (Hgd^{-/-} 29.3) appeared to be an outlier with very high HGA levels compared with controls and 0.125mg cohort littermates, perhaps exhibiting a reduced sensitivity to nitisinone. The high variability within this group may be an indication that this was just below an effective dose and not quite reaching the critical therapeutic point to have a beneficial effect for the majority of mice. Conversely, another apparent outlier within the 0.125mg cohort (Hgd^{-/-} 29.2) showed very low HGA levels at the mid-term bleed with a value closer to the cohort receiving 2mg nitisinone. Interestingly, within Hgd^{-/-} 29.2, tyrosine was the least elevated out of the cohort and HPPA and HPLA were similar to control levels. Unfortunately, this mouse developed a persistent sore on its tail that would not heal and had to be culled prior to terminal metabolite measurements. Nevertheless, this could be an example of an enhanced response to nitisinone and better endogenous metabolic control within the mouse, supporting the notion of tailored nitisinone therapy according to patient sensitivity [72].

Mice receiving 0.5mg/L and 2mg/L nitisinone had significantly reduced ochronotic pigmentation and plasma HGA concentrations reduced by 61% and 78% of control respectively. This suggests plasma HGA must be lowered to a critical threshold concentration before deposition of pigment within connective tissue is affected. In this case, the critical levels for plasma HGA appeared to be between 40-60umol/L. Below 40umol/L resulted in a dramatic reduction in pigmentation whereas above 60umol/L pigmentation was similar to control and showed maximal levels of ochronosis (Fig 4.32). Mice receiving 0.5mg/L nitisinone exhibited lower pigmentation levels, suggesting that this dose provided a prophylactic effect for the joints from ochronosis whilst also producing a less pronounced degree of tyrosinemia than the higher 2mg/L dose (Fig 4.31). This is an important finding for human therapeutic use. Some patients show high sensitivity to nitisinone related tyrosinemia despite restricting dietary protein that manifests as a painful corneal keratopathy and requires cessation of treatment whilst these symptoms subside [138, 139]. Tailoring the dose of nitisinone for these patients so it provides a practical compromise of lowering HGA to relatively harmless levels whilst ensuring the degree of tyrosinemia is minimised in order to prevent adverse effects and guarantee continuous treatment is thus important for improved therapeutic outcome.

4.4.2 Dosing to reduce elevation of tyrosine

Along with HGA, a clear dose-response was observed for plasma concentrations of tyrosine and its associated phenolic metabolites, HPPA and HPLA, reiterating the efficacy of nitisinone (Fig 4.16, Fig. 4.17). Plasma tyrosine concentrations in Hgd^{-/-} control mice were similar to those of untreated AKU patients but the elevation of plasma tyrosine and its metabolites, HPPA and HPLA post-nitisinone were more marked in the Hgd^{-/-} mouse (Table 1, appendix). The 0.5mg/L and 2mg/L nitisinone doses used in this study equate to higher concentrations than used in human AKU studies, which would explain the higher degree of tyrosinemia observed. Tyrosinemia is well tolerated in the mouse as the general metabolic activity of this species is far greater than in humans [140]. The mouse liver and kidneys are therefore capable of withstanding greater metabolic stresses due to their ability to rapidly induce and resynthesise enzymes to enable clearance of metabolic products [141]. The mg/kg concentration was determined for each mouse dose used in this study for comparison with those used in previous human studies [55, 56]. Calculations were based on a 30g mouse consuming 4-6ml drinking water per day [136, 137] and equated to 0.0175-

0.025 mg/kg, 0.07-0.1mg/kg and 0.25-0.4mg/kg for 0.125mg/L, 0.5mg/L and 2mg/L respectively. The recent SONIA1 human study had used 10mg per day, being the nearest readily available dose, but this had to be reduced in some patients due to keratopathy presumed secondary to high tyrosine. The SONIA1 study concluded 8mg daily as the most efficacious dose for AKU patients, which equates to 0.114mg/kg for a 70kg patient. Within this study, the 0.5mg/L or 0.07-0.1mg/kg dose is closest to the SONIA1 8mg human dose and provided a practical compromise of lowering plasma HGA sufficiently to reduce pigmentation whilst also producing a lower degree of tyrosinemia than higher doses. This degree of congruence in the two species is surprising and promising for facilitating tailoring of treatment.

4.4.3 HPPA and HPLA

The degree of tyrosinemia and elevation of HPPA and HPLA in the 0.5mg/L and 2mg/L nitisinone treated cohorts were more pronounced in the mid-term bleed than the terminal bleed. Lock et al compared acute and chronic dosing in the mouse and showed repeated exposure to nitisinone reduces the extent of tyrosinemia. They observed a single dose of 10mg/kg nitisinone in mice caused elevation of tyrosine to a maximum of 1200umol/L whilst 6 weeks daily administration of doses up to 160mg/kg also resulted in tyrosinemia but this was 50% lower than in the single dose cohort. They proposed this might reflect the increasing ability of the mouse liver TAT to metabolise tyrosine to HPPA and to facilitate clearance in the urine [141]. The differences observed in this study may also be an example of the mouse acclimatising to the nitisinone induced tyrosinemia and becoming more efficient at urinary clearance of tyrosine and its phenolic metabolites HPPA and HPLA, between mid-term and terminal plasma samples. Upon further reflection, although the terminal bleed tyrosine levels were lower than the mid-term bleed, both treatment periods would be considered as chronic dosing (20 and 40 weeks of daily dosing). More so, the 20 week bleed could not be considered as an acute dose for comparison with the Lock et al study who only used a single dose. The possibility that the unexpected discrepancies in plasma levels of tyrosine, HPPA and HPLA between mid and terminal bleeds were methodological is investigated further in chapter five of this thesis.

Normally, plasma HPPA concentrations are low or undetectable due to HPPD conversion of HPPA to HGA. HPPD inhibition via nitisinone causes HPPA to increase and exert product inhibition on the enzyme tyrosine amino transferase (TAT) and its conversion of tyrosine to HPPA. This product inhibition of TAT by HPPA and the resulting elevation of tyrosine produce the tyrosinemia observed as a side effect of nitisinone therapy. The conversion of HPPA to HPLA is normally a dormant process. This alternative endogenous pathway can be activated to increase tyrosine degradation and excretion via the kidneys in an attempt to counteract elevated tyrosine [135]. Tyrosine, HPPA and HPLA all undergo renal clearance and urinary excretion but much of the tyrosine is reabsorbed explaining the observed higher levels of plasma tyrosine compared with HPPA and HPLA, which are more readily excreted in the urine [142].

Within the terminal bleeds, two mice in the 0.5mg cohort had tyrosine values just below 500umol/L (454.7 and 478.1) and both had equal levels of HPPA/HPLA (20.5/21.8umol/L and 21.5/20.4umol/L respectively). All other mice within this cohort had tyrosine values between 500-600umol/L and HPLA that exceeded HPPA by 5-10umol/L. As tyrosine levels were elevated further in the 2mg nitisinone cohort, HPLA then exceeded HPPA values by up to 10-40 umol/L. This could suggest that conversion of HPPA to HPLA exceeds TAT synthesis of HPPA occurs once plasma tyrosine reaches >500umol/L. HPLA was higher than HPPA in mice once tyrosine reached this value suggesting this is around a critical point where the HPPA to HPLA conversion pathway is activated. Upon further analysis, mid-term bleeds did not show the same trend with HPPA and HPLA values being much higher in the 0.5mg and 2mg bleed cohorts and HPLA never exceeding HPPA values. This was another example of the curious metabolite discrepancies found between bleeds.

4.4.4 HGA variability

There was high variability in plasma HGA concentrations consistent with that observed in AKU patients [55, 56, 58] and previous murine studies [70, 72] (Fig. 4.4, Fig. 4.5, Table 4.1). This variability was apparent within mice of the same cohort (often littermates of the same inbred strain) and within the same mouse at different time points. The highest 2mg dose of nitisinone appeared to reduce HGA variability in the 20 week, mid term bleed. Terminal bleed coefficients of variation were lower than mid bleed in all but the 0.125mg nitisinone cohort due to the high outlier mentioned previously (Hgd/- 29.3). Interestingly, the coefficient of variation for the control cohort was markedly lower in the terminal (18.2%)

than mid bleed (35.4%) despite receiving no therapy. Once more, this was an unexpected finding and seemed unlikely simply due to variation as all mice within the control cohort had significantly reduced plasma HGA in terminal bleeds compared to mid term bleeds. This finding was investigated further in chapter five.

4.4.5 Mid-term and terminal bleed metabolite discrepancies

Many of the metabolites varied significantly between mid and terminal bleeds not only in nitisinone treated cohorts but also in control mice. For this reason, it was necessary to investigate possible explanations for this. Unexpectedly, despite the control receiving no pharmacological intervention, all but one mouse showed significant decreases of between 30-70% in HGA between mid and terminal bleeds. This goes against previous work by Preston et al who observed that although plasma HGA is subject to variation, it does not rise or fall significantly over the untreated Hgd^{-/-} mouse lifetime [70]. An explanation for the differences observed between mid and terminal bleeds could be the site or method of plasma sampling. Mid-term bleeds were obtained from one of the paired lateral caudal veins in the lower third of the tail after the mouse had been incubated in a heat box at 38 degrees Celsius for several minutes to aid with vasodilation. Terminal bleeds were obtained directly from the brachial artery after schedule 1 culling with an overdose of pentobarbitone sodium. In hindsight, here lies a weakness of the study – terminal bleeds should have been sampled from the tail immediately prior to culling to provide measurements that were better comparable with mid bleed samples although there was no prior reason to expect a systematic difference. Administration of pentoject prior to the terminal bleed sampling could have also affected plasma metabolites. As all cohorts showed significant differences in metabolites between mid and terminal bleeds, a further study investigating the effect of sampling method on plasma metabolites was designed and implemented, the results of which form chapter five of this thesis.

Notwithstanding a possible methodological explanation, the lower plasma HGA between mid and terminal bleeds in control and nitisinone treated mice (Fig. 4.6) could have been due to an increased rate of ochronosis and pigment deposition between 20 and 40 weeks of age in the Hgd^{-/-} mouse. Perhaps HGA polymerisation and deposition into cartilaginous tissue during the interval between bleeds aided to remove some HGA from the blood

causing a reduction in plasma concentrations. The 0.125mg nitisinone treated cohorts had reduced levels of HGA but this dose was not sufficient to reduce pigmentation therefore additional HGA was reduced by ochronosis. The reduction in HGA in the 2mg cohort between mid and terminal bleeds was much smaller than other cohorts, perhaps because HGA was lowered sufficiently to prevent pigment deposition so the rate of ochronosis due to increased age had less of an effect. The Hgd^{-/-} natural history study carried out by Keenan et al found extensive increase in pigmentation levels between 20 and 40 weeks which would support this [72] but conversely, Preston et al reported plasma HGA was relatively constant throughout the lifetime of the mouse despite pigmentation increasing through life; chapter five examines these discrepancies in more detail.

Phenylalanine demonstrated the least fluctuation out of the metabolites measured in control and nitisinone treated cohorts. Mid-term bleeds showed a significant elevation in mice receiving 2mg/L nitisinone compared with control, this statistically significant difference was not evident in the terminal bleeds due to increased intra-cohort variation but values were still raised (Fig. 4.7, Fig. 4.8). As an essential amino acid, phenylalanine cannot be synthesised by the body and is obtained solely through diet [142]. Phenylalanine hydroxylation to tyrosine is an irreversible process so elevated tyrosine levels as a result of nitisinone should not directly affect phenylalanine levels. The increase in the 2mg nitisinone cohort could be due to normal variation of food intake within the mice although this would most likely also be seen in other cohorts and was not. Mice were maintained on a normal protein diet throughout the study so phenylalanine intake remained similar but could have fluctuated slightly depending on the mouse's intake of food prior to plasma sample collection. A possible explanation could be that the effects of elevated tyrosine in the 2mg cohort increased the mouse appetite by affecting the thyroids production of thyroxine, effectively inducing a state of hyperthyroidism in an attempt to clear or utilise the surplus tyrosine. In support of this, a study by Diarra and colleagues found hyperthyroidism decreased tyrosinemia and endogenous tyrosine levels in the striatum, adrenals and heart in rats. They concluded that the thyroid status of the rat can influence tyrosine uptake mechanisms and catecholamine synthesis and that this is likely due to thyroid hormones modulation of tyrosine hydroxylase activity, the enzyme which catalyses the rate limiting step in catecholamine biosynthesis [143]. This connects to another possible explanation whereby the increase in tyrosine is stimulating dopamine production

(a catecholamine), that is also linked to regulation of appetite and motivation to consume food [144, 145]. A study by Hardman and colleagues examining the effects of tyrosine depletion on appetite found participants reported significantly lower levels of hunger following a fixed-test meal relative to non-tyrosine depleted controls [146]. The opposite could be occurring in the 2mg cohort with the increased plasma tyrosine stimulating dopamine synthesis and in turn, the related motivational components of eating and stimulation of appetite.

4.4.6 Limitations

Finally, an accepted limitation of this chapter is the lack of behavioural and motor function testing after 40 weeks treatment with nitisinone. This could have provided data examining the effects of chronic nitisinone dosing in the Hgd^{-/-} mice on learning and memory and would have been valuable to compare with data obtained in chapter 3. Unfortunately, this was a missed opportunity due to time constraints and should be considered for the future licencing process.

The findings of this chapter demonstrated the systematic dose response of metabolites in the tyrosine pathway to nitisinone treatment. Data revealed plasma HGA and pigmentation are correlated but that this relationship does not appear to be linear with HGA having to be reduced to a critical level prior to pigmentation being affected. This chapter also demonstrated that nitisinone dose can be tailored to provide a protective HGA and ochronotic pigmentation lowering effect whilst also minimising the elevation of tyrosine. These findings have positive implications for AKU patients with a predisposition to tyrosine toxicity.

5. Investigating the arteriovenous blood metabolome relating to Alkaptonuria in the BALB/c Hgd^{-/-} mouse.

5.1 INTRODUCTION

This study was designed to investigate unexpected discrepancies between plasma metabolites in samples collected from BALB/c Hgd^{-/-} cohorts within the nitisinone long-term dose response study. The plasma metabolite results detailed in chapter 4 of this thesis (Fig. 5.1) indicated significant differences between metabolites measured in the mid-term bleeds and those measured in the terminal bleed. This was the case for all nitisinone treated cohorts; a reduction in plasma HGA was expected due to the proven HPPD inhibiting mode of action of nitisinone shown to be efficacious within 1-2 weeks [55, 56, 58]. Mid-term plasma sampled after 20 weeks treatment with nitisinone showed a dose related decrease in HGA but unexpectedly, terminal plasma sampled after 40 weeks treatment showed significant further decreases in HGA. Previous studies in humans [55, 56, 99] and mice [70, 72] have shown nitisinone reduces plasma HGA within 1-2 weeks and that these levels remain relatively constant with continued treatment of the same dose. Furthermore, within the long-term dose response study, a significant difference (\downarrow 46%) in plasma HGA was also observed within the control cohort between mid and terminal plasma samples, the mice from which had received no treatment or exposure to nitisinone within their lifetime. This difference in plasma HGA in control mice was in contradiction of previous work by Preston et al who concluded plasma HGA levels, although subject to variation, show no significant rise or fall over the Hgd^{-/-} mouse lifetime [55].

Arteriovenous discrepancies do exist for some metabolites between types of blood samples. Lactate for example, where arterial blood is considered the "gold standard" sample due to having constant concentrations irrespective of sample site. This is because arterial blood is derived from a mixed venous blood composition (since all venous fields drain into the right atrium), providing a representative sum of all sources of tissue lactate production. By contrast, the concentration of lactate in venous blood can vary depending on the site of sampling because of variation in local tissue lactate production with central venous samples considered superior to peripheral venous samples [147-148]. Along with lactate, it has long been accepted that arteriovenous differences in glucose and nitrous oxide exist, highlighting the difficulty in measuring and comparing metabolic parameters between one blood compartment and another [149-152]. A recent paper [153] investigating arteriovenous metabolomics in humans found significant differences in phenylalanine, a

member of the tyrosine pathway, which raises the question whether this could have implications for the other pathway metabolites such as HGA.

The literature indicates that the significant differences in metabolites observed between plasma samples in chapter 4 may have been methodological. In the aforementioned study, mid-term plasma samples were collected from one of the lateral tail veins without sedation. Prior to tail vein sample collection, mice were heated in an incubator to incite vasodilatation and briefly held in a Perspex restrainer to minimise risk of injury during sample collection. At the end of the study, terminal plasma samples were collected from the brachial vessels, providing a more arterial-like blood supply. Terminal bleed samples were collected after mice had been culled with an overdose of Pentoject (pentobarbitone) for which little research is available for its acute effects on the metabolome. A murine study by Clark and colleagues [154] reported that overdose with Pentoject resulted in a significant increase in serum miR-122 (a biomarker of liver injury) to a much greater extent than mice culled with CO₂. They also reported significantly higher levels of miR-122 in samples obtained via cardiac puncture (i.e. post-cull) compared with those obtained via tail bleed, indicating that differences can exist between arteriovenous metabolites sampled minutes apart in the same animal. In consideration of these findings along with the results of chapter 4, the following studies were designed to assess whether the metabolite fluctuations were methodological providing an unintentional, yet clinically relevant finding that could have implications for future work.

5.1.1 Study 1

Investigation into the differences in metabolites between tail and terminal bleeds from chapter 4, examining the effect of collection tube and collection site

- 9 BALB/c Hgd^{-/-} mice (5 nitisinone treated, 4 control)
- 2 x consecutive tail (venous) bleeds (approx 70ul each) into microvettes
- Pentoject overdose and once unresponsive:
- Terminal bleed (via brachial vessels) collected firstly in a microvette (70ul) and then into a monovette (1ml).

Both venous tail bleeds were sampled within several seconds of each other. Venous tail bleeds and arterial terminal bleed were sampled a maximum of 5 minutes apart (the time for Pentoject to take effect).

5.1.2 Study 2

Investigation into the trend of decreasing HGA in tail bleeds in control mice.

- 2 BALB/c Hgd^{-/-} control mice
- 5 x consecutive tail (venous) bleeds into microvettes were taken to see if the trend in falling of HGA continues
- Pentoject overdose and once unresponsive:
- Terminal bleed (via brachial vessels) collected into microvette (150-200ul).

Consecutive venous tail bleeds were sampled within several seconds of each other. Venous tail bleeds and arterial terminal bleed were sampled a maximum of 5 minutes apart (the time for Pentoject to take effect).

5.1.3 Study 3

Investigation into differences in HPPA and HPLA between venous tail and terminal arterial bleeds in nitisinone treated mice.

- 3 BALB/c Hgd^{-/-} nitisinone treated mice
- 5 x consecutive tail bleeds were taken to see if the trend in falling of HGA continues,
- Pentoject overdose and once unresponsive:
- Terminal bleed (via brachial vessels) collected into microvette (150-200ul).

Consecutive venous tail bleeds were sampled within several seconds of each other. Venous tail bleeds and arterial terminal bleed were sampled a maximum of 5 minutes apart (the time for Pentoject to take effect).

5.1.4 Study 4

Investigation into the effect of cull method on metabolites in nitisinone treated and control mice.

- BALB/c Hgd^{-/-} mice (4 nitisinone treated, 3 control)
- 5 x consecutive tail bleeds were taken to see if the trend in falling of HGA continues
- Manual culling
- Terminal bleed (via brachial vessels) collected into microvette (150-200ul).

Consecutive venous tail bleeds were sampled within several seconds of each other. Venous tail bleeds and arterial terminal bleed were sampled a maximum of 45 seconds apart (the time taken to cull via cervical dislocation and incise the axilla to reach the brachial vessels).

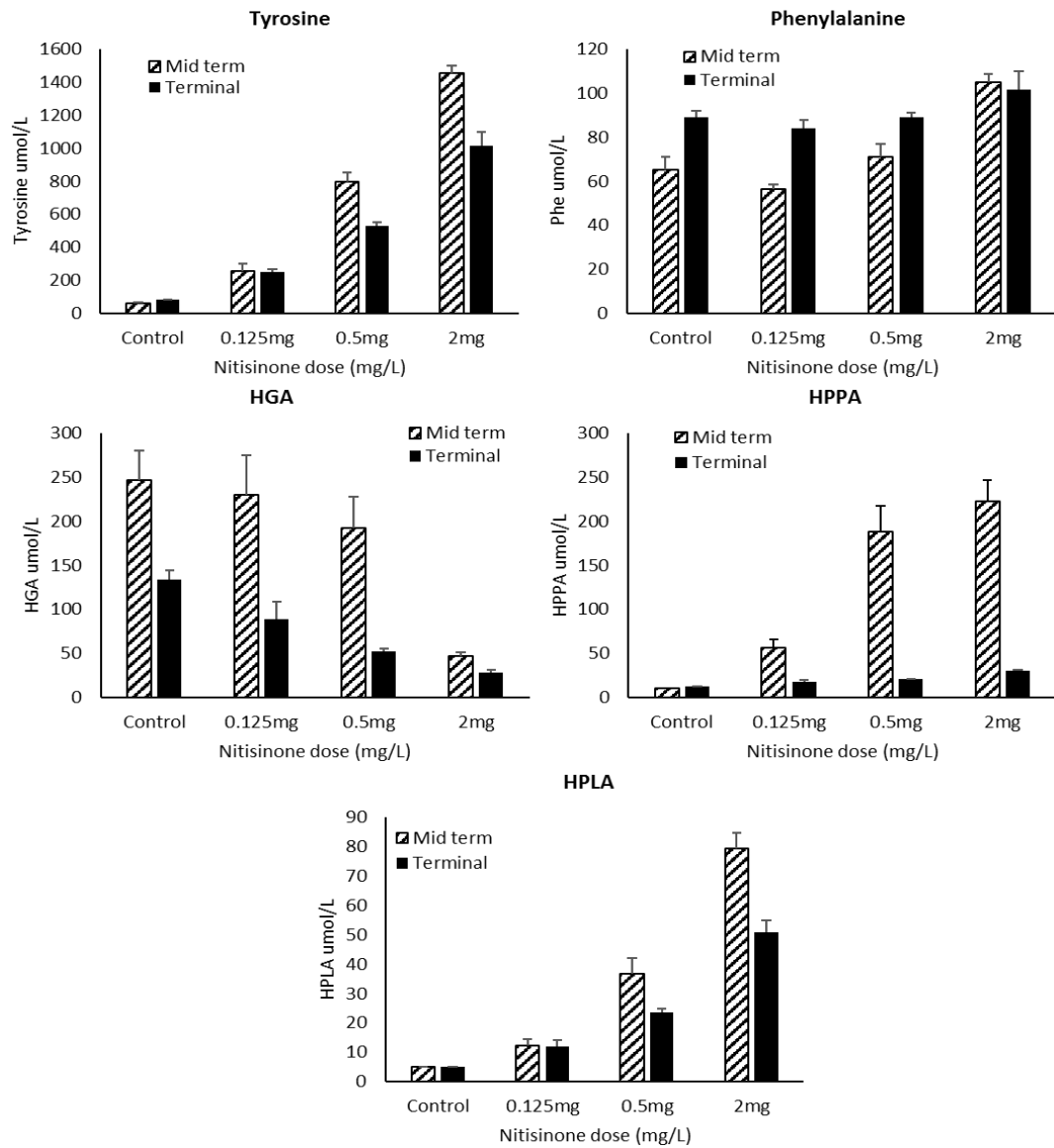


Figure 5.1 - Differences in metabolites between mid-term and terminal bleeds in BALB/c Hgd^{-/-} mice from the long-term dose response study (chapter 4). The inconsistencies in metabolite values, especially within those of control mice, influenced the decision to carry out the subsequent study discussed within this chapter. Mean \pm SEM.

5.2 HYPOTHESIS AND AIM OF STUDY

Hypothesis: Within the Hgd^{-/-} mouse, circulating blood will show the same concentration of tyrosine breakdown pathway intermediates irrespective of point of sampling.

Although there is high inter-individual and inter-sample variability in both mice and humans for HGA and tyrosine, the long-term dose response study in chapter four also showed a significant difference in the mean concentrations of HPPA and HPLA between mid and terminal bleeds for all doses of nitisinone investigated. The primary aim of this study was to investigate these differences in plasma metabolite concentrations between mid-term and terminal bleed samples. It was necessary to examine differences between sampling method to assess whether the observed variation in metabolites were methodological due to differences within sample site, sample collection or culling method.

5.3 RESULTS

This study began by investigating methodological inconsistencies between the sample collection tubes and sampling site. Within the long-term dose response study (chapter 4), mid-term bleeds were sampled via one of the lateral tail veins into microvette collection tubes. Terminal bleeds were sampled from the brachial vessels into monovette collection tubes immediately after schedule one culling with Pentoject. The difference in choice of collection tubes had been solely due to the larger volume of blood that can be collected from the terminal sample site. Both samples were centrifuged and processed identically to obtain plasma for analysis. For the first part of the study contained within this chapter, two consecutive tail bleeds were collected, each approximately 70ul, into microvette tubes. Mice were then immediately culled via intraperitoneal overdose of Pentoject and two terminal bleeds were collected from the brachial vessels, one into microvette (70ul) and the other into a monovette (1ml) for comparison. Both venous tail bleeds were sampled within several seconds. Venous tail bleeds and arterial brachial bleeds were sampled a maximum of 5 minutes apart (time for pentoject to take effect).

5.3.1 Effect of sample collection tube

There was no significant effect of collection tube (microvette/monovette) on tyrosine breakdown metabolites between brachial vessel samples in control or nitisinone treated Hgd^{-/-} mice. Samples prepared from both collection tubes showed similar plasma metabolite values (Fig. 5.2). This was also the first indication that plasma metabolite concentrations sampled from the brachial vessels were less variable than those sampled from the tail vein (Fig. 5.3).

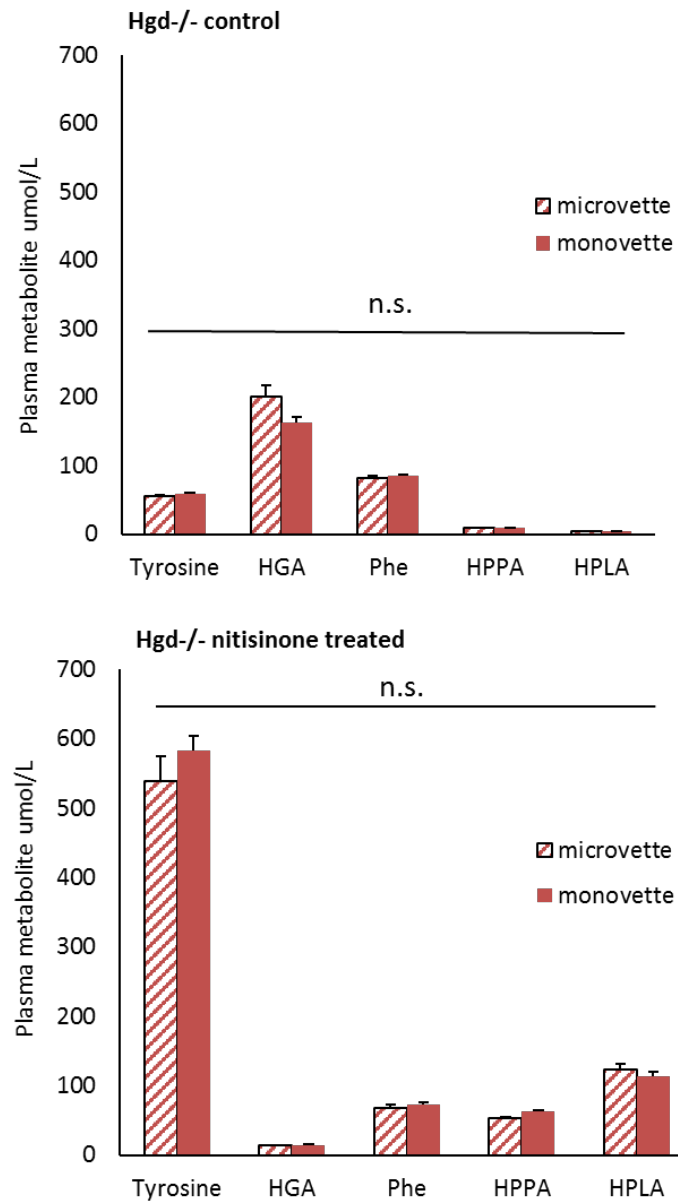


Figure 5.2 - Collection tube had no significant effect on metabolite values between brachial arterial blood samples in control or nitisinone treated BALB/c Hgd-/- mice. Mean \pm SEM plasma metabolite values shown. Treated n=5 control n=4.

5.3.2 Differences in metabolites between tail bleeds

Plasma HGA values showed variation between tail bleeds sampled just seconds apart (Fig. 5.3). Control and nitisinone treated mice showed a decreasing trend in HGA for the second tail bleed. Paired t test results showed differences between the two tail bleeds in control mice were statistically significant ($t(3)= 3.4319$ $P=0.0415$), differences in nitisinone treated mice were not significant ($t(4)= 2.0057$ $P=0.1154$). There was no significant variation in the other metabolites between tail bleeds.

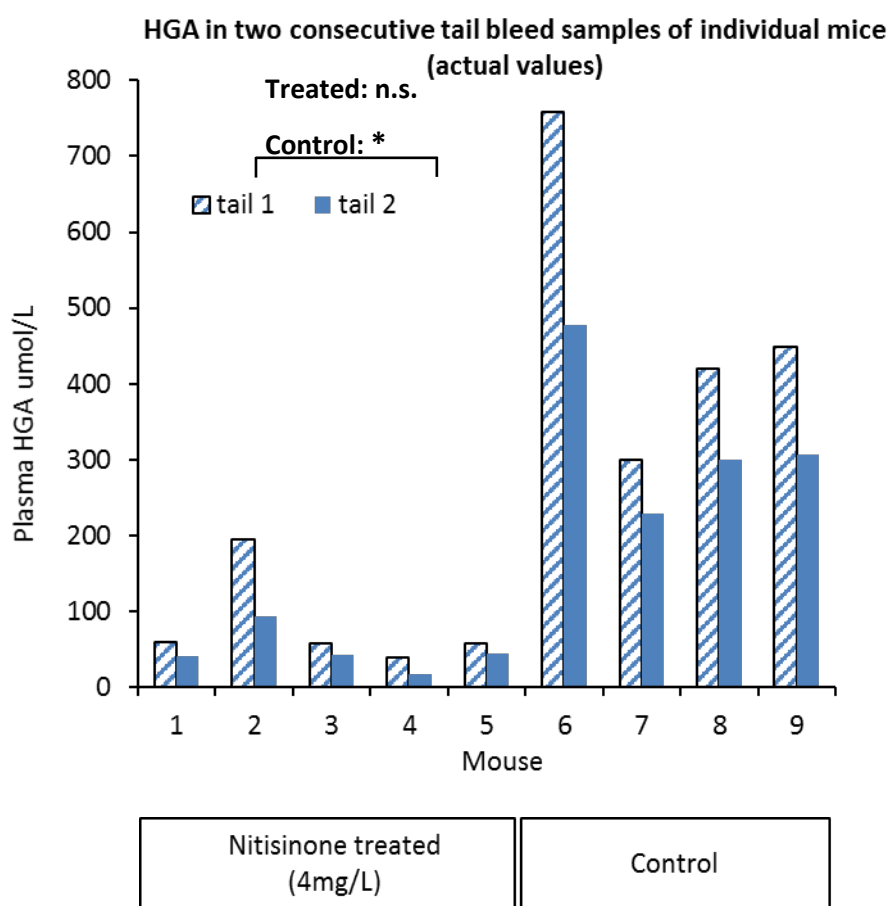


Figure 5.3 - Plasma HGA values decrease between two consecutive tail bleeds sampled seconds apart. HGA variation is more apparent in control mice when nitisinone has not lowered plasma levels but all mice showed the same decreasing trend.

5.3.3 Differences in metabolites between sample site (venous/arterial)

To compare venous and arterial bleeds, the mean of both venous tail bleeds (tail 1 and 2) and brachial arterial bleeds (microvette/monovette) were calculated to create mean \pm SEM values for each metabolite in nitisinone treated (n=5) and control (n=4) cohorts. Mean HGA values were significantly lower in arterial bleeds compared to venous bleeds in nitisinone treated (t(9) = 3.1795 P=0.0112) and control (t(7) = 3.7064 P=0.0076) cohorts. In nitisinone treated cohorts, HPPA was also significantly lower in arterial bleeds compared with venous bleeds (t(9) = 9.7695 P=0.0001). The opposite was the case for its metabolite, HPLA, which was significantly higher in arterial than venous bleeds (t(9)= 15.5979 P=0.0001) (Fig. 5.4).

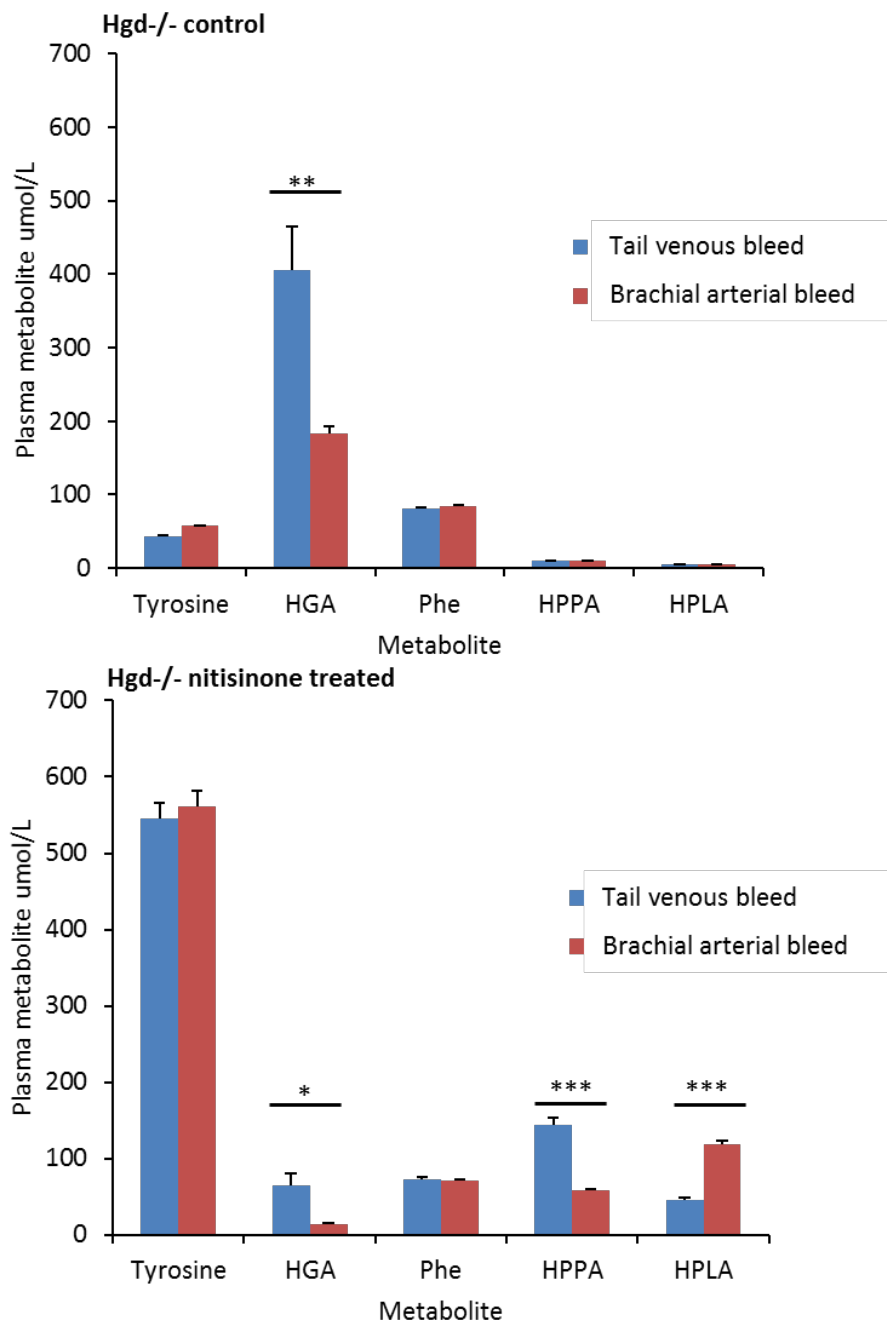


Figure 5.4 - HGA values were significantly lower in brachial bleeds in control mice. HGA and HPPA were significantly lower in brachial bleeds and HPLA was significantly higher in brachial bleeds in nitisinone treated mice. Tyrosine and phenylalanine showed no significant variation between bleeds. Mean \pm SEM plasma metabolite values shown. Treated n=5 control n=4. * P=<0.05 ** P = <0.01 * = P<0.001.**

5.3.4 Five consecutive tail bleeds

After finding a decreasing trend in HGA values between two consecutive tail bleeds and between tail and brachial arterial bleeds, we next investigated whether this decreasing trend continued in tail bleeds until these reached arterial bleed values. We hypothesised that if a number of consecutive tail bleeds were sampled, the peripheral venous blood would be rapidly replaced with that from a more central arterial supply and values may become more similar. This was investigated in control (n=2) and treated mice (n=3) so the differences in HGA (control), HPPA and HPLA (treated) could be further examined. Five consecutive tail bleeds were sampled from the right lateral tail vein, mice were culled with Pentoject and a terminal arterial bleed was sampled from the brachial vessels.

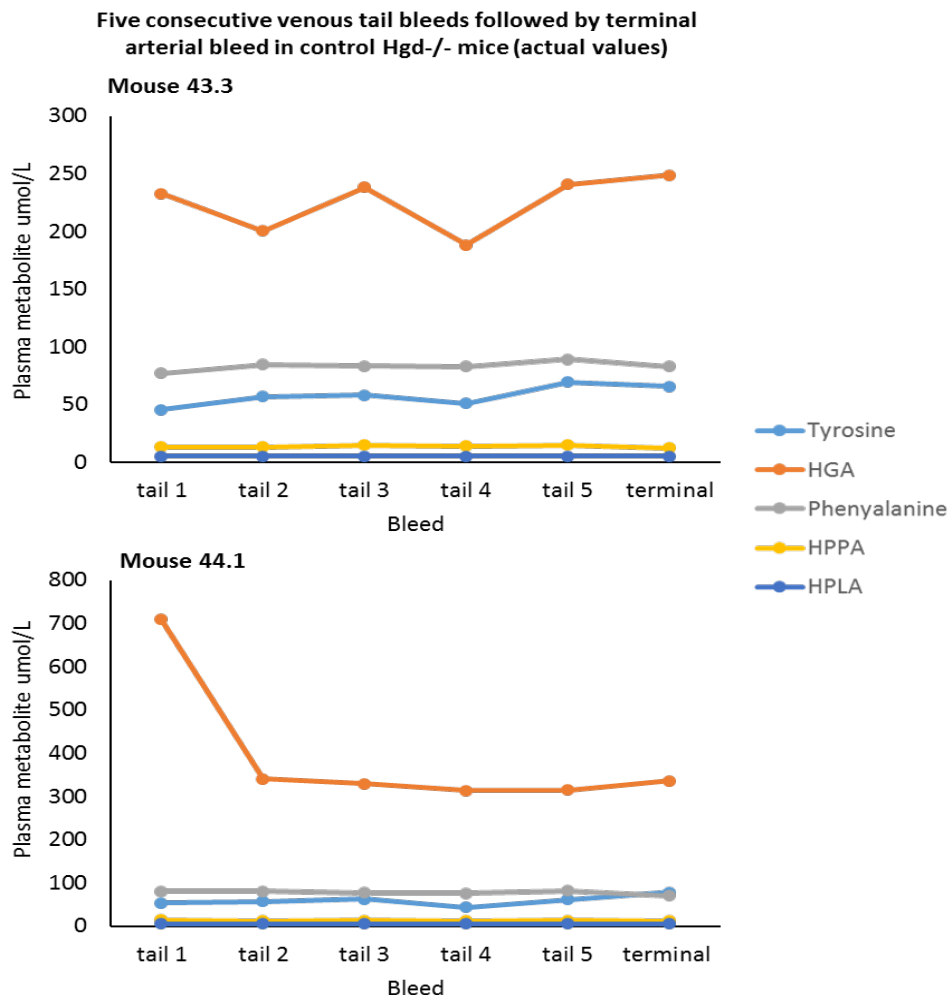
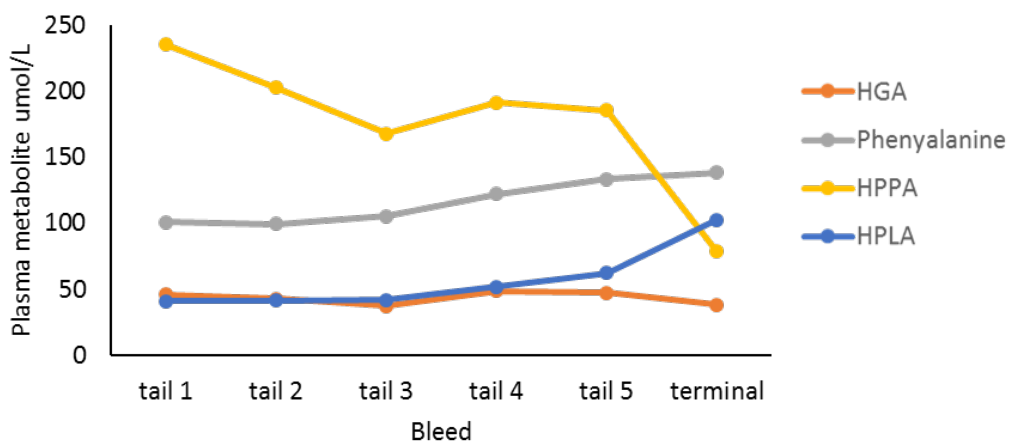


Figure 5.5 - Control mice showed variation in HGA between tail bleeds. Mouse 44.1 showed a dramatic 63% decrease in plasma HGA between tail 1 and tail 2 bleeds which then levelled for subsequent bleeds. Mouse 43.3 showed five variable tail bleed HGA values but less variation between tail and terminal bleeds.

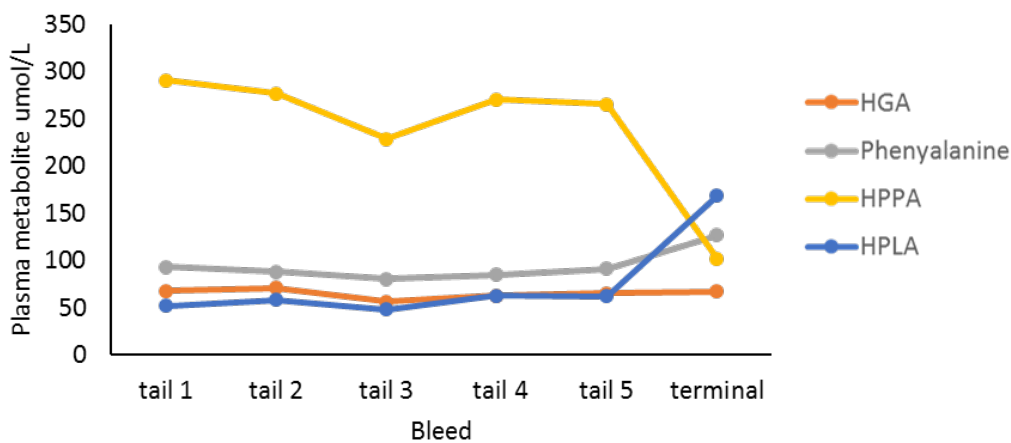
As observed in the previous experiments, the metabolites that varied significantly were HGA in control cohorts (Fig. 5.5) and HPPA and HPLA in nitisinone treated cohorts (Fig. 5.6). One of the control mice (43.3) showed fluctuating HGA between successive tail bleeds. Interestingly, this was the first mouse investigated who showed similar terminal bleed plasma HGA to tail bleed values (tail bleed mean 220umol/L, terminal 249umol/L). The other control mouse (44.1) had an extremely high first tail bleed of HGA value of 709umol/L, the subsequent four tail bleeds lowered to within normal range (for an untreated Hgd^{-/-} mouse) and remained similar in the terminal bleed. In past studies, occasional mice have shown extremely high HGA values and these have usually been considered as outliers or erroneous values. It was intriguing to see that this high HGA value reduced by over 60% within a matter of seconds and from the same sample site suggesting these past high values may not have been due to human or analytical error as previously assumed. HPPA and HPLA followed the same trend as in previous experiments with HPPA being reduced in terminal arterial bleeds compared to tail bleeds, with the opposite being the case for HPLA. These metabolites did not differ significantly between successive tail bleeds (Fig. 5.6).

Five consecutive venous tail bleeds followed by terminal arterial bleed in nitisinone treated Hgd^{-/-} mice (actual values)

Mouse 44.2



Mouse 44.3



Mouse 46.1

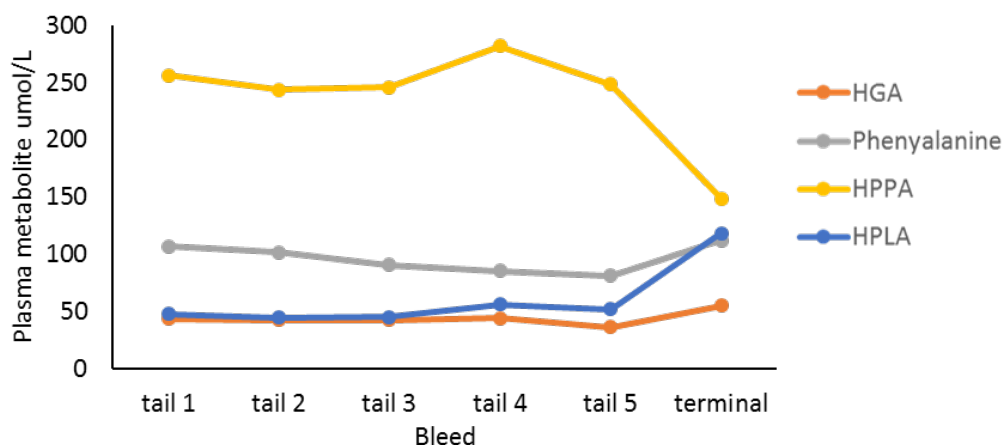


Figure 5.6 - Variation in HGA is masked by the therapeutic effect of nitisinone in treated Hgd^{-/-} mice. This variation is now apparent in HPPA and HPLA between tail and terminal bleeds. Tyrosine removed for clarity.

5.3.5 Cull method

Cull method was subsequently investigated as a possible cause for the observed variation in metabolites between venous tail and terminal arterial samples. In the long-term dose response study (chapter 4) and the previous studies discussed within this chapter, mice were culled prior to terminal sample collection with an intraperitoneal overdose of Pentoject (pentobarbitone). In the previous studies of this chapter, this was performed immediately after tail bleed plasma samples had been collected. For the following study, five consecutive venous tail bleeds were sampled followed by manual culling via cervical dislocation. Arterial samples were then collected from the brachial vessels. Control (n=3) and nitisinone treated (n=4) cohorts were used for consistency with previous experiments. The data was then compared to data from the previous studies where the pentobarbitone cull method was used. If a significant effect of cull method was observed, this would only apply to terminal arterial samples as culling takes place between tail and terminal bleeds and would therefore have no effect on tail bleed plasma metabolites.

The metabolites showing significant variation from each mouse are presented below to show each mouse followed a similar trend and this was not simply due to individual variation. Tyrosine and phenylalanine, as previously shown, did not vary significantly between bleeds so have been removed for clarity. Control mice once more showed highly variable plasma HGA, both between consecutive venous tail bleeds and between venous tail and terminal arterial bleeds. However, mean terminal bleed HGA values were lower than tail bleed values. Once again, a control mouse within this study (55.2) had an extremely high HGA value at the first tail bleed (829.5 μ mol/L) which steadily reduced with subsequent bleeds over a period of 20 to 30 seconds until it was within the normal range for an untreated Hgd^{-/-} mouse. Conversely, mouse 55.1 showed HGA values that increased significantly between the first to third tail bleed (258.7, 350.3, 567.4 μ mol/L) which then reduced in the subsequent tail and terminal bleeds. Interestingly, although these control mice had vastly variable tail bleed HGA values, they had all showed similar lower levels in the terminal arterial bleed, within approximately 60 μ mol/L of each other (Fig. 5.7).

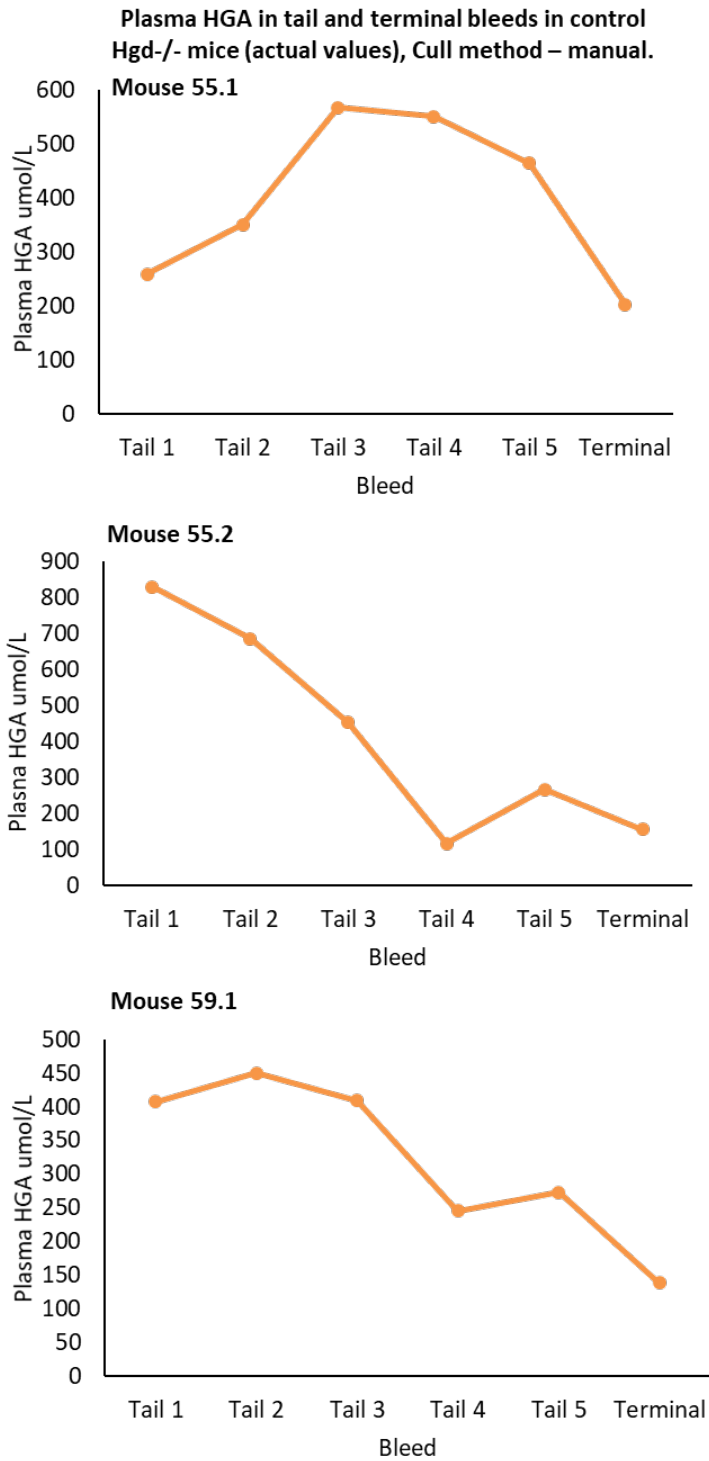


Figure 5.7 - Tail bleed HGA values in control mice once again showed high intra and inter-mouse variability. HGA was lowest in terminal bleeds with these values being within ± 60 umol/L range between the three mice despite previous tail HGA values differing substantially between these mice.

Nitisinone treated mice showed the established trend of steadily reducing HPPA between tail bleed 1 and terminal bleeds as observed in the previous studies. The decrease in HPPA between the final tail bleed (tail 5) and terminal bleed was still present. Interestingly, the sharp increase in HPLA between the final tail bleed and terminal bleed that was observed in the previous studies was not as apparent (Fig. 5.8). HPLA levels showed minimal variation and were relatively stable across all bleeds in the nitisinone treated mice. As mice within this study were culled manually via cervical dislocation, this could be an indication that the pentobarbitone was responsible for the significant increase in HPLA between final tail bleed and terminal bleeds that were previously observed in nitisinone treated Hgd^{-/-} mice (Fig. 5.4, Fig 5.6).

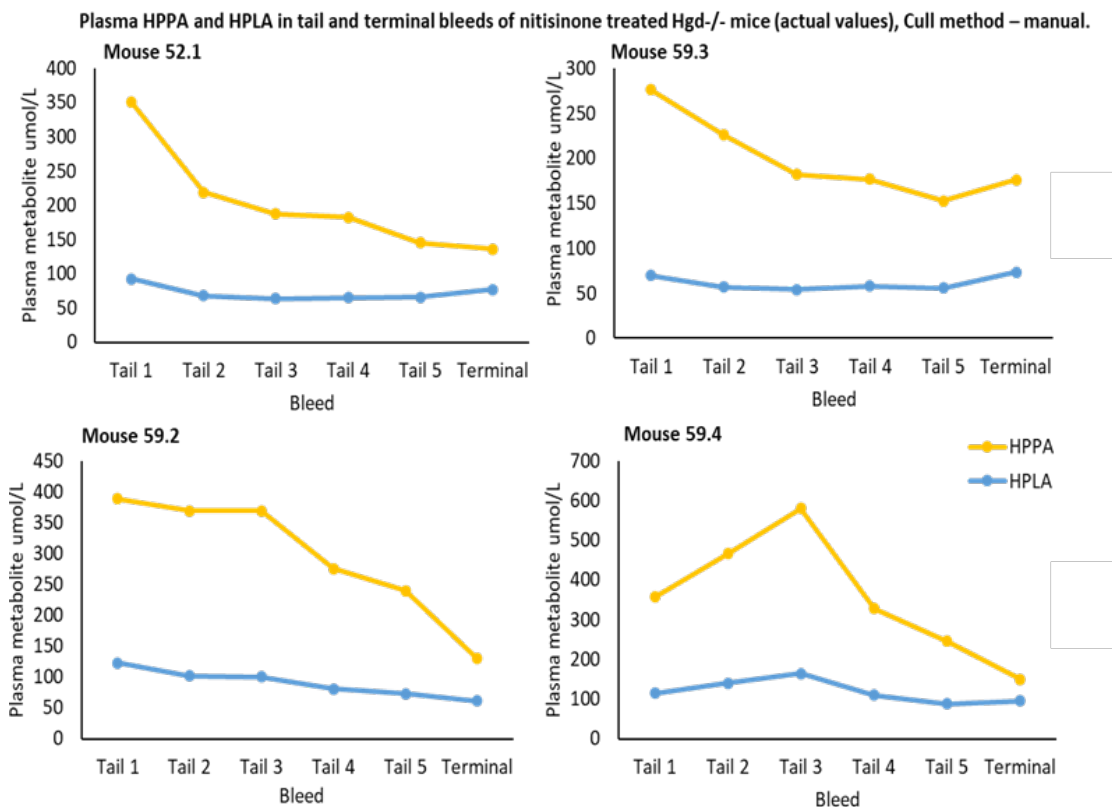


Figure 5.8 - HPPA values in treated mice followed the same trend as observed in previous studies – lower levels in terminal arterial bleeds compared to tail bleeds. HPLA was much less variable with similar concentrations across bleeds. Mice culled with pentobarbitone from previous studies showed a sharp increase in HPLA between the final tail bleed and terminal bleed. This trend is absent in manually culled mice suggesting the increase in HPLA may have been an effect relating to pentobarbitone administration.

5.3.6 Combined data from terminal arterial bleeds to assess cull method

Mean metabolite data from all terminal arterial bleeds within this chapter (control n=9, nitisinone treated n=12) were then combined to assess the significance of cull method on terminal bleed metabolites. To reiterate, mice within the final study (Fig.5.7, Fig. 5.8) were culled manually via cervical dislocation. This data was then compared with the data obtained from the previous experiments where mice were culled via overdose of Pentोजect in order to determine whether Pentोजect, as a pharmacological agent, was causing the differences in terminal arterial values for HGA in control mice and HPPA/HPLA in nitisinone treated mice.

Cull method had no significant effect on terminal bleed mean HGA values for control mice (Fig. 5.9A) with plasma concentrations similar irrespective of cull method ($t(7)=0.898$ $P=0.3990$) (manual: 207.3 ± 30.67 , Pentोजect: 165.5 ± 19.3). Cull method had a statistically significant effect on HPPA ($t(10)=5.653$ $P=0.0002$) (manual: 148.0 ± 10.3 , Pentोजect: 75.54 ± 7.5) and HPLA ($t(10)=3.395$ $P=0.0068$) (manual: 77.0 ± 7.0 , Pentोजect: 115.48 ± 7.1) in nitisinone treated mice (Fig. 5.9B&C). For HPPA, terminal plasma values were higher in mice that were culled manually. HPLA showed the opposite with plasma values being higher in mice culled with Pentोजect. This could indicate that Pentोजect is in some way interacting with these metabolites and the mechanism of HPPA to HPLA conversion.

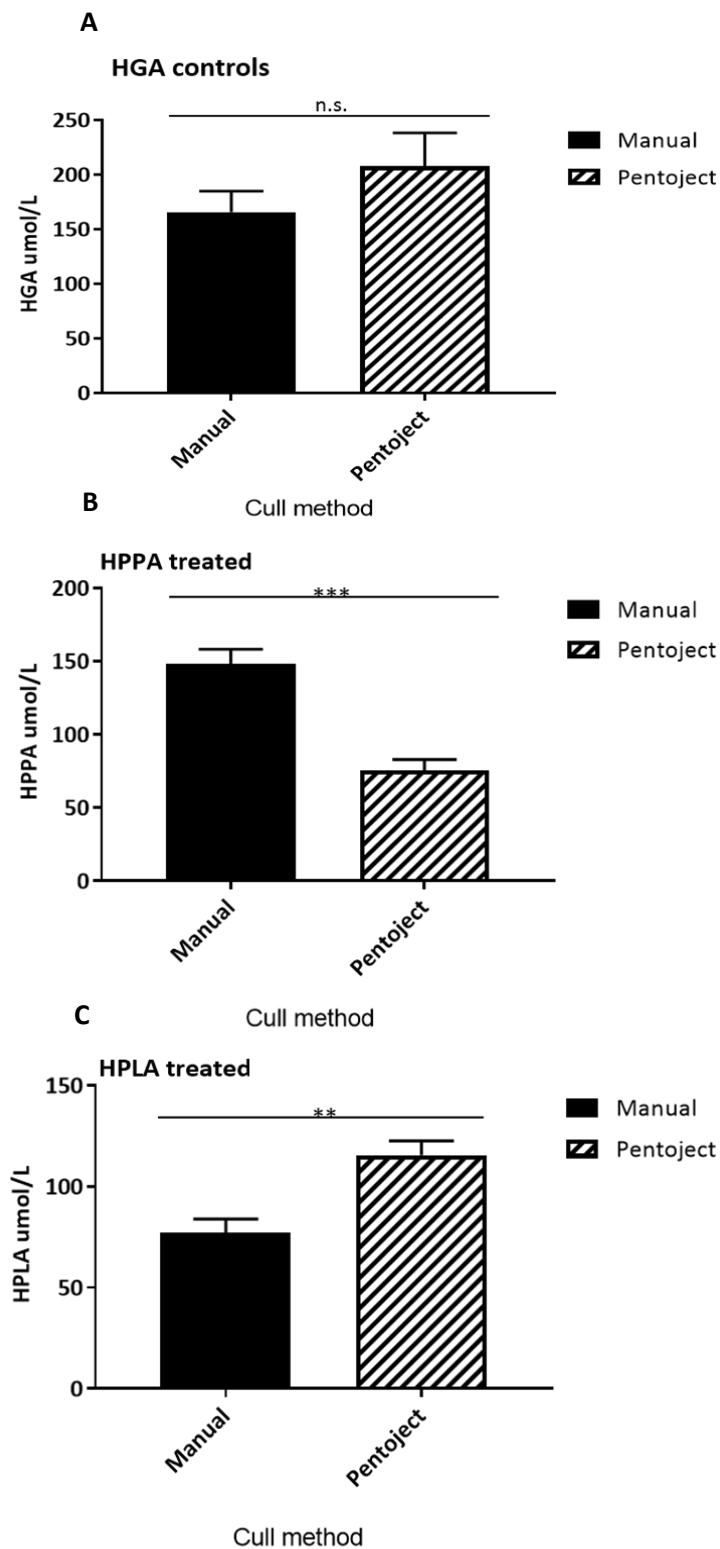


Figure 5.9 - Culling with Pentoject had a significant effect on HPPA and HPLA terminal arterial plasma values compared to manual culling in nitisinone treated Hgd^{-/-} mice (B, C). Cull method had no significant effect on HGA values in terminal arterial bleeds of control Hgd^{-/-} mice (A). Mean \pm SEM terminal bleed plasma metabolite values shown. Control: manual n=3, Pentoject n=6. Nitisinone treated: manual n=4, Pentoject n=8. ** = P<0.01 * = P<0.001.**

To examine this effect of Pentोजect further, the last tail bleed (sample taken immediately prior to culling) and the terminal arterial bleed for both cull methods were analysed for HPPA and HPLA. This showed HPLA sharply increased after Pentोजect administration in terminal bleeds. This increase is absent for HPLA in manually culled mice. HPPA showed the same reduction between tail and terminal bleeds for both cull methods although the reduction was more pronounced in mice culled with Pentोजect (Fig. 5.10).

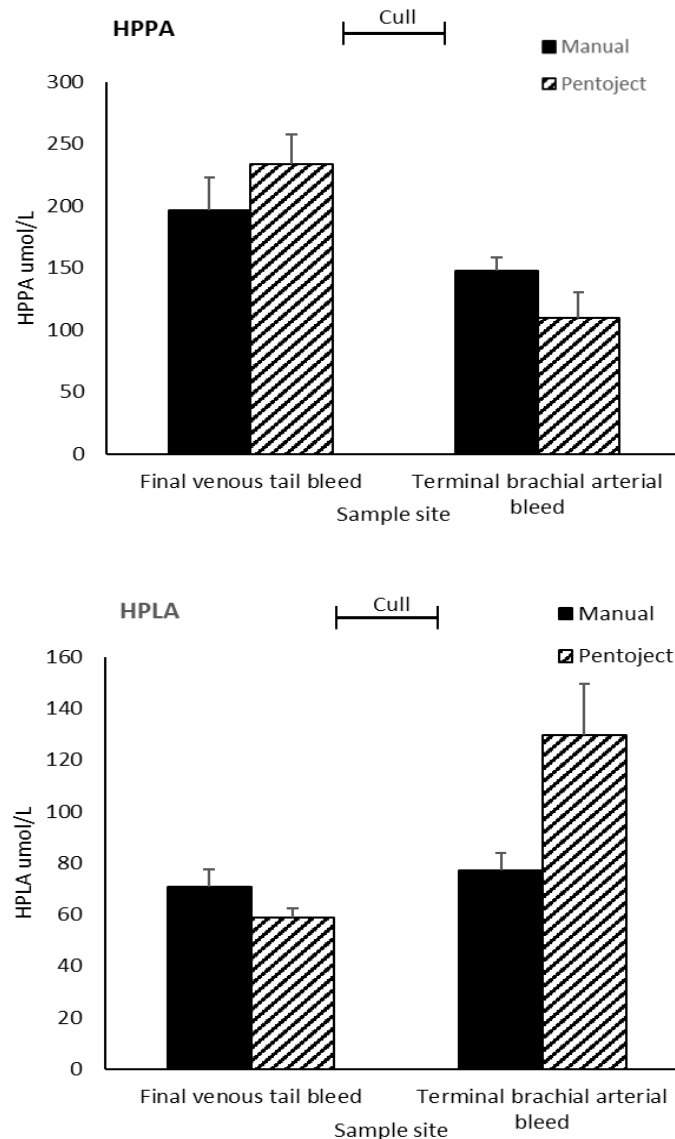


Figure 5.10 - Administration of Pentोजect has a significant effect on terminal bleed HPPA and HPLA plasma values of Hgd^{-/-} BALB/c nitisinone treated mice. Pentोजect results in a sudden increase in HPLA which is absent in manually culled mice. The reduction of HPPA between venous tail and terminal arterial bleeds is more marked with Pentोजect. Mean \pm SEM.

5.3.7 Combined data from venous tail and terminal bleeds

Combined venous tail and brachial arterial bleed data from this chapter (n=21 mice) showed HGA was consistently significantly lower in terminal bleeds of control Hgd^{-/-} mice compared to tail bleeds (Fig. 5.11). ANOVA confirmed that type of bleed (tail 1, tail 2 or terminal) had a significant effect on plasma HGA ($F(2,38) = 19.16$ $P < 0.0001$) (Table 5.1). This is in agreement with metabolite findings within the long-term dose response study in chapter four. Treatment with nitisinone masked this effect due to lowering plasma HGA levels so although this meant there was no statistically significant difference between bleeds; tail bleed values were still lower. The effect was observed in all but one of the twenty-one mice investigated suggesting this is a not just a methodological finding and HGA is genuinely lower in blood sampled from the brachial vessels compared to blood sampled from peripheral venous vessels. Similarly, type of bleed also had a significant effect on HPPA and HPLA plasma values (ANOVA $F(2,38)=23.23$ $P < 0.0001$ and $F(2,38)=5.986$ $P < 0.0055$ respectively) (Table 5.1) and as observed in the long-term dose response study, HPPA and HPLA were found to be significantly different between venous tail and brachial arterial bleed samples in nitisinone treated mice. HPPA is lower in blood sampled from the brachial vessels compared to blood sampled from peripheral venous vessels (Fig. 5.12A). The opposite occurs for HPLA with this metabolite being higher in blood sampled from the brachial vessels compared to blood sampled from peripheral venous vessels (Fig. 5.12B), although this effect was more marked in mice culled with Pentoject (Fig. 5.10). Phenylalanine varied significantly between type of bleed in nitisinone treated mice (ANOVA $F(2,38)=3.498$ $P=0.0403$) (Table 5.1) but this was much less pronounced than HGA, HPPA and HPLA (Fig. 5.13). Tyrosine was the most consistent metabolite within this study showing no significant variations across blood sample sites (Fig. 5.14).

Metabolite	Significance from Tukey multiple comparisons post hoc test (P value)					
	Tail 1 - Tail 2		Tail 1 - Terminal		Tail 2 - Terminal	
	Control	Treated	Control	Treated	Control	Treated
HGA	0.0256	n.s.	<0.0001	n.s.	0.0004	n.s.
HPPA	n.s.	n.s.	n.s.	<0.0001	n.s.	0.0001
HPLA	n.s.	n.s.	n.s.	0.0002	n.s.	0.0001
Phenylalanine	n.s.	n.s.	n.s.	0.0360	n.s.	0.0080
Tyrosine	n.s.	n.s.	n.s.	n.s.	n.s.	n.s.

Table 5.1 - Tukey multiple comparisons results from ANOVA post hoc tests of combined venous tail and brachial arterial bleed data (n=21 mice).

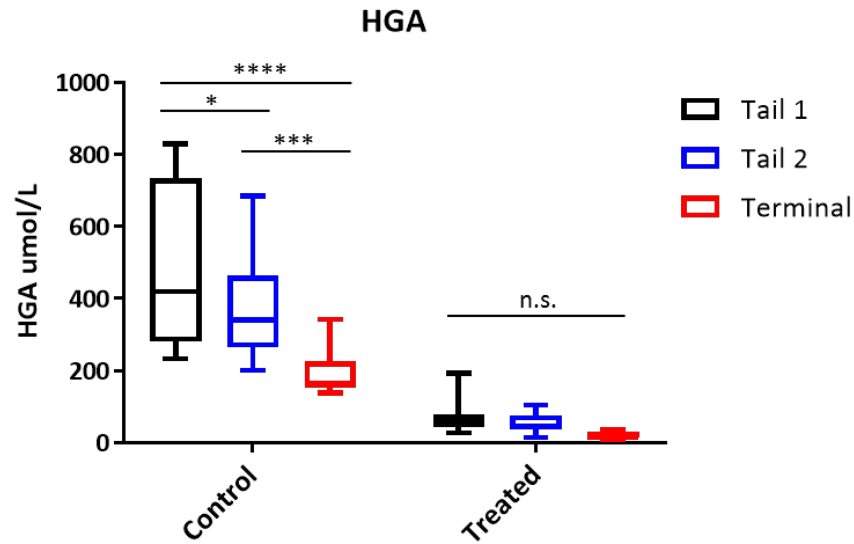


Figure 5.11 – Plasma HGA was lower in blood sampled from brachial vessels (terminal) compared to peripheral venous blood (tail) in BALB/c Hgd^{-/-} mice. This statistically significant effect is masked in treated mice but values are still lower in terminal arterial bleeds than venous tail bleeds for both control and nitisinone treated cohorts. Control n=9, treated n=12 . Significance from Tukey multiple comparisons post hoc test. * = P<0.05, *** = P<0.001, **** = P<0.0001.

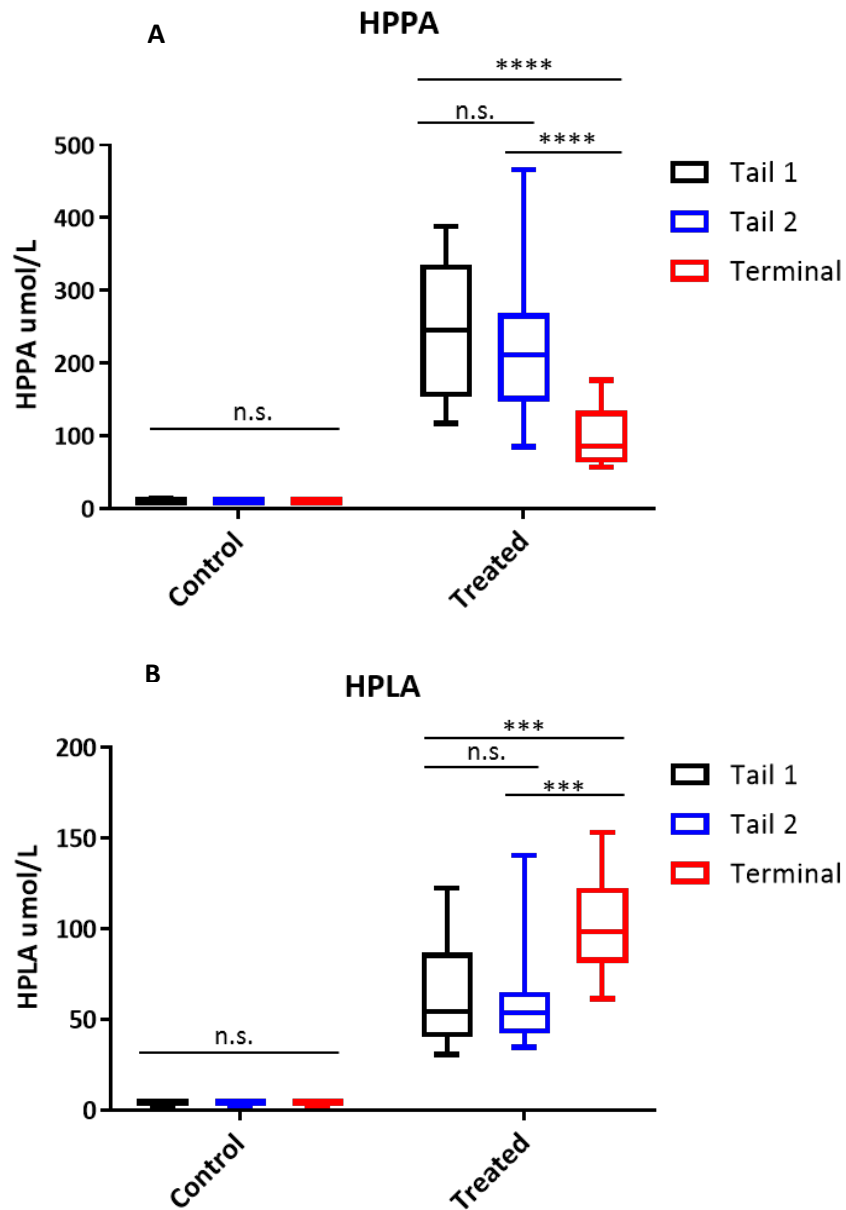


Figure 5.12 – Plasma HPPA was lower (A) and HPLA higher (B) in blood sampled from brachial vessels (terminal) compared to peripheral venous blood (tail) in BALB/c Hgd^{-/-} mice. These metabolites are low or undetectable in controls where the effect is instead observed in the downstream metabolite HGA. Control n=9, treated n=12. Significance from Tukey multiple comparisons post hoc test. *** = P<0.001, **** = P<0.0001.

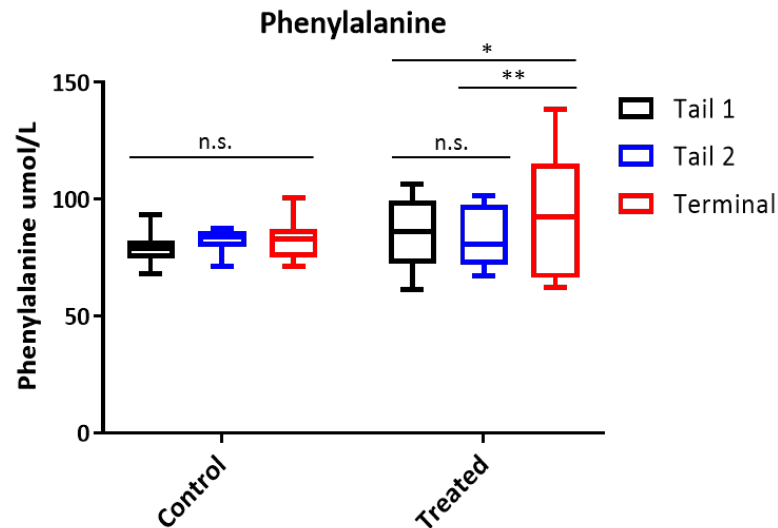


Figure 5.13 – Phenylalanine was slightly elevated in blood sampled from brachial vessels (terminal) compared to peripheral venous blood (tail) in nitisinone treated BALB/c Hgd^{-/-} mice. This statistically significant result appeared to be likely due to higher terminal bleed intra-cohort variation than observed in tail bleeds as mean plasma phenylalanine values were similar.

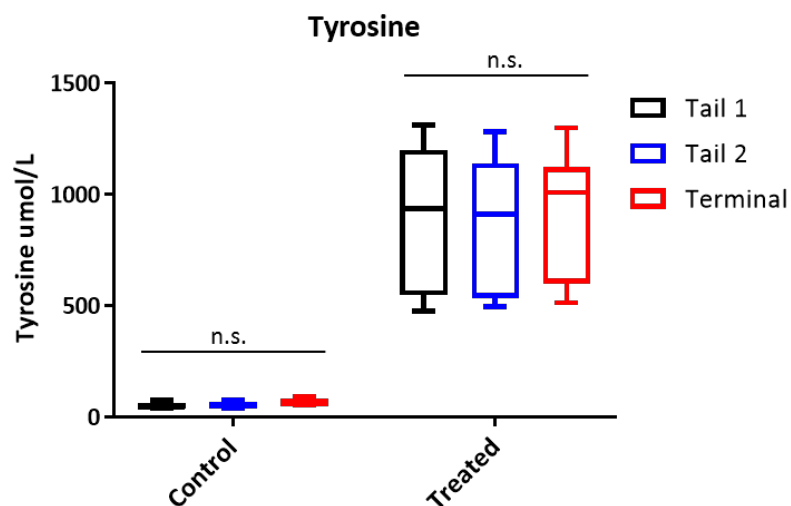


Figure 5.14 – Tyrosine showed no significant fluctuations between plasma sample site in control or nitisinone treated BALB/c Hgd^{-/-} mice. Elevated plasma concentrations in treated mice are due to HPPD inhibition by nitisinone. Significance from Tukey multiple comparisons post hoc test.

5.4 DISCUSSION

The findings of this chapter demonstrate the importance of standardisation of blood sample site for measurement of tyrosine breakdown metabolites in the Hgd^{-/-} mouse, particularly when repeated blood sampling is required. The metabolite inconsistencies observed within the long-term dose response study were methodological due to differences between sample site which prior to this study were unknown. HGA, as the main metabolite of concern with regards to AKU, was the most variable between blood compartments, and therefore this is an important finding with implications for future research. These systematic differences in metabolites between site of sampling should be considered in some past and all future experiments as the inconsistencies are large enough to mask important therapeutic effects if not considered when comparing samples. Tail samples should be collected pre-cull for accurate comparison with previous plasma samples. The results do not support the hypothesis, consequently the method and location of serial blood sampling needs careful planning and further investigation.

HGA was consistently found to be lower in blood sampled from brachial vessels compared to peripheral venous blood. When sampling from the brachial vessels, the axilla was incised and vessels severed to collect the sample. This sample would have provided a mixed, more central blood supply as the brachial vessels include the brachial artery and deep brachial veins. Blood sampled from this site may have had lower HGA due to more recent renal clearance of metabolites compared to venous peripheral blood. Evidence from a recent study by Taylor and Vercruyssen [59] suggests HGA must reach an alkalinity threshold prior to conversion into pigment. Arterial blood has a slightly higher (alkali) pH compared to venous blood, although these pH differences are very slight due to homeostasis [155]. Perhaps the slightly alkali environment results in more HGA being converted into pigment thus removing the metabolite from blood within the arterial supply, explaining the lower concentrations compared to venous blood. Increased tissue trauma would also have been an artefact of brachial samples due to incising of the axilla prior to sample collection. Brachial bleeds also exposed blood to surrounding tissues as it pooled into the body cavity prior to collection. HGA may have been taken up by these surrounding tissues, although this would have to be a very rapid mechanism so is unlikely.

Conversely, higher HGA concentrations in venous blood may also indicate that HGA is being released from the collagenous tissues. Some control mice demonstrated extremely high HGA levels (>700umol/L) in the first tail bleed which decreased over subsequent bleeds to become lowest in the terminal sample (Fig. 5.5, Fig 5.7). We had proposed that previous high outliers in tail bleeds could be due to relatively poor renal processing within that particular mouse but these findings show that in subsequent tail bleeds, HGA levels quickly reached normal limits for an untreated Hgd^{-/-} mouse suggesting no renal issues. A possible explanation for this could have been blood stasis where stagnation of blood within the tail, perhaps due to less efficient peripheral circulation, meant the blood had longer contact with the tissues to collect waste metabolites compared to faster flowing arterial blood. Upon further reflection, prior to tail vein sample collection, mice were warmed in a heat box to enhance blood flow to allow for easier sample collection. Heating would have likely reduced the effect of blood stasis within the tail by inducing vasodilation. Considering this, another explanation could be that increasing the mouse's body temperature may have in turn increased metabolic rate and HGA production. The high HGA value within the first tail bleed which gradually reduced during consecutive bleeds may have been related to this increase in body temperature. Mice were removed from the heat box to collect samples therefore body temperature would have lowered slightly with each successive bleed resulting in the lower HGA values. Future work could include taking tail bleed samples without the use of a heat box to compare values and see if such high variation still occurs.

In nitisinone treated mice, HGA was lowered by HPPD inhibition but the metabolite discrepancies between venous and brachial vessel samples were then found in HPPA and HPLA, metabolites upstream from HPPD inhibition. HPPA was higher in venous blood and dropped in terminal samples with the opposite occurring for its metabolite, HPLA. The conversion pathway of HPPA to HPLA is currently unknown but it appears to be activated as an alternative route for the clearance of tyrosine when elevated. Culling method had a significant effect on the terminal bleed values of these metabolites (Fig. 5.9, Fig. 5.10). For HPPA, terminal plasma values were higher in mice that were culled manually. Pentोजect appeared to cause a decrease in terminal HPPA values. The opposite was observed for HPLA with Pentोजect appearing to cause a marked increase in terminal bleed values. The increase in HPLA was much less obvious or absent in mice that were manually culled (Fig. 5.8). As HPLA is a metabolite of HPPA, when HPPA decreases it would be assumed HPLA is

being synthesised and increases as a result. These findings could indicate that Pentोजect is in some way interacting with these metabolites or catalysing the mechanism of HPPA to HPLA conversion. A study by Overmyer and colleagues investigating the impact of anesthesia and euthanasia on metabolomics of mammalian tissues found significant fold change decreases in serum metabolites including tyrosine and phenylalanine compared to cervical dislocation when the use of Pentोजect was implemented [156]. Methodological inconsistencies with regards to manual and Pentोजect culling method must also be considered. When culled with Pentोजect, terminal bleeds were sampled after several minutes; the time for the drug to take effect and the mouse to become unresponsive. For manual culling, terminal bleeds were sampled within a matter of seconds as the process of cervical dislocation causes immediate death. Pentोजect (pentobarbitone) causes death via respiratory arrest; terminal arterial blood sampled from Pentोजect culled mice may therefore have had a lower pH due to respiratory acidosis as ventilation and circulation would have been reduced or absent for a longer period of time. Perhaps HPPA to HPLA conversion takes place at a lower pH, as in the pentोजect culled mice, or endogenous factors released during the several minutes prior to sampling aid with the conversion. Lactate dehydrogenase (LDH) is released into the bloodstream during tissue damage or cell death and could be a potential candidate [157].

Arteriovenous perturbations in metabolites may have also been a result of the stress response associated with culling which could in turn cause release of cortisol and corticosterone [156]. During tail bleeds, mice were warmed in a heat box then gently held in a restrainer prior to sample collection. This would almost definitely induce a stress response due to the environmental stressor of increase temperature (37°C) along with the psychological effect of temporary restraint [158]. During terminal bleeds, it could be argued that manually culling would induce less of a stress response as the cervical dislocation method is completed within a matter of seconds. The highest stress response between all of the sampling methods would likely be overdose with Pentोजect as this takes several minutes for the mouse to become completely unresponsive and during this time the mouse will hyperventilate. Cortisol levels have been shown to peak in as little as 3 minutes when stress is induced within a mouse so this could affect plasma metabolite levels [159]. Interestingly, administration of cortisol to rodents has been shown to induce tyrosine aminotransferase (TAT) in the liver, responsible for converting tyrosine to HPPA [160, 161]

so stress response may have been a real contributing factor to the observed fluctuations in tyrosine metabolites between bleeds.

Tyrosine was the most stable metabolite between blood compartments in both control and treated mice which was surprising considering the large elevation observed during nitisinone treatment. Phenylalanine showed slight arteriovenous differences in treated mice within this study but not to the scale observed in chapter four where it was elevated for all cohorts in terminal bleeds. A possible reason for the elevation in phenylalanine within the long-term study could be that mice were 20 weeks older in the terminal bleed than in mid-term bleeds. At 43 weeks of age, when terminal bleeds were collected, the mice would have had an increased bodyweight and food consumption compared to at 23 weeks when mid-term bleeds were collected. Phenylalanine is an essential amino acid that is derived from dietary protein. In support of this, a paper investigating amino acid concentrations in children by Lepage et al [162] demonstrated that phenylalanine concentrations tended to increase throughout childhood and adolescence.

With long-term studies comes the practicalities of long-term plasma sampling. These studies often require serial samples to be collected that must be obtained whilst adhering to the Home Office guidelines for volumes of blood taken. This is a maximum of 15% total blood volume within one month and a maximum of 10% total blood volume within any one bleed. This study has established how sensitive the metabolome is to variations between blood compartment, cull method and, in the case of HGA, bleeds sampled seconds apart from the same site. Venous tail bleeds are the preferred method for serial sampling within our lab as they are quick and simple to perform, minimising stress for the mouse. HGA is one of the primary metabolites of interest in AKU, it is therefore crucial that accurate plasma values are obtained for analysis. The differences in plasma HGA values observed between consecutive tail bleeds within this study suggest it may be advantageous to take 3 separate tail bleeds during future studies in order to use the average value of these for subsequent analysis. As the metabolite differences between consecutive tail bleeds may have been due to increased metabolic rate as a result of warming prior to sample collection, it may be beneficial to try a different sampling method. Sampling from the lateral saphenous vein is a relatively quick method of obtaining serial blood samples from mice and does not require the animal to be warmed for sample collection. Anaesthesia is not necessary and mice are conscious throughout the procedure [163-164]. Comparison of

metabolites values between tail vein and saphenous vein samples would allow the effects of warming on the metabolome, if any, to be investigated further.

6. General Discussion

AKU is a chronic and progressive disease with multi-system involvement involving devastating joint damage and lifelong pain from early adulthood. Despite advances in the understanding and molecular basis of the condition, and identifying HGA as the key player in morbidity, over a century has passed since Garrod described AKU but still no definitive treatment is available. Nitisinone is a treatment option that has the potential to lower HGA levels from a young age, effectively halting the disease in its tracks and vastly improving disease prognosis later in life. Nitisinone use in children has, up until now, only been used for the treatment of HT-1 in which fatal complications arise if left untreated. Concerns regarding the safety of elevation of tyrosine in children as an adverse effect of nitisinone treatment have justly been aired. This thesis presents novel data that neither nitisinone itself, nor the associated elevation of tyrosine has a detrimental effect on learning, memory or motor function in young Hgd^{-/-} mice. It also demonstrates that plasma HGA and ochronotic pigmentation are correlated but that this correlation is not linear, HGA must be reduced to a critical level before pigmentation is significantly reduced. Additionally, this thesis shows that there are large discrepancies between the arteriovenous metabolome relating to AKU, which should be considered when comparing experimental blood samples and in designing sampling protocols for future studies.

The findings of chapter three reported no detrimental effect of nitisinone treatment or the related-tyrosine elevation, which is encouraging for treatment of children with AKU. Concerns regarding the neurotoxicity of elevated tyrosine, especially during brain development, have been raised because of the cognitive development issues occasionally reported in HT-2 and HT-3. Neurocognitive developmental impairment has also been reported in some HT-1 nitisinone treated children. Within these conditions, high tyrosine levels are present from birth as the result of a genetic mutation or treatment with nitisinone. Genetic deficiency of TAT, the first enzyme of the tyrosine degradation pathway, in HT-2 means the conversion of tyrosine into HPPA is reduced. It has been suggested that mitochondrial aspartate aminotransferase acts as a compensatory substitute to aid with tyrosine excretion via HPPA [164] but nevertheless, tyrosine levels tend to be highest in this condition (>1000umol/L). Within AKU, on the other hand, the TAT tyrosine conversion pathway is functional, enabling renal processing and urinary excretion of HPPA/HPLA when tyrosine is elevated by nitisinone therapy. HT-3 has a closer metabolic resemblance to nitisinone treatment in AKU as inhibition of HPPD is present in both. Only a few cases of

HT-3 have been reported in the literature with mixed clinical findings including some asymptomatic cases [115, 165] suggesting that the high tyrosine concentration alone does not participate directly in the neuronal damage described within these patients. HPPD deficiency and high tyrosine in HT-3 is probably also present during the prenatal period, during vital stages of neurocognitive development. Three cases of women with HT-1 who received nitisinone throughout pregnancy are described in the literature, with the children reported as suffering no adverse effects and normal psychomotor development within the first years of life [67-69]. Similar to those with HT-3, these children would have also experienced elevated tyrosine during their prenatal development, further suggesting that the neurological dysfunction in HT-3 is not directly due to elevation of tyrosine and that other factors must be involved. Nitisinone treatment for children with AKU would use lower doses than in the treatment of HT-1 and this would be combined with a protein-restricted diet to ensure tyrosine levels remained within clinically set safety limits. Tyrosine is required by the brain for the synthesis of the catecholamines, but techniques to regulate uptake by the brain when levels are elevated during nitisinone treatment could be beneficial. Tyrosine is a large neutral amino acid (LNAA) which shares a common transporter across the blood brain barrier with other LNAA such as tryptophan and the branched chain amino acids (BCAA). The ingestion of dietary LNAA has been shown to modify tryptophan and tyrosine uptake into the brain and their conversion to serotonin and catecholamine's, respectively [166]. Choi and colleague demonstrated that ingesting BCAA reduces tyrosine concentrations due to competitive inhibition of the LNAA transporter [167]. This could potentially be used as a precautionary measure to regulate uptake of tyrosine within the brain alongside nitisinone therapy and a protein controlled diet.

The data from chapter three also showed that differences between learning ability in the MWM were an effect of genotype and not treatment with nitisinone. There were no significant differences in any of our multiple measured parameters between control and treated cohorts, which was encouraging as this indicated nitisinone treatment did not have a detrimental effect on the learning process. Both control and treated wild type cohorts showed preference to the target quadrant and performed better overall within the MWM task. Both Hgd^{-/-} cohorts were slower at learning during acquisition trials compared to wild type and showed no preference to the target quadrant during the probe trial. This probably

indicated relatively poor spatial learning and reference memory within the Hgd^{-/-} mice. Such a characteristic has not been documented previously. Dopamine and the activation of hippocampal and striatal D1R and D5R dopamine receptors are known to be involved in spatial learning and memory processing [93]. Deletion or dysregulation of these receptors has been shown to produce deficits in acquisition of spatial memory and reduced hippocampal activation within the MWM [86, 91]. Dopamine is also extensively involved in the mesolimbic system that mediates motivated behaviour [168]. Aversive stimuli, such as the MWM, have been shown to stimulate dopamine synthesis as mice are motivated to escape the pool [169]. Hgd^{-/-} mice were noticeably more docile and seemed less anxious to be handled from the beginning. This could suggest the Hgd^{-/-} genotype demonstrate poor spatial learning, but could also be interpreted as an indication of reduced aversive behaviour and a reduction in motivated behaviour due to influences of the genotype on the dopaminergic system. Tyrosine is a precursor to the catecholamine neurotransmitters including dopamine. Administration of tyrosine has also been shown to increase acetylcholinesterase activity in rats [170], responsible for breaking down Acetylcholine, which itself also plays a role in learning and memory. As AKU is a condition affecting tyrosine catabolism, these neural systems could feasibly be implicated.

The characteristic features of HT-3 can include occasional loss of balance and coordination. Motor function assessment in chapter 3 showed Hgd^{-/-} control and treated mice displayed no indications of intermittent ataxia or deficits in gross motor function. Chapter three also contained the results of a novel assessment of gait in the Hgd^{-/-} mouse using the Catwalk XT automated platform. The chosen parameters, also used by other centres for the assessment of mouse models of OA, showed no obvious signs of pathologically altered gait. Symptomatic joint pathology in human AKU patients often presents from the third decade and progressively worsens with age [96]. Hgd^{-/-} cohorts were between 17 to 39 weeks when gait was analysed, as this is when the ochronotic phase of the disease has been shown to be present [70]. Mice are quadrupedal therefore the load on weight bearing joints is reduced compared to human locomotion. With reduced load bearing, the joint damage relating to ochronosis and its effect on gait may take much longer to manifest in the mouse. It would be interesting to assess gait in Hgd^{-/-} aged mice to assess whether symptoms of ochronotic osteoarthropathy were apparent in older mice when kidney and liver function were also likely to be less efficient. The principle of lower severity in mice

than in humans with analogous musculoskeletal mutations producing chronic disease is not unusual. For example, the mdx mouse that shows the mutation analogous to that producing Duchenne muscular dystrophy in human is much less affected in terms of motor function than human patients.

Prior to this thesis, the correlation of HGA and ochronotic pigmentation remained unidentified. Results from chapter four indicated a correlation does exist although this is not linear. The critical plasma levels for HGA appeared to be between 40-60 μ mol/L. Below 40 μ mol/L resulted in a dramatic reduction in pigmentation whereas above 60 μ mol/L pigmentation was similar to control and showed maximal levels of ochronosis. This builds upon *in vitro* work by Tinti and colleagues that suggests 10 μ mol/L HGA is insufficient to cause ochronosis [106]. These findings are encouraging for facilitating tailored nitisinone treatment as it suggests a personalised dose of nitisinone can be used that lowers HGA to levels that prevent ochronosis while simultaneously keeping elevation of tyrosine to a minimum. This is particularly important for those AKU patients who demonstrate tyrosine toxicity independent of peak plasma levels as it would mean that they might be able to receive continuous treatment with minimised risk of ocular symptoms necessitating withdrawal of treatment. Chapter four also showed there was a surprising degree of congruence between Hgd^{-/-} mice and humans in the effect of nitisinone dose. The SONIA1 human study concluded that the 8mg daily dose, which equates to 0.114mg/kg for a 70kg human, was most efficacious for AKU patients. Within the Hgd^{-/-} mouse study in chapter 4, the 0.5mg/L dose, which equates to 0.007-0.01mg/kg for a 30g mouse, provided a practical compromise of lowering HGA sufficiently to reduce pigmentation whilst also producing a lower degree of tyrosinemia than higher doses. This reaffirms the importance of the Hgd^{-/-} mouse as an appropriate model to clarify pathophysiology and test therapies for AKU.

The data presented in chapter five showed, for the first time, that the metabolome of tyrosine breakdown products, specifically HGA, HPPA and HPLA, were labile in the compartments of the circulating blood. This is important to consider when comparing samples, as differences are significant enough to mask potential therapeutic effects. Chapter five also stressed the importance of sampling tail bleeds pre-cull for comparison with previous serial samples during long-term studies. The use of pentobarbitone for

humane killing had significant effects on the tyrosine phenolic metabolites HPPA and HPLA, which are themselves important to analyse for evaluating tyrosine clearance during nitisinone treatment. Within the arteriovenous metabolome study, one group of five nitisinone treated littermates had tyrosine levels of around 500umol/L whilst receiving a dose of 4mg/L. All other mice receiving the same dose had tyrosine levels of >1000umol, typical within the Hgd^{-/-} model. The lower plasma tyrosine levels within these five littermates suggest that they may have had a genetic advantage that enabled more efficient clearance of tyrosine. Plasma tyrosine levels are a reflection of inhibition of HPPD and the ability to clear tyrosine from the blood stream. HPPA and HPLA plasma values within the five littermates did not differ significantly from the other mice within the study, suggesting additional tyrosine was not cleared by increases in this excretory pathway. Increased tyrosine clearance by another mechanism may have been taking place, such as enhanced production of melanin or hormones. Another possible explanation may be that these mice had HPPD that was less sensitive to nitisinone inhibition, allowing a percentage of the tyrosine to be catabolised into HGA. Intriguingly, only one of the five littermates had HGA that was higher than would be expected when receiving the 4mg/L dose of nitisinone and this value was still much lower than found in untreated Hgd^{-/-} mice. This suggests that these mice were just as sensitive to nitisinone as other treated mice but in addition, they exhibited a tyrosine clearance mechanism, other than HPPA and HPLA, that was more efficient.

During the work reported in this thesis, we observed no cases of Hgd^{-/-} or WT mice that displayed any obvious signs of ocular lesions that affected vision when receiving the highest doses of nitisinone (2mg or 4mg). Mice within the long-term study in chapter four had prolonged elevation of tyrosine (>1000umol/L) for around 40 weeks and still appeared to have no obvious ocular symptoms, although the cornea was not specifically examined. WT and Hgd^{-/-} mice within the MWM study in chapter three all had tyrosine levels >1100umol/L during testing, with one wild type mouse exceeding 1800umol/L, and showed no deficits during the visible platform test – a test specifically designed to alert the experimenter to mice with visual defects. This reconfirms that the mouse has superior mechanisms than in human to tolerate such high plasma tyrosine with no obvious adverse effects. One mouse within the study reported in chapter four developed a cutaneous lesion at the base of the tail that would not heal and consequently had to be culled prior to the

end of the study. This mouse was part of the 0.125mg nitisinone cohort and had the least elevated tyrosine value within the cohort suggesting that this event was not a cutaneous symptom relating to tyrosine toxicity.

A final point to consider is the role of tyrosinase in the synthesis of ochronotic pigmentation. Taylor and colleagues [41] mentioned a potentially useful link that is so far missing from the literature – an individual with both AKU and albinism that could provide further clues for any potential action of tyrosinase in the disease process of AKU. This thesis used BALB/c mice - an albino inbred mouse strain that results from a cysteine to serine substitution at position 85 of the tyrosinase gene. This mutation leads to non-functioning tyrosinase and is the reason why the BALB/c mouse is also considered a murine model of human tyrosinase negative oculocutaneous albinism [171-172]. This thesis therefore used a model that combines both AKU and albinism. Control and low dose nitisinone treated Hgd^{-/-} cohorts within chapter three displayed ochronotic pigmentation. Previous studies using BALB/c Hgd^{-/-} mice have also demonstrated ochronotic pigmentation [70-72]. The natural history study by Keenan and colleagues reported BALB/c (as used in this study) and BL/6 mice (which possess functional tyrosinase) to have similar pigmentation levels [71]. BALB/c mice in fact had a slightly higher pigmented chondron count range than BL/6 after 60 weeks of age, suggesting tyrosinase does not play a leading role and that other factors must mediate the synthesis of pigment in this model.

In summary, the work presented within this thesis presents novel findings to support the future licensing of nitisinone for use in AKU and opens the door to treatment in young patients. Early treatment has the potential to prevent the accumulating damage of high HGA during childhood and improve patient prognosis in later life. The results indicate no detrimental effect of nitisinone treatment on cognition or motor function in young BALB/c mice and demonstrate the feasibility of patient-tailored treatment to provide protection from ochronosis whilst minimising the adverse effects of elevated tyrosine. This thesis also presents novel data on the lability of the arteriovenous metabolome relating to AKU and suggests possible conditions relating to the HPPA to HPLA excretory conversion pathway.

7. Future work

The findings presented in this thesis have uncovered several lines of research that should be pursued in order to build upon the current understanding of the pathophysiology of AKU, along with the effects of nitisinone treatment.

7.1 Investigate differences between arteriovenous metabolome in AKU humans

HGA plasma levels were shown to widely vary between venous and mixed arterial blood in the Hgd^{-/-} mouse. It would be interesting to see if this was the case for humans with AKU and whether mixed arterial samples would give more accurate HGA results. A minimally invasive way to obtain a more arterial-like supply would be to sample from the hand after it had been placed in a warmed box to assist with vasodilation. This method is currently being implemented in human patients for a tyrosine tracer study within our AKU research group. It would be interesting to analysis this metabolite data to see if differences between arteriovenous samples were apparent. An arterial sample could also be taken with permission from an AKU patient during arthroplasty surgery to compare with a previous venous sampled from the same patient.

7.2 Heterozygous mice for further MWM trials

The results from chapter three highlighted that it would be useful to perform future trials with a control colony that were as closely matched to the Hgd^{-/-} mice as possible. It would be helpful to repeat some of the studies in heterozygous mice generated by crossing some of the homozygous colony back with WT mice and selecting the heterozygotes that have the mutation in only one allele (Hgd^{+/-}). This would eliminate as far as possible the non-AKU genetic differences between strains. A transgenic mouse model is currently being developed at the University of Liverpool with the hope this will give an even more accurate AKU model. As the model will be clean Hgd gene knock out, this will also eliminate the unknown non-AKU genetic differences resulting from random mutagenesis.

7.3 Measuring catecholamines in the mouse brain

The results from chapter three suggested that the Hgd^{-/-} genotype could affect the catecholamines within the mouse brain. Measuring these neurotransmitters, with a specific

focus on dopamine, in control and nitisinone treated Hgd^{-/-} and WT mice would allow analysis to see if any of these were elevated or depleted as a result of the genotype or treatment. Similar work is currently underway within the Royal Liverpool University Hospital's Department of Clinical Biochemistry and Metabolic Medicine.

7.4 Gait analysis with weight matched Hgd^{-/-} and WT mice

The gait analysis results in chapter three were affected by differences within bodyweight. Further analysis of age and bodyweight matched Hgd^{-/-} and WT mice should be carried out to enable a more sensitive measure of pathological gait that may occur in AKU mice. This could also be investigated in aged nitisinone treated and control Hgd^{-/-} mice to assess whether gait is more severely affected in later life, as in AKU patients.

7.5 Quantification of OA in Hgd^{-/-} nitisinone treated mice

Some control and nitisinone treated mice showed signs of OA within chapter four. Ochronotic pigmentation is linked to early onset OA therefore this could be expected in control mice, but surprisingly, treated mice who had reduced HGA from weaning also showed OA of the tibio-femoral joint. This suggests factors other than high HGA are involved in the joint damage observed in AKU. It may also suggest that even low amounts of HGA can cause joint damage despite pigmentation being minimal or absent. A long-term study involving quantification of OA in nitisinone treated and control Hgd^{-/-} cohorts, with age matched WT mice for comparison, would allow this to be investigated further.

7.6 Cull method effect on HPPA/HPLA

Chapter five indicated that culling with Pentoject had a significant effect on HPPA and HPLA values. Whether this was due to the pharmacological agent itself or endogenous factors released upon its administration is unknown. Further investigation into what caused this effect could potentially elucidate the mechanism or conditions required for stimulation of the HPPA to HPLA conversion pathway.

7. References

1. Garrod AE: **A contribution to the study of alkaptonuria.** *Medico-Chirurgical Transactions* 1899, **82**:369–394.
2. Garrod AE: **About alkaptonuria.** *Lancet* 1901, ii: 1484–1486.
3. Garrod AE: **The incidence of alkaptonuria: A study in chemical individuality** (1902) *The Yale Journal of Biology & Medicine* 2002, **75**(4):221-231.
4. Garrod AE, Hele TS: **The uniformity of the homogentisic acid excretion in alkaptonuria.** *The Journal of Physiology* 1905, **33**(3):198-205.
5. Garrod AE, Clarke JW: **A new case of alkaptonuria.** *The Biochemical Journal* 1907, **2**(5-6):217-220.
6. Garrod AE: **The croonian lectures on inborn errors of metabolism.** *The Lancet* 1908, **172**(4427):1-7.
7. Neubauer O: **Über den Abbau der Aminosäuren im gesunden und kranken Organismus.** *Deutsches Archiv Fur Klinische Medizin* 1909, **95**:211-256.
8. Lee SL, Stenn FF: **Characterization of mummy bone ochronotic pigment.** *The Journal of the American Medical Association* 1978, **240**(2):136-138.
9. Stenn FF, Milgram JW, Lee SL *et al*: **Biochemical identification of homogentisic acid pigment in an ochronotic Egyptian mummy.** *Science* 1977, **197**:566-568.
10. Boedeker C: **Ueber das Alcapton: ein neuer Beitrag zur Frage: welche Stoffe des Harns können Kupferreduction bewirken?** *Z Ration Med* 1859, **7**:130-145.
11. Virchow R: **Ein Fall von allgemeiner Ochronose der Knorpel und knorpelähnlichen Theile.** *Virchows Archiv* 1866, **37**:212–219.
12. Wolkow M, Baumann E: **Ueber das Wesen der Alkaptonurie.** *Physiologische Chemie* 1891, **15**:228–285.
13. Siťaj S: **Artropatia alcaptonurica.** *Bratislavske Lekarske Listy* 1947, **27**(4), 1–9.
14. Urbánek T, Siťaj Š: **Simultaneous occurrence of alkaptonuria, ochronotic arthropathy and Bechterews disease.** *Fysiatr. Vestn. Cesk. Fysiatr.* 1955, **33**:85–91.
15. Siťaj Š, Červeňanský, J, Urbánek T: **Alkaptonuria and ochronosis, (in Slovak).** *SAV Publishing, Bratislava* 1956, 156.
16. La Du BN, Zannoni VG, Laster L *et al*: **The nature of the defect in tyrosine metabolism in alcaptonuria.** *The Journal of Biological Chemistry* 1958, **230**(1):251-260.
17. La Du BN, Seegmiller JE, Laster L *et al*: **Alcaptonuria and ochronotic arthritis.** *Bulletin on the Rheumatic Diseases* 1958, **8**(9):163-164.

18. Pollak MR, Chou YH, Cerda JJ *et al*: **Homozygosity mapping of the gene for alkaptonuria to chromosome 3q2**. *Nature Genetics* 1993, **5**:201–204.
19. Phornphutkul C, Introne WJ, Perry MB *et al*: **Natural history of alkaptonuria**. *The New England Journal of Medicine* 2002, **347**(26):2111-2121.
20. Mistry JB, Bukhari M, Taylor AM: **Alkaptonuria**. *Rare Diseases* 2013, **1**:e27475.
21. Zatkova A, de Bernabe DB, Polakova H *et al*: **High frequency of alkaptonuria in Slovakia: evidence for the appearance of multiple mutations in HGO involving different mutational hot spots**. *American Journal of Human Genetics* 2000, **67**(5):1333-1339.
22. Al-Sbou M, Mwafi N, Lubad MA: **Identification of forty cases with alkaptonuria in one village in Jordan**. *Rheumatology International* 2012, **32**(12):3737-3740.
23. Sakthivel S, Zatkova A, Nemethova M *et al*: **Mutation screening of the HGD gene identifies a novel alkaptonuria mutation with significant founder effect and high prevalence**. *Annals of Human Genetics* 2014, **78**(3):155-64.
24. Ranganath LR, Jarvis JC, Gallagher JA: **Recent advances in management of alkaptonuria (invited review; best practice article)**. *Journal of Clinical Pathology* 2013, **66**(5):367-373.
25. Fisher AA, Davis MW: **Alkaptonuric ochronosis with aortic valve and joint replacements and femoral fracture: A case report and literature review**. *Clinical Medicine & Research* 2004, **2**(4):209-215.
26. Ozmanevra R, Guran O, Karatosun V *et al*: **Total knee arthroplasty in ochronosis: A case report and critical review of the literature**. *Joint Diseases & Related Surgery* 2013, **24**(3):169-172.
27. Gallagher JA, Dillon JP, Sireau N *et al*: **Alkaptonuria: An example of a “fundamental disease”—A rare disease with important lessons for more common disorders**. *Seminars in Cell & Developmental Biology* 2016, **52**:53–57.
28. Hughes AT, Milan AM, Christensen P *et al*: **Urine homogentisic acid and tyrosine: Simultaneous analysis by liquid chromatography tandem mass spectrometry**. *Journal of Chromatography B* 2014, **963**:06-112.
29. Bory C, Boulieu R, Chantin C *et al*: **Diagnosis of alcaptonuria: rapid analysis of homogentisic acid by HPLC**. *Clinica Chimica Acta; International Journal of Clinical Chemistry* 1990, **189**(1):7-11.
30. Jacomelli G, Micheli V, Bernardini G *et al*: **Quick Diagnosis of Alkaptonuria by Homogentisic Acid Determination in Urine Paper Spots**. *Journal of Inherited*

- Metabolic Disease Reports* 2017, **31**:51–56.
31. Granadino B, Beltran-Valero de Bernabe D, Fernandez-Canon JM *et al*: **The human homogentisate 1,2-dioxygenase (HGO) gene.** *Genomics* 1997, **43**(2):115-122.
 32. Laschi M, Tinti L, Braconi D *et al*: **Homogentisate 1,2 Dioxygenase is Expressed in Human Osteoarticular Cells: Implications in Alkaptonuria.** *Journal of Cellular Physiology* 2012, **227**:3254–3257.
 33. Nemethova M, Radvanszky J, Kadasi L *et al*: **Twelve novel HGD gene variants identified in 99 alkaptonuria patients: focus on ‘black bone disease’ in Italy.** *European Journal of Human Genetics* 2016, **24**:66–72.
 34. Zatkova A: **An update on molecular genetics of alkaptonuria (AKU).** *Journal of Inherited Metabolic Disease* 2011, **34**(6):1127-1136.
 35. Fernandez-Canon JM, Granadino B, Beltran-Valero de Bernabe D *et al*: **The molecular basis of alkaptonuria.** *Nature Genetics* 1996, **14**(1):19-24.
 36. Taylor AM, Hsueh MF, Ranganath LR *et al*: **Analysis of cartilage biomarkers of turnover and ageing in the osteoarthropathy of alkaptonuria.** *Osteoarthritis & Cartilage* 2011, **19**:S80.
 37. Taylor AM, Hsueh MF, Ranganath LR *et al*: **Cartilage biomarkers in the osteoarthropathy of alkaptonuria reveal low turnover and accelerated ageing.** *Rheumatology* 2017, **56**(1):156-164.
 38. Taylor AM, Wlodarski B, Prior IA *et al*: **Ultrastructural examination of tissue in a patient with alkaptonuric arthropathy reveals a distinct pattern of binding of ochronotic pigment.** *Rheumatology* 2010, **49**(7):1412-1414.
 39. Chow WY, Taylor AM, Reid DG *et al*: **Collagen atomic scale molecular disorder in ochronotic cartilage from an alkaptonuria patient, observed by solid state NMR.** *Journal of Inherited Metabolic Disease* 2011, **34**(6):1137-1140.
 40. Taylor AM, Boyde A, Wilson PJ *et al*: **The role of calcified cartilage and subchondral bone in the initiation and progression of ochronotic arthropathy in alkaptonuria.** *Arthritis & Rheumatism* 2011, **63**(12):3887-3896.
 41. Taylor AM, Kammath V, Bleakley A: **Tyrosinase, could it be a missing link in ochronosis in alkaptonuria?** *Medical Hypotheses* 2016, **91**:77–80.
 42. Ellaway CJ, Holme E, Standing S *et al*: **Outcome of tyrosinemia type III.** *Journal of Inherited Metabolic Disease* 2001, **24**:824–32.

43. Keller JM, Macaulay W, Nercessian OA *et al*: **New developments in ochronosis: review of the literature.** *Rheumatology International* 2005, **25**:81–85.
44. Merolla G, Dave A, Pegreff F *et al*: **Shoulder arthroplasty in alkaptonic arthropathy: A clinical case report and literature review.** *Musculoskeletal Surgery* 2012, **96**(1):93-99.
45. Zannoni VG, Lomtevas N, Goldfinger S: **Oxidation of homogentisic acid to ochronotic pigment in connective tissue.** *Biochimica et Biophysica Acta* 1969, **177**:94-105.
46. Mayatepek E, Kallas K, Anninos A *et al*: **Effects of ascorbic acid and low-protein diet in alkaptonuria.** *European Journal of Pediatrics* 1998, **157**(10):867-868.
47. Wolff JA, Barshop B, Nyhan WL *et al*: **Effects of ascorbic acid in alkaptonuria: alterations in benzoquinone acetic acid and an ontogenic effect in infancy.** *Pediatric Research* 1989, **26**:140-4.
48. Sealock RR, Silberstein HE: **The control of experimental alcaptonuria by means of vitamin C.** *Science* 1939, **90**(2344):517.
49. Braconi D, Laschi M, Amato L *et al*: **Evaluation of anti-oxidant treatments in an in vitro model of alkaptonic ochronosis.** *Rheumatology* 2010, **49**(10):1975-83.
50. de Haas V, Carbasius Weber EC, de Klerk JB *et al*: **The success of dietary protein restriction in alkaptonuria patients is age-dependent.** *Journal of Inherited Metabolic Disease* 1998, **21**:791-8.
51. Lock E, Ranganath LR, Timmis O: **The role of nitisinone in tyrosine pathway disorders.** *Current Rheumatology Reports* 2014, **16**(11):457–464.
52. Gil JA, Wawrzynski J, Waryasz GR: **Orthopedic Manifestations of Ochronosis: Pathophysiology, Presentation, Diagnosis, and Management.** *American Journal of Medicine* 2016, **129**(5):536,e1-6.
53. Knudsen CG, Lee DL, Michaely WJ *et al*: **Discovery of the triketone class of HPPD inhibiting herbicides and their relationship to naturally occurring beta-triketones.** *Allelopathy in Ecological Agriculture and Forestry*. Dordrecht: Kluwer Academic Publishers 2000, 101–111.
54. Moran GR: **4-Hydroxyphenylpyruvate dioxygenase.** *Archives of Biochemistry and Biophysics* 2005, **433**:117-128.
55. Ranganath LR, Milan AM, Hughes AT *et al*: **Suitability Of Nitisinone In Alkaptonuria 1 (SONIA 1): an international, multicentre, randomised, open-label, no-treatment controlled, parallel-group, dose-response study to investigate the effect of once**

- daily nitisinone on 24-h urinary homogentisic acid excretion in patients with alkaptonuria after 4 weeks of treatment. *Annals of the Rheumatic Diseases* 2016, **75**(2):362-7.
56. Introne WJ, Perry MB, Troendle J *et al*: **A 3-year randomized therapeutic trial of nitisinone in alkaptonuria.** *Molecular Genetics & Metabolism* 2011, **103**(4):307-314.
57. Stewart RMK, Brigg MC, Jarvis JC *et al*: **Reversible Keratopathy Due to Hypertyrosinaemia Following Intermittent Low-Dose Nitisinone in Alkaptonuria: A Case Report.** *Journal of Inherited Metabolic Disease Reports* 2014, **17**: 1-6.
58. Suwannarat P, O'Brien K, Perry MB : **Use of nitisinone in patients with alkaptonuria.** *Metabolism: Clinical & Experimental* 2005, **54**(6):719-728.
59. Taylor AM, Vercruyse KP: **Analysis of melanin-like pigment synthesised from homogentisic acid, with or without tyrosine, and its implications in alkaptonuria.** *Journal of Inherited Metabolic Disease Reports* 2017, **35**:79-85.
60. Lewis RW, Botham JW: **A review of the mode of toxicity and relevance to humans of the triketone herbicide 2-(4-methylsulfonyl-2-nitrobenzoyl)-1, 3-cyclohexanedione.** *Critical Reviews in Toxicology* 2013, **43**(3):185-199.
61. Henderson MJ, Faraj BT, Ali FM *et al*: **Tyrosine transaminase activity in normal and cirrhotic liver.** *Digestive Diseases and Sciences* 1981, **26**:124-128.
62. Lock EA, Gaskin P, Ellis MK *et al*: **Tissue distribution of 2-(2-nitro-4-trifluoromethylbenzoyl)cyclohexane-1,3-dione (NTBC): Effect on enzymes involved in tyrosine catabolism and relevance to ocular toxicity in the rat.** *Toxicology & Applied Pharmacology* 1996, **141**(2):439-447.
63. Lock EA, Ellis MK, Gaskin P *et al*: **From toxicological problem to therapeutic use: The discovery of the mode of action of 2-(2-nitro-4-trifluoromethylbenzoyl)-1,3-cyclohexanedione (NTBC), its toxicology and development as a drug.** *Journal of Inherited Metabolic Disease* 1998, **21**(5):498-506.
64. Lock EA, Gaskin P, Ellis MK *et al*: **Tyrosinemia produced by 2-(2-nitro-4-trifluoromethylbenzoyl)-cyclohexane-1,3-dione (NTBC) in experimental animals and its relationship to corneal injury.** *Toxicology and Applied Pharmacology* 2006, **215**(1): 9-16.
65. Thimm E, Herebian D, Assmann B *et al*: **Increase of CSF tyrosine and impaired serotonin turnover in tyrosinemia type I.** *Molecular Genetics and Metabolism* 2011, **102**(2):122-5.

66. Jae I, Janes T, Lukowiak K: **The role of serotonin in the enhancement of long-term memory resulting from predator detection in *Lymnaea*.** *Journal of Experimental Biology*. 2010, **213**:3603-3614.
67. Vanclooster A, Devlieger R, Meersseman W *et al*: **Pregnancy during nitisinone treatment for tyrosinaemia type I: first human experience.** *Journal of Inherited Metabolic Disease Reports*. 2012, **5**:27–33.
68. Garcia Segarra N, Roche S, Imbard A *et al*: **Maternal and fetal tyrosinemia type I.** *Journal of Inherited Metabolic Disease* 2010, **33**(3):507–510.
69. Kassel R, Sprietsma L, Rudnick DA. **Pregnancy in an NTBC-treated patient with hereditary tyrosinemia type I.** *Journal of Pediatric Gastroenterology and Nutrition* 2015, **60**(1):5–7.
70. Preston AJ, Keenan CM, Sutherland H *et al*: **Ochronotic osteoarthropathy in a mouse model of alkaptonuria, and its inhibition by nitisinone.** *Annals of the Rheumatic Diseases* 2014, **73**(1):284-289.
71. Taylor AM, Preston AJ, Paulk NK *et al*: **Ochronosis in a murine model of alkaptonuria is synonymous to that in the human condition.** *Osteoarthritis & Cartilage* 2012, **20**(8):880-886.
72. Keenan CM, Preston AJ, Sutherland H *et al*: **Nitisinone arrests but does not reverse ochronosis in alkaptonuric mice.** *Journal of Inherited Metabolic Disease Reports* 2015, **24**: 44-50.
73. Montagutelli X, Lalouette A, Coude M *et al*: **aku, a mutation of the mouse homologous to human alkaptonuria, maps to chromosome 16.** *Genomics* 1994, **19**(1):9-11.
74. Kress W, Schmidt SR, Halliger-Keller B *et al*: **The genetic defect of the alkaptonuric mouse (aku).** *Mammalian Genome* 1999, **10**(1):68-70.
75. Grompe M, Lindstedt S, al-Dhalimy M *et al*: **Pharmacological correction of neonatal lethal hepatic dysfunction in a murine model of hereditary tyrosinaemia type I.** *Nature Genetics* 1995, **10**(4):453-60.
76. Levin ED, Buccafusco JJ: **Animal Models of Cognitive Impairment.** *Boca Raton (FL): CRC Press/Taylor & Francis* 2006. <https://www.ncbi.nlm.nih.gov/books/NBK2533>
77. Van Meer P, Raber J: **Mouse Behavioural Analysis in Systems Biology.** *Biochemical Journal* 2005, **389**(3):593–610.

78. Roedel A, Storch C, Holsboer F *et al*: **Effects of light or dark phase testing on behavioural and cognitive performance in DBA mice.** *Laboratory Animals* 2006, **40**:371–381.
79. Peirson SN, Brown LA, Pothecary CA *et al*: **Light and the laboratory mouse.** *Journal of Neuroscience Methods* 2017, <https://doi.org/10.1016/j.jneumeth.2017.04.007>
80. Hawkins P, Golledge HDR: **The 9 to 5 Rodent – Time for Change? Scientific and animal welfare implications of circadian and light effects on laboratory mice and rats.** *Journal of Neuroscience Methods* 2017, <https://doi.org/10.1016/j.jneumeth.2017.05.014>
81. Bains RS, Wells S, Sillito RR *et al*: **Assessing mouse behaviour throughout the light/dark cycle using automated in-cage analysis tools.** *Journal of Neuroscience Methods* 2017, <https://doi.org/10.1016/j.jneumeth.2017.04.014>
82. Morris RG: **Spatial localisation does not depend on the presence of local cues.** *Learning and Motivation* 1981, **12**:239-260.
83. Morris RG, Garrud P, Rawlins JN *et al*: **Place navigation impaired in rats with hippocampal lesions.** *Nature* 1982, **297**(5868):681-683.
84. D’Hooge R, De Deyn PP: **Applications of the Morris water maze in the study of learning and memory.** *Brain Research Reviews* 2001, **36**(1):60-90.
85. Camors D, Jouffrais C, Cottureau BR *et al*: **Allocentric coding: Spatial range and combination rules.** *Vision Research* 2015, **109**:87-98.
86. Vorhees CV, Williams MT: **Morris water maze: Procedures for assessing spatial and related forms of learning and memory.** *Nature Protocols* 2006, **1**(2):848-858.
87. John S: **MorrisWaterMaze.svg.** (25 November 2010). Retrieved from <https://commons.wikimedia.org/wiki/File:MorrisWaterMaze.svg>
88. Langui D, Lachapelle F, Duyckaerts C: **Animal models of neurodegenerative diseases.** *Medecine Sciences* 2007, **23**(2):180-6.
89. de Quervain DJ, Roozendaal B, McGaugh JL: **Stress and glucocorticoids impair retrieval of long-term spatial memory.** *Nature* 1998, **394**(6695):787-90.
90. Riedel G, Micheau J, Lam AG *et al*: **Reversible neural inactivation reveals hippocampal participation in several memory processes.** *Nature Neuroscience* 1999, **2**(10):898-905.
91. Xing B, Kong H, Meng X *et al*: **Dopamine D1 but not D3 receptor is critical for spatial learning and related signaling in the hippocampus.** *Neuroscience* 2010, **169**(4):1511-1519.

92. Stensola T, Moser EI: **Grid Cells and Spatial Maps in Entorhinal Cortex and Hippocampus.** *Micro-,Meso- and Macro-Dynamics of the Brain. Cham (CH): Springer* 2016.
93. Sariñanaa J, Tonegawaa S: **Differentiation of Forebrain and Hippocampal Dopamine 1-Class Receptors, D1R and D5R, in Spatial Learning and Memory.** *Hippocampus* 2016, **26**(1):76–86.
94. Mandillo S, Heise I, Garbugino L *et al*: **Early motor deficits in mouse disease models are reliably uncovered using an automated home-cage wheel-running system: a cross-laboratory validation.** *Disease Models & Mechanisms* 2014 **7**:397-407.
95. Brooks S, Dunnett S: **Tests to assess motor phenotype in mice: a user's guide.** *Nature Reviews Neuroscience* 2009, **10**(7):519-529.
96. Barton GJ, King SL, Robinson MA *et al*: **Age-Related Deviation of Gait from Normality in Alkaptonuria.** *Journal of Inherited Metabolic Disease Reports* 2015, **24**:39-44.
97. Dunham NW, Miya TS: **A note on a simple apparatus for detecting neurological deficit in rats and mice.** *Journal of the American Pharmacists Association* 1957, **46**:208–209.
98. Wang Z, Miller RE, Malfait AM: **Assessment of motor coordination and balance after destabilization of the medial meniscus in mice.** *Osteoarthritis and Cartilage* 2016, **24**:S455-S456.
99. Gertsman I, Barshop BA, Panyard-Davis J *et al*: **Metabolic Effects of Increasing Doses of Nitisinone in the Treatment of Alkaptonuria.** *Journal of Inherited Metabolic Disease Reports* 2015, **24**:13–20.
100. Rana AQ, Saeed U, Abdullah I *et al*: **Alkaptonuria, more than just a mere disease.** *Journal of Neurosciences in Rural Practice* 2015, **6**(2):257-260.
101. Das AM: **Clinical utility of nitisinone for the treatment of hereditary tyrosinemia type-1 (HT-1).** *The Application of Clinical Genetics* 2017, **10**:43-48.
102. Hoffer LJ: **Parenteral Nutrition: Amino Acids.** *Nutrients* 2017, **9**(3):257.
103. Helliwell TR, Gallagher JA, Ranganath L: **Alkaptonuria--a review of surgical and autopsy pathology.** *Histopathology* 2008, **53**(5):503-512.
104. Bory C, Boulieu R, Chantin C *et al*: **Homogentisic acid determined in biological fluids by HPLC.** *Clinical Chemistry* 1989, **35**(2):321-322.

105. Glasson SS, Chambers MG, Van Den Berg WB *et al*: **The OARSI histopathology initiative – recommendations for histological assessments of osteoarthritis in the mouse.** *Osteoarthritis & Cartilage* 2010, **18**, Supplement 3(0):S17-S23.
106. Tinti L, Taylor AM, Santucci A *et al*: **Development of an in vitro model to investigate joint ochronosis in alkaptonuria.** *Rheumatology* 2011, **50**(2):271-277.
107. Gouveia K & Hurst JL: **Optimising reliability of mouse performance in behavioural testing: the major role of non-aversive handling.** *Scientific Reports* 2017, **7**:44999.
108. Hurst JL & West RS: **Taming anxiety in laboratory mice.** *Nature Methods* 2010, **7**:825–826.
109. Glasson SS, Blanchet TJ, Morris EA: **The surgical destabilization of the medial meniscus (DMM) model of osteoarthritis in the 129/SvEv mouse.** *Osteoarthritis & Cartilage* 2007, **15**(9):1061-1069.
110. Bendadi F, de Koning TJ, Visser G *et al*: **Impaired cognitive functioning in patients with tyrosinemia type I receiving nitisinone.** *The Journal of Pediatrics* 2014, **164**(2):398-401.
111. Pohorecka MI, Biernacka M, Jakubowska-Winecka A *et al*: **Behavioral and intellectual functioning in patients with tyrosinemia type I.** *Pediatric Endocrinology, Diabetes, and Metabolism* 2012, **18**(3):96–100.
112. Thimm E, Richter-Werkle R, Kamp G *et al*: **Neurocognitive outcome in patients with hypertyrosinemia type I after long-term treatment with NTBC.** *Journal of Inherited Metabolic Disease* 2012, **35**(2):263-8.
113. De Laet C, Terrones V, Jaeken J *et al*: **Neuropsychological outcome of NTBC-treated patients with tyrosinemia type 1.** *Developmental Medicine & Child Neurology* 2011, **53**:962–964.
114. García MI, De la Parra A, Arias C *et al*: **Long-term cognitive functioning in individuals with tyrosinemia type 1 treated with nitisinone and protein-restricted diet.** *Molecular Genetics and Metabolism Reports* 2017, **11**:12–16.
115. Cerone R, Holme E, Schiaffino MC *et al*: **Tyrosinemia type III: diagnosis and ten year follow-up.** *Acta Paediatrica* 1997, **86**(9):1013–1015.
116. Hillgartner MA, Coker SB, Koenig AE *et al*: **Tyrosinemia type 1 and not treatment with NTBC causes slower learning and altered behaviour in mice.** *Journal of Inherited Metabolic Disease* 2016, **39**:673-682.
117. Beninger RJ, Miller R: **Dopamine D1-like receptors and reward-related incentive learning.** *Neuroscience & Biobehavioural Reviews* 1998, **22**(2):335–345.

118. Colzato LS, Jongkees BJ, Sellaro R *et al*: **Working memory reloaded: Tyrosine repletes updating in the N-back task.** *Frontiers in Behavioural Neuroscience* 2013, **7**:200.
119. Kühn S, Düzel S, Colzato L *et al*: **Food for thought: association between dietary tyrosine and cognitive performance in younger and older adults.** *Psychological Research* 2017, **81**:1-10.
120. Eisenhofer G, Tian H, Holmes C *et al*: **Tyrosinase: a developmentally specific major determinant of peripheral dopamine.** *FASEB Journal* 2003, **10**:1248-55.
121. Sparrow LM, Pellatt E, Yu SS *et al*: **Gait changes in a line of mice artificially selected for longer limbs.** *Peer Journal* 2017, **5**:3008.
122. Parvathy SS, Masocha W: **Gait analysis of C57BL/6 mice with complete Freund's adjuvant-induced arthritis using the CatWalk system.** *BMC Musculoskeletal Disorders* 2013, **14**(14):19.
123. Ferland CE, Laverty S, Beaudry F *et al*: **Gait analysis and pain response of two rodent models of osteoarthritis.** *Pharmacology Biochemistry and Behavior* 2011, **97**(603):10.
124. Hoffmann MH, Hopf R, Niederreiter B *et al*: **Gait changes precede overt arthritis and strongly correlate with symptoms and histopathological events in pristane-induced arthritis.** *Arthritis Research & Therapy* 2010, **12**(41):10.
125. Simjee SU, Pleuvry BJ, Coulthard P: **Modulation of the gait deficit in arthritic rats by infusions of muscimol and bicuculline.** *Pain* 2004, **109**(453):60.
126. Coulthard P, Pleuvry BJ, Brewster M *et al*: **Gait analysis as an objective measure in a chronic pain model.** *Journal of Neuroscience Methods* 2002, **116**(197):213.
127. Jacobs BY, Kloefkorn HE, Allen KD: **Gait Analysis Methods for Rodent Models of Osteoarthritis.** *Current Pain and Headache Reports* 2014, **18**(10):456.
128. Lakes EH, Allen KD: **Gait Analysis Methods for Rodent Models of arthritic disorders: reviews and recommendations.** *Osteoarthritis and cartilage* 2016, **24**:1837-1849
129. Allen KD, Griffin TM, Rodriguiz RM *et al*: **Decreased Physical Function and Increased Pain Sensitivity in Mice Deficient for Type IX Collagen.** *Arthritis Research & Therapy* 2007, **9**(6):123.
130. Bozkurt A, Deumens R, Scheffel J *et al*: **CatWalk gait analysis in assessment of functional recovery after sciatic nerve injury.** *Journal of Neuroscience Methods* 2008, **173**:91-98.

131. Bozkurt A, Scheffel J, Brook GA *et al*: **Aspects of static and dynamic motor function in peripheral nerve regeneration: SSI and CatWalk gait analysis.** *Behavioural Brain Research* 2011, **219**:55-62.
132. Costa LM, Simões MJ, Maurício AC *et al*: **Methods and protocols in peripheral nerve regeneration experimental research: Part IV – kinematic gait analysis to quantify peripheral nerve regeneration in the rat.** *International Review of Neurobiology* 2009, **87**:127-139.
133. Deumens R, Jaken RJP, Marcus MAE *et al*: **The CatWalk gait analysis in assessment of both dynamic and static gait changes after adult rat sciatic nerve resection.** *Journal of Neuroscience Methods* 2007, **164**:120-130.
134. Möller KÄ, Berge OG, Hamers FPT: **Using the CatWalk method to assess weight-bearing and pain behaviour in walking rats with ankle joint monoarthritis induced by carrageenan: effects of morphine and rofecoxib.** *Journal of Neuroscience Methods* 2008, **174**:1-9.
135. Beloborodova NV, Khodakova AS, Bairamov IT *et al*: **Microbial Origin of Phenylcarboxylic Acids in the Human Body.** *Biochemistry (Moscow)* 2009, **74**(12):1657-1663.
136. Bachmanov AA, Reed DR, Beauchamp GK *et al*: **Food Intake, Water Intake, and Drinking Spout Side Preference of 28 Mouse Strains.** *Behavior Genetics* 2002, **32**(6): 435–443.
137. Al-Dhalimy M, Overturf K, Finegold M *et al*: **Long-Term Therapy with NTBC and Tyrosine-Restricted Diet in a Murine Model of Hereditary Tyrosinemia Type I.** *Molecular Genetics and Metabolism* 2002, **75**: 38–45.
138. Khedr M, Judd S, Briggs MC *et al*: **Asymptomatic Corneal Keratopathy Secondary to Hypertyrosinaemia Following Low Dose Nitisinone and a Literature Review of Tyrosine Keratopathy in Alkaptonuria.** *Journal of Inherited Metabolic Disease Reports* 2017, **35**: 1-7.
139. Stewart RMK, Brigg MC, Jarvis JC *et al*: **Reversible Keratopathy Due to Hypertyrosinaemia Following Intermittent Low-Dose Nitisinone in Alkaptonuria: A Case Report.** *Journal of Inherited Metabolic Disease Reports* 2014, **17**: 1-6.
140. Holliday MA, Potter D, Jarrah A *et al*: **The relation of metabolic rate to body weight and organ size.** *Pediatric Research* 1967, **1**(3): 185-95.

141. Lock EA, Gaskin P, Ellis MK *et al*: **Tissue distribution of 2-(2-nitro-4-trifluoromethylbenzoyl)-cyclohexane-1,3-dione (NTBC) and its effect on enzymes involved in tyrosine catabolism in the mouse.** *Toxicology* 2000, **144**(1–3): 179-187.
142. Hall MG, Wilks MF, Provan WM *et al*: **Pharmacokinetics and pharmacodynamics of NTBC (2-(2-nitro-4-fluoromethylbenzoyl)-1,3-cyclohexanedione) and mesotrione, inhibitors of 4-hydroxyphenyl pyruvate dioxygenase (HPPD) following a single dose to healthy male volunteers.** *Journal of Clinical Pharmacology* 2001, **52**:169-177.
143. Diarra A, Lefauconnier JM, Valens M *et al*: **Tyrosine content, influx and accumulation rate, and catecholamine biosynthesis measured in vivo, in the central nervous system and in peripheral organs of the young rat. Influence of neonatal hypo- and hyperthyroidism.** *Archives of Physiology and Biochemistry* 1989, **97**(5):317-32.
144. Frank S, Veit R, Sauer H *et al*: **Dopamine Depletion Reduces Food-Related Reward Activity Independent of BMI.** *Neuropsychopharmacology* 2016, **41**(6):1551-9.
145. Bjork JM, Grant SJ, Chen G *et al*: **Dietary tyrosine/phenylalanine depletion effects on behavioural and brain signatures of human motivational processing.** *Neuropsychopharmacology* 2014, **39**(3):595-604.
146. Hardman CA, Herbert VM, Brunstrom JM *et al*: **Dopamine and food reward: effects of acute tyrosine/phenylalanine depletion on appetite.** *Physiol Behav.* 2012, **105**(5):1202-7.
147. Higgins C: **Lactate measurement: arterial versus venous blood sampling.** Retrieved from acute-care-testing.org Jan 2017.
148. Reminiac F, Saint-Etienne C, Runge I *et al*. **Are central venous and arterial lactate interchangeable. A human retrospective study.** *Anesthesia & Analgesia* 2012, **115**(3):605-10.
149. Chan YK, Davis PF, Poppitt SD *et al*: **Influence of tail versus cardiac sampling on blood glucose and lipid profiles in mice.** *Laboratory Animals* 2012, **46**(2):142-147.
150. Gibbs EL, Lennox WG, Nims LF *et al*: **Arterial and cerebral venous blood: Arterial-venous differences in man.** *The Journal of Biological Chemistry* 1942, **144**:325–332.
151. Glassberg BY: **The arteriovenous difference in blood sugar content.** *Archives of Internal Medicine* 1930, **46**:605–609.

152. Cicinelli E, Ignarro LJ, Schonauer LM *et al*: **Different plasma levels of nitric oxide in arterial and venous blood.** *Clinical Physiology* 1999, **5**:440-2.
153. Ivanisevic J, Elias D, Deguchi H *et al*: **Arteriovenous Blood Metabolomics: A Readout of Intra-Tissue Metabostasis.** *Scientific Reports* 2015, **5**:12757.
154. Clarke JI, Forootan SS, Lea JD *et al*: **Circulating levels of miR-122 increase post-mortem, particularly following lethal dosing with pentobarbital sodium: implications for pre-clinical liver injury studies.** *Toxicology Research.* 2017, **6**:406-411.
155. Middleton P, Kelly A M, Brown J *et al*: **Agreement between arterial and central venous values for pH, bicarbonate, base excess, and lactate.** *Emergency Medicine Journal* 2006 **23**:622–624.
156. Overmyer KA, Thonusin C, Qi NR *et al*: **Impact of Anesthesia and Euthanasia on Metabolomics of Mammalian Tissues: Studies in a C57BL/6J Mouse Model.** *PLoS ONE* 2015, **10**(2):e0117232.
157. Chan FK, Moriwaki K, De Rosa MJ: **Detection of Necrosis by Release of Lactate Dehydrogenase (LDH) Activity.** *Methods in Molecular Biology* 2013, **979**:65–70.
158. Golub MS, Campbell MA, Kaufman FL *et al*: **Effects of restraint stress in gestation: implications for rodent developmental toxicology studies.** *Birth Defects Research. Part B, Developmental and Reproductive Toxicology* 2004, **71**:26–36.
159. Gong S, Miao Y, Jiao GZ *et al*: **Dynamics and Correlation of Serum Cortisol and Corticosterone under Different Physiological or Stressful Conditions in Mice.** *PLoS ONE* 2015, **10**(2): e0117503.
160. Alam SQ, Boctor AM, Rogers QR *et al*: **Some Effects of Amino Acids and Cortisol on Tyrosine Toxicity in the Rat.** *The Journal of Nutrition* 1967, **93**(3):317-323.
161. Panin LE, Usynin IF: **Role of glucocorticoids and resident liver macrophages in induction of tyrosine aminotransferase.** *Biochemistry.* 2008, **73**(3):305-9.
162. Lepage N, McDonald N, Dallaire L *et al*: **Age-specific distribution of plasma amino acid concentrations in a healthy pediatric population.** *Clinical Chemistry* 1997, **43**(12):2397-402.
163. Hem A, Smith AJ, Solberg P: **Saphenous vein puncture for blood sampling of the mouse, rat, hamster, gerbil, guinea pig, ferret and mink.** *Laboratory animals* 1998, **32**(4):364-368.

164. Diehl KH, Hull R, Morton D *et al*: **A good practice guide to the administration of substances and removal of blood, including routes and volumes.** *Journal of applied Toxicology*. 2001, **21**(1): 15-23.
165. Psarelli EE, Cox T, Ranganath L: **Clinical development of nitisinone for alkaptonuria (developakure) - a rare disease clinical trials design.** *Trials* 2013, **14**(1):29.
164. Lowell A, Goldsmith LA, Thorpe J *et al*: **Hepatic Enzymes of Tyrosine Metabolism in Tyrosinemia II.** *Journal of Investigative Dermatology* 1979, **73**(6):530-532.
165. Szymanska E, Sredzinska M, Ciara E *et al*: **Tyrosinemia type III in an asymptomatic girl.** *Molecular Genetics and Metabolism Reports* 2015, 5:48–50.
166. Fernstrom JD: **Large neutral amino acids: dietary effects on brain neurochemistry and function.** *Amino Acids* 2013, **45**(3):419-30.
167. Choi S, Disilvio B, Fernstrom MH *et al*: **Oral branched-chain amino acid supplements that reduce brain serotonin during exercise in rats also lower brain catecholamines.** *Amino Acids* 2013, **45**(5):1133-42.
168. Taylor AMW, Becker S, Schweinhardt P *et al*: **Mesolimbic dopamine signaling in acute and chronic pain: implications for motivation, analgesia, and addiction.** *Pain* 2016, **157**(6):1194-1198.
169. Bromberg-Martin ES, Matsumoto M, Hikosaka O: **Dopamine in motivational control: rewarding, aversive, and alerting.** *Neuron* 2010, **68**(5):815-34.
170. Ferreira GK, Carvalho-Silva M, Gonçalves CL *et al*: **L-Tyrosine administration increases acetylcholinesterase activity in rats.** *Neurochemistry International* 2012, **61**:1370–1374.
171. Beermann F, Ruppert S, Hummler E *et al*: **Rescue of the albino phenotype by introduction of a functional tyrosinase gene into mice.** *The EMBO Journal* 1990, **9**(9):2819-26.
172. Shibahara S, Okinaga S, Tomita Y *et al*: **A point mutation in the tyrosinase gene of BALB/c albino mouse causing the cysteine -P serine substitution at position 85.** *European Journal of Biochemistry* 1990, **189**:455 -461.
173. Nestler EJ, Hyman SE: **Animal Models of Neuropsychiatric Disorders.** *Nature Neuroscience* 2010, **13**(10):1161–1169.
174. Luong TN, Carlisle HJ, Southwell A: **Assessment of Motor Balance and Coordination in Mice using the Balance Beam.** *Journal of Visualized Experiments* 2011, **49**:2376.

175. Gómez C, Delgado-García M, Santiago-Mejía J *et al*: **Swimming Performance: A Strategy to Evaluate Motor Dysfunction after Brain Ischemia in Mice.** *Journal of Behavioural and Brain Science* 2013, **3**:584-590.
176. Brooks SP, Pask T, Jones L *et al*: **Behavioural profiles of inbred mouse strains used as transgenic backgrounds. I: motor tests.** *Genes, Brain and Behaviour* 2004, **3**:206–215.
177. Moser VC: **Functional Assays for Neurotoxicity Testing.** *Toxicologic Pathology* 2010, **39**(1):36-45.
178. Colotla VA, Flores E, Oscos A *et al*: **Effects of MPTP on locomotor activity in mice.** *Neurotoxicology and Teratology* 1990, **12**:405-407.
179. Giraldo G, Brooks M, Giasson BI: **Locomotor differences in mice expressing wild-type human α -synuclein.** *Neurobiology of Aging* 2018, **65**:140-148.
180. Kondziela W: **Eine neue method zur messung der muskularen relaxation bei weissen mausen.** *Archives Internationales De Pharmacodynamie Et De Therapie.* 1964, **152**:277–284.
181. Golledge H: **Euthanasia.** Retrieved from <https://www.nc3rs.org.uk/euthanasia> April 2017.
182. Bulfield G, Siller WG, Wight PA: **X chromosome-linked muscular dystrophy (mdx) in the mouse.** *Proceedings of the National Academy of Sciences* 1984, **81**:1189–1192.
183. Chen YJ, Cheng F, Sheu ML: **Detection of subtle neurological alterations by the Catwalk XT gait analysis system.** *Journal of Neuroengineering and Rehabilitation* 2014, **11**:62.

Appendix: Long-term dose response study metabolite data & pigmented chondron counts

Nitisinone dose (mg/L)	n	Metabolite	Mean (umol/L)	SD	SEM	Coefficient of variation
BALB/c Hgd -/- Mid bleed - 20 weeks						
0	7	Tyrosine	60.6	12.6	4.8	20.8
		HGA	247.3	87.5	33.1	35.4
		Phenylalanine	65.0	15.0	5.7	23.1
		HPPA	<10.0	-	-	-
		HPLA	<5.0	-	-	-
0.125	6	Tyrosine	257.0	110.8	41.9	43.1
		HGA	229.6	119.3	45.1	52.0
		Phenylalanine	56.3	6.0	2.3	10.7
		HPPA	56.9	24.4	9.2	42.9
		HPLA	12.1	5.7	2.2	47.1
0.5	7	Tyrosine	796.7	137.3	56.0	17.2
		HGA	192.2	86.6	35.3	45.1
		Phenylalanine	71.0	14.3	5.8	20.1
		HPPA	188.5	69.4	28.3	36.8
		HPLA	36.8	12.5	5.1	34.0
2	7	Tyrosine	1455.3	120.3	45.5	8.3
		HGA	47.4	10.7	4.0	22.6
		Phenylalanine	104.9	9.9	3.73	9.4
		HPPA	222.4	62.6	23.6	28.1
		HPLA	79.4	13.9	5.3	17.5
BALB/c Hgd -/- Term bleed - 40 weeks						
0	7	Tyrosine	83.6	4.3	1.8	5.1
		HGA	133.8	24.4	10.0	18.2
		Phenylalanine	89.1	7.3	3.0	8.2
		HPPA	12.7	0.3	0.1	2.4
		HPLA	<5.0	-	-	-
0.125	6	Tyrosine	249.3	45.3	18.5	18.2
		HGA	89.1	47.6	19.4	53.4
		Phenylalanine	84.0	9.1	3.7	10.8
		HPPA	18.2	3.5	1.4	19.2
		HPLA	12.0	4.9	2.0	40.8
0.5	6	Tyrosine	531.3	54.4	22.2	10.2
		HGA	51.9	9.5	3.9	18.3
		Phenylalanine	89.0	4.8	1.9	5.4
		HPPA	20.4	0.8	0.3	3.9
		HPLA	23.6	3.0	1.2	12.7
2	6	Tyrosine	1015.0	218.4	82.6	21.5
		HGA	28.7	5.9	2.2	20.6
		Phenylalanine	101.6	21.9	8.3	21.6
		HPPA	30.3	3.5	1.3	11.6
		HPLA	50.7	11.3	4.3	22.3
AKU Human – SONIA1 4 week data						
0	8	Tyrosine	56.0	15	5.3	27.8
		HGA	30.5	12.4	4.4	32.4
		Phenylalanine	54.6	16.7	5.9	30.7

		HPPA	13.8	5.6	2.0	40.4
		HPLA	<5	-	-	-
1	8	Tyrosine	653.0	106	37.5	16.2
		HGA	ND	-	-	-
		Phenylalanine	53.5	5.7	2.0	10.7
		HPPA	37.5	15.6	5.5	41.6
		HPLA	47.2	26.2	9.3	55.5
2	8	Tyrosine	715.0	171	60.5	23.9
		HGA	ND	-	-	-
		Phenylalanine	51.6	13.0	4.6	25.2
		HPPA	43.2	12.5	4.4	28.9
		HPLA	47.1	7.9	2.8	16.8
4	8	Tyrosine	803.0	155	54.8	19.3
		HGA	ND	-	-	-
		Phenylalanine	53.8	12.2	4.3	22.6
		HPPA	49.6	15.3	5.4	30.8
		HPLA	79.5	54.8	19.4	68.9
8	8	Tyrosine	813.0	145	15.9	17.8
		HGA	ND	-	-	-
		Phenylalanine	54.3	11.6	4.1	21.4
		HPPA	56.2	15.4	5.4	27.4
		HPLA	78.7	20.1	7.1	25.5

Table 1 - Plasma metabolites measured at 20 and 40 weeks in control and nitisinone treated BALB/c Hgd^{-/-} mouse from long-term dose response study (chapter 4). Human data obtained via personal communication from SONIA1 study [55] ND, not detected (below 3.1umol/L).

BALB/c Hgd ^{-/-}	Nitisinone dose (mg/L)	Cellular pigmentation count	Cellular + peri-cellular pigmentation count
30.1	0 Control	250	449
30.2	0 Control	197	427
30.3	0 Control	119	248
30.4	0 Control	170	287
30.5	0 Control	115	235
30.6	0 Control	258	369
29.1	0.125	106	299
29.3	0.125	211	477
29.4	0.125	248	359
29.5	0.125	247	433
29.6	0.125	252	425
29.7	0.125	123	195
24.1	0.5	77	131
24.2	0.5	29	44
26.1	0.5	33	75
26.2	0.5	44	98
26.3	0.5	22	51
26.4	0.5	53	129
13.1	2	5	22
13.2	2	3	12
13.3	2	4	16
13.4	2	13	46
13.5	2	4	12
13.6	2	7	35
13.7	2	0	10

Table 2 - Quantification of ochronotic pigmentation in 43 week old, control and nitisinone treated BALB/c Hgd^{-/-} mice from long-term dose response study (chapter 4). Both classifications of pigmentation included.